INVESTIGATIONS OF INDOOR THERMAL AND AIR FLOW CONDITIONS IN A TOBACCO WAREHOUSE

A Thesis Submitted to the
Graduate School of Engineering and Science
İzmir Institute of Technology
in Partial Fulfillment of the Requirements for the Degree of

DOCTOR OF PHILOSOPHY

in Architecture

by
Mümine GERÇEK ŞEN

July 2023
İZMİR

We approve the thesis of **Mümine GERÇEK ŞEN**

Examining Committee Members:

Prof. Dr. Tahsin BAŞARAN
Department of Architecture, İzmir Institute of Technology

Prof. Dr. Mustafa Emre İLAL
Department of Architecture, İzmir Institute of Technology

Assoc. Prof. Dr. Ziya Haktan KARADENİZ
Department of Energy Systems Engineering, İzmir Institute of Technology

Prof. Dr. Yenal AKGÜN
Department of Architecture, Dokuz Eylül University

Assoc. Prof. Dr. Mehmet Akif EZAN
Department of Mechanical Engineering, Dokuz Eylül University

20 July 2023

Prof. Dr. Tahsin BAŞARAN
Supervisor, Department of Architecture,
İzmir Institute of Technology

Prof. Dr. Koray KORKMAZ
Head of the Department of Architecture

Prof. Dr. Mehtap EANES
Dean of the Graduate School of
Engineering and Sciences

ACKNOWLEDGEMENTS

I would like to express the most profound appreciation to my thesis supervisor, Prof. Dr. Tahsin Başaran, for giving me the opportunity to work with him and for his guidance and persistent help throughout my studies. I am also grateful to my thesis monitoring committee members, Prof. Dr. Mustafa Emre İlal and Assoc. Prof. Dr. Ziya Haktan Karadeniz.

I would also like to thank Ahmet Okumuş on behalf of the company 'Oryantal Tütün Paketleme (OTP)', for allowing me to conduct my studies on-site and for the many valuable information about the sector. In addition, I am very grateful for the invaluable support of the Warehouse Manager, Önder Öngel. His contributions to the whole process during field studies, his endless patience with my questions, and my visits many times were always encouraging for me to keep going even in the hardest times.

I would also like to express my gratitude to Assoc. Prof. Dr. Murat Barışık for allowing me to use his laboratory and facilities to conduct my work. I am very grateful for his unconditional support throughout my computational analysis process.

I am also thankful to my friends Gülçin Özen, Mina Yavuz Aslan, İlker Güçü, and my laboratory mate Ali Berkay Avcı for giving me support, courage, and strength whenever I needed. Thank you for being not just colleagues but for being real friends.

I would also like to thank my parents Kemal and Kalbiye Gerçek, and my brother Hüseyin Gerçek for their endless support. It meant the world to me that you tried with all your strength to push all the obstacles out of my way and try to make everything easier for me, even in the most difficult times of our lives. I will always feel your eternal love deep in my heart.

Last, but not least, I am very grateful to my husband "Tüm" for his endless care, kindness, and support. Thank you for expressing your belief in me any time I feel frustrated. Thank you for helping me to get over the hard times. I could not have done it without you.

ABSTRACT

INVESTIGATIONS OF INDOOR THERMAL AND AIR FLOW CONDITIONS IN A TOBACCO WAREHOUSE

This study investigates the thermal performance and indoor environment conditions of naturally and hybrid ventilated industrial buildings. Numerical analyses and experimental measurements were conducted in a tobacco warehouse in İzmir, Turkey. Parametric analyses were performed with three different approaches: i) 15 architectural design strategies are evaluated by using a sensitivity analysis. It is found that roof insulation thickness, shading projection factor, and shading angle have significant impact on heating and cooling requirements. In addition, the most influential factors on operational CO_2 emissions are thickness of insulation material and conductivity of thermal insulation material. ii) Vertical and volumetric temperature gradients, crucial for stored product quality, are assessed through field measurements and CFD simulations. Ceiling-mounted radiant cooling systems reduced indoor temperatures by 3°C, while floor heating systems increased temperatures by 7°C, ensuring a consistent range of 21-25°C by providing a range at defined indoor temperature values. Maximum loads are determined as 12.9W/m^2 for cooling and 39.6W/m^2 for heating. iii) The air change effectivenesses of different ventilation conditions are analysed. Four additional fans improved air exchange quality and decreased the volumetric mean age of air (AoA) from 1230 to 525 seconds. It is indicated that, while additional fans may decrease the mean AoA, maximizing the fan operation capacities is not obligatory to achieve increased air change effectiveness. Besides, the analysis of various fan operation scenarios significantly improves indoor environment conditions and energy efficiency. This thesis emphasizes the importance of design parameters in influencing indoor environmental conditions and energy consumption. The investigation of thermal air mixing and conditioning strategies underscores the need for a combined experimental and numerical approach. The findings contribute to effective solutions for warehouses storing temperature-sensitive products, ensuring optimal storage conditions and mitigating temperature variations during logistics operations.

ÖZET

BİR TÜTÜN DEPOSUNDAKİ İÇ MEKAN TERMAL VE HAVA AKIŞ ŞARTLARININ İNCELENMESİ

Bu çalışma, doğal ve hibrit havalandırmalı endüstriyel binaların ısıl performansını ve iç ortam koşullarını araştırmaktadır. Sayısal analizler ve deneysel ölçümler İzmir'de bulunan bir tütün deposunda gerçekleştirilmiştir. Üç farklı yaklaşımla parametrik analizler yapılmıştır: i) 15 mimari tasarım stratejisi duyarlılık analizleri kullanılarak değerlendirilmiştir. Çatı yalıtım kalınlığı, gölgeleme projeksiyon faktörü ve gölgeleme açısının ısıtma ve soğutma gereksinimlerini önemli ölçüde etkilediği bulunmuştur. Ayrıca işletme CO_2 emisyonlarını en çok etkileyen faktörler yalıtım malzemesi kalınlığı ve ısı yalıtım malzemesinin iletkenliğidir. ii) Depolanan ürün kalitesi için çok önemli olan dikey ve hacimsel sıcaklık gradyanları, saha ölçümleri ve CFD simülasyonları aracılığıyla değerlendirilmiştir. Tavana monte radyant soğutma sistemleri, iç ortam sıcaklıklarını 3°C düşürürken, yerden ısıtma sistemleri sıcaklıkları 7°C artırarak, 21-25°C'lik tutarlı; tanımlı iç ortam sıcaklık değerlerinde bir aralık sağlamaktadır. Maksimum yükler soğutma için 12,9W/m^2, ısıtma için 39,6W/m^2 olarak belirlenmiştir. iii) Farklı havalandırma koşullarının hava değişim etkisi analiz edilmiştir. Dört ek fan, hava değişim kalitesini iyileştirmiş ve havanın ortalama yaşını 1230 saniyeden 525 saniyeye düşürmüştür. Ek fanlar havanın ortalama yaşını düşürebilirken, artan hava değişim etkinliği elde etmek için fan çalışma kapasitelerinin maksimize edilmesinin zorunlu olmadığı ortaya çıkmıştır. Ayrıca, çeşitli fan çalışma senaryolarının analizi, iç ortam koşullarının ve enerji verimliliğinin iyileştirilmesinde önemli bir etkiye sahiptir. Bu tez, iç ortam koşullarını ve enerji tüketimini etkilemede tasarım parametrelerinin önemini vurgulamaktadır. Termal hava karıştırma ve şartlandırma stratejilerinin araştırılması, birleşik bir deneysel ve sayısal yaklaşıma duyulan ihtiyacın altını çizmektedir. Bulgular, sıcaklığa duyarlı ürünleri depolayan ambarlar için etkili çözümlere katkıda bulunurken, optimum depolama koşulları sağlamakta ve lojistik operasyonlar sırasında oluşan sıcaklık değişimlerini azaltmaktadır.

TABLE OF CONTENTS

TABLE OF CONTENTS v
LIST OF FIGURES vii
LIST OF TABLES xiii

CHAPTER 1. INTRODUCTION 1
1.1. Problem Definition 2
1.2. Aim and Scope of the Thesis 4
1.3. Outline of the Thesis 5

CHAPTER 2. LITERATURE REVIEW 8
2.1. Tobacco Warehouses 9
2.2. Review of the Previous Work 14
2.3. Air Flow and Thermal Analysis of Warehouses 18
2.3.1. Energy-Oriented Approaches 18
2.3.2. Thermal Stratification in Warehouses 24
2.3.3. Ventilation Approaches on Warehouses 32

CHAPTER 3. RESEARCH APPROACH AND METHODOLOGY 51
3.1. Case Building 52
3.1.1. The Climate Data 54
3.1.2. Indoor Environment Conditions 55
3.1.3. Measurement Setup 56
3.1.4. On-site Measurements 58
3.2. CASE A: Energy Performance Analyses 66
3.2.1. Energy Simulation Model 66
3.2.1.1. Calibration of the OpenStudio Model 68
3.2.1.2. Building Performance Assessment 71
3.2.2. Pre-Processing 72
3.2.3. Simulations 74
3.3. CASES B&C: CFD Model 75
3.3.1. Grid Generation 78

3.3.2. Governing Equations 80
3.3.3. CFD Modeling 82
3.3.3.1. Case B: Thermal Stratification 82
3.3.3.2. Case C: Indoor Ventilation 85

CHAPTER 4. RESULTS 87
4.1. Experimental Measurement Results 87
4.2. Numerical Analysis Results 90
4.2.1. CASE A: Energy Simulation Results 90
4.2.2. CASES B&C: CFD Analyses 94
4.2.2.1. Model Validation 94
4.2.2.2. CASE B: Thermal Stratification 97
4.2.2.3. CASE C: Indoor Ventilation 106

CHAPTER 5. DISCUSSIONS AND CONCLUSION 118
5.1. Discussions 118
5.2. Conclusion 120

REFERENCES 122

APPENDICES
APPENDIX A 132
APPENDIX B 138
APPENDIX C 141
APPENDIX D 150
APPENDIX E 159

LIST OF FIGURES

Figure **Page**

Figure 1.1. Global final energy consumption by sectors 1

Figure 1.2. The general framework of thesis 7

Figure 2.1. Effect of varying roof insulation thickness while maintaining wall insulation 20

Figure 2.2. Effect of varying wall insulation thickness while maintaining roof insulation 20

Figure 2.3. Annual energy consumption with various glazing systems glass..... 21

Figure 2.4. SRCs for the most influential parameters regression 22

Figure 2.5. Differences in energy usage and emissions among various types of (a) warehouses and (b) equipment..... 23

Figure 2.6. Contours of temperature plotted on slices through the warehouse domain for the fan-off case (left) and fan-on case (right). Apex heights of (a) 12.5m, (b) 15.0m, (c) 17.5m and (d) 20.0m. The outside temperature is 4°C..... 26

Figure 2.7. Graphs illustrating the vertical fluctuation of monthly average temperatures in the four warehouses 27

Figure 2.8. Evaluation of the thermal stratification between the aboveground warehouse (a) without air conditioning and (b) with air conditioning..... 28

Figure 2.9. Temperature profile comparison between the measurements and the simulation results. (a) for L1 and (b) for L2 of the QT warehouse, and (c), (d) (e) and (f) are for L1, L2, L3, and L4 for the warehouse 30

Figure 2.10. Typical air-conditioning systems in large space buildings: (a) entire space air-conditioning system with MV, (b) stratified air-conditioning system with MV, (c) occupant zone air-conditioning system with DV, and (d) occupant zone air-conditioning system with RF and DV..... 31

Figure 2.11. Natural ventilation design scheme 1..... 34

Figure 2.12. Natural ventilation design scheme 2..... 35

Figure 2.13. Natural ventilation design scheme 3..... 36

Figure **Page**

Figure 2.14. Cross-section results left is the temperature, and velocity is the right. The cases are, from top to bottom: (1) winter case mixing, (2) summer case mixing, (3) winter case displacement, and (4) summer case displacement 37
Figure 2.15. Distributions of air velocity, pressure, and temperature 39
Figure 2.16. Hybrid ventilation strategy (Karava et al., 2012) 40
Figure 2.17. The mixed mode/hybrid cooling control algorithm for occupied (left) and unoccupied periods (right) 41
Figure 2.18. Schematic diagrams of the two warehouses 42
Figure 2.19. Schematic diagram of the MG stadium. The fresh air duct system has been marked in green 43
Figure 2.20. Schematic diagrams of two warehouses 43
Figure 2.21. Velocity streamlines distributions at the axial center plane of the computational model 44
Figure 2.22. First ventilation scenario (three AHUs, one for each area) of the warehouse 45
Figure 2.23. Second ventilation scenario (one AHU for the central and other areas) of the warehouse 46
Figure 2.24. Configurations of air supplying system (a) and the position of vents and slabs at the local working zone (b) 46
Figure 2.25. Contours of mean air temperature at the vertical (y –z) plane of (x = 30 m) within the local cooling zone with six different supplying velocities 47
Figure 2.26. Model of the simplified building: (a) mixing ventilation subtype (MV) and (b) displacement ventilation/radiant floor subtype (DV or RF + DV) 48
Figure 2.27. Air-volume balance in the railway station: (a) winter and (b) summer 48
Figure 2.28. Temperature and velocity contours (cross-sectional planes) (X. Liu et al., 2020) 49
Figure 3.1. The framework of research methodology 51
Figure 3.2. The location of the case study 53
Figure 3.3. The tobacco warehouse with surrounding buildings 53
Figure 3.4. Storage of tobacco bales inside the warehouse 56

Figure **Page**

Figure 3.5. Location of the selected building 57
Figure 3.6. The data logger, Green Eye – Desktop Environmental Monitor 57
Figure 3.7. Installation of the data loggers for field measurements 58
Figure 3.8. Inside temperature measured in July 2020 59
Figure 3.9. Inside temperature measured in August 2020 60
Figure 3.10. Inside temperature measured in January 2021 61
Figure 3.11. Inside temperature measured in February 2021 62
Figure 3.12. Inside temperature measured in March 2021 62
Figure 3.13. Relative humidity ratios measured between 2020 June and 2021 October 64
Figure 3.14. CO_2 concentrations measured between 2020 June and 2021 October 65
Figure 3.15. Three-dimensional OpenStudio model of the case building 66
Figure 3.16. Schematic plan (up) and section (down) of the storage zones 67
Figure 3.17. The usage of air walls for thermal stratification modeling 68
Figure 3.18. Visualization of the project simulation process 71
Figure 3.19. The calculation domain 76
Figure 3.20. Side view of the meshing from the three-dimensional model 79
Figure 3.21. Partial view of the generated mesh from model 79
Figure 3.22. CFD model for thermal stratification studies 83
Figure 3.23. Existing and proposed fan locations 86
Figure 4.1. Yearly measured temperature data 88
Figure 4.2. The most influential factors for annual heating consumption 91
Figure 4.3. The most influential factors for annual cooling consumption 92
Figure 4.4. The most influential factors for operational CO_2 emissions 93
Figure 4.5. Comparison between experimental and CFD temperature results 95
Figure 4.6. Location of the planes in the CFD model 97
Figure 4.7. Curves of the vertical stratification of the monthly average temperatures from the fall to spring period 98
Figure 4.8. Curves of the vertical stratification of the monthly average temperatures for the summer period 99
Figure 4.9. Velocity contours (0-0.8 m/s) of floor heating scenarios for (from left to right) January, February, and March 102

Figure **Page**

Figure 4.10. Velocity contours (0-0.5 m/s) of ceiling cooling scenarios for (from left to right) July, August, and September 103
Figure 4.11. Vertical temperature gradient comparison among various months: (a) the coldest (floor heating) and (b) the warmest months (ceiling-mounted cooling) 104
Figure 4.12. Current case fan scenarios; a) both at full capacity 12 m/s, b) both fans at 8 m/s, c) fan 1 at 12 m/s and fan 2 at 6 m/s 107
Figure 4.13. Velocity contours of the current case fan scenarios; a) both at full capacity 12 m/s, b) both fans at 8 m/s, c) fan 1 at 12 m/s and fan 2 at 6 m/s (Planes are 1,2 and 3; from top to bottom) 108
Figure 4.14. Velocity streamlines for the cases with additional four fans: 110
Figure 4.15. UDF for calculating the mean AoA 112
Figure 4.16. AoA at the current case fan scenarios; a) Case 1, b) Case 2, c) Case 3 .. 113
Figure 4.17. AoA at the cases with additional four fans; a) Case 4, b) Case 5 113
Figure 4.18. Spatial averaged mean AoA distribution within the planes along the z-direction 114
Figure A.1. Inside temperature measured in June 2020 132
Figure A.2. Inside temperature measured in September 2020 132
Figure A.3. Inside temperature measured in October 2020 133
Figure A.4. Inside temperature measured in November 2020 133
Figure A.5. Inside temperature measured in December 2020 134
Figure A.6. Inside temperature measured in April 2021 134
Figure A.7. Inside temperature measured in May 2021 135
Figure A.8. Inside temperature measured in June 2021 135
Figure A.9. Inside temperature measured in July 2021 136
Figure A.10. Inside temperature measured in August 2021 136
Figure A.11. Inside temperature measured in September 2021 137
Figure A.12. Inside temperature measured in October 2021 137
Figure B.1. Inside temperature values of 2020 and 2021 from the H1 level 138
Figure B.2. Inside temperature values of 2020 and 2021 from the H2 level 138
Figure B.3. Inside temperature values of 2020 and 2021 from the H3 level 139
Figure B.4. Inside temperature values of 2020 and 2021 from the H4 level 139
Figure B.5. Inside temperature values of 2020 and 2021 from the H5 level 140

Figure **Page**

Figure C.1. CO_2 concentration values in June 2020 141
Figure C.2. CO_2 concentration values in July 2020 141
Figure C.3. CO_2 concentration values in August 2020 142
Figure C.4. CO_2 concentration values in September 2020 142
Figure C.5. CO_2 concentration values in October 2020 143
Figure C.6. CO_2 concentration values in November 2020 143
Figure C.7. CO_2 concentration values in December 2020 144
Figure C.8. CO_2 concentration values in January 2021 144
Figure C.9. CO_2 concentration values in February 2021 145
Figure C.10. CO_2 concentration values in March 2021 145
Figure C.11. CO_2 concentration values in April 2021 146
Figure C.12. CO_2 concentration values in May 2021 146
Figure C.13. CO_2 concentration values in June 2021 147
Figure C.14. CO_2 concentration values in July 2021 147
Figure C.15. CO_2 concentration values in August 2021 148
Figure C.16. CO_2 concentration values in September 2021 148
Figure C.17. CO_2 concentration values in October 2021 149
Figure D.1. Relative humidity values in June 2020 150
Figure D.2. Relative humidity values in July 2020 150
Figure D.3. Relative humidity values in August 2020 151
Figure D.4. Relative humidity values in September 2020 151
Figure D.5. Relative humidity values in October 2020 152
Figure D.6. Relative humidity values in November 2020 152
Figure D.7. Relative humidity values in December 2020 153
Figure D.8. Relative humidity values in January 2021 153
Figure D.9. Relative humidity values in February 2021 154
Figure D.10. Relative humidity values in March 2021 154
Figure D.11. Relative humidity values in April 2021 155
Figure D.12. Relative humidity values in May 2021 155
Figure D.13. Relative humidity values in June 2021 156
Figure D.14. Relative humidity values in July 2021 156
Figure D.15. Relative humidity values in August 2021 157
Figure D.16. Relative humidity values in September 2021 157

Figure **Page**

Figure D.17. Relative humidity values in October 2021 158
Figure E.1. Velocity contours on planes (a), (b), (c), and (d) for the current case fan scenarios; Case 1 (left), Case 2 (middle), Case 3 (right)..... 159
Figure E.2. AoA distribution within the 2 m plane along the z direction; a) Case 1, b) Case 2, c) Case 3 160
Figure E.3. AoA distribution within the 4 m plane along the z direction; a) Case 1, b) Case 2, c) Case 3 160
Figure E.4. AoA distribution within the 6 m plane along the z direction; a) Case 1, b) Case 2, c) Case 3 161
Figure E.5. AoA distribution within the 8 m plane along the z direction; a) Case 1, b) Case 2, c) Case 3 161
Figure E.6. AoA distribution within the 10 m plane along the z direction; a) Case 1, b) Case 2, c) Case 3 162
Figure E.7. AoA distribution within the 12 m plane along the z direction; a) Case 1, b) Case 2, c) Case 3 162
Figure E.8. AoA distribution within the 2 m plane along the z direction: 163
Figure E.9. AoA distribution within the 4 m plane along the z direction: 163
Figure E.10. AoA distribution within the 6 m plane along the z direction:..... 164
Figure E.11. AoA distribution within the 8 m plane along the z direction:..... 164
Figure E.12. AoA distribution within the 10 m plane along the z direction:..... 165
Figure E.13. AoA distribution within the 12 m plane along the z direction:..... 165

LIST OF TABLES

Table **Page**

Table 2.1. City-based tobacco production in Turkey in 2022 and 2021 11

Table 2.2. The general framework of the previous literature 17

Table 3.1. Statistical properties of inside temperature, relative humidity, and CO_2 concentrations inside the warehouse 63

Table 3.2. Calibration results of the OpenStudio Simulations 70

Table 3.3. Lower and upper boundaries for the architectural design parameters were investigated. 73

Table 3.4. Heat transfer coefficient calculations for roof, floor, and exterior walls 77

Table 3.5. Outside and ground temperatures for selected periods 78

Table 3.6. Monthly heat generation rates for the roof, north and east directions 84

Table 4.1. Measured temperature differences between 2020 June-December 89

Table 4.2. Measured temperature differences between 2021 January-October 89

Table 4.3. Validation results of the CFD model 96

Table 4.4. Results and coefficients of the linear regression model: R^2, standard error, and the temperature difference (ΔT) 100

Table 4.5. Monthly consumption values for thermal conditioning 105

Table 4.6. Cases used for the simulations with various fan arrangements. 110

Table 4.7. The mean AoA, air changes per hour, and air change effectiveness for all scenarios 116

CHAPTER 1

INTRODUCTION

Since, the impacts of climate change are noticeable worldwide, creating sustainable and energy-efficient solutions using advanced technological applications has been the current issue. At the same time, these solutions created the need for sufficient abilities to design with climate.

Architecture does not only aim to protect from severe climatic conditions but also to reduce the need for energy, as well as the impacts on the environment. Therefore, the call for energy-efficient building design is growing because the energy consumed by buildings is in significant amounts. For instance, it is shown in Figure 1.1 that, the construction industry is responsible for 30% of final energy consumption and 36% of global final energy consumption when combined with buildings construction sectors (Masanet, 2017).

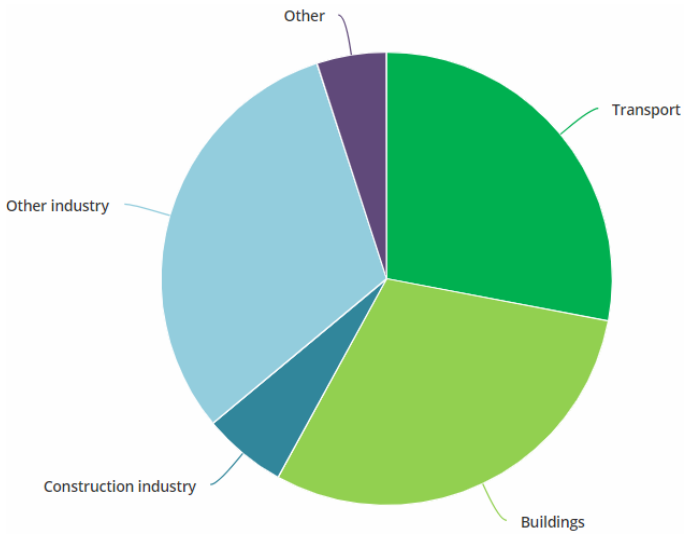

Figure 1.1. Global final energy consumption by sectors.
(Source: Masanet, 2017)

At that point, one of the most important concerns in architectural design is about the reaction of architecture to climatic elements, as well as the contribution of

climatological factors to architectural design. Combination of the wind, temperature, relative humidity, and radiation are some of the components which can provide both user comfort and efficiencies in energy and environmental performance of the buildings.

1.1. Problem Definition

The industrial sector accounted for 38% of global final energy consumption in 2021 and is projected to grow at an average rate of 3% per year. However, industrial emissions have increased by over 70% since 2000 due to rising global demand for industrial goods and only modest increases in energy efficiency (Conti & Holtberg, 2022). The latest studies assess that logistical supply chains cause about 10% of global CO_2 emissions (Dhooma & Baker, 2012). The economic and environmental effects of warehouse management have drawn more attention from companies in recent years.

In sectors such as storage, maintaining control over air temperature is essential since some stored products may easily be affected or influenced. Temperature and relative humidity are the most significant environmental factors affecting the physical quality of goods (Nunes et al., 2009). Deficiencies in the storage environment can cause undesired physicochemical changes and a loss of quality in stored products (H. Liu et al., 2011; Park et al., 2012; Shi et al., 2013; J. Wang et al., 2017). Besides, inadequate indoor conditions in industries can lead to extensive expenses for administration and wasted products (Rohdin & Moshfegh, 2011).

In terms of commercial buildings, storage structures are among the buildings that should be examined priorly in terms of design criteria, providing the desired indoor conditions and energy consumption characteristics. Special attention is required to keep the storage conditions of the products at certain intervals and to provide a stable preservation environment (Rushton et al., 2017). Since the storage conditions required are various, storage structures are divided into different groups. Mainly, agricultural, and industrial buildings require unique specifications such as height, temperature, or humidity needs. Depending on the product, every item has a different indoor temperature range. While agricultural buildings may differ in terms of livestock or agricultural product storage, industrial buildings have standard terms when referring to temperature ranges, namely ambient, air-conditioned, refrigerated, and cold/frozen.

Within the context of the logistics sector, warehouses play a significant role in consuming a growing portion of energy and have the potential to be designed with greater efficiency. Their contribution to greenhouse gas (GHG) emissions and subsequent impact on global warming cannot be disputed. Specifically, warehouse operations are responsible for approximately 11% of the logistics industry's worldwide GHG emissions (Doherty & Hoyle, 2009).

Energy-intensive practices are observed in air-conditioned, refrigerated, and cold/frozen warehouses, where significant amounts of energy are consumed to maintain optimal internal air conditions for climate-sensitive items. Even ambient warehouses require temperature control mechanisms to ensure a dry environment despite temperature fluctuations, especially when storing high-value or perishable goods. Thus, careful consideration needs to be given to internal air conditioning in both climate-controlled and ambient warehouses.

Warehousing companies are increasingly recognizing the need to consider the environmental and social impacts of their operations, extending their focus beyond purely operational and economic objectives. These sustainability factors have often been neglected as important indicators of performance by many companies. Governments and businesses worldwide are now placing greater importance on environmental awareness. For instance, certain European countries have established certain objectives for improving energy efficiency. In Germany, it is targeted to reduce primary energy consumption by 20% for private houses, industrial corporations, and local companies by 2020 compared to 2008 (Federal Ministry for Economic Affairs and Energy, 2016). Similarly, the Chinese government is actively promoting climate change policies by allocating additional research finances to this subject (Kitagawa, 2017). Therefore, there has been a growing focus on green and sustainable practices in warehousing, leading to numerous research studies on management concepts, technologies, and equipment aimed at reducing energy demands and overall emissions in warehouses.

Accordingly, the significant criteria for better-performing warehouses and the focus have been given on the thermal conditions, indoor environment conditions, and energy performance as well as possible design solutions for more sensitive architectural and energy-efficient strategies. Finally, how the proposed thesis will be structured by indicating the objectives and research questions, research and methodological approaches, and potential contributions of the content of the thesis to the discipline are aimed to be emphasized.

1.2. Aim and Scope of the Thesis

This thesis mainly aims to provide investigations for energy-efficient improvement of indoor conditions in large-scale warehouses containing hygroscopic materials. Assessing the sensitivities of design parameters on building energy performance for underlining the most effective parameters for decreasing required energy consumption as well as clarifying the possible ventilation solutions for optimal indoor environment for stored tobacco in hot humid climates are the primary objectives of the study.

The objectives to accomplish the aim of the thesis are stated as follows:

- Preventing the deteriorating effects of excessive temperature increases in summer, sudden temperature drops in winter, and fluctuations in storage volumes in hot humid climates on hygroscopic materials.
- Development of proposals in the digital environment to reduce the heat transfer to the warehouse to prevent excessive temperature rise.
- Determination of possible risky storage areas in the warehouse due to the temperature stratification experienced throughout the year and aging of the air depending on the storage arrangement.
- Analysing natural and mechanical ventilation possibilities in the digital environment to prevent excessive temperature rise and achieve the desired indoor environment conditions.
- Development of an energy-efficient solution for the cooling and ventilation of the entire space that can be used when necessary to keep the warehouse at the desired temperature and humidity.
- To minimize the risk of deterioration in the storage of tobacco which is a very important and valuable product for the country's economy, proposals for modifications in architectural elements as well as hybrid ventilation solutions are aimed at the improvement of existing warehouses.

The scientific and technological contribution of this project can be explained under the following headings:

- A holistic approach will be taken not only by presenting architectural solutions but also by studying hybrid ventilation methods so that energy-efficient solutions will be produced while improving indoor environment conditions.

- While indoor conditions in tobacco warehouses are tried to be controlled only based on experiences until now, they can be optimized using numerical data.
- Being an energy-efficient and user-friendly system approach, it can provide an increase in building performance.
- Ability to guide professionals for performance improvements on existing warehouses as well as numerical information for future warehouse designs.

1.3. Outline of the Thesis

This section provides an academic explanation of the outline of the thesis that focuses on the analysis of tobacco warehouses and their air flow dynamics. It comprises five chapters that delve into the problem definition, aims and scope of the research, and the detailed outline of the thesis. Additionally, it explores previous work related to tobacco warehouses, air flow, and thermal analysis in such facilities, as well as the utilization of energy and ventilation approaches. The subsequent chapters examine a specific case study, the climate data involved, measurement setup, on-site measurements, energy simulation models, CFD modeling, thermal stratification analysis, and the results obtained from energy simulations and CFD analyses.

The first chapter begins by defining the problem at hand, which centers around the analysis of tobacco warehouses. The aim and scope of the thesis are outlined, emphasizing the specific objectives and boundaries of the research. The chapter sets the foundation for the subsequent chapters, providing a clear understanding of the purpose and goals of the study.

The second chapter explores the characteristics and features of tobacco warehouses. It examines the unique aspects of these facilities, considering factors such as size, design, indoor environment, and specific requirements for tobacco storage. Furthermore, a comprehensive review of previous work is conducted, encompassing relevant research studies, academic literature, and industry reports about tobacco warehouses. This review serves to provide a comprehensive understanding of the existing knowledge and gaps in the field. It also focuses on the analysis of air flow and thermal characteristics within tobacco warehouses. A detailed examination of thermal stratification phenomena that occur in such facilities is provided. The chapter then delves into energy-oriented approaches, exploring strategies and methods for optimizing energy

efficiency within tobacco warehouses. Moreover, ventilation approaches specific to warehouses are discussed, highlighting various techniques and technologies employed to enhance indoor environment conditions.

The third chapter presents a specific case study within the context of tobacco warehouses. It describes the climate data used for the study and outlines the measurement setup to collect relevant data. The chapter further introduces energy simulation models, specifically focusing on the OpenStudio model to assess the building's performance. Additionally, computational fluid dynamics (CFD) modeling techniques are employed to analyze air flow patterns, governing equations, grid generation, boundary conditions, and validation of the CFD model. The chapter concludes with a presentation of the simulation results obtained from both energy simulation and CFD analyses.

The fourth chapter explains the results collected from each case studied. Initially, field measurement results are presented that are collected and gathered from the site. Then, energy simulation results are given, and conclusions collected from the analysis of Case A are presented. Finally, CFD analysis results in Cases B&C are explained under two headings as thermal stratification and indoor ventilation.

The final chapter includes a summary of the concluding remarks. The impacts of design and ventilation strategies are presented for future studies. Several significant building design parameters, and guidance for improving natural, mechanical, and hybrid ventilation systems are laid out to provide a foundation for generalized indoor environment conditions and optimal storage conditions that can be applied to the built environments and early design processes in hot-humid climates.

Overall, the thesis targets to provide an academic explanation of the outline of a thesis that examines tobacco warehouses and their air flow dynamics. It covers various aspects, including problem definition, aims and scope of the research, review of previous work, air flow and thermal analysis, a case study, measurement setup, energy simulation, and CFD modeling. The objective of this thesis is to enhance the existing understanding and insights within the realm of tobacco warehouses by investigating their unique characteristics and providing insights into improving energy efficiency and ventilation strategies.

The general framework of the thesis can be seen in Figure 1.2. The first column in Figure 1.2 contains the main chapter titles in this thesis along with chapter numbers. Subsections are indicated in the other two columns. Different cases (CASE A, B, and C specified in Figure 1.2) were studied in terms of the basic thermal and flow problems

determined in the selected study area to analyze the thermal performance and indoor conditions of tobacco warehouses, and to develop solutions. In this context, firstly, the measurements inside and outside the studied warehouse were evaluated. The determined cases were carried out on energy simulation analyses, temperature stratification, and indoor ventilation (under the title of CFD analyses), respectively.

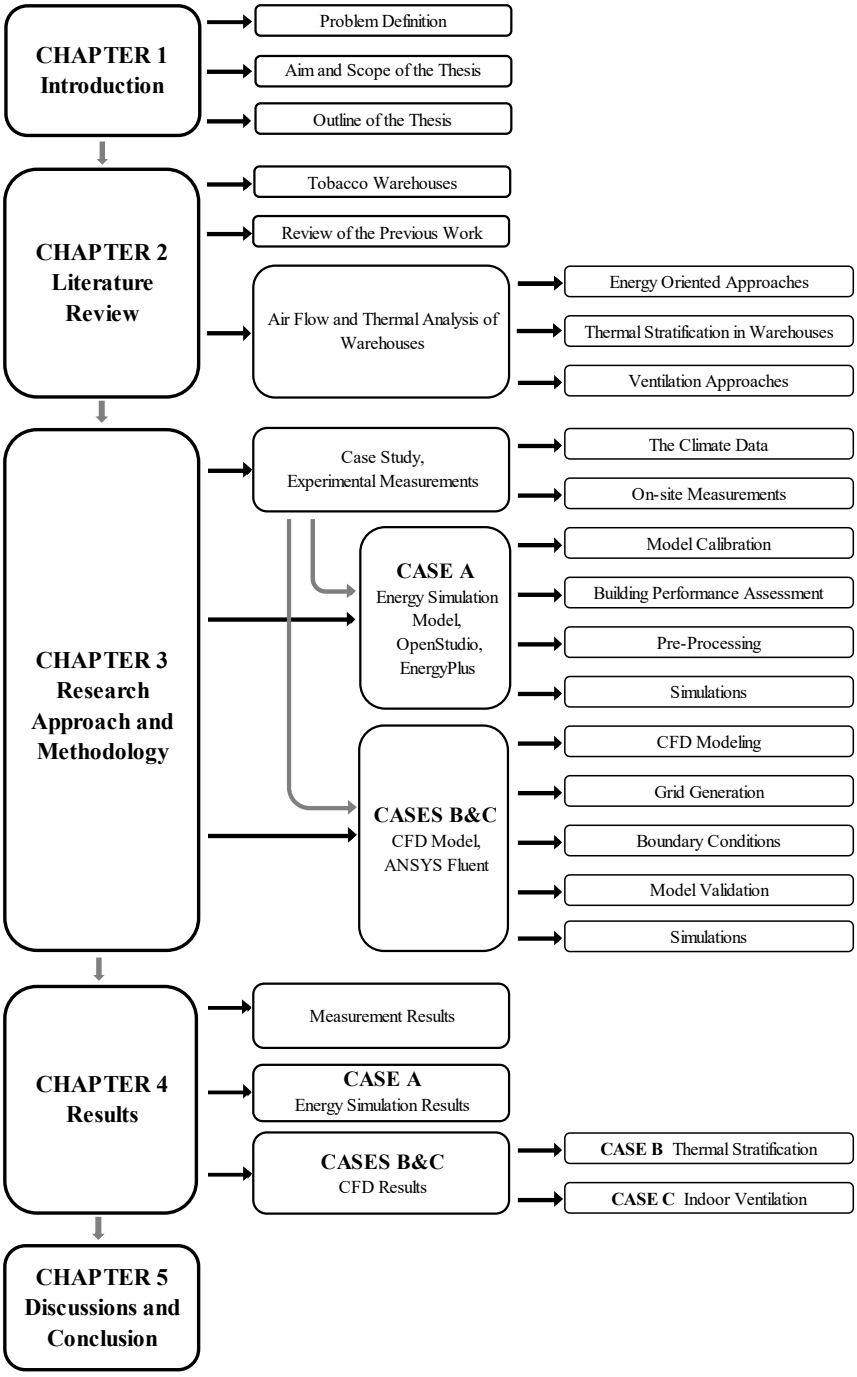

Figure 1.2. The general framework of thesis

CHAPTER 2

LITERATURE REVIEW

Rapid increases in energy demands, especially in cooling loads, and GHG emissions occur with the temperature increases caused by global warming and the increases in people's expectation of thermal comfort within the built environment. Therefore, the significance of providing thermally comfortable and user-friendly environments for buildings as well as the need for designers to reconsider the entire life cycle of buildings has gained more importance recently. Additionally, as a broader field, design with climate elements has been prioritized by considering global climatic problems and is still taking particular attention of architects and engineers with many points to be explored, especially for subsequent improvements in early design stages of buildings or retrofits in existing buildings (Krautheim M., Pasel R, 2014).

Consequently, the impact of architectural design has increased in terms of both its physical properties and climatic issues. The growing awareness of climatic concerns related to design processes could also enhance the local relevancy of structures as well as create more case-specific and sophisticated architectural solutions. Accordingly, the buildings in recent research are mostly divided into two main categories commercial and residential. In terms of commercial buildings, storage structures are among the buildings that should be examined based on design criteria, optimal indoor thermal conditions, and energy consumption characteristics. This is because special care needs to be taken to maintain the storage conditions of the products to certain standards and to ensure a stable protection environment, which has great economic value.

Warehouses play a critical role as essential nodes within supply chains across various industries. The rapid expansion of the e-trade sector and the escalating demand for mass customization have significantly amplified the need for store facilities and structures (Angel et al., 2006). As integral components of logistics operations, warehouses contribute to the emission of GHG, thereby exerting a substantial impact on global warming.

More precisely, warehousing activities are responsible for approximately 11% of the total GHG emissions generated by the logistics sector at a global level (Doherty &

Hoyle, 2009). Consequently, organizations are extending their strategic focus beyond conventional operational and economic objectives to encompass broader environmental and social considerations associated with warehousing practices. These sustainability aspects have often been disregarded by companies (Elkington, 1998). However, there is a growing acknowledgment among governments and corporations to address these issues by fostering intensified environmental consciousness and implementing significant measures.

In line with this global trend, there is a growing emphasis on adopting green and sustainable practices within warehousing operations. This heightened attention has resulted in the emergence of numerous research findings exploring management concepts, technologies, and equipment aimed at reducing both the carbon footprint and energy requirements of warehouses (Trust, 2007; Wiedmann & Minx, 2008).

2.1. Tobacco Warehouses

When considering commercial buildings, storage structures are among the others that should be examined first in terms of design criteria and providing the desired indoor conditions as well as energy and environmental efficiency. Particular emphasis should be given to keeping the storage conditions of the products at certain intervals and providing a stable preservation environment, and this has great economic value (Rushton et al., 2017). Although cold storage is fully equipped with conditioned ventilation systems, changing climatic conditions due to global warming reveal the need for mechanical air conditioning in raw material warehouses where natural ventilation is emphasized, while the importance of hybrid ventilation is increasing gradually (Calegari et al., 2016; Shiao et al., 2011).

Natural, mechanical, or hybrid ventilation methods are implemented for conditioning the warehouses. Natural ventilation is the most popular method since its possibility of low maintenance and first investment cost. However, increasing temperature trends because of global warming also affected the indoor air conditions of warehouses, so additional systems are started to be required for optimal indoor conditions. Accordingly, the usage of hybrid ventilation systems has increased over the years. Nevertheless, current studies on the use of hybrid ventilation in storage structures and the development of numerical approaches in this regard are found to be quite limited (Calegari et al., 2016; Delsante & Vik, 2000; Heiselberg, 2002; Y. Li & Heiselberg,

2003). For this reason, more attention needs to be paid to the design and operation of functional and energy-efficient approaches. At this point, there is a need to analyze mixed systems in which natural and mechanical ventilation work together so that optimal indoor environment settings can be provided as well as keeping the conditions constant.

Since the storage conditions required by each product are different, storage structures are also divided into different groups. For example, studies on heat and flow analyses in livestock and cold storage (Cook & Sproul, 2011; W. Li, 2016; Liberati & Zappavigna, 2010; Rojano et al., 2018) show that systematic information gathered from calculations and field experiments have a great impact on energy-oriented approaches. It also influences the economy, and it has an economic contribution potential by reducing the energy expenditure of the facilities while preserving product quality. At that point, when the evaluations of the building design parameters and building energy performance characteristics are examined, it is seen that the indoor environment conditions (interior air exchange coefficient, indoor temperature, humidity, and CO_2 values) are the most significant parameters in the buildings where hygroscopic products (tea, coffee, cocoa, tobacco, etc.) are stored. There are several problems to be considered in terms of these types of buildings. Vertical temperature gradients are critical for stored products at different levels. To solve these problems, ventilation solutions gain importance for increasing indoor environmental conditions. Various ventilation approaches are implemented in warehouses and the improvements should also be energy and environmentally friendly.

Considering the need for research focusing on improving the storage conditions of hygroscopic products, especially in Turkey, tobacco, which is among the main export items, has a long-standing priority in the country's economy as one of the most important products of the agricultural sector. With the beginning of tobacco farming extending to the Ottoman period, investments and breakthroughs made in the development of tobacco farming in the country showed a great increase in the first years of the Republic. Since 1940, tobacco production has been included in the scope of support programs (Ataseven, 2005).

Based on the data, in 2017, Turkey has been the eighth country in the overall ranking in terms of tobacco planting area, and the fifth country in terms of tobacco production (FAOSTAT, 2022). Due to its economic size and the fact that it is an agricultural product that has been in the lives of the people of the country for a very long

time, it is seen that one of the prominent raw materials is tobacco when focusing on the improvement of storage conditions.

Except for Central Anatolia, almost all climatic regions of Turkey are suitable for tobacco production, which has become a traditional agricultural branch (SPO, 2007). Table 2.1. shows the top ten cities with the highest tobacco production in 2021 and 2022 in Turkey. The grey-colored three cities are the ones with more than 10000 tons of produced tobacco.

Table 2.1. City-based tobacco production in Turkey in 2022 and 2021.
(Source: TUIK, 2023)

Ranking	2022		2021	
	City	Production (tons)	City	Production (tons)
1	Adıyaman	19968	Adıyaman	17910
2	Denizli	17453	Denizli	12013
3	Manisa	11353	Manisa	11266
4	Uşak	9868	Batman	5990
5	Samsun	6025	Samsun	4780
6	Hatay	2795	Uşak	4494
7	Batman	2571	Aydın	2642
8	Aydın	2294	Malatya	2550
9	Malatya	2236	Hatay	1640
10	Balıkesir	1605	Tokat	1575

Existing studies on animal husbandry and cold storage (Cook & Sproul, 2011; W. Li, 2016; Liberati & Zappavigna, 2010; Rojano et al., 2018) stressed that systematic information collected from the calculations and field experiments have major impacts on energy-oriented approaches and they have potentials to contribute economically by reducing energy expenditure and maintaining product quality of the facilities.

However, many storage facilities in the country operate without any HVAC systems. Existing studies focusing on agricultural product storage in Turkey point out that ideal conditions are ventilated, cool temperatures with high to moderate humidity and they should be stabilized to avoid deteriorations in the crop (Karaman et al., 2009; Kibar, 2012; Kibar et al., 2015).

Due to the possibility of the product waiting for months in tobacco storage, the risks posed by inadequate storage conditions on the preservation of tobacco without losing its properties are important problems that cannot be ignored. In this direction, it can cause serious economic and large-scale losses. Besides, experiments by Wang et al. (Wang et al., 2017) indicated that temperature and moisture content have interactive effects on carcinogenic chemicals during burley tobacco storage.

Since strict indoor environment conditions like cold storage are not imposed for hygroscopic products, only non-systematic interventions in the regulation of storage conditions are applied. They are often insufficient and cause large increases in storage, cost, and energy. For this reason, instead of ensuring the continuity of the process by producing daily palliative solutions to eliminating the problems that arise in the warehouses of tobacco and similar indoor conditions; considering the possible economic losses, it is of great importance to develop active and passive air conditioning systems to store similar hygroscopic products, especially tobacco, under the desired ideal conditions, which can contribute to the storage sector.

The existing literature is examined and although there are studies on the storage of substances that need different indoor conditioning, tobacco, etc., which is processed and prepared for export, publications examining the storage conditions of hygroscopic products and their thermodynamic changes during the waiting period and suggesting an experimentally studied ventilation system on this subject have not become widespread. There are deficiencies in studies within the national and international literature, focusing on providing improvement proposals or methodical approaches for tobacco storage in terms of active and passive air conditioning and indoor environment conditions. Besides, there is a need for research focusing on developing more efficient and effective solutions, including all processes starting from tobacco planting to consumption of the product, especially on improving the storage conditions, since tobacco is an agricultural product of this economic size and has been densely occupied in the life of the people of the country for a long time.

Nevertheless, there are important criteria that require particular attention when specifically examining tobacco and its storage. The first of these is the deterioration effects that seasonal changes may cause on stored tobacco, and this is of much greater importance, especially in regions with extreme temperature increases. At this point, some criteria should be taken into consideration by professionals. Higher humidity and temperature will lead to excessive annealing, discoloration, and mildew (TEA, 2017).

Therefore, the water vapor ratio and temperature of the environment constitute the priority criteria. The low rate of moisture in the air slows down and delays the ripening of tobacco and their physical properties of them may deteriorate because of excessive drying. If the temperature value is lower or higher than the optimal level, the environment must be kept at an appropriate level with more attention to the humidity to protect the tobacco.

To ensure a positive flow of tobacco in this period, the optimal annealing rate of tobacco should be around 13-14%. For obtaining this required amount of tobacco, the optimal relative humidity of the environment is approximately between 50-65% and the temperature is around 21-25 ° C (Jang et al., 2007; Shi et al., 2013). In fact, on rainy days of spring and autumn, humidity and temperature may increase. These periods may require more careful work for protection and maintenance, as the conditions can initiate excessive annealing, discoloration, and mildew in tobacco (SPO, 2007).

The research focusing on tobacco warehouses in terms of providing optimal indoor conditions and energy consumption characteristics is quite inadequate when studies about building design parameters and building energy performance characteristics are examined. The focus should also be given to the assessment of the internal environment of stored products, mainly considering the aspects of (1) the heat exchanged through ventilation; (2) stabilizing the indoor temperature and relative humidity which changes due to chemical reactions of stored products; and (3) the intents to decrease the energy demand. Moreover, due to the significant share of the tobacco industry in the economy, specifically for tobacco storage, more attention should be given to the design and maintenance of functional and energy-efficient buildings for practitioners.

In the study, which focuses on proposing a comprehensive investigation by using natural and mechanical air conditioning together, it is foreseen that field studies should be carried out on a tobacco warehouse, representing all storage structures where hybrid ventilation can be applied. Another important problem is the warehousing conditions in the Mediterranean climate regions, where the greatest effects of global warming are seen, mostly affected by the increases in the cooling load, and where the summers are hot.

2.2. Review of the Previous Work

Storage buildings play a crucial role in modern logistics sectors, providing efficient storage and distribution of goods. As these facilities continue to grow in number and size, it becomes imperative to analyze and understand the various factors influencing their design, operation, and environmental impact. Accordingly, the current literature explores four key topics related to warehouses: design decisions, energy and environmental impacts, thermal stratification, and ventilation strategies. By examining these topics, gaining valuable insights into optimizing warehouse performance and minimizing their ecological footprint is possible.

To examine the topics of energy and environmental impacts, thermal stratification, ventilation strategies, and design decisions in warehouses, a range of methodologies are employed. These methodologies enable researchers and professionals to gain insights and make informed decisions regarding warehouse design and operation.

According to existing studies, thermal stratification refers to the layering of air with different temperatures within a warehouse space. This phenomenon occurs due to variations in heat sources, inadequate insulation, and poor ventilation. Uncontrolled thermal stratification can result in temperature imbalances, reduced energy efficiency, and discomfort for workers (Barbaresi et al., 2015; Porras-Amores et al., 2014; Wang & Li, 2017). To address this issue, warehouse designers should incorporate effective insulation techniques, consider heat sources in layout planning, and implement appropriate cooling and ventilation strategies (W. Li, 2016; Rohdin & Moshfegh, 2011).

Warehouses consume significant amounts of energy, contributing to both economic costs and environmental consequences (Cook & Sproul, 2011; Daheng, 2010a; Ezzeldin & Rees, 2013; Liberati & Zappavigna, 2010). Energy consumption primarily arises from lighting, heating, cooling, and material handling systems. Warehouse owners and operators can mitigate these impacts by adopting energy-efficient practices such as installing LED lighting, employing advanced HVAC systems, utilizing natural lighting, and implementing smart controls (Dhooma & Baker, 2012; Fichtinger et al., 2015; Karava et al., 2012; Pudleiner & Colton, 2015; Schulze & Eicker, 2013). Additionally, renewable energy sources like solar panels and wind turbines can be integrated into warehouse design to reduce dependence on fossil fuels and decrease GHG emissions (Accorsi et al.,

2017; Huang & Gurney, 2016; Lewczuk et al., 2021; Rai et al., 2011; Ries et al., 2017; Seifhashemi et al., 2018).

Warehouse design decisions have a significant impact on operational efficiency and environmental sustainability. Optimal warehouse layout, incorporating considerations such as product flow, storage capacity, and ease of material handling, can enhance operational productivity (Accorsi et al., 2017; Liberati & Zappavigna, 2010; Pudleiner & Colton, 2015; Rai et al., 2011; Ries et al., 2017; Rojano et al., 2018). Furthermore, the use of sustainable construction materials, efficient space utilization, and strategic location planning can minimize resource consumption, waste generation, and transportation-related emissions.

Proper ventilation is vital for maintaining a healthy and comfortable indoor environment in warehouses. Ventilation helps remove pollutants, control temperature, and humidity levels, and prevent the buildup of hazardous gases. Natural ventilation systems, such as windows, louvers, and vents, can be employed to maximize airflow and reduce the need for mechanical ventilation (Calegari et al., 2016; X. Liu et al., 2020; Rojano et al., 2018; Spindler & Norford, 2009). Additionally, advanced technologies like heat recovery systems and air circulation fans can improve energy efficiency while ensuring optimal environmental conditions.

On-site measurements play a crucial role in understanding the actual energy consumption, thermal conditions, and ventilation effectiveness within warehouses (Barbaresi et al., 2015; Calegari et al., 2016; Dhooma & Baker, 2012; Estelles, 2018). By collecting real-time data, researchers can identify areas of improvement and validate the performance of implemented strategies. Computational Fluid Dynamics (CFD) models offer a powerful tool for simulating and analyzing airflow patterns, temperature distributions, and pollutant dispersion within warehouse spaces (Ding et al., 2018; Ho et al., 2010; Rohdin & Moshfegh, 2011; Rojano et al., 2018). These models enable researchers to evaluate various ventilation scenarios and optimize the design of ventilation systems.

Energy analysis models, such as building energy simulation software, allow for a comprehensive assessment of energy consumption, identifying areas of inefficiency and suggesting energy-saving measures. Analytical approaches, involving mathematical equations and calculations, aid in evaluating thermal stratification phenomena, determining heat transfer rates, and assessing the thermal comfort of warehouse occupants (Daheng, 2010a; Lewczuk et al., 2021; W. Li, 2016; Liberati & Zappavigna,

2010; Spindler & Norford, 2009). By employing these methodologies, researchers and practitioners can delve deeper into the complex dynamics of warehouses and develop effective strategies to optimize their performance while minimizing their environmental impact.

In the realm of ventilation-oriented research within warehouses, studies have gone beyond analyzing the existing ventilation systems and have focused on proposing innovative solutions to optimize airflow and indoor environment conditions. These research endeavors have explored the implementation of central ventilation systems, which allow for centralized control of air distribution and quality throughout the warehouse space (Ding et al., 2018; Estelles, 2018; Karava et al., 2012; X. Liu et al., 2020; Mei et al., 2018a; Spindler & Norford, 2009). Additionally, various control strategies have been developed to ensure efficient and effective ventilation, such as demand-controlled ventilation (DCV) that adjusts airflow based on occupancy levels or pollutant concentrations (Pudleiner & Colton, 2015; Rojano et al., 2018; Schulze & Eicker, 2013). Furthermore, researchers have explored the implementation of hybrid ventilation systems, which combine natural and mechanical ventilation methods to capitalize on the benefits of both approaches (Calegari et al., 2016; Ezzeldin & Rees, 2013; Karava et al., 2012). These advancements in ventilation-oriented research offer valuable insights and practical recommendations for warehouse designers and operators to improve ventilation effectiveness and create better-performing indoor environments.

Examining the key topics of energy and environmental impacts, thermal stratification, ventilation strategies, and design decisions provides valuable insights into enhancing warehouse performance while minimizing their ecological footprint. By implementing energy-efficient practices, addressing thermal stratification issues, employing proper ventilation strategies, and making informed design decisions, warehouse owners and operators can significantly reduce energy consumption, improve indoor environment conditions, and mitigate environmental impacts. Continued research and innovation in these areas may contribute to the development of sustainable warehouse practices, supporting a greener future for the logistics industry.

The general framework of the current literature mentioned in this chapter is visualized systematically in Table 2.2. The more detailed literature survey focusing on the main problems that occurred in storage spaces, energy-oriented approaches to solve these problems, and various ventilation improvement proposals as well as the deficiencies in the literature are explained comprehensively in the following section.

Table 2.2. The general framework of the previous literature.

Author	Warehouse topic				Methodology				Approach to ventilation			
	Energy/ env. impacts	Thermal stratification	Vent. strategy	Design decisions	On-site meas.	CFD model	Energy analysis model	Analytical	System proposal	Central system	Control strategy	Hybrid vent.
Spindler and Norford (2009)			✓					✓		✓	✓	
Daheng (2010)	✓							✓				
Ho et al (2010)			✓			✓	✓		✓			
Liberati and Zappavigna (2010)	✓			✓	✓			✓				
Cook and Sproul (2011)	✓			✓			✓					
Rai et al (2011)	✓			✓			✓					
Rohdin and Moshfegh (2011)		✓	✓		✓	✓		✓	✓	✓		
Dhooma and Baker (2012)	✓				✓							
Karava et al (2012)	✓				✓					✓		✓
Ezzeldina and Reesb (2013)	✓		✓				✓			✓		✓
Schulze and Eicker (2013)	✓		✓				✓				✓	
Porras-Amores et al (2014)		✓			✓							
Fichtinger et al (2015)	✓		✓				✓	✓				
Pudleiner and Colton (2015)	✓			✓			✓				✓	
Calegari et al (2016)			✓		✓							✓
Huang and Gurney (2016)	✓						✓					
Li (2016)		✓	✓		✓	✓			✓			
Accorsi et al. (2017)	✓			✓				✓				
Ding et al (2017)			✓		✓				✓			
Ries et al. (2017)	✓			✓			✓					
Wang and Li (2017)		✓			✓	✓			✓			
Ding et al (2018)			✓		✓	✓		✓	✓	✓		
Estelles (2018)					✓					✓		
Mei et al (2018)					✓	✓			✓	✓		
Rojano et al (2018)			✓	✓	✓	✓					✓	
Seifhashemi et al. (2018)	✓			✓	✓	✓	✓					
Liu et al (2020)			✓		✓	✓				✓		
Lewczuk et al (2021)	✓							✓				

2.3. Air Flow and Thermal Analysis of Warehouses

Warehouses play a crucial role as pivotal points within supply chains across diverse industries. The continuous expansion of the online retail industry and the rising demand for customized products have resulted in a heightened requirement for warehouse space and infrastructure (Angel et al., 2006). Apart from the prominent factors influencing the energy and environmental attributes of buildings, careful consideration needs to be given to the thermophysical conditions within the storage facilities and the provision of consistent indoor air conditions for the stored goods.

The design of storage buildings should consider, together with the structural, functional, and dimensional aspects, as well as the ventilation conditions aimed at obtaining the best internal environment for product storage. To achieve this purpose, the result that should generally be pursued is the balance between the theoretical requirements and the realizable conditions concerning specific climatic conditions with the added limitation that the building's operation should be economically sustainable. For example, it may be hard to meet the optimal internal climate during the daytime because of the high external temperatures in hot climatic regions. However, it is possible to try to maximize the benefit of the drops in night temperature so that the negative effects of the conditions during the daytime may be minimized. Therefore, the objective for building design should be the optimization of the internal conditions considering the general pattern of the studied environment. Accordingly, improvements in the building design, material selections, and ventilation conditions, as well as the placement of the products within the building should be site-specific and considered carefully.

2.3.1. Energy-Oriented Approaches

Warehouse buildings have a significant impact on energy consumption and the depletion of natural resources throughout their lifespan (Rai et al., 2011). The relationship between energy usage in warehouses and climatic conditions, especially in summer, is crucial, as energy consumption can rise by over 100% during the daytime due to external and internal temperature connections (Huang & Gurney, 2016). Research in this area has addressed several important aspects, including energy reduction, GHG emissions, building design, and optimal material utilization.

Dhooma & Baker (2012) investigated energy consumption in different end-use categories within warehouses. They developed a framework to identify opportunities for energy savings, focusing on four warehouses operating in the same sector. The study revealed significant potential for energy reduction in specific end-use categories, particularly HVAC and lighting.

Furthermore, Colicchia et al. (2013) emphasized the significance of materials installed in warehouse buildings and their impact on GHG emissions. Energy efficiency initiatives aimed at reducing the environmental impact of warehouses often involve adjustments to lighting, heating, air-conditioning, and ventilation systems, particularly in warmer places (Fichtinger et al., 2015). Policies targeting lighting and HVAC systems designed to minimize environmental impacts were also highlighted.

Regarding the optimization of warehouse design to achieve energy efficiency, Daheng (2010) introduced the application of grey relational analysis, a method capable of handling multiple decision-making problems. The research examined eleven quantitative Green Building Evaluation criteria, such as building orientation, roof insulation, and natural ventilation. Additionally, economic and management factors were included to evaluate the overall sustainability. By employing grey relational analysis, the study offered valuable insights into the impact of each factor on energy conservation.

Another study by Cook & Sproul (2011) investigated a retail warehouse building and employed simulation software to assess its energy requirements. Figure 2.1, Figure 2.2, and Figure 2.3. illustrate the annual energy consumption results for roof and wall insulation as well as different glazing systems. The simulation results indicated that lighting was the primary factor in energy consumption. By implementing several variations such as insulation, sawtooth roofs, selective glazing, natural ventilation, lamp replacements, and lighting controls, the simulation has shown a drop in energy demand of up to 73%.

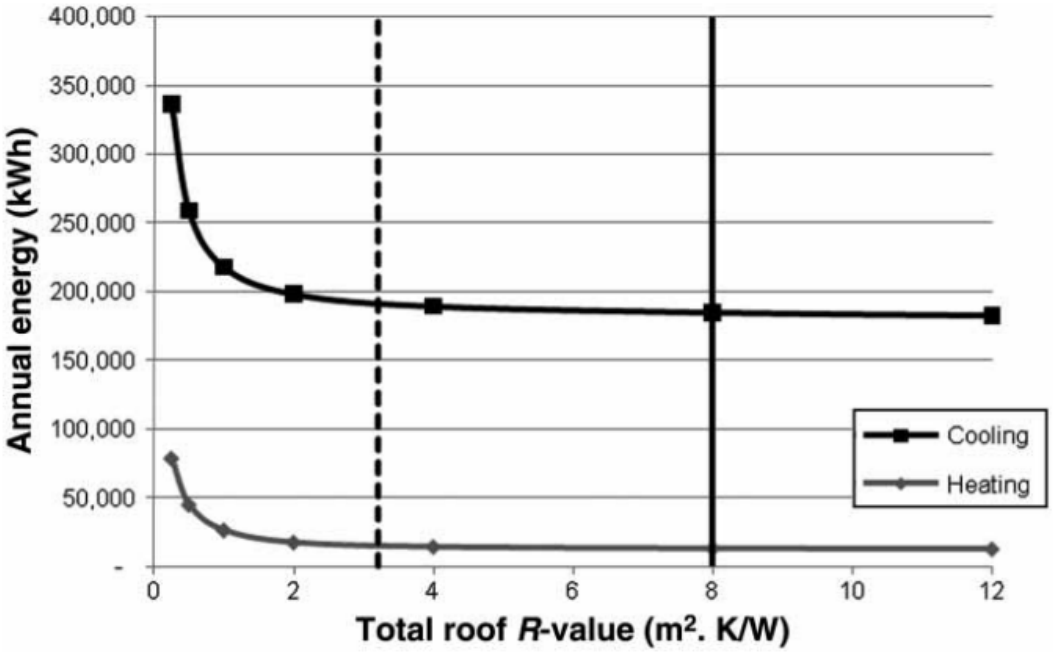

Figure 2.1. Effect of varying roof insulation thickness while maintaining wall insulation (Source: Cook & Sproul, 2011)

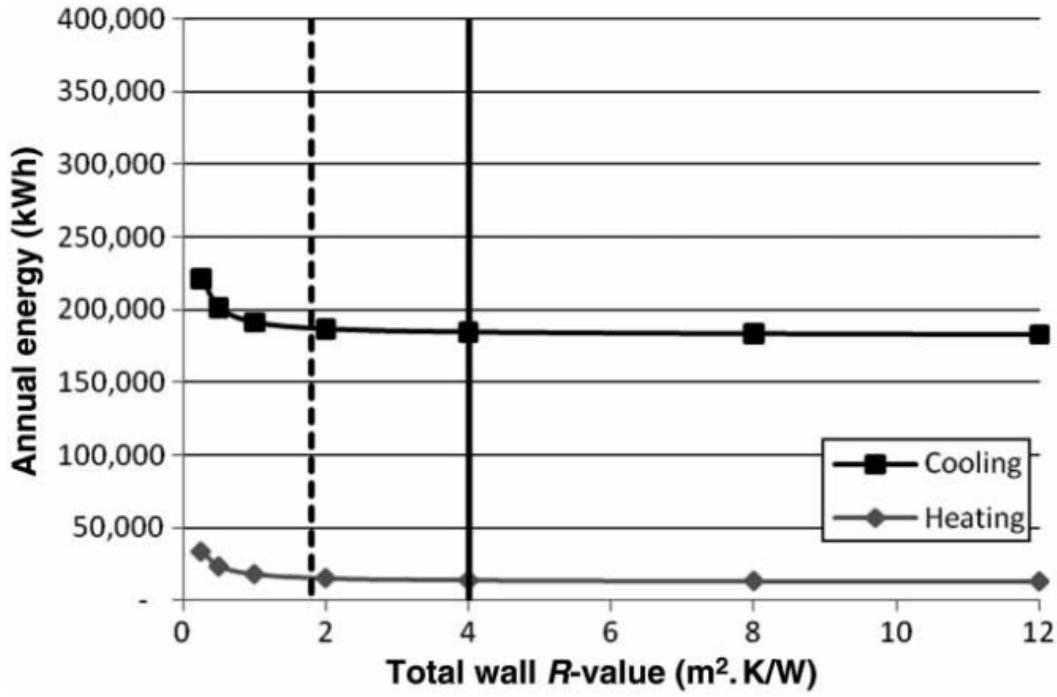

Figure 2.2. Effect of varying wall insulation thickness while maintaining roof insulation (Source: Cook & Sproul, 2011)

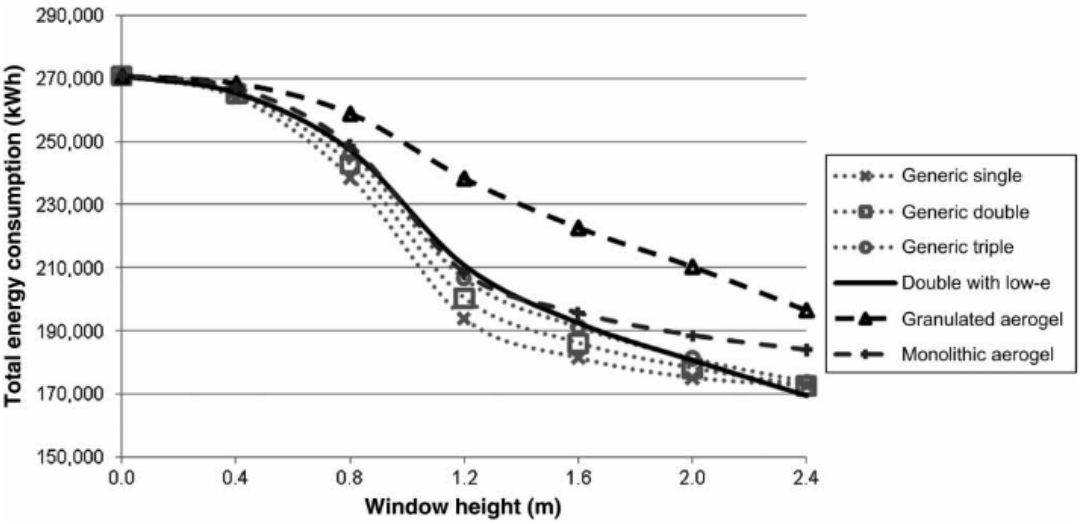

Figure 2.3. Annual energy consumption with various glazing systems glass (Source: Cook & Sproul, 2011)

Similarly, Rai et al. (2011) conducted a study that aimed to address the life cycle emissions of a distribution warehouse by focusing on operational solutions. The researchers analyzed the impact of design decisions and insulation materials on GHG emissions. The study utilized a conventional distribution center in the UK as a case study, evaluating building emissions over 25 years under three different insulation scenarios: low, medium, and high levels of insulation. Additionally, Colicchia et al. (2013) emphasized the role of materials installed in warehouse buildings in influencing GHG emissions. They highlighted the importance of adjusting lighting, heating, air-conditioning, and ventilation systems from an environmentally friendly perspective, particularly in warmer environments, as a primary energy efficiency initiative (Fichtinger et al., 2015). The study also mentioned specific strategies targeting lighting and HVAC systems to reduce the overall environmental impact of warehouses.

Pudleiner & Colton (2015) performed sensitivity analyses and created a model to measure the impact of design parameters on energy usage in warehouse buildings, employing the Net-Zero Energy building design approach. The research focused on several parameters such as external wall insulation, window characteristics, infiltration, natural ventilation, lighting, and equipment. The aim was to quantify the effects of these factors on energy consumption within warehouse buildings in a warm climate. Through a case study of a warehouse, the researchers investigated the relative importance of these parameters. The study also examined different building controls and architectural design

parameters, such as evaporator fans, lighting, defrost, plug loads, and thermostats (Figure 2.4). The findings demonstrated that the U-values of wall and roof insulation had a significant impact on reducing energy consumption in warehouses.

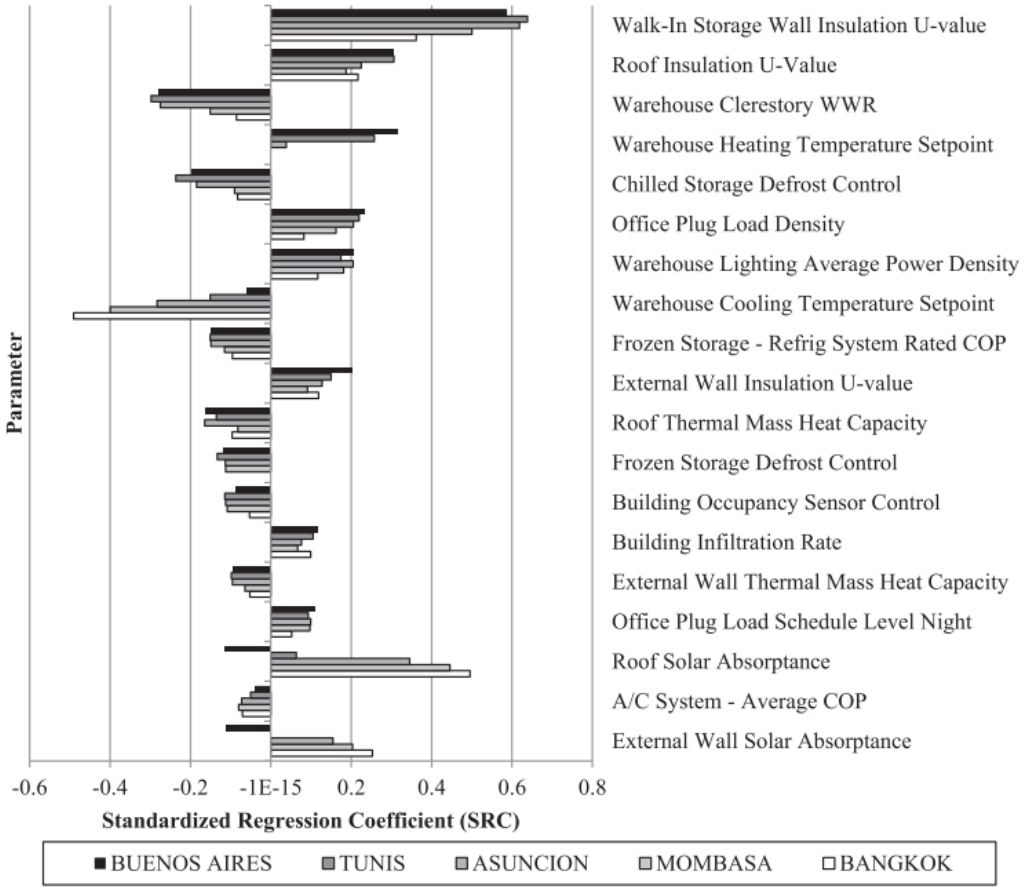

Figure 2.4. SRCs for the most influential parameters regression
(Source: Pudleiner & Colton, 2015)

Ries et al. (2017) conducted an empirical analysis using data from the United States to investigate the influence of various warehouse design factors on GHG emissions. The study found that different warehouse scenarios, such as block-place store, narrow-aisle, and automated storage/retrieval systems (AS/RS), had varying levels of emissions, with block-place store exhibiting the lowest and narrow-aisle and AS/RS warehouses having the highest emissions. The researchers also examined the impact of different technologies on emissions and found that switching from standard incandescent lamps to more energy-efficient options like fluorescents or LEDs could significantly reduce lighting energy consumption by 80% to 90%. This reduction in energy

consumption translated to a potential decrease in emissions ranging from 20% to 34% for the median warehouse (Figure 2.5). Additionally, the study proposed a simulation approach involving three different warehouses and conducted a long-term analysis to identify specific scenarios that could effectively mitigate emissions in warehouse operations.

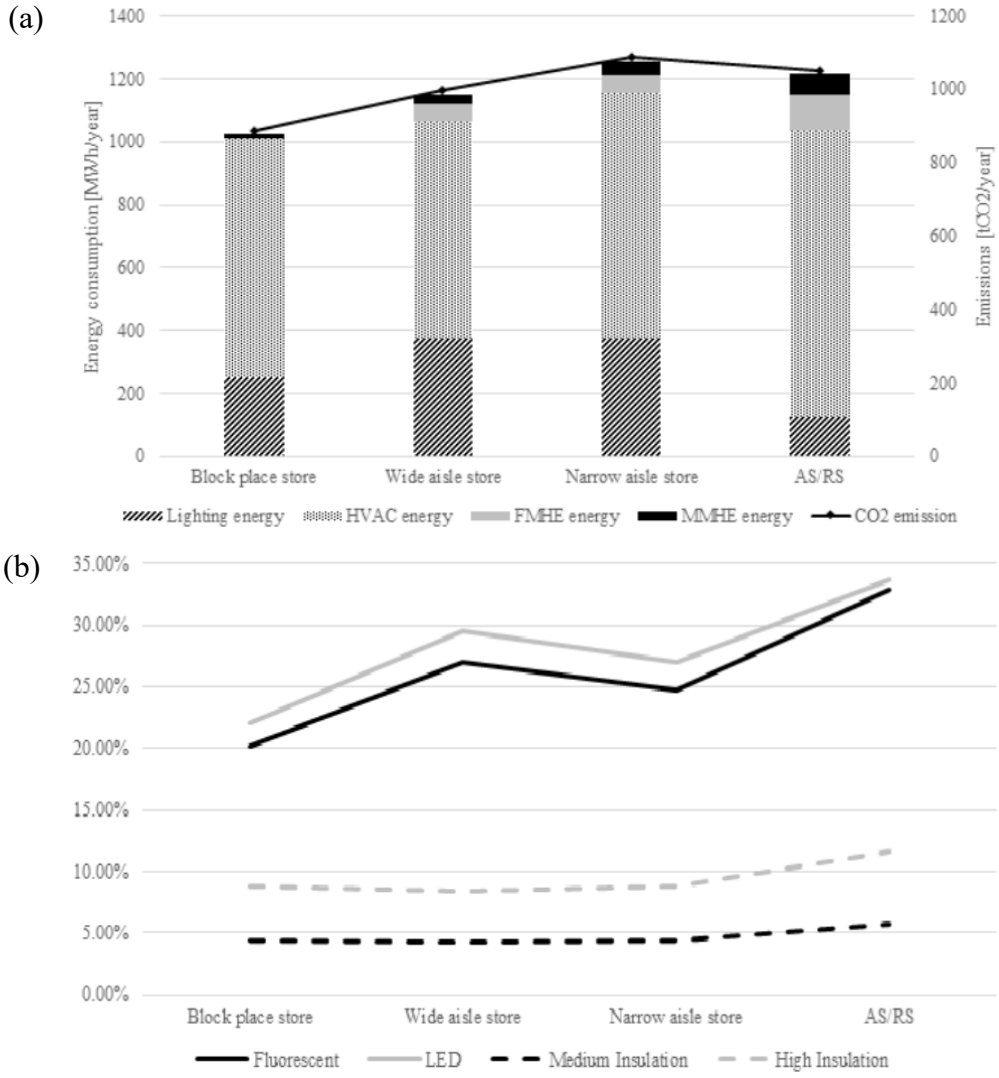

Figure 2.5. Differences in energy usage and emissions among various types of (a) warehouses and (b) equipment (Source: Ries et al., 2017)

Seifhashemi et al. (2018) focused on retail buildings and generated a computational approach to assess the impact of implementing cool roofs on warehouse energy consumption. The study demonstrated multiple benefits of this technology,

including reduced energy consumption, cost savings, improved thermal comfort, and decreased cooling energy demand across different climatic zones.

Accorsi et al. (2017) projected a multi-objective model for designing warehouse buildings, intending to optimize sizing parameters to decrease cycle time, total cost, and carbon footprint throughout the building's lifespan. The model aimed to strike a balance between building dimensions, storage capacity, and material handling performance.

Lewczuk et al. (2021) presented a methodology for assessing storage space and assessing energy consumption in warehouses. The study considered energy consumption related to material handling equipment operation, building maintenance, and energy generation from rooftop photovoltaic systems. The authors estimated operational costs for different scenarios and calculated an automation index to compare energy consumption and the level of mechanization and automation in warehouses. The research highlighted that a significant portion of energy consumption is attributed to maintaining warehouse buildings, especially in facilities with lower levels of automation.

2.3.2. Thermal Stratification in Warehouses

Controlling air temperature is vital in sectors like storage, primarily due to the vulnerability of stored products. The physical quality of goods is greatly influenced by temperature and relative humidity, making these environmental factors of the highest importance (Nunes et al., 2009). Deficiencies in the storage environment can cause unwanted alterations in the physical and chemical characteristics of stored products resulting in a decrease in their overall quality (H. Liu et al., 2011; Park et al., 2012; Shi et al., 2013; J. Wang et al., 2017). Conversely, inadequate indoor conditions in industries can lead to extensive costs for management and wasted products (Rohdin & Moshfegh, 2011).

Warehouses are large industrial buildings, and air temperature fluctuations are critical aspects that must be considered thoroughly in indoor environment design. There are two issues to be considered vertical temperature variations and overall temperature changes inside the volume. In large industrial warehouses, warm air tends to rise under the influence of buoyancy forces, resulting in a positive vertical temperature gradient between the floor and ceiling, which creates a phenomenon called thermal stratification (ASHRAE, 2017). This vertical temperature difference can cause product deterioration if

it persists for a prolonged period. Therefore, in higher building spaces, temperature stratification is considered one of the main issues in providing diffused temperature gradients in adjacent lower and upper spaces. Thermal stratification commonly occurs in large industrial warehouses and storage facilities, especially during winter seasons (Boon & Battams, 1988; R. W. Bottcher et al., 1988; L. L. Wang & Li, 2017), in buoyancy-driven ventilated spaces, including displacement (Calay et al., 2000; Gilani et al., 2016; Gil-Lopez et al., 2017) and/or underfloor ventilation systems (Kobayashi et al., 2017; Kong & Yu, 2008; Rhee et al., 2015; Tsai et al., 2014; X. Wang et al., 2011), and during natural ventilation in large spaces (Brandan & Alejandra, 2012; Dominguez Espinosa & Glicksman, 2017) throughout cooling seasons.

Initial research investigations primarily focused on studying the vertical temperature distribution within warehouses. These studies highlighted the existence of two distinct air layers characterized by different temperature gradients. The first layer extended from the floor level up to 2 meters in height, exhibiting its temperature gradient, while the second layer below the ceiling also spanned up to 2 meters and maintained a uniform temperature (Andersen, 1998; Aynsley, 2005). Notably, factors such as roof geometry, door type, and ceiling height were determined to have negligible effects on the overall temperature distribution (Saïd et al., 1996).

Previous studies aimed to quantify thermal stratification levels by assessing temperature differences and gradients. For example, (Aynsley, 2005) reported a vertical temperature gradient of 1.4°C per meter in a building heated at the floor level, while (Owen, 2010) observed a temperature gradient of 1°C per meter in a warehouse case study. Owen (2010) also noted that thermal stratification was observed in all cases when the fan was switched off, whereas complete destratification occurred in all cases with the fan operating.

Figure 2.6 illustrates the temperature contours across the warehouse areas, revealing that, when the fan was turned off, stratification levels were similar for different warehouse heights, ranging from 0.5°C to 1°C per meter. Conversely, a uniform temperature distribution was evident in all cases when the fan was switched on.

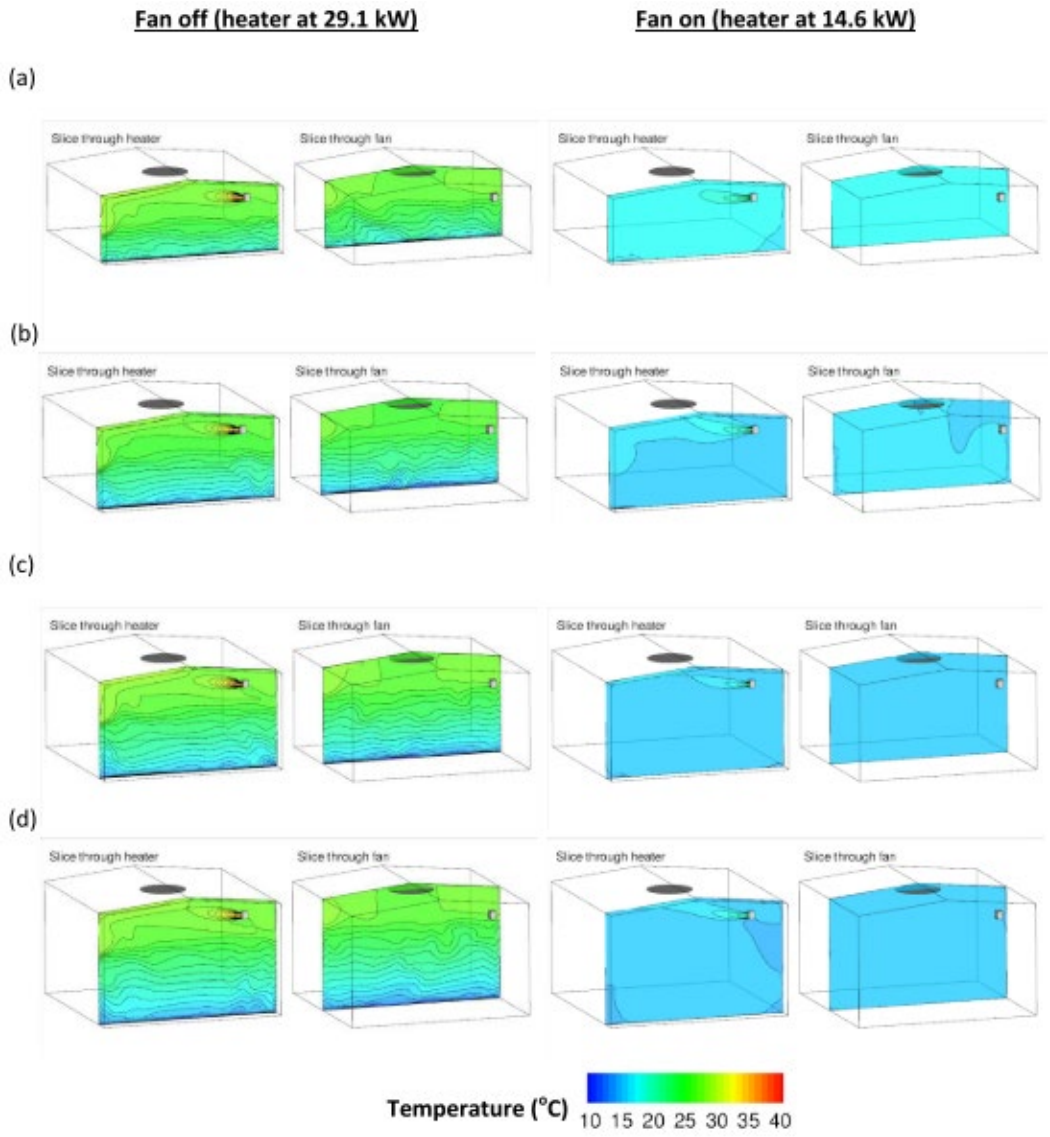

Figure 2.6. Contours of temperature plotted on slices through the warehouse domain for the fan-off case (left) and fan-on case (right). Apex heights of (a) 12.5m, (b) 15.0m, (c) 17.5m and (d) 20.0m. The outside temperature is 4°C (Source: Owen, 2010).

The climatic conditions of the building's location are also significant in terms of the thermal stratification that occurs. In colder regions, an even distribution of hot air inside the volume is desired during the winter season, whereas preventing the accumulation of hot air and creating different levels of temperature gradients during the summer is crucial for warehouses located in hot humid climates. However, during most of the winter or summer, the uncontrolled air infiltration, which exhibits prominent characteristics of buoyancy-driven ventilation (X. Liu et al., 2018; Saïd et al., 1996), has led to not only an unsatisfactory indoor thermal environment but also a high level of

energy consumption for space heating and cooling (X. Liu et al., 2018; Saïd et al., 1996; B. Wang et al., 2017).

One of the most widely adopted ventilation strategies in large spaces in a region with cold winters and hot summers is tunnel ventilation in summer. In this strategy, ventilating air is drawn into one end of the volume and exhausted at the other end (B. et al., 1998), generating higher air speeds that increase the convective heat exchange between indoor and ventilation air.

The tunnel system is often used with an evaporation cooling pad installed behind the inlet when the outdoor temperature is high. After evaporation cooling, the inlet air is of low temperature and high humidity (Hongwei et al., 1994). Furthermore, Porras-Amores et al. (2014) studied the vertical temperature variations in different warehouse placements. The temperature profile for each month is represented by the monthly averages (Figure 2.7).

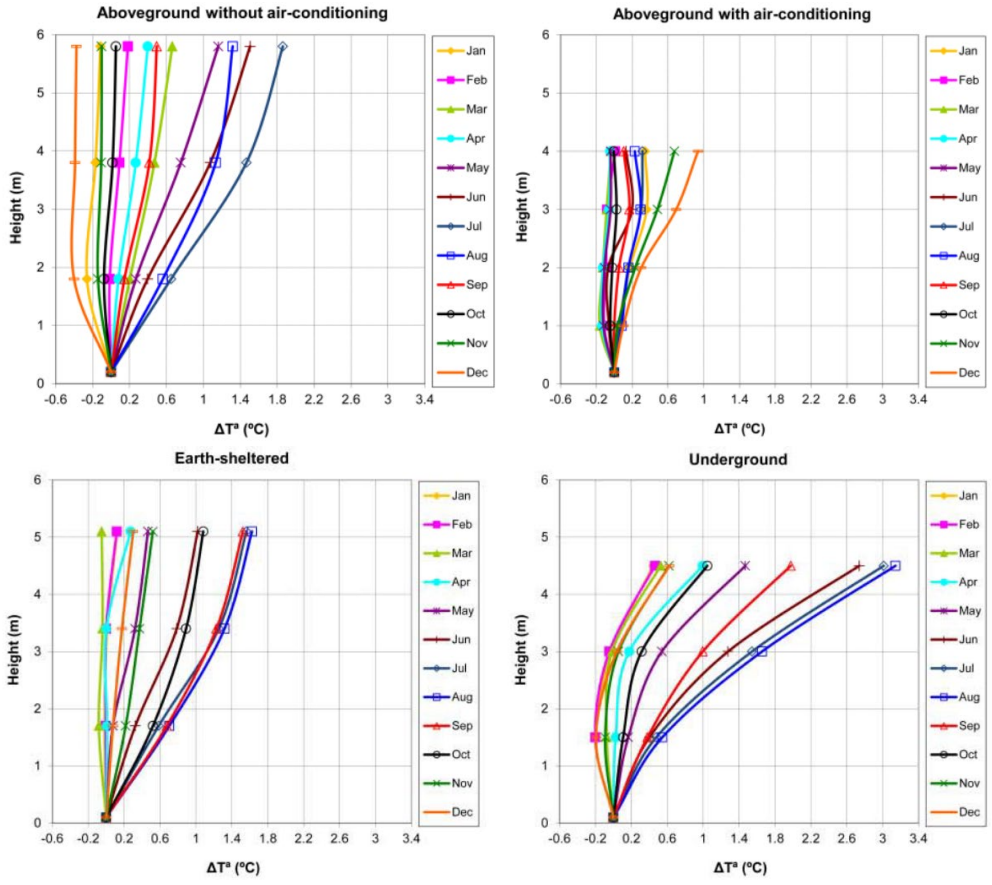

Figure 2.7. Graphs illustrating the vertical fluctuation of monthly average temperatures in the four warehouses (Source: Porras-Amores et al., 2014)

It is also concluded in the study that the cooling performance of the air conditioning system minimizes the vertical temperature differences throughout the day, reducing them to negligible levels (Figure 2.8).

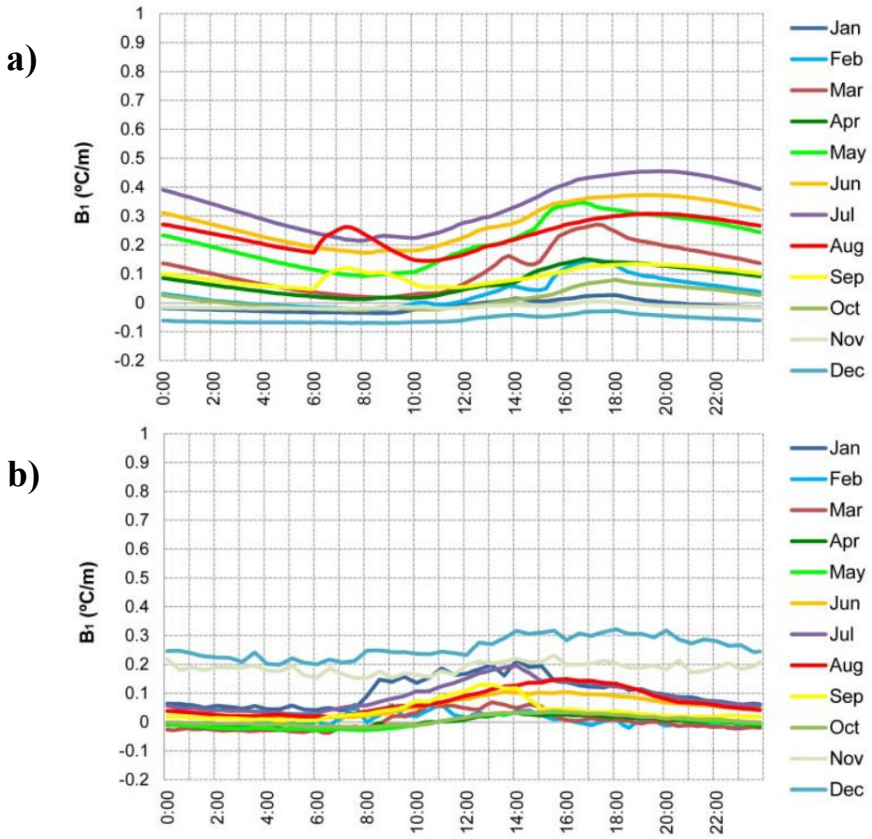

Figure 2.8. Evaluation of the thermal stratification between the aboveground warehouse (a) without air conditioning and (b) with air conditioning (Source: Porras-Amores et al., 2014).

On the other hand, previous research using numerical simulations (Ho et al., 2010) emphasizes that diffused temperature in a large space can be accomplished through the accurate design and positioning of cooling units. Techniques called thermal destratification, such as circulating and mixing air from different levels, are used to reduce or remove thermal stratification and provide diffused air inside.

Compared with field and wind tunnel experiments, CFD is found to be a time and cost-saving approach that is feasible for fully controlling external factors and experimental variables. Additionally, CFD can obtain all relevant environmental information within the simulation zone, and the airflow pattern can be analyzed

quantitatively and qualitatively, unlike tests that have limited measurement points. The issue of simulation accuracy remains a topic of debate unless proper validation and verification processes are undertaken (Rong et al., 2016). In a study conducted by Rohdin & Moshfegh, (2011), the objective was to assess the effectiveness of CFD in the planning of new systems or the renovation of existing industrial ventilation systems. The researchers specifically investigated the performance of two distinct supply principles within a process characterized by high levels of contaminants, considering factors such as temperature and density stratification.

When comparing mixing and displacement ventilation systems at a facility, the difference in performance between the two systems was smaller in summer cases (Porras-Amores et al., 2014). In another investigation, the objective was to investigate the vertical temperature fluctuations in warehouses, measure their rate, and analyze their patterns over the course of the year. The findings revealed that the utilization of air conditioning equipment played a significant role in preserving a uniform indoor environment, disrupting stratification, and reducing the discrepancies in temperature along the vertical axis. In their studies, (W. Li, 2016; L. L. Wang & Li, 2017), the authors researched to identify thermal stratification characteristics in five different warehouses through field measurements. Furthermore, they examined the impact of mechanical air mixing using fans through numerical simulations based on CFD simulations (L. L. Wang & Li, 2017).

They recommended installing a series of bucket fans beneath the ceiling of the warehouse as the most effective method for mixing air. In the studies of L. L. Wang & Li, (2017), the authors conducted a study where they examined various techniques to reduce vertical temperature differences within two industrial warehouses. This investigation involved collecting real-world data and utilizing CFD simulations. They pointed out that there exists an optimal number of these devices, beyond which the destratification performance could not be further improved significantly.

When it comes to evaluating ventilation efficiency, commonly employed measures involve analyzing and adjusting airflows using variable speed drives and time control, managing input temperatures, and incorporating heat recovery mechanisms. The research focuses on identifying the potential for energy savings through improved ventilation techniques that address thermal destratification, leading to more effective maintenance of ideal workplace conditions and up to a 38% reduction in energy consumption in a typical warehouse (L. L. Wang & Li, 2017) (Figure 2.9).

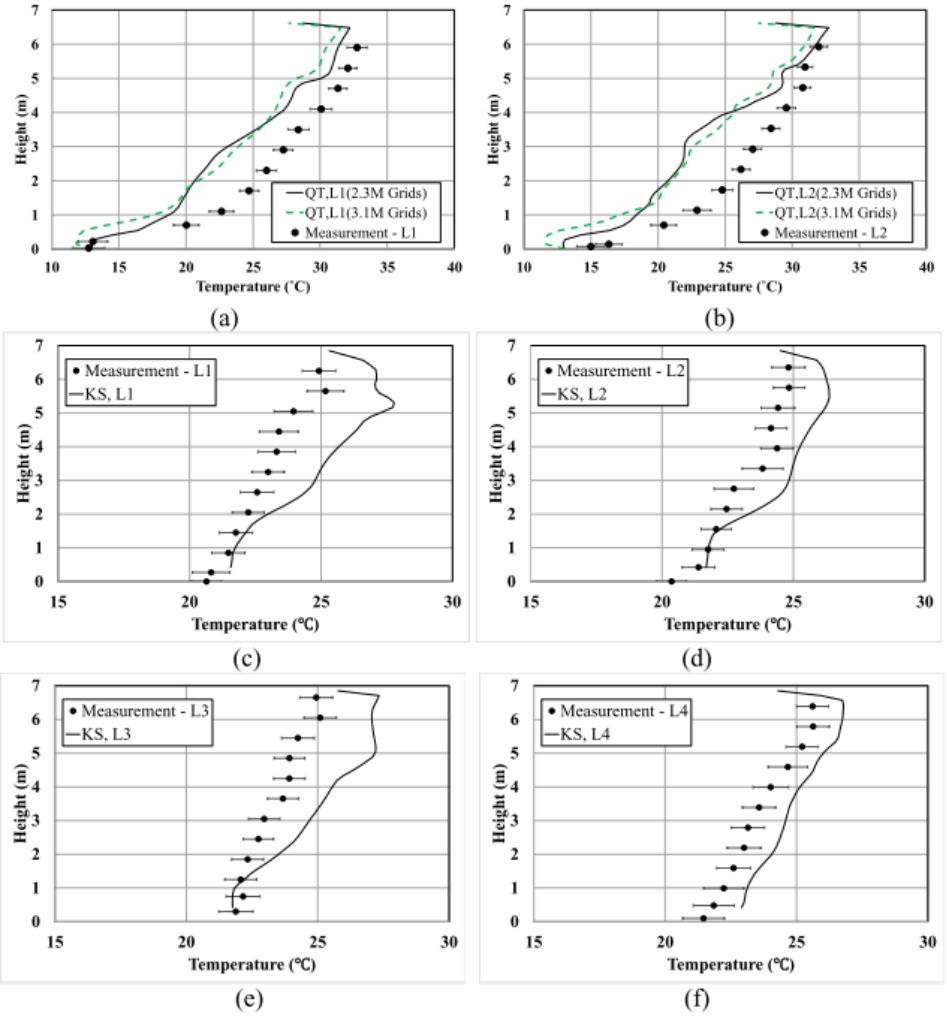

Figure 2.9. Temperature profile comparison between the measurements and the simulation results. (a) for L1 and (b) for L2 of the QT warehouse, and (c), (d) (e) and (f) are for L1, L2, L3, and L4 for the warehouse (Source: L. L. Wang & Li, 2017).

The impact of mechanical ventilation systems on air infiltration under heating and cooling conditions is a matter of concern, particularly in existing large-scale buildings, where a comprehensive theoretical analysis is lacking (X. Liu et al., 2020). Various types of mechanical ventilation systems, including the entire space air-conditioning system, stratified air-conditioning system, and occupant zone air-conditioning system with displacement ventilation or radiant floor, are commonly employed in large-scale buildings. These systems exhibit variations in terms of where and how heat is released or absorbed, leading to unique patterns of temperature stratification within indoor environments (X. Liu et al., 2020) (Figure 2.10).

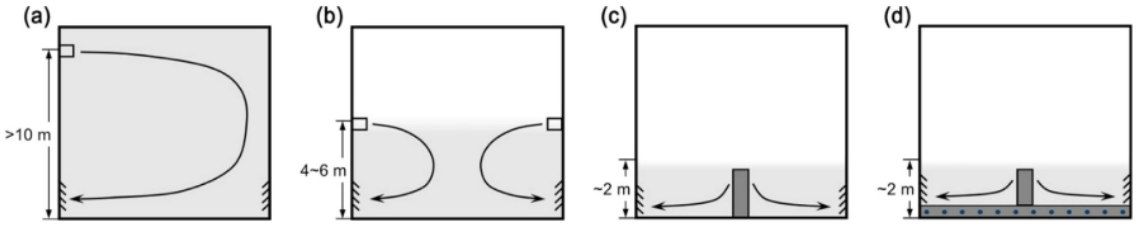

Figure 2.10. Typical air-conditioning systems in large space buildings: (a) entire space air-conditioning system with MV, (b) stratified air-conditioning system with MV, (c) occupant zone air-conditioning system with DV, and (d) occupant zone air-conditioning system with RF and DV (Source: X. Liu et al., 2020).

Despite the growing interest in retrofit interventions for temperature management in warehouses, there are still gaps in the literature. For example, there is limited research on the effectiveness of retrofit interventions in reducing energy consumption and improving temperature management in warehouses. There is a lack of multifaceted studies on vertical temperature fluctuations and changes in temperature over time, both of which can be harmful and lead to the deterioration of stored products. Additionally, there is a lack of standardization in the design and implementation of retrofit interventions, making it difficult to compare and evaluate the effectiveness of different interventions. Consequently, further research is needed to develop guidance for the design and implementation of retrofit interventions and to evaluate their effectiveness in improving temperature management and reducing energy consumption in warehouses.

These findings highlighted the importance of developing proposals for air conditioning inside buildings. Besides, the need for retrofit interventions in warehouses to improve temperature management has become increasingly important in recent years due to their significant role in the supply chain of various industries. Proper temperature management is essential for maintaining the quality of stored products and reducing energy consumption. Given the limited knowledge regarding air fluctuations in warehouses, this study offers a broad perspective on the development of thermal gradients in warehouses situated in hot and humid climates, specifically focusing on the warmest and coldest months of the year.

The study aims to explore the potential of retrofit interventions on warehouses to enhance their temperature management through both experimental and numerical methods. In this study, a theoretical model that represents the steady airflow driven by buoyancy-induced air infiltration in a large single-zone building is developed and the

accuracy of the model is confirmed. The validation process involved collecting field measurements and conducting numerical simulations. Consequently, the study monitors and analyses the vertical gradients of indoor temperature existing in a tobacco warehouse for a period of sixteen months. Later, the critical months for the stored product were identified so that possible solutions can be examined to increase indoor air distribution while providing a stable temperature gradient over a period.

By filling the gap in the literature, this study will identify retrofit interventions that can be implemented to manage these gradients and maintain a uniform temperature distribution. This research will provide practical insights for warehouse managers and stakeholders. Besides, the results may be valuable to the energy-efficient design and management of air conditioning systems in large space buildings.

2.3.3. Ventilation Approaches on Warehouses

Ventilation is necessary for buildings to remove 'stale' air and replace it with 'fresh' air: It helps to moderate internal temperature and humidity, replenishing oxygen, and reducing the accumulation of moisture, odors, bacteria, CO_2, and other contaminants that can build up inside, as well as creating air movement which also improves the indoor environment conditions.

Ventilation in buildings can be classified as 'natural' or 'mechanical'. Natural ventilation is driven by pressure differences between one part of a building and another or pressure differences between the inside and outside. Natural ventilation is generally preferable to mechanical ventilation as it will typically have lower capital, operational, and maintenance costs. However, there are certain circumstances in which natural ventilation may not be possible. Some of the issues can be avoided or mitigated by careful design, and mixed mode or assisted ventilation might be possible, where natural ventilation is supplemented by mechanical systems. On the other hand, mechanical (or forced) ventilation is driven by fans or other mechanical plants where mechanical ventilation is necessary it can be:

- A circulation system such as a ceiling fan, which creates internal air movement, but does not introduce fresh air.
- A localized exhaust system operates by creating a negative pressure within a structure, expelling air from space. This pressure change prompts the influx of fresh air

from the outside through gaps in the building envelope and deliberate, passive vents. Exhaust ventilation is most appropriate for colder climates, since in warmer climates, depressurization can draw moist air into wall cavities where it may condense and cause moisture damage.

- A supply system, in which fresh outside air is blown into the building by inlet fans, creating a higher internal pressure than the outside air. Supply ventilation systems allow better control of the air that enters the volume compared to exhaust ventilation systems. Supply ventilation systems work best in hot or mixed climates. Since they pressurize the inside, these systems have the potential to cause moisture problems in cold climates.
- A vacuum system, in which stale internal air is extracted from the building by an exhaust fan, creating lower pressure inside the building than the outside air.
- A balanced system that uses both inlet and extract fans, maintaining the internal air pressure at a similar level to the outside air and so reducing air infiltration and draughts.

In commercial (non-residential) buildings, mechanical ventilation is driven by air handling units (AHU) connected to ductwork within the building that supplies air to and extracts air from interior spaces. In general, AHU comprises an insulated box that forms the housing for; filter racks or chambers, and a fan (or blower).

Extracting internal air and replacing it with outside air can increase the need for heating and cooling. This can be reduced by re-circulating a proportion of internal air with the fresh outside air, or by heat recovery ventilation (HRV) that recovers heat from extracted air to pre-heat incoming fresh air using counter-flow heat exchangers.

In this context, large space storage buildings, such as warehouses are one of the most significant subjects to be focused on since they contribute most to the consumption of energy and natural resources (Rai et al., 2011). Besides, for optimal storage conditions, they require certain indoor air properties depending on the type of stored product Accordingly, it becomes significant to study ventilation systems within these buildings comprehensively and find ideal case-specific air circulation strategies. By investigating the current literature, it is possible to decide on certain ventilation approaches that can be suitable for the case building in this study.

The objective of Tran (2013)'s study was to put forward and examine strategies for incorporating natural ventilation in the design of high-performing non-residential structures located in hot and humid climates. The study focused on retrofitting an existing

university building in Honolulu and evaluated three different natural ventilation design schemes. Design scheme 1 utilized a cross-ventilation approach, where outdoor air entered through opposite ventilation ducts, circulated within the spaces, and was subsequently exhausted through ventilation windows on the opposite side of the building facade (Figure 2.11).

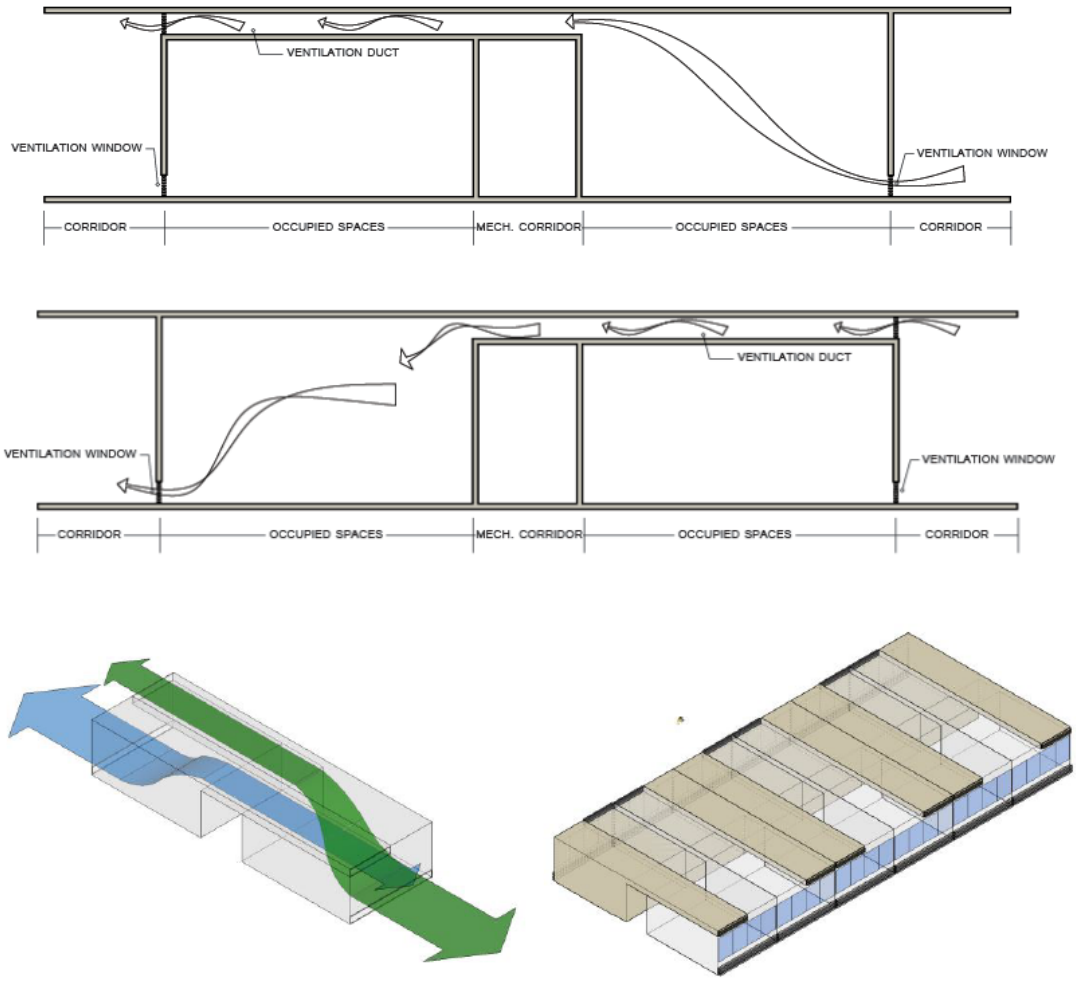

Figure 2.11. Natural ventilation design scheme 1
(Source: Tran, 2013)

In Design Scheme 2, a hybrid ventilation method was utilized, employing the wind tower effect to improve cross ventilation. Similar to scheme 1, fresh outdoor air was introduced into occupied areas through ventilation windows, ducts, and supplementary openings linked to the mechanical corridor. This approach relied on a combination of wind pressure and stack effect to drive the airflow, resulting in bidirectional airflow

within the ventilation shaft caused by the combined effects of wind-induced pressure and buoyancy-driven force (Figure 2.12).

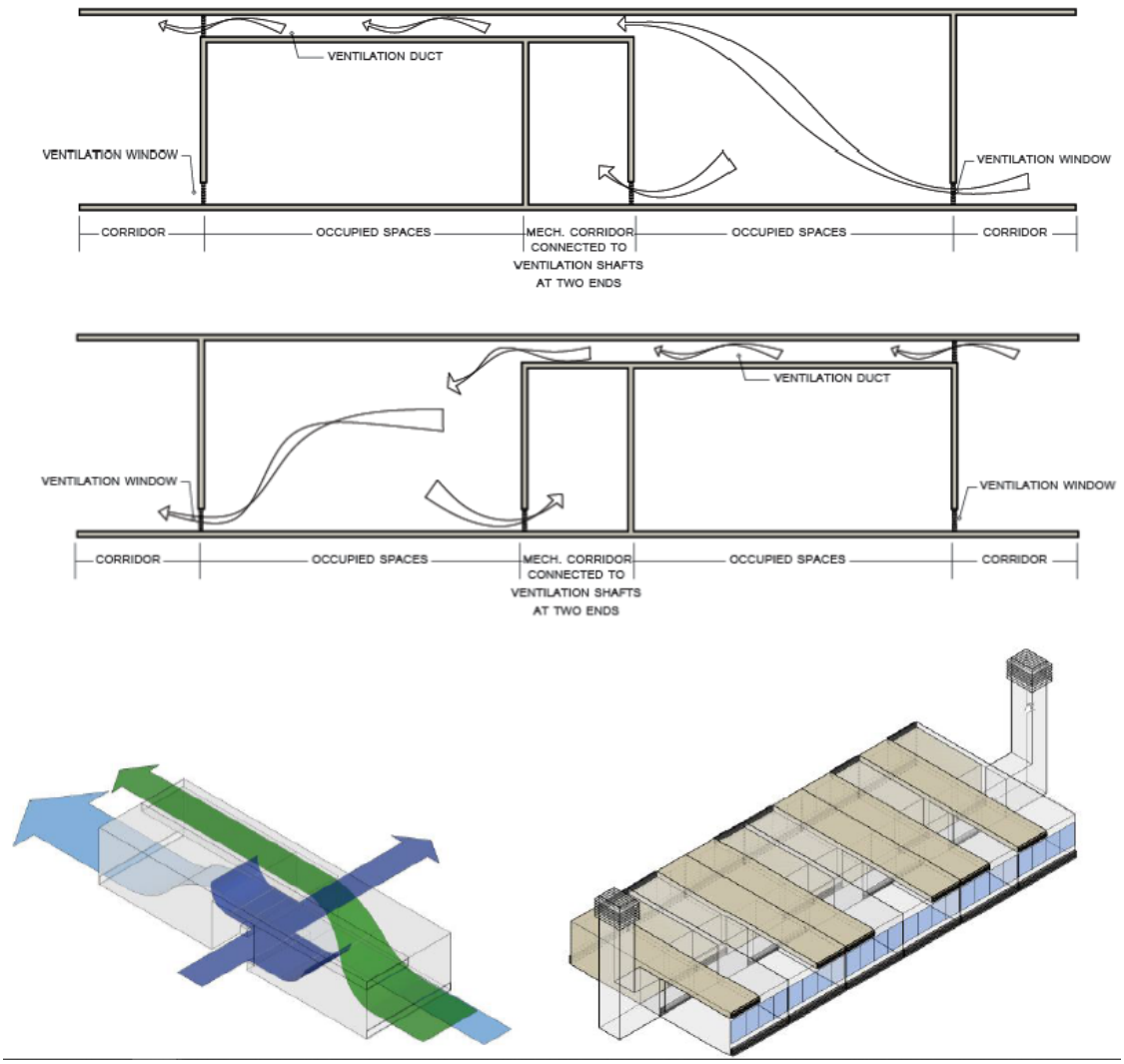

Figure 2.12. Natural ventilation design scheme 2
(Source: Tran, 2013)

The third scenario expands on the concepts of scheme 2 by introducing a modification that involves replacing the two ventilation shafts positioned at opposite ends of the mechanical corridor with vertical ventilation shafts situated within the central mechanical corridor. This design takes advantage of the building's existing structure, where the central mechanical corridors extend to the roof. As a result, ventilation ducts can extract stagnant air from occupied spaces and expel it through outlet openings located at the roof level (Figure 2.13).

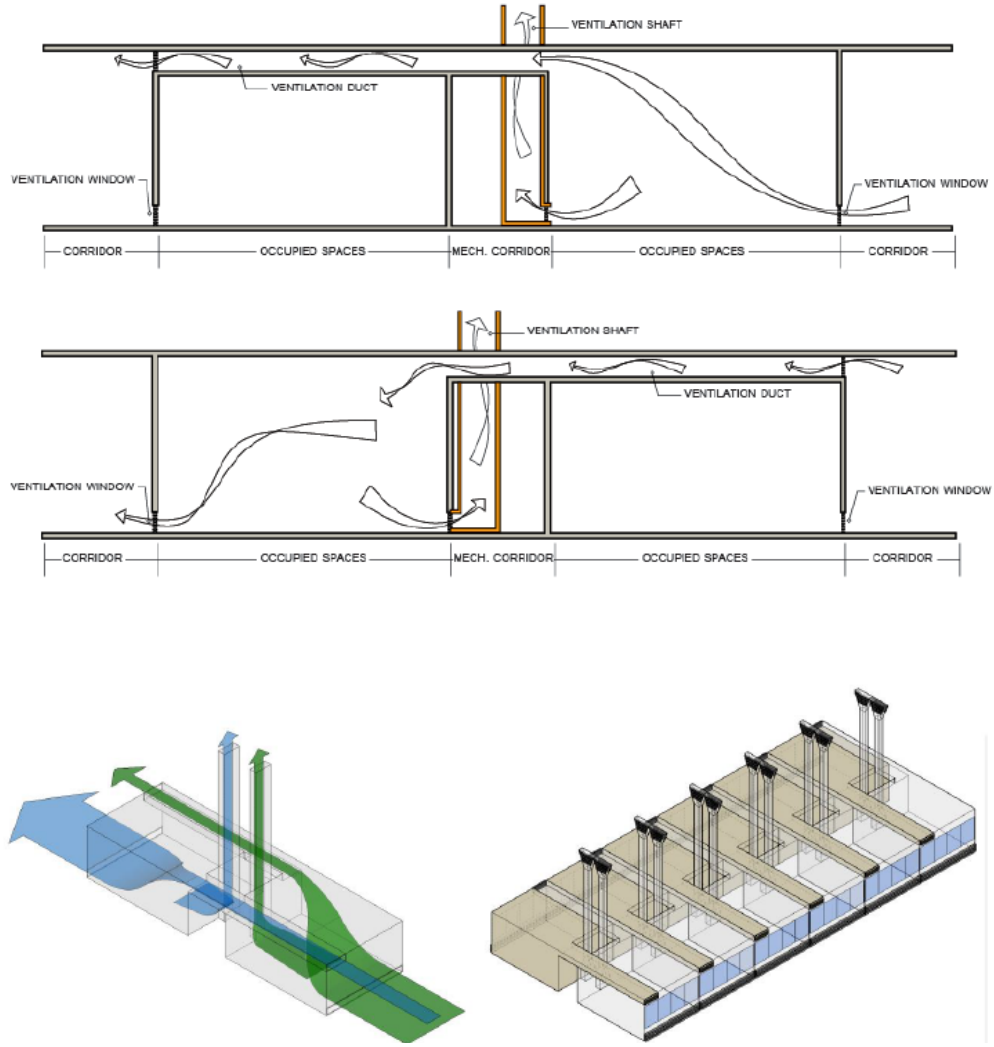

Figure 2.13. Natural ventilation design scheme 3
(Source: Tran, 2013)

The findings of the study by Tran, (2013) indicate that relying solely on cross-ventilation is insufficient to provide satisfactory thermal comfort to residents within an acceptable range of discomfort hours. Nevertheless, the integration of vertical ventilation ducts improves the effectiveness of natural ventilation design scenarios. These enhanced scenarios revealed that either the ventilation ducts or the ventilation windows could be completely closed, rendering one of them unnecessary in the design of natural ventilation systems. This adjustment not only mitigates the potential transmission of outdoor noise through the openings of ventilation channels and windows but also improves overall indoor environmental conditions.

Rohdin & Moshfegh (2011) conducted a study to assess the effectiveness of using CFD in the planning and renovation of industrial ventilation systems. The researchers

specifically examined two different supply principles within a contaminant-intensive process characterized by temperature and density stratification. Figure 2.14 displays the cross-sectional simulation results.

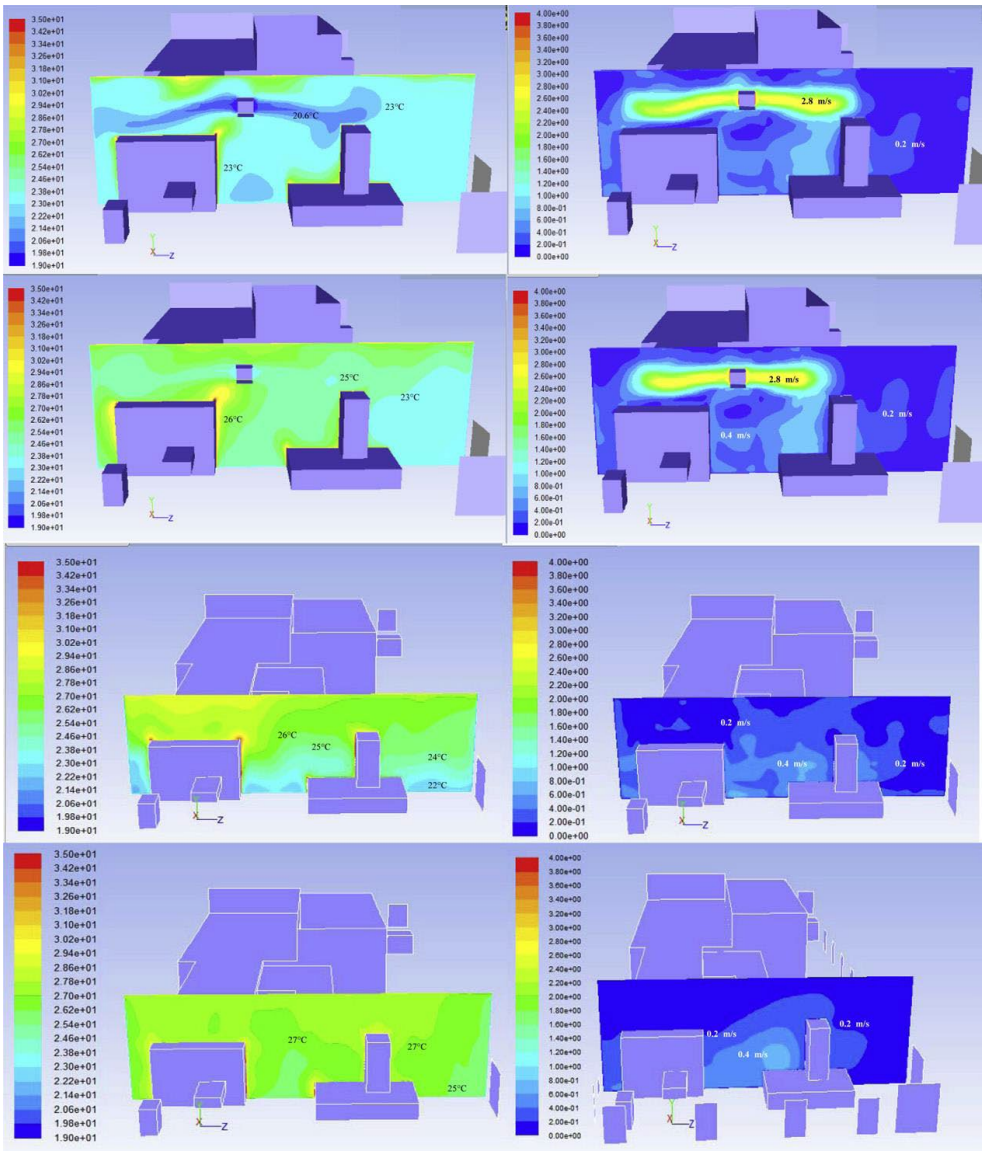

Figure 2.14. Cross-section results left is the temperature, and velocity is the right. The cases are, from top to bottom: (1) winter case mixing, (2) summer case mixing, (3) winter case displacement, and (4) summer case displacement (Source: Rohdin & Moshfegh, 2011)

When comparing the mixing and displacement ventilation systems in the facility, it was observed that the displacement system exhibited higher contaminant removal efficiency during winter, along with improved heat removal effectiveness. In the summer

cases, the performance gap between the two systems was smaller. However, the overall performance of the displacement system diminished as the temperature difference between the supplied air and the room air decreased, resulting in a decline in its effectiveness due to the reduced stack effect.

Teitel et al. (2008) claim that axial or radial fans are widely used in the ventilation of large space storage buildings. Besides, when forced ventilation is used, the fans should be capable of moving large quantities of air with a relatively low-pressure drop. It is also indicated that, since the heat load on warehouses usually varies during the year and each day, variable frequency drives could be another means for controlling ventilation. More importantly, the study shows that variable speed fans can provide continuous air movement within the building and thus minimize the regions of stagnant hot and humid air, allow a more homogeneous air velocity inside, and allow a continuous supply of atmospheric air with oxygen in cases where it is needed.

Spindler & Norford (2009) utilized a data-driven thermal model to evaluate the influence of window and internal openings, as well as fan operation, on building thermal conditions. The study aimed to rank and select suitable cooling strategies to maintain temperatures within a specified range during occupied periods while minimizing fan energy consumption. Four control modes were considered: full-speed fan operation, buoyancy- and wind-driven airflow without a fan, wind-driven cross ventilation without a fan, and closed buildings without a fan. The study also investigated the optimal selection of control modes during different periods within a day. The findings indicated that incorporating mechanical air conditioning allows for maintaining comfortable conditions throughout occupied periods, but it necessitates the implementation of an additional control mode. In the case of a variable-speed fan, if the variable cooling capacity is available, the air conditioner mode can be subdivided into sub-modes, each catering to a different capacity.

Ho et al. (2010) presented an analysis of air velocity and temperature distribution within a refrigerated warehouse. The study focused on a refrigerated space equipped with ceiling-type cooling units located in front of arrays of palletized product packages. Steady-state air flow and heat transfer were numerically simulated using a three-dimensional model.

A parametric analysis was conducted, considering different blowing air velocities and locations of cooling units. Figure 2.15 illustrates the visualization of air velocity, pressure, and temperature distributions. The analysis revealed that higher blowing air

velocities and/or positioning the cooling units lower and closer to the arrays of product packages led to improved cooling effectiveness and temperature uniformity within the refrigerated space.

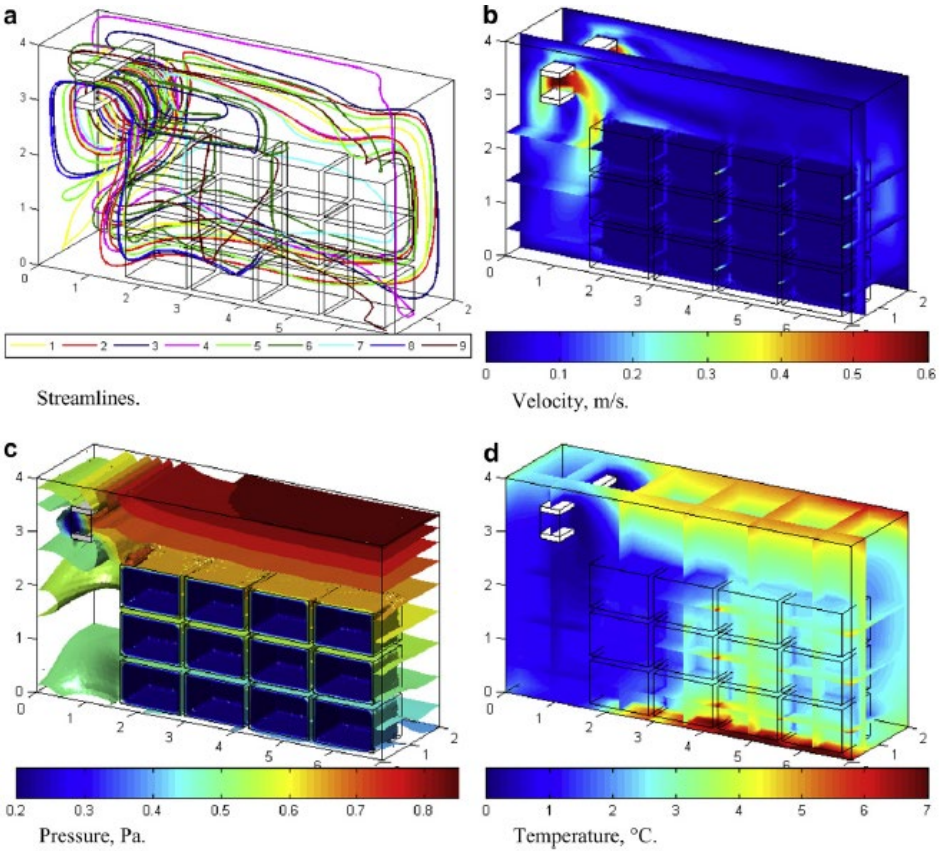

Figure 2.15. Distributions of air velocity, pressure, and temperature
(Source: Ho et al., 2010)

Karava et al. (2012) conducted a study on mixed-mode cooling strategies in buildings characterized by hybrid ventilation and high levels of exposed thermal mass. The research involved an experimental setup in a real-occupied institutional building, where motorized facade openings were integrated with an atrium. The authors focused on evaluating night cooling strategies aimed at pre-cooling the thermal mass. These strategies involved the use of variable low-temperature setpoints to regulate airflow through the operation of motorized grilles or a potentially variable-speed fan.

The hybrid ventilation concept, illustrated in Figure 2.16, involves cool outdoor air entering the building through corridor inlet grilles. The air is then transferred to the

atrium, where it heats up and moves upwards through the atria-connecting grilles. Finally, the heated air is exhausted through the outlet vent located at the top of the atrium.

Based on the relative strengths of wind pressure and stack pressure, the airflow dynamics in the building can facilitate the entry of air through corridor inlet grilles on one side while being exhausted through inlet grilles on the other side, as depicted by the bidirectional arrows in Figure 2.16. The research findings indicate that the hybrid ventilation system was active for approximately 30% of the cooling season (April to October), and the utilization of free cooling proved capable of meeting a significant portion of the cooling demands. Moreover, the investigation of mixed-mode cooling strategies, incorporating motorized grilles with variable low-temperature setpoints for nighttime operation, revealed that the inflowing air at lower temperatures enhanced the cooling capacity, leading to increased cooling storage within the thermal mass.

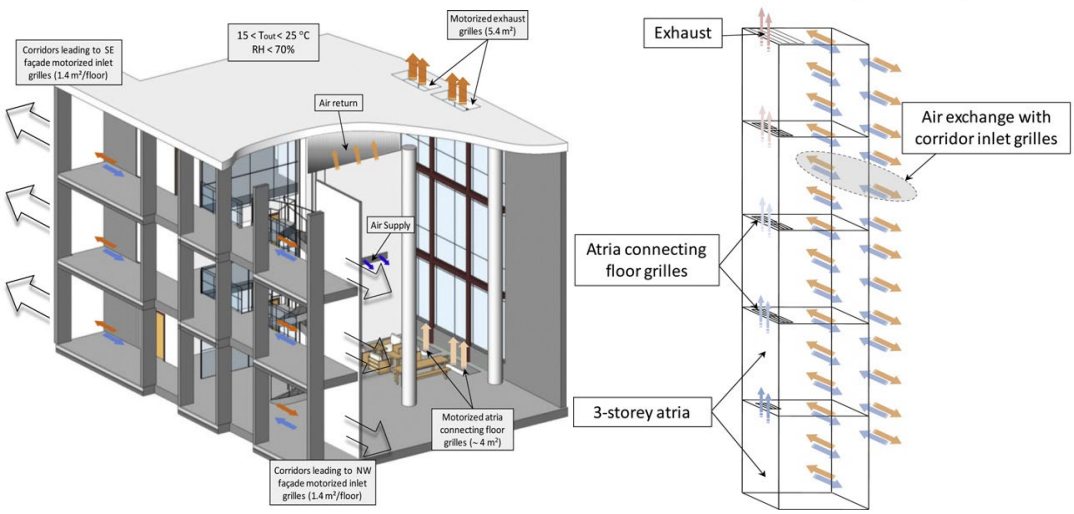

Figure 2.16. Hybrid ventilation strategy
(Source: Karava et al., 2012)

Ezzeldin & Rees (2013) conducted a comprehensive assessment of various mixed-mode cooling strategies for office buildings in arid climates, considering different levels of internal heat gain. The study focused on four representative cities. The base cases involved active cooling systems, namely constant air volume (CAV) and variable air volume (VAV) air conditioning, along with a radiant cooling system with CAV fresh air supply (C). In the simulations of the active systems, air-cooled chillers were utilized as cooling sources for both air handlers and the radiant system.

The study investigated various mixed mode cooling systems, encompassing different combinations of ventilation strategies. These included a simple mixed mode ventilation approach, which involved utilizing natural ventilation during working hours and switching to an active system during peak conditions. Additionally, the study examined the integration of a night convective cooling strategy. Other configurations explored included mixed mode ventilation combined with direct evaporative cooling, as well as mixed mode ventilation coupled with radiant cooling elements linked to either a cooling tower (indirect evaporative cooling) or borehole heat exchangers (earth cooling).

The mixed mode cooling algorithms employed in the analyses are depicted in Figure 2.17. The simulation results were evaluated based on defined thermal comfort criteria and the potential reductions in energy consumption of the cooling systems.

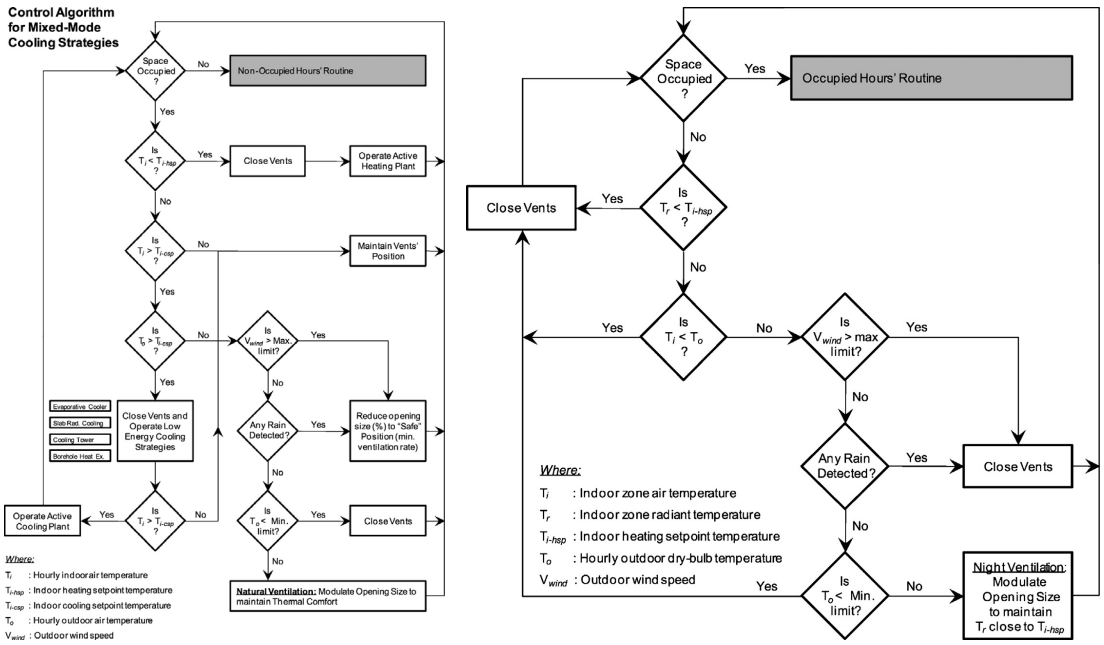

Figure 2.17. The mixed mode/hybrid cooling control algorithm for occupied (left) and unoccupied periods (right) (Source: Ezzeldin & Rees, 2013)

The findings indicated that hybrid approaches, which combine active air-conditioning systems with natural ventilation, have the potential to reduce plant energy consumption by approximately 50% compared to conventional active air-conditioning systems. Consequently, it is recommended to consider the implementation of mixed-mode cooling strategies in arid climates.

Li (2016) highlights the significance of axial turbine fans, an alternative type of fan installed below the ceilings in warehouses. These fans are characterized by their compact size compared to traditional ceiling fans and deliver higher-speed and more concentrated airflow. Consequently, the airflow from axial turbine fans exhibits greater penetration length. The study primarily involves field measurements to assess thermal stratification conditions in warehouses. It also develops a method to simulate large warehouses using CFD simulations, incorporating heating processes and fan mixing. Additionally, the effectiveness of different fan settings in mitigating thermal stratification in large warehouses is explored.

The study incorporates CFD models of various warehouses. Figure 2.18 presents two models illustrating the positions of stored products and ventilation equipment within the buildings. The left photo in Figure 2.18, displays a space heated by an electronic heater suspended below the ceiling. It features an internal fan at the heater's inlet and a bucket fan operating beneath the ceiling to facilitate air mixing in the warehouse. In the same figure, the right photo depicts a building heated by warm air supplied from the mechanical room, along with six baseboard heaters situated beneath windows on the exterior wall near ground level.

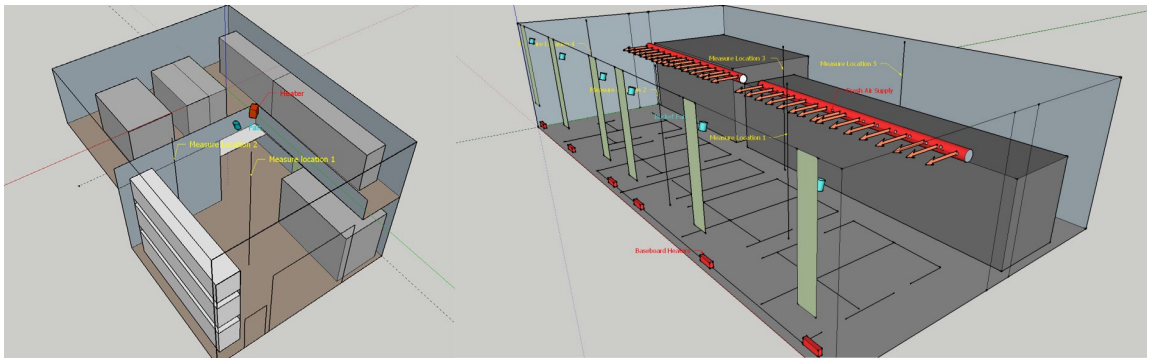

Figure 2.18. Schematic diagrams of the two warehouses
(Source: W. Li, 2016)

Eight fans, consisting of six bucket fans and two ceiling fans, are employed to facilitate air mixing. Figure 2.19 illustrates the HVAC system configuration within the stadium. Along the side walls, two rows of air diffusers are positioned to supply air into the stadium, while an additional 12 fabric diffusers are strategically distributed below the ceiling. The fabric diffusers direct conditioned air downward.

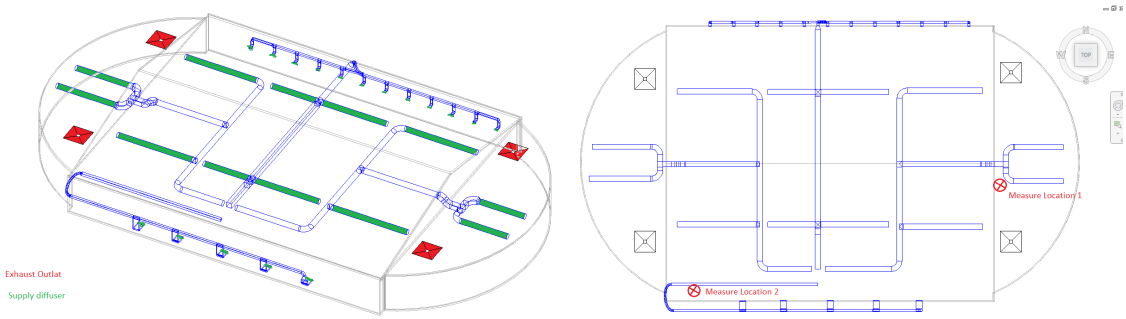

Figure 2.19. Schematic diagram of the MG stadium. The fresh air duct system has been marked in green (Source: W. Li, 2016)

Comparisons were made between scenarios with the bucket fan operating and with the bucket fan turned off. The findings demonstrated a noticeable improvement in temperature mixing when the mixing fan was in operation. Furthermore, a comparison was conducted between scenarios with the ceiling fan and bucket fan, revealing that the ceiling fan proved to be more effective in neutralizing temperature differences compared to the bucket fan (W. Li, 2016).

Figure 2.20 depicts two configurations of warehouse heating systems. The left diagram presents a building heated by infrared heaters suspended below the ceiling, accompanied by six additional heaters positioned along the warehouse's exterior perimeter. In the right diagram of the same figure, a warehouse is equipped with two types of heaters, specifically infrared heaters and forced air heaters, integrated into the building. Additionally, 18 standard ceiling fans are installed within the warehouse to facilitate air mixing.

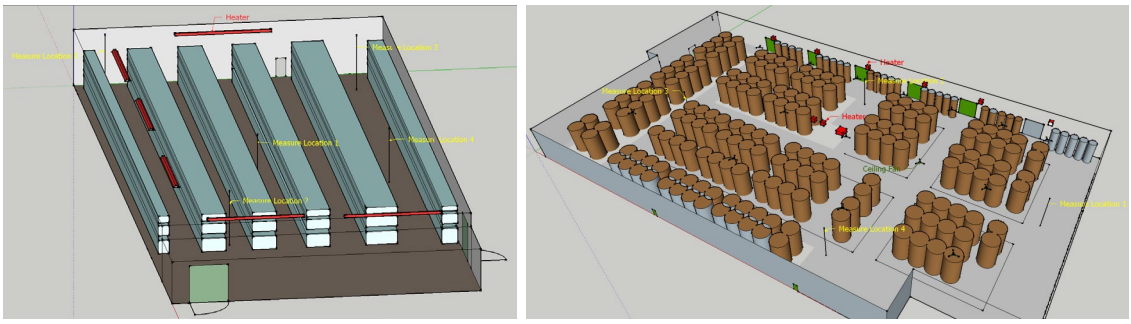

Figure 2.20. Schematic diagrams of two warehouses
(Source: W. Li, 2016)

Ding et al. (2018) also conducted another study by focusing on mixing fans and analyzing fans with different designs. The field studies aimed to find the optimal design of mixing fans to apply to improve air mixing in agricultural buildings. The study analyzed various combinations of diffuser angles and lengths, then revealed the best option. Figure 2.21 shows the CFD analysis results of some scenarios.

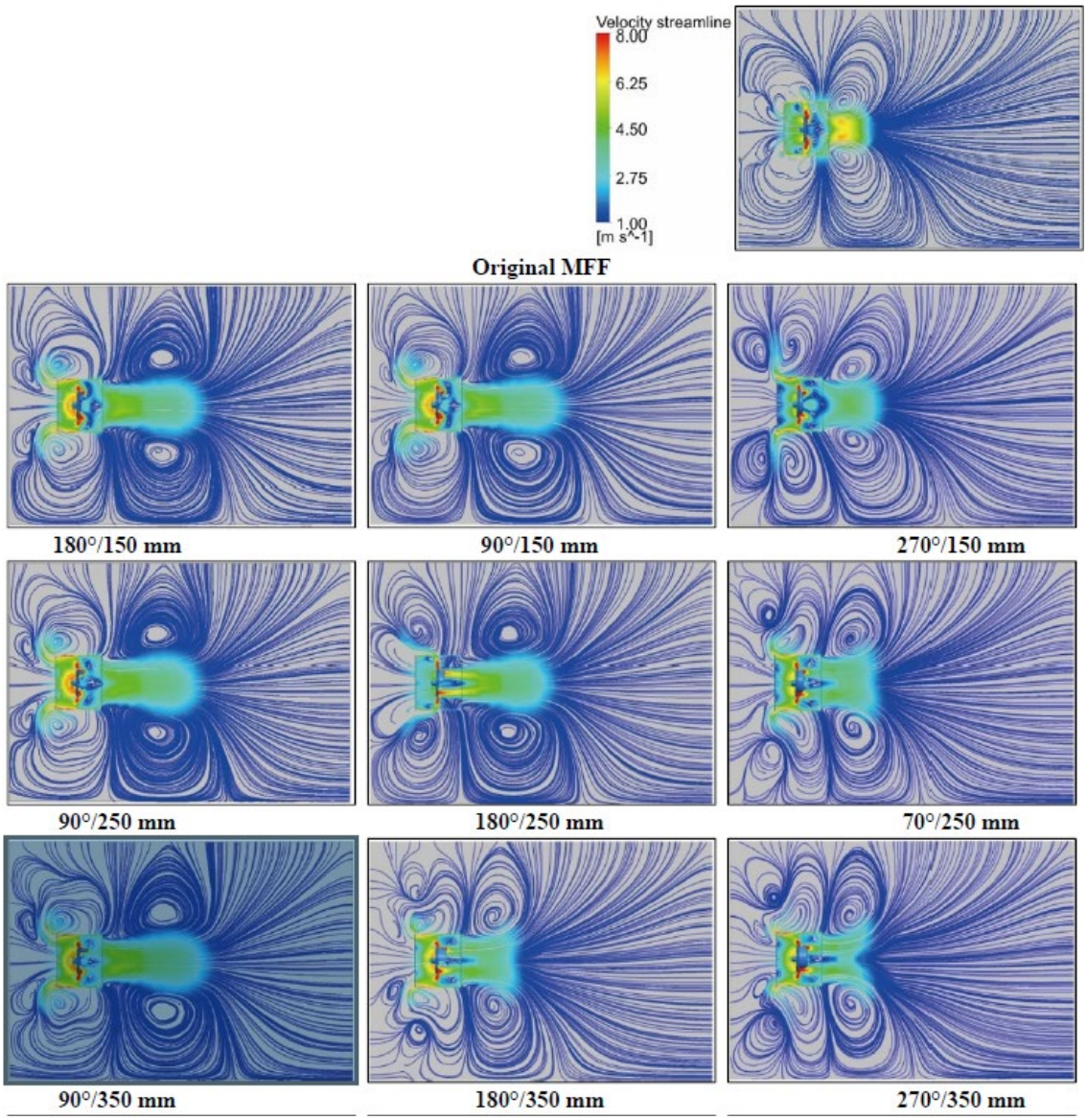

Figure 2.21. Velocity streamlines distributions at the axial center plane of the computational model (Source: Ding et al., 2018)

Estelles (2018) conducted a study to enhance the ventilation system of a warehouse building, focusing on two different scenarios. In the first scenario, the existing setup was improved by implementing three separate air handling units for different areas of the building (Figure 2.22).

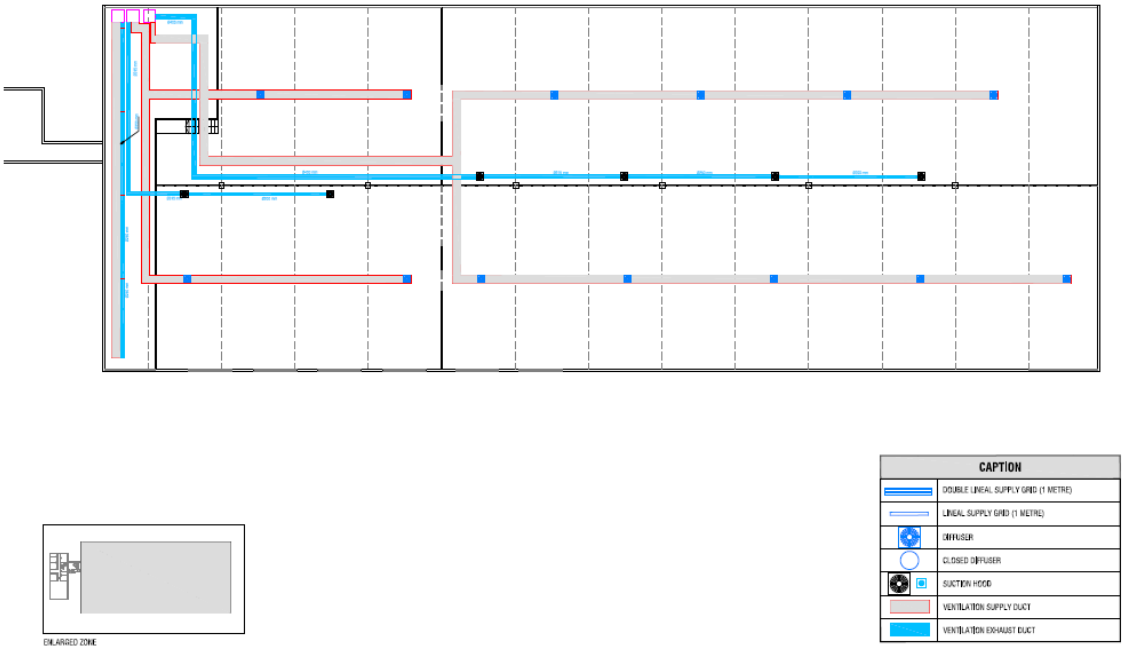

Figure 2.22. First ventilation scenario (three AHUs, one for each area) of the warehouse (Source: Estelles, 2018)

The following scenario involved combining the AHUs assigned to provide fresh air to the warehousing areas into a single unit that serves both spaces (Figure 2.23). The study aimed to identify the appropriate AHU, equipped with a heat recovery system, and design an efficient ventilation duct system to achieve energy savings through heat demand reduction.

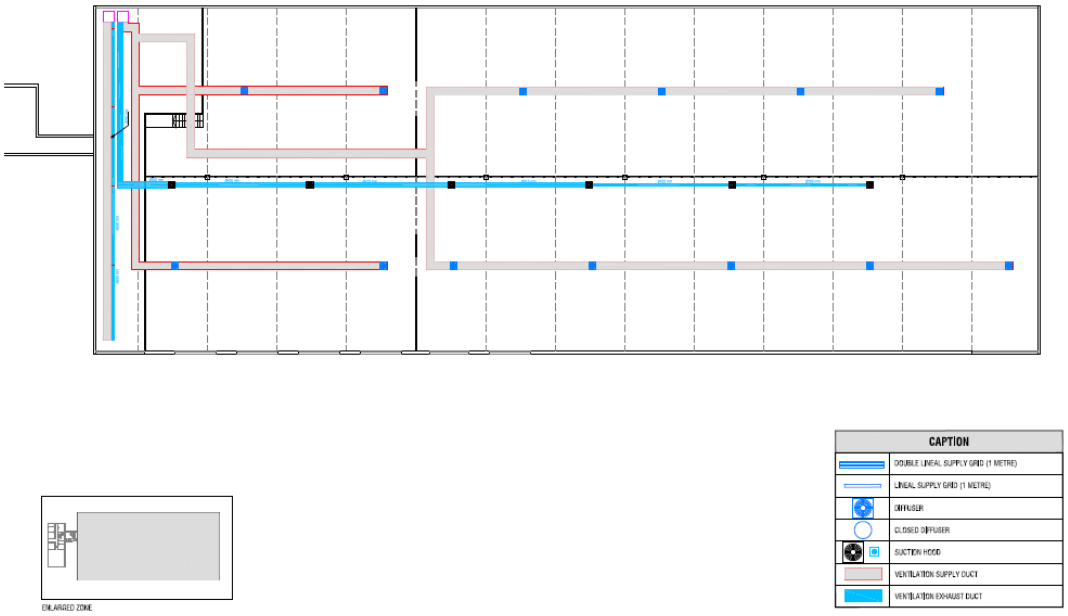

Figure 2.23. Second ventilation scenario (one AHU for the central and other areas) of the warehouse (Source: Estelles, 2018)

Mei et al. (2018) have investigated buoyancy-driven natural ventilated flows assisted by a localized cooling system with assisting mechanical fans in an industrial building by CFD models and on-site measurements. The effects of a couple of supplying vents at the ground third floor and a slab on top of it, on the cooling space below the slab, are shown in Figure 2.24.

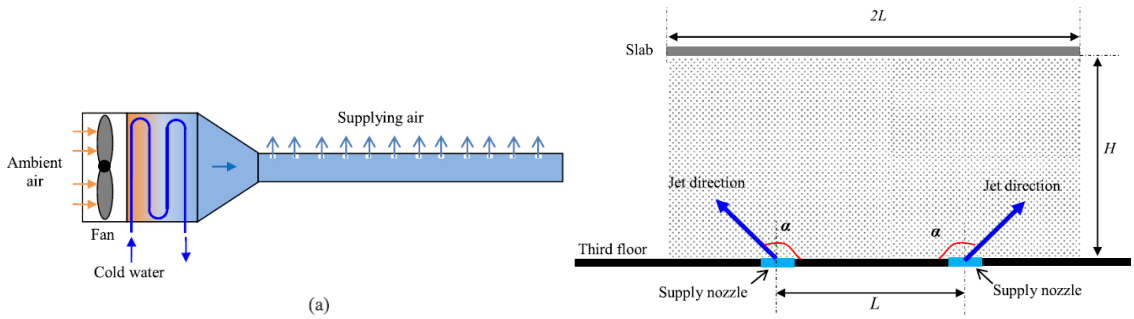

Figure 2.24. Configurations of air supplying system (a) and the position of vents and slabs at the local working zone (b) (Source: Mei et al., 2018b)

Different cooling effects of simulated scenarios are also shown in Figure 2.25. After investigating the effects of supplying air jet angle, supplying air velocity, and

supplying air temperature, the simulation results implied that decreases in air temperature and increases in air exchange efficiency are related to the ejection direction and velocity.

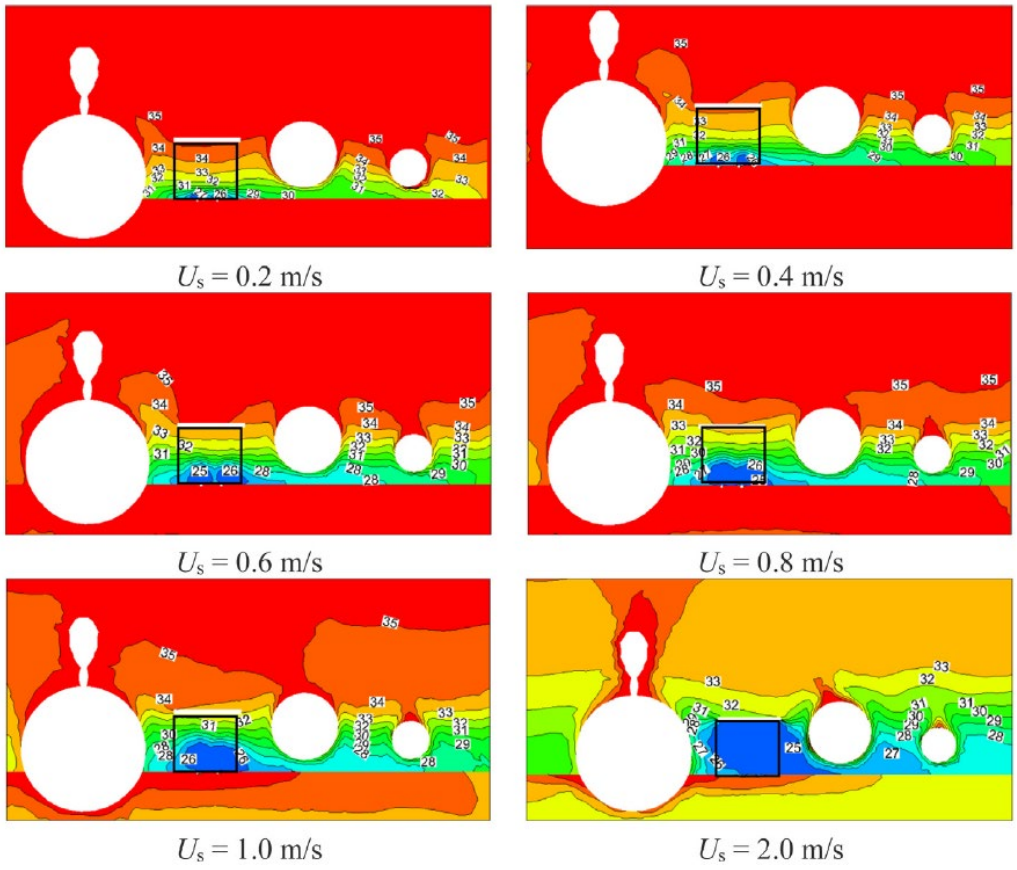

Figure 2.25. Contours of mean air temperature at the vertical (y –z) plane of (x = 30 m) within the local cooling zone with six different supplying velocities (Source: Mei et al., 2018b)

Liu et al. (2020) pointed out that air-conditioning systems have a notable influence on air infiltration in large space buildings. A CFD model of a railway station was established and installed with typical air-conditioning systems, i.e., mixing ventilation (MV), displacement ventilation (DV), and radiant floor with displacement ventilation (RF + DV).

It is indicated that a uniform vertical temperature distribution in the heating condition has the potential to reduce air infiltration rate, which is best corresponded by RF + DV. Accordingly, these can reduce the air infiltration rate in the heating condition

and save a certain amount of the heating capacity as well as reduce the air infiltration rate in the cooling condition and save some of the cooling capacity.

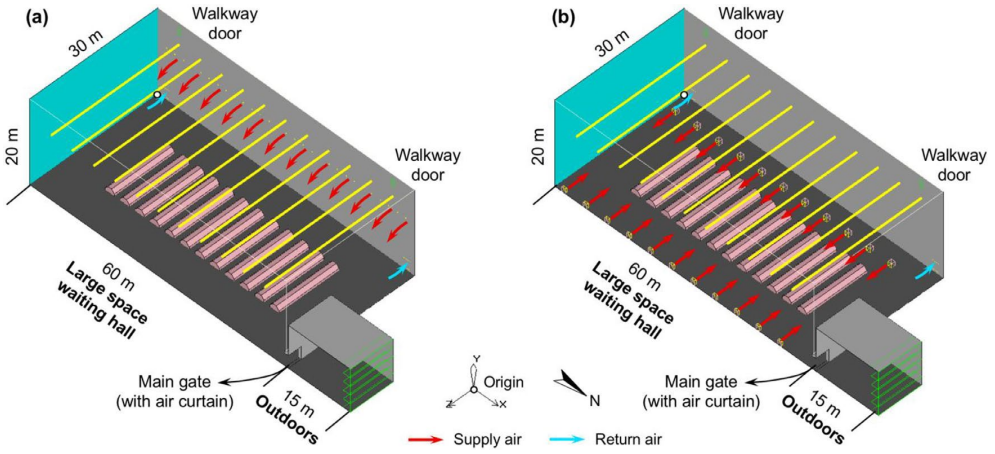

Figure 2.26. Model of the simplified building: (a) mixing ventilation subtype (MV) and (b) displacement ventilation/radiant floor subtype (DV or RF + DV) (Source: X. Liu et al., 2020)

Figure 2.27 illustrates the distributions of the air velocities at the main gate and walkway doors.

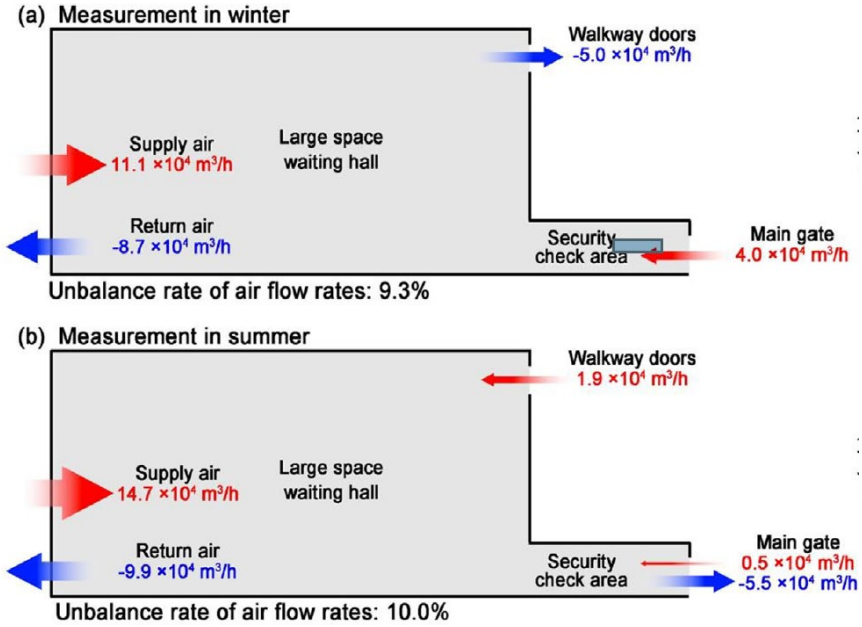

Figure 2.27. Air-volume balance in the railway station: (a) winter and (b) summer (Source: X. Liu et al., 2020)

Accordingly, three different mechanical ventilation scenarios with displacement ventilation and radiant floor with displacement ventilation analysis results can be seen in Figure 2.28. It is possible to see the impacts of different ventilation strategies on air circulation inside the volume. The stratification occurrence results depending on the selected mechanical ventilation type are also found in these figures. The balance between an increase in indoor air exchange rates and equal diffusion of air inside should be considered while making decisions about the ventilation type (X. Liu et al., 2020).

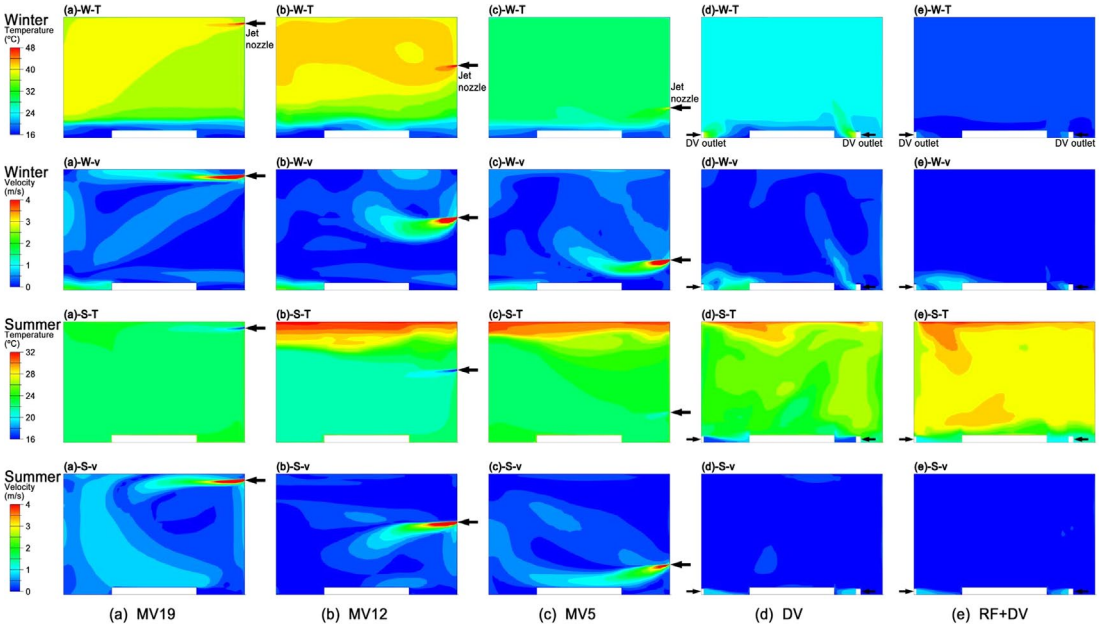

Figure 2.28. Temperature and velocity contours (cross-sectional planes)
(Source: X. Liu et al., 2020)

Regarding the existing literature, certain approaches to natural, mechanical, and hybrid ventilation systems in large space buildings are investigated. At that point, it is significant to focus on suitable strategies for case building while eliminating the inapplicable cases.

Initially, natural ventilation is one of the most common methods that's used in every type of building. It is utilized as an effective passive cooling system to significantly reduce the energy used by air conditioning systems in buildings. Besides, existing studies claim that Turkey is suitable for using natural ventilation for cooling purposes. The studies also show that natural ventilation can be used to provide a thermally comfortable

indoor environment during both the summer and the winter seasons, while indoor air quality can be maintained for all opening typologies (Ayata, 2009; Orung et al., 2016; Schulze & Eicker, 2013). The effectiveness of summer cooling and thermal comfort in buildings is heavily influenced by the chosen natural ventilation strategy. Proper control over the openings plays a critical role in all scenarios, as improper regulation can result in excessive cooling or overheating of the indoor spaces.

In addition, the selected warehouse building is in use, and the openings are placed in certain positions. Accordingly, it is significant to focus on directing incoming air inside the volume, and proposing various additional elements that can direct air through the openings. Besides, daily behavior of outside air needs to be observed so that control strategies on openings for increasing natural ventilation quality might be produced. On the other hand, considering various types of mechanical ventilation systems, or analyzing several methods to find out the optimal solution has more potential to study providing a combined natural and mechanical ventilation approach. It is possible to make various inferences about ventilation system applications to the case building.

At that point, hybrid ventilation strategies gained more importance. Hybrid ventilation is aimed at securing as much benefit as possible from natural ventilation while taking advantage of the added security of mechanical ventilation. Three typical types of mixed-mode systems should be considered for the current study, namely alternate use of natural and mechanical ventilation, fan-assisted natural ventilation, and concurrent use of natural and mechanical ventilation.

During the decisions about the hybrid ventilation system to be applied, the natural ventilation mode, the mechanical ventilation mode, and the control strategies should also be analyzed. In this way, it can be possible to identify issues such as the point at which natural driving forces fail to fulfill ventilation demand and the periods when mechanical ventilation is more energy efficient than natural ventilation. During these studies analysis methods are needed to perform some significant tasks such as to size ventilation systems for both ventilation modes, to evaluate system performance, e.g., indoor environment conditions and thermal comfort parameters; to select the control and ventilation strategies for optimum energy efficiency; to evaluate heat transfer processes, pollutant dispersion, energy consumption, and life cycle cost, etc.

CHAPTER 3

RESEARCH APPROACH AND METHODOLOGY

This research involves mainly on-site studies and three cases with various methodologies used separately for each case. The framework of the study and these three cases is shown in Figure 3.1. The general workflow of the research is generated under two main headings. The first section of the study includes experimental measurements which are conducted on-site. The explanations about the case building are explained under subsection 3.1.

Numerical analyses are examined in the second section under three different cases. The second column in the figure shows these main headings. While the branches of numerical analyses are shown under the following columns as Case A, B, and C. Experimental measurements are explained under four sections. On the other hand, Case A included energy performance analyses while Case B and C are used for conducting the CFD analyses. These three cases are explained comprehensively in subsections 3.2 and 3.3. The last column of the figure shows the detailed explanations of these subsections.

<table>
<tr><td rowspan="4">EXPERIMENTAL MEASUREMENTS</td><td colspan="3" rowspan="4">Case Building (Section 3.1)</td><td>Introduction of case building</td></tr>
<tr><td>Climatic conditions of the building location</td></tr>
<tr><td>Measurement equipment installation</td></tr>
<tr><td>On-site measurements</td></tr>
<tr><td rowspan="6">NUMERICAL ANALYSES</td><td rowspan="3">CASE A (Section 3.2)</td><td rowspan="3">Energy performance analyses</td><td colspan="2">Extracting the simulation weather data from Case Building chapter, section 2</td></tr>
<tr><td colspan="2">Conduction of energy performance analyses with numerical background of OpenStudio and Energyplus</td></tr>
<tr><td colspan="2">Investigating the impact of architectural parameters on annual heating, cooling demands as well as operational CO_2 emissions</td></tr>
<tr><td rowspan="3">CASES B&C (Section 3.3)</td><td rowspan="3">CFD analyses</td><td rowspan="2">CASE B
Thermal Stratification</td><td>Case Building chapter, section 4 data is used for stratification analyses</td></tr>
<tr><td>Energy equations are included</td></tr>
<tr><td rowspan="2">CASE C
Indoor Ventilation</td><td>Fan properties information from Case Building chapter are used</td></tr>
<tr><td>Energy equations are not included</td></tr>
</table>

Figure 3.1. The framework of research methodology

Initially, on-site measurements are conducted to gather temperature, relative humidity, and CO_2 concentration data about the target building. Secondly, Case A includes energy performance analyses to observe the impacts of various architectural parameters on annual heating, cooling demands, and operational CO_2 emissions of the building. Finally, in Cases, B&C, the collected data, along with relevant building information, serve as the basis for subsequent numerical simulations aimed at reconstructing the thermal stratification conditions within the building.

Utilizing a CFD model capable of representing the building's thermal characteristics, simulations are conducted to explore the effectiveness of different indoor environment strategies. Case B is generated to analyze the thermal stratification occurring inside the warehouse. By integrating the energy equations into the CFD model and using on-site measurement data, vertical temperature gradience inside is observed. On the contrary, in Case C, energy equations are not included, instead fan properties are integrated into the model and indoor ventilation conditions are investigated. Specifically, hybrid ventilation models incorporating both mechanical and natural ventilation methods are employed, and design solutions for enhancing energy efficiency are investigated. The objective is to assess the impact of various settings on reducing energy demand within the building.

3.1. Case Building

The warehouse building selected as the case study is a tobacco warehouse building located in İzmir, a city in the west of Turkey. The city has a typical Mediterranean climate which is characterized by hot humid summers and mild winters.

The building is located in Torbalı which is far from the seaside and located at the inner part of İzmir. Field experiments are carried out in this building. The building is inside an industrial building complex manufactured by Alliance Tobacco Inc. Even though the complex is constructed in 2002, the selected storage building is built in 2016. The current location of the building is shown in Figure 3.2.

Figure 3.2. The location of the case study

The building is arranged on the south-north orientation with a surrounding of several other large-scale industrial buildings as can be seen in Figure 3.3. The building is based on the floor plan and construction of a typical existing storage building in Turkey.

Figure 3.3. The tobacco warehouse with surrounding buildings

The storage space has air inlets on each sidewall as well as transportation doors on north-south facades. There are two axial fans located on the external walls. During colder weather, the sidewall air inlets are open at specific hours, allowing uniform fresh air to enter inside. In warm weather, the place is conditioned mostly naturally, while relative humidity conditions are tried to be balanced with the help of conditioning processes applied to stored tobacco stacks. The storage is mostly collected along the length of the warehouse from north to south.

3.1.1. The Climate Data

The selected building for the case study is in İzmir, Turkey. The weather conditions for the studied city are mostly hot, humid in summer, and rainy in winter, as a representation of the Mediterranean climate.

The proximity to the Aegean Sea makes summer and winter relatively temperate, summers are hot and dry in contrast to mild and rainy winters, as well. July and August are the hottest months of summer, and January and February are the coldest of winter. The average maximum temperature is around 38°C during the summer period, whereas the average minimum in winter varies between 0°C and -3°C. Besides, the annual mean temperature is approximately 17.9°C, while the mean relative humidity is around 65% (TSMS, 2022).

The climate conditions of the area can add to the internal gains of a building, causing excessive heat gains if care is not taken to control it, particularly in the warmer months of the year. Many commercial buildings in Turkey use much more energy over the course of a year for cooling than they use for heating, because of large areas of unshaded glazing and poorly insulated opaque surfaces that absorb and transfer large amounts of solar radiation into the building. While high levels of solar radiation can cause excessive heat gains, they also indicate a potential to utilize a photovoltaic system efficiently. Design solutions may allow for the incorporation of photovoltaic systems, as well.

3.1.2. Indoor Environment Conditions

In warehousing, the quality of the stored raw material is among the priority issues to ensure continuity in line with the indoor air quality of the environment and systematic approaches. Air exchange coefficient, indoor temperature, humidity values, and CO_2 concentration are the most important parameters in determining indoor environment conditions in large-volume storage buildings (Childs et al, 1970; Xin et al, 2018; Liu et al., 2020).

When the criteria are examined, it has been found that the internal air exchange coefficient in the storage structures should be around 6 ACH (Scharnow, 1986). When this value is exceeded, there is a risk of drying, breaking, and fragmentation of tobacco leaves. In addition, due to the nature of tobacco, the importance of fixing this coefficient increases due to the increase in the CO_2 concentration as the fermentation continues constantly. Therefore, it is necessary to measure the CO_2 level in the indoor environment. Accordingly, 1500 ppm provides adequate air quality, while 1400 ppm and below indicates that the indoor air is in good condition in most cases (CEN, 2019; Active House Alliance, 2020).

Tobacco must be at certain temperature and humidity values, as well. The tobacco temperature to be supplied should be approximately 21-25°C and the moisture concentration of tobacco should be about 13% (Scharnow, 1986). The relative humidity ratio inside the volume should also be between 50-65%. If the required humidity balance is maintained, it is not an issue that the environment in which the tobacco is stored may reach low or high temperatures for a short time from time to time. However, if the required relative humidity is not achieved or is higher than the optimal range, tobacco bales start to discolor and the leaf quality decreases.

Stacking of the tobacco bales is standardized with universally same-sized boxes as well as the external frames (Figure 3.4). In the current structure, the storage zone is carried out with maximum capacity in many months of the year. Due to the intensive placement of the containers where the tobacco is stored, it is quite difficult to provide adequate ventilation homogeneously and to provide the desired conditions. At the same time, there are likely dead zones in space. Along with the high temperature in the outdoor environment, high-temperature values which can be dangerous for tobacco are reached in the indoor environment and temperature stratification is observed in the space.

Figure 3.4. Storage of tobacco bales inside the warehouse

Internal and external temperature measurements are taken hourly and continuously from one point in the warehouse. The internal temperature measured values are the average of the temperature values taken from one measuring point in each of the four adjacent warehouses that interact with each other through open doors, and there is no significant difference between the tanks in the hourly measured values. The temperature sensors are regularly calibrated at intervals of 6 months and are approximately 12 meters above the ground.

The risk of deterioration in the stored tobacco increases due to the outdoor temperatures rising during the summer months and reaching the maximum levels in July-August and September since the structure is in a hot and humid city like İzmir. Due to these instabilities throughout the year, natural and mechanical-driven solutions are needed to provide the necessary indoor conditions throughout the period when tobacco is stored intensively. During the solutions to be produced, at least 12-month temperature fluctuations are needed to be monitored to prevent these problems, since they are not only seasonal but also a year-round problem, and it is of great importance to produce solutions by analyzing the measured data.

3.1.3. Measurement Setup

The measurements were carried out over the course of one year in a tobacco bale storage warehouse equipped with two fan systems, located in İzmir, Turkey (38°12'18.0"N, 27°22'01.7"E). The building is part of a tobacco industrial complex and

is divided into four zones. One of the zones, highlighted in red in Figure 3.5 was selected for the measurements and designated for storage purposes. The building is oriented in a North-South direction and measures 83 meters in length and 27 meters in width. The sidewall height is 12.5 meters, and the rooftop height is 14 meters.

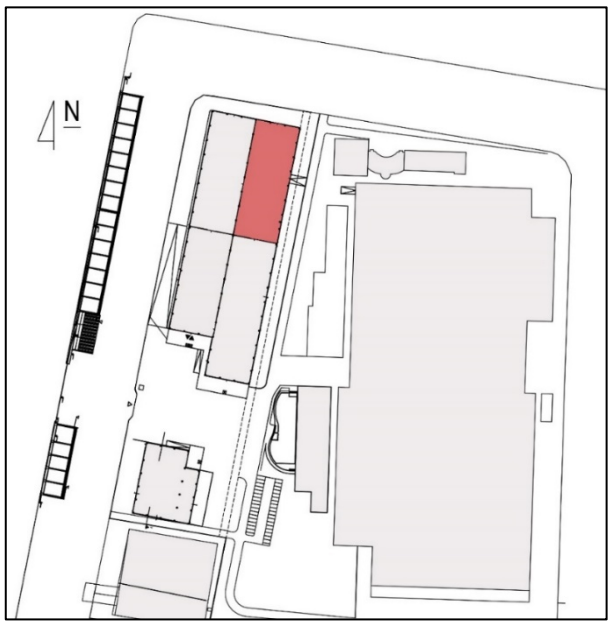

Figure 3.5. Location of the selected building

Field measurements of the warehouse started on 2020, June 16, and ended in 2021, on November 8. The temperature, relative humidity, and CO_2 concentration values are measured at different heights using Green Eye–Desktop Environmental Monitor (Figure 3.6).

Figure 3.6. The data logger, Green Eye – Desktop Environmental Monitor

The vertical spacing among data loggers was adjusted according to the ceiling height of the measured building which is 14.5 m at the highest point. The distance between data loggers is 2.5 m so a total of five points were measured vertically (Figure 3.7).

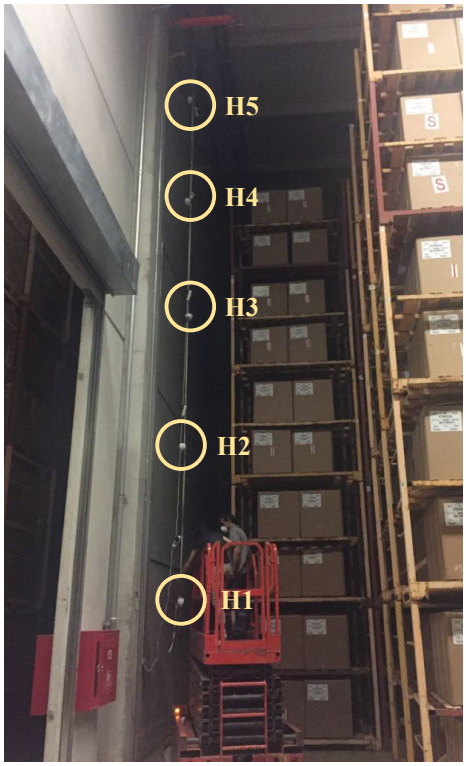

Figure 3.7. Installation of the data loggers for field measurements

Every month, the data is transferred to the computer via a USB connection to collect and store data from the loggers regularly. Temperature, relative humidity, and CO_2 readings were taken every five minutes. The uncertainties were quantified as CO_2 (±50 ppm); humidity (±3% [10% to 90%]); temperature (±0.6°C) for data loggers used. The outdoor temperature values are requested from the company, the data collected belongs to the setup that has already been applied outside of the building.

3.1.4. On-site Measurements

The data loggers are numbered from 1 to 5 and indicated as H1, H2, H3, H4, and H5. The lowest number indicates the data logger placed at 2m which is the lowest level,

while the fifth logger is for the data logger located at 12 m. The numbering of the lines in figures is assigned accordingly.

As indicated in Figure A.1, Figure 3.8, Figure 3.9, and Figure A.2; starting from June until September (mostly in July and August) the highest temperature values are observed. The green band in the figure indicates the critical indoor temperature required for optimal tobacco storage conditions. Accordingly, it is seen that these months are the most critical period inside the warehouse. The 21-25°C range is accepted as the maximum limit of inside temperature; however, the temperature is always higher than the limits. These are the most significant months to be considered while designing inside air conditioning systems.

The risk of deterioration in tobacco bales caused by higher temperatures is one of the most dangerous factors in terms of affecting the quality of tobacco leaves. Therefore, natural, mechanical, or hybrid ventilation solutions are needed to provide optimal environmental conditions within the volume.

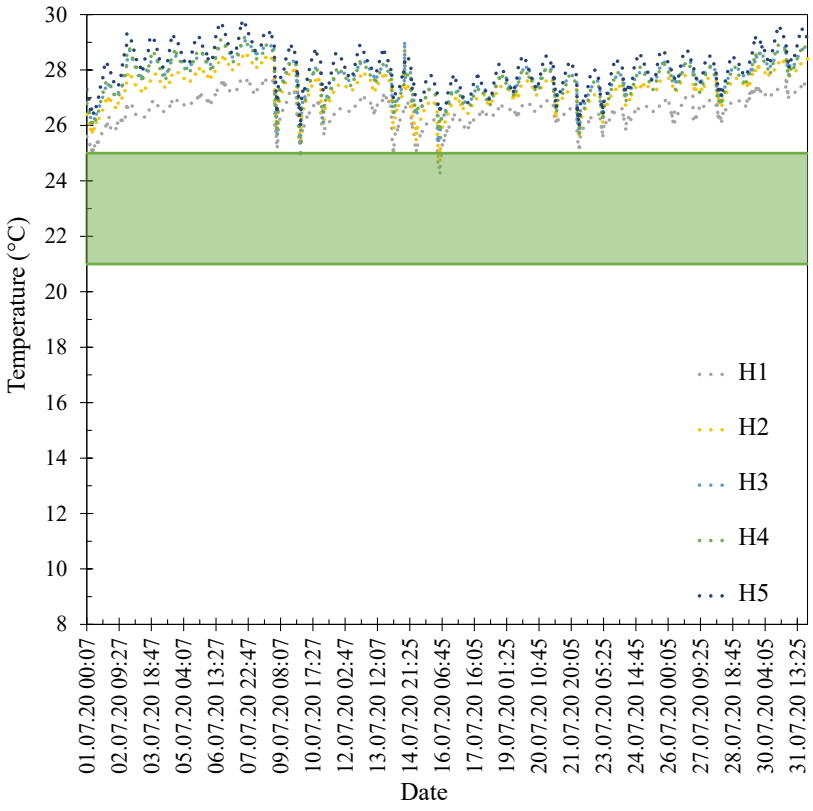

Figure 3.8. Inside temperature measured in July 2020

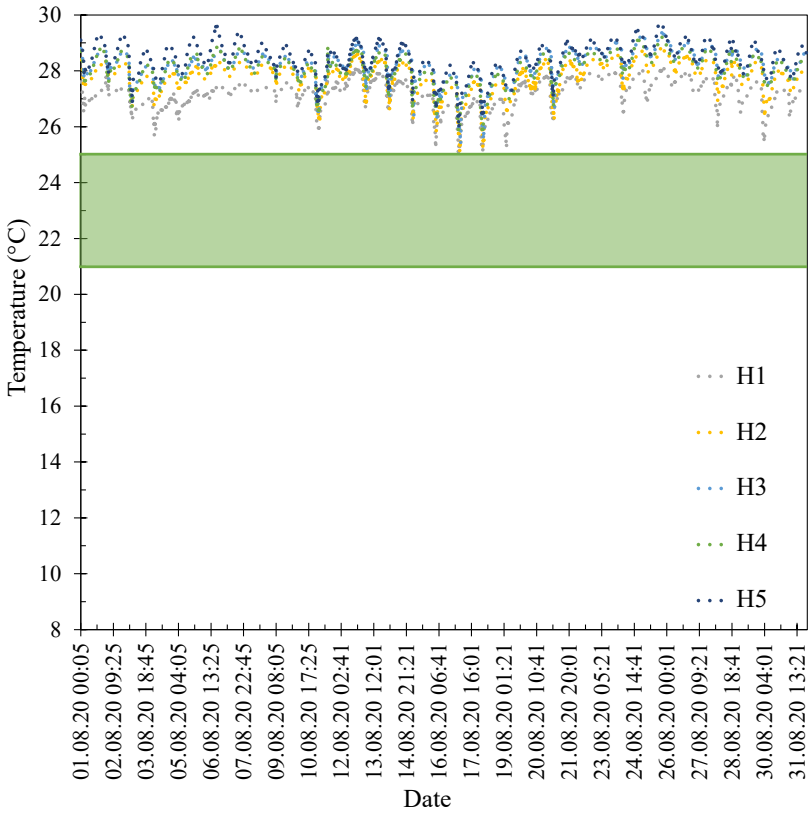

Figure 3.9. Inside temperature measured in August 2020

Although September is the month that temperature drops are observed, the thermal conditions of the warehouse are still not low enough to be within the acceptable range. On the other side, since the temperature continues diminishing after mid-October higher temperature risks disappear so that the values get lower than 21°C. The detailed representation of these changes is shown in Figure A.3.

The temperature stays within acceptable ranges in October and continues diminishing during the following months until June. The temperature decreases can be followed by the figures between Figure A.4 and Figure A.7. It is seen that high-temperature values are no longer a major problem and there will be no need for mechanical ventilation support within this period. Even though the temperature rises, and decreases are observed during these months, it is always under the critical limits of required values for the ideal storage conditions of tobacco bales.

Since the measured values in June, July, August, and September 2020 are the most critical periods in terms of increasing temperature, it is important to observe the same period in 2021, as well. Figure A.8, Figure A.9, Figure A.10 and Figure A.11 cover these

months and it is seen that the same critical temperature trend is observed in these months again. However, the comparison between the values of September shows that the values are lower in 2021 than the previous year. Besides, Figure A.12 shows the temperature trend in October, and the values are back in the acceptable limits.

Starting from October until February temperature values continue diminishing until almost 12°C. The increases are observed starting from the beginning of March. It is possible to see that higher temperature values are closer to the limit range while temperature drops reach significantly lower points between January and March.

On the other hand, as shown in Figure 3.10, Figure 3.11, and Figure 3.12, the coldest months are January, February, and March. The temperature is below 20°C in January and it drops down to 8°C in February. These fluctuations cause a temperature difference between the optimal conditions which is 13°C lower than the minimal acceptable temperature for optimal storage conditions.

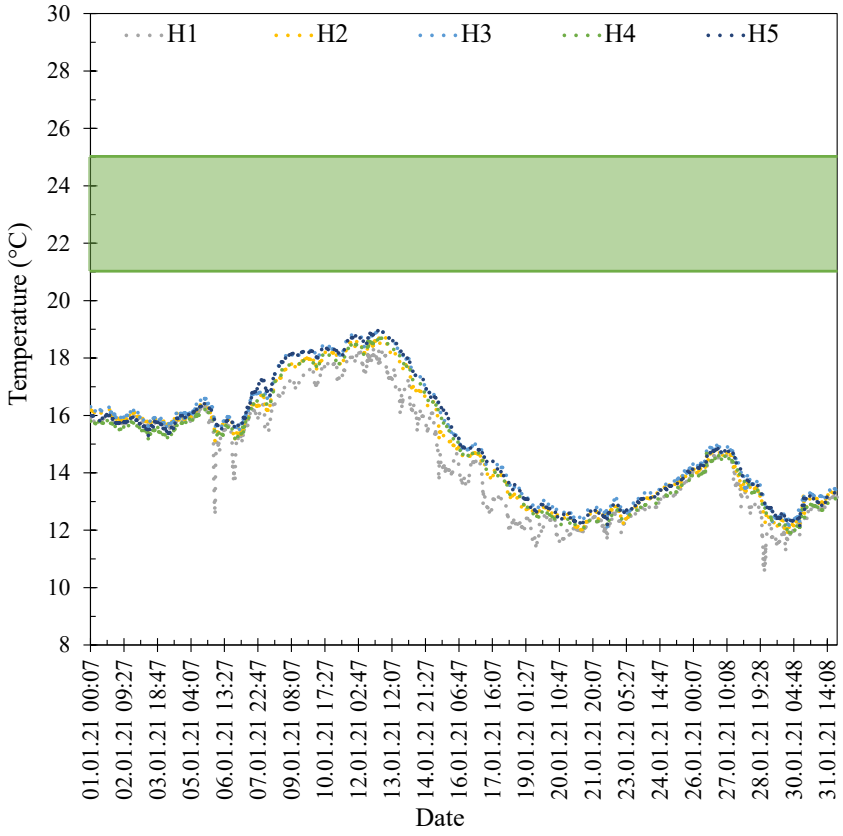

Figure 3.10. Inside temperature measured in January 2021

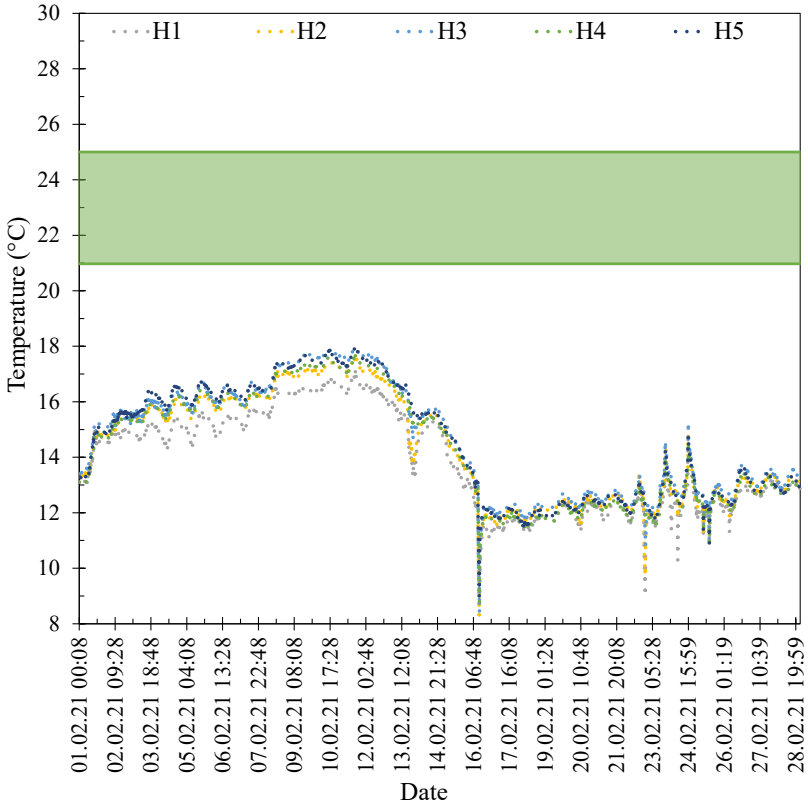

Figure 3.11. Inside temperature measured in February 2021

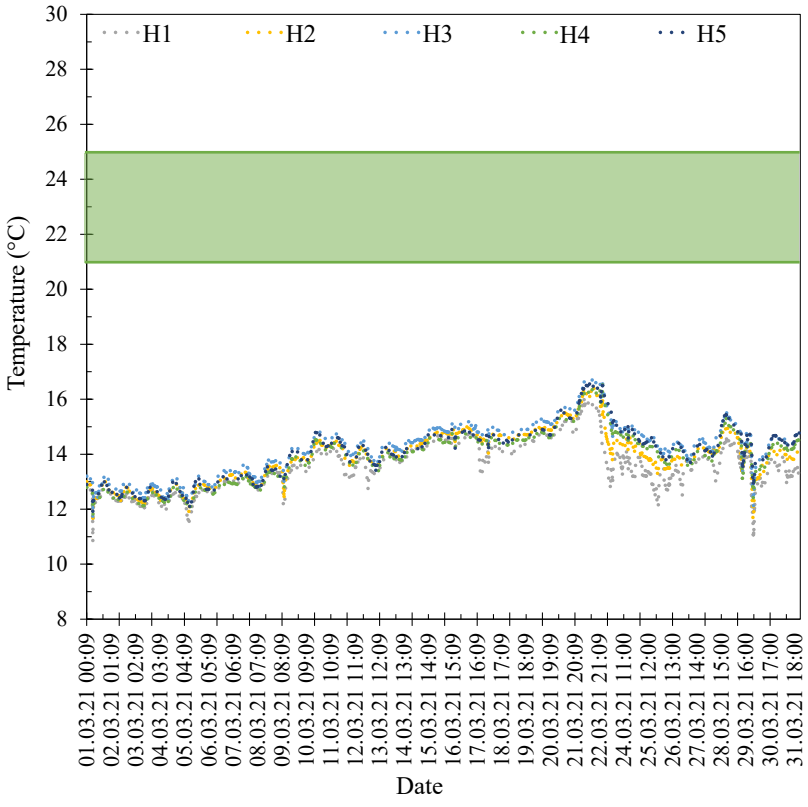

Figure 3.12. Inside temperature measured in March 2021

The observations about the comparison between the same months of 2020 and 2021, concurrent months are analyzed in figures between Figure B.1 and Figure B.5. The comparison includes June, July, August, September, and October in 2020 and 2021.

H1-2020, H2-2020, H3-2020, H4-2020, and H5-2020 symbols are used for the values collected from the months in 2020, while H1-2021, H2-2021, H3-2021, H4-2021, and H5-2021 show the temperature trends of the months in 2021. Initially, all five figures show that the temperature values are similar between June and August, whereas the values are lower in 2021. The difference increases every month and reaches its highest point in October.

Since each figure belongs to different levels in the volume, it is possible to see that, as the measurement level within the volume increases, the temperature values of each year get closer to each other. Figure B.5 represents the closest temperature trends that belong to the +12.5 m level inside the warehouse.

Lastly, statistical numbers about CO_2 concentrations also point out several significant issues. One of the critical months in terms of the amount of CO_2 gases is November and December. Moreover, maximum amounts in these months also show that the concentration sometime increases so much that the values reach over 4000ppm which is significantly higher than the acceptable range. The overall framework of the inside temperature, relative humidity, and CO_2 concentrations and their numerical explanation can be seen in Table 3.1.

Table 3.1. Statistical properties of inside temperature, relative humidity, and CO_2 concentrations inside the warehouse

	June	July	August	September	October	November	December	January	February	March
Average Air Temp.	25.5	27.5	28.0	26.0	22.0	19.6	18.1	14.9	14.3	13.9
Max. Air Temp.	27.1	28.9	29.0	28.2	24.3	20.2	20.7	18.8	17.6	16.3
Min. Air Temp.	24.3	25.3	25.7	22.0	18.9	18.2	14.6	12.0	8.7	11.5
Air Temp Stand. Dev.	0.6	0.6	0.5	1.1	1.1	0.2	1.8	2.0	1.9	1.0
Average RH	62.5	58.2	56.1	56.5	58.8	64.8	65.6	65.7	61.2	62.9
Max. RH	66.0	66.5	65.8	67.7	78.3	73.4	74.2	80.1	72.9	71.7
Min. RH	38.1	45.7	40.0	47.5	38.2	41.7	49.4	47.6	38.0	50.2
RH Stand. Dev.	3.3	3.8	3.5	3.3	7.5	5.3	5.1	7.1	7.7	5.1
Average CO_2 Conc.	909.7	645.7	603.8	439.2	632.5	1672.1	1136.4	780.1	766.5	1290.8
Max. CO_2 Conc.	1576.5	1057.1	1115.4	611.0	1633.4	4228.8	4225.6	2035.0	1661.0	2779.0
Min. CO_2 Conc.	333.6	354.6	396.0	388.0	387.0	156.8	189.2	343.0	335.8	388.4
CO_2 Conc. Stand. Dev.	304.6	171.1	124.7	39.0	290.2	1015.7	969.3	363.8	246.6	619.6

It is also important to analyze relative humidity ratios inside the warehouse since the acceptable limit is between 50-65 %. Therefore, keeping the humidity between these values is crucial for the quality of tobacco as well as avoiding deterioration in tobacco leaves. The general trend of relative humidity ratios inside the warehouse within 2020 June and 2021 October is visualized in Figure 3.13.

The green-colored band is the acceptable range for optimal humidity levels in warehouses. Higher values than the acceptable range are deteriorating for stored products (tobacco in this case). Even though the decrease in relative humidity around the summer period is observed, it is possible to say that the remaining times of the year will not be considered a threat to the stored tobacco bales.

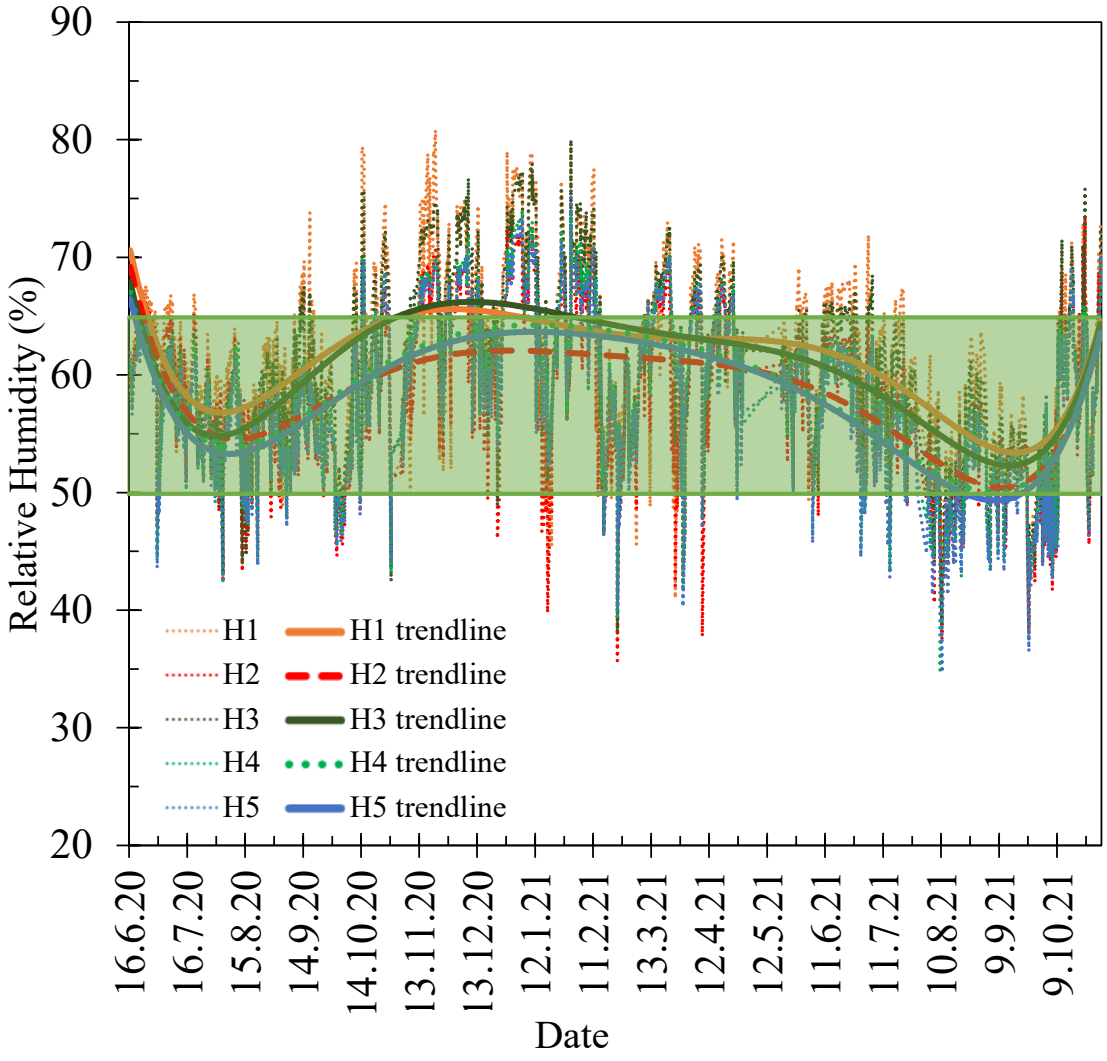

Figure 3.13. Relative humidity ratios measured between 2020 June and 2021 October

The CO_2 concentrations measured in the storage are shown in Figure 3.14. The red line shows the critical limit for the gas density within storage which is indicated around 1500ppm. A significant number of increases are stated only around November and December. Even though there are instant rises of concentrations because of the movements near the data loggers during tobacco bale transportation.

The trendlines show that critical limits are not exceeded significantly throughout the measurement period. Therefore, it is possible to see that CO_2 concentration fluctuations are not one of the concerns related to the case building.

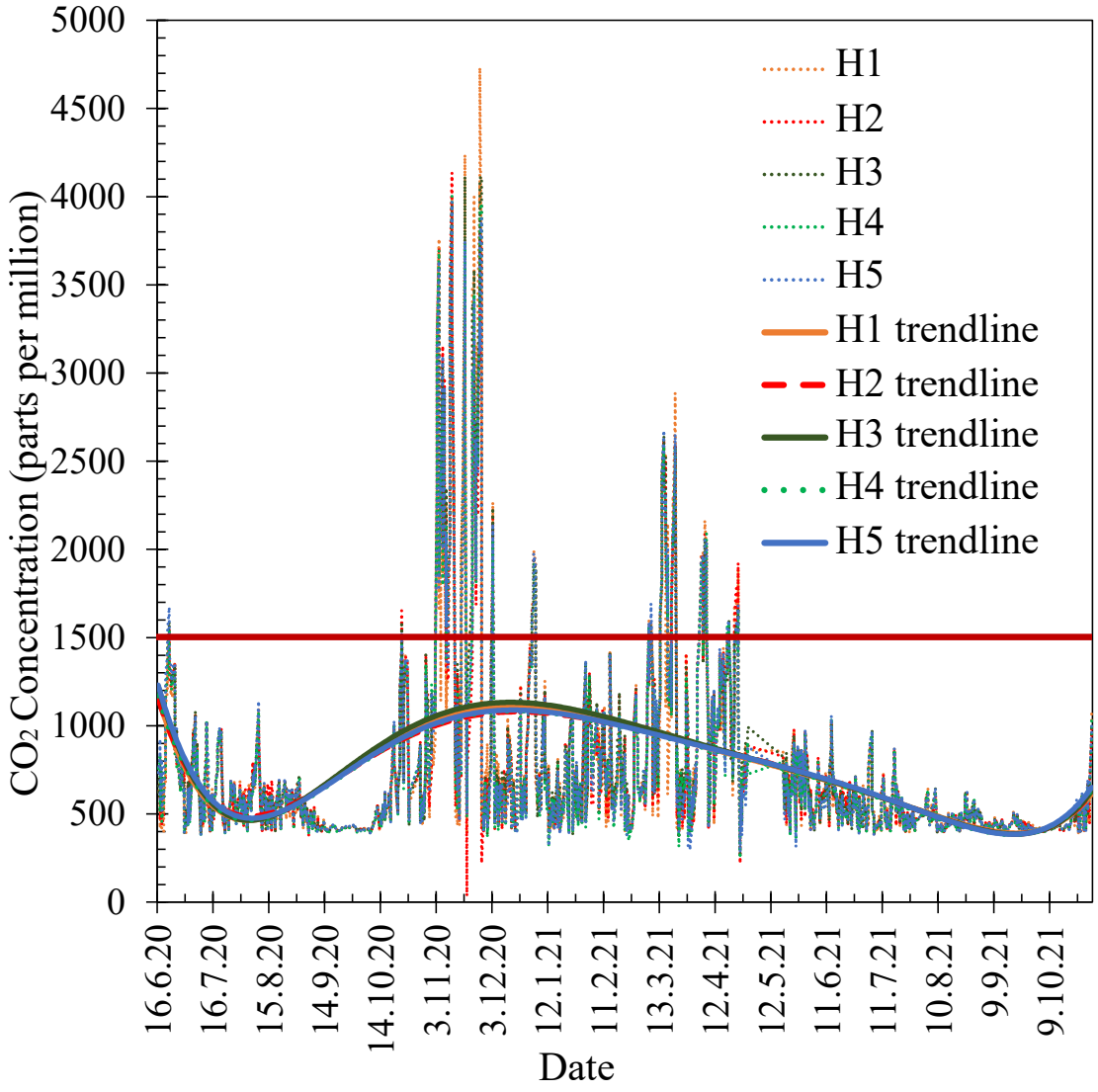

Figure 3.14. CO_2 concentrations measured between 2020 June and 2021 October

3.2. CASE A: Energy Performance Analyses

3.2.1. Energy Simulation Model

The energy performance analyses are conducted after generating the computational model and accuracy validation. The energy performance analyses are carried out in OpenStudio and EnergyPlus programs. An OpenStudio model has been generated for the energy analyses of the building (Figure 3.15).

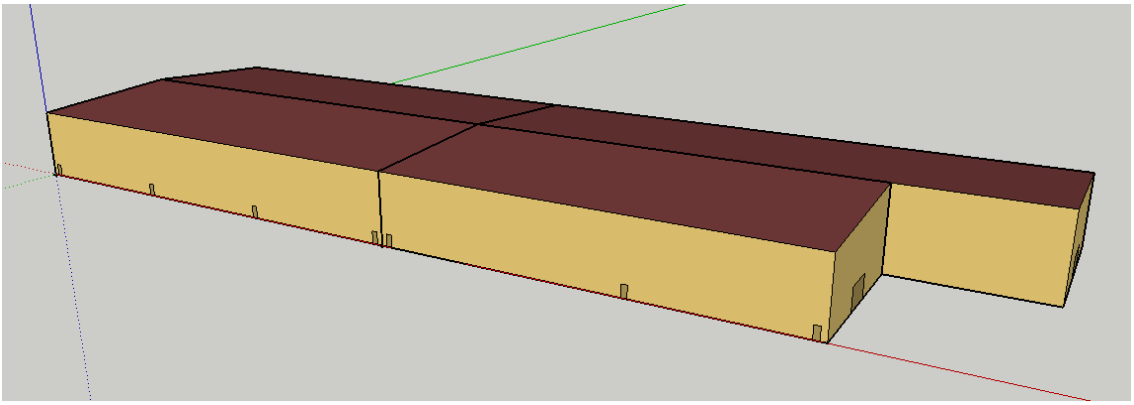

Figure 3.15. Three-dimensional OpenStudio model of the case building

The overall warehouse building contains four different storage zones and the reference volume for the current study is indicated in Figure 3.16. The dimensions of this zone are about 85 m x 29 m. The area of the studied storage zone is around 2500 m^2 and the volume of the reference space, where the highest point of the roof is approximately 14.5 m, is around 35000 m^3.

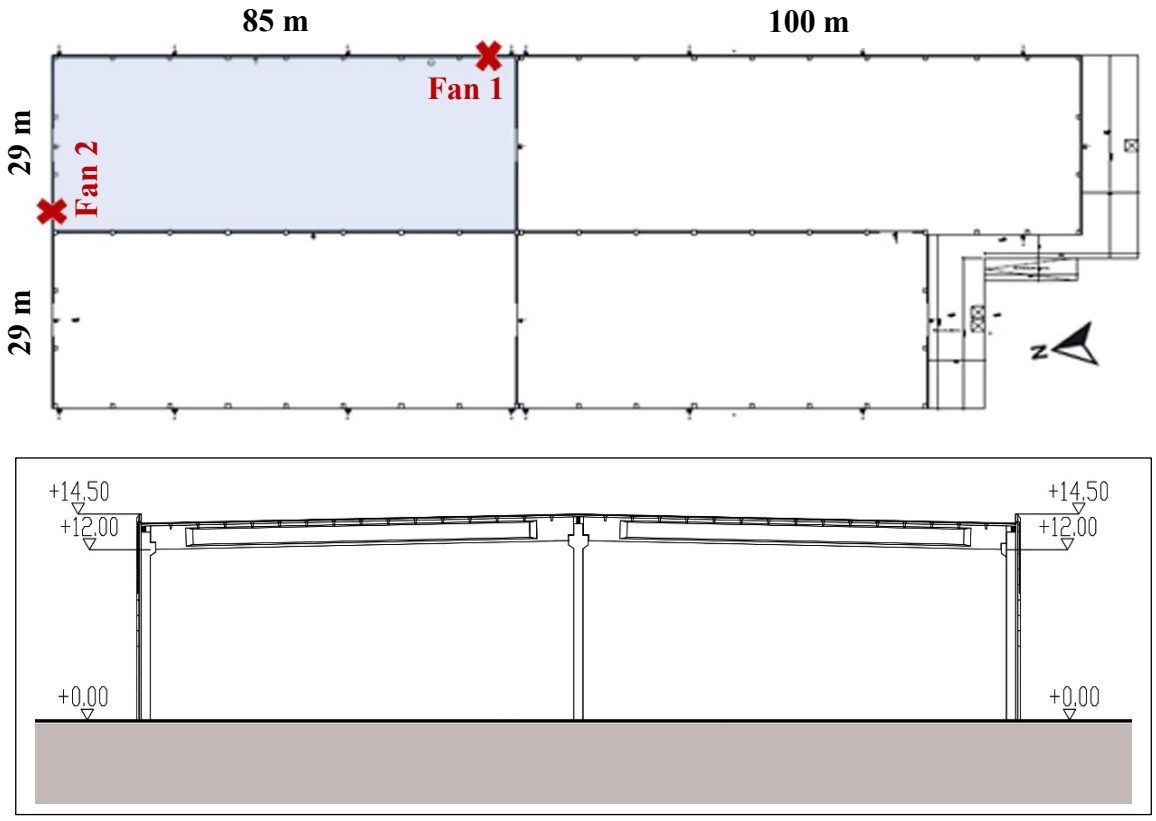

Figure 3.16. Schematic plan (up) and section (down) of the storage zones

To account for the large volume of stored product zones and the presence of thermal stratification within these zones, various techniques have been investigated to replicate these conditions in computer-based models. Barbaresi et al., (2015) conducted a study on wine storage warehouses, focusing on the necessary conditions to maintain specific indoor temperatures for optimal wine preservation.

The study aimed to identify an effective and efficient modeling approach suitable for common types of wine storage buildings. One of the objectives was to evaluate the reliability and accuracy of different solutions for discretizing the internal volume into thermal zones using horizontal "airwalls." This evaluation was based on comparing the outputs of digital simulations with real thermal data recorded in practice.

Two different modeling approaches were analyzed using EnergyPlus thermal simulation software. The internal space was modeled as consisting of either one or two thermal zones. The simulation results were then compared with three years of monitored data from a specific case study, followed by a validation and acceptability procedure. The findings demonstrated that the method employed was a reliable tool for assessing the

reliability of results in aboveground building modeling. Moreover, the appropriateness of using "airwalls" as horizontal partitions was confirmed.

Therefore, the zone selected for the studies has been divided into five levels by using air walls (Figure 3.17). The positioning of the air walls has been decided according to the temperature differences observed from field measurements. The horizontal placement of the air walls in the computer-based model can also be seen in the figure.

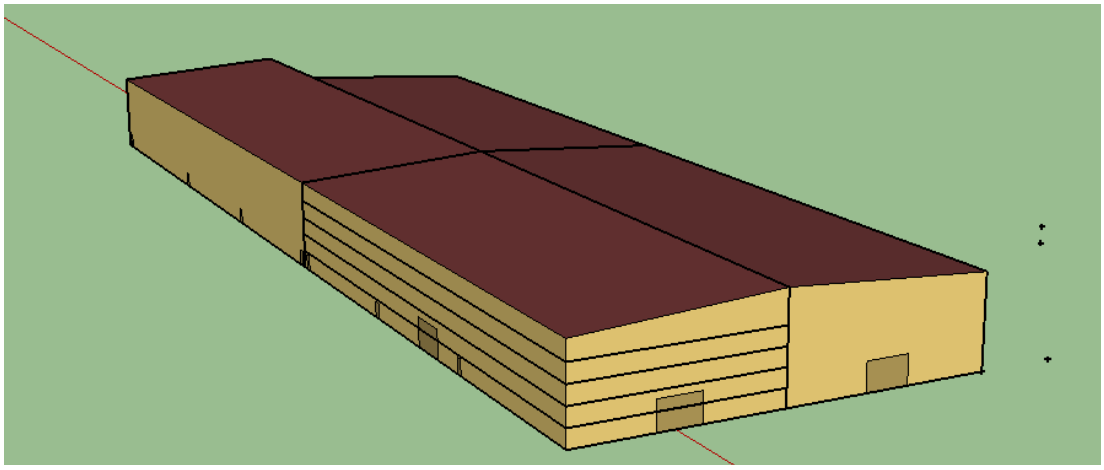

Figure 3.17. The usage of air walls for thermal stratification modeling

After the modeling process of the building, materials, and the occupancy schedule of the warehouse are defined comprehensively within the program. The climate data of İzmir is also imported into the program as well as the definitions of the building type (defined as warehouse) and no forced ventilation tool has been specified for this case.

3.2.1.1. Calibration of the OpenStudio Model

Calibration is an important procedure after modeling in terms of having a reliable design. “ASHRAE 14 guideline 14-2002: Measurement Energy and Demand Savings” (ASHRAE, 2002b), calibration method is followed to standardize the OpenStudio model. ASHRAE 14 guideline 14-2002 suggests calculating and checking different statistical indicators. Two of these indicators are selected for the current study. One of them is *Mean Bias Error (MBE)* and the other is the *Coefficient of Variation of Root Mean Square (CV(RMSE))*.

MBE (Mean Bias Error) represents the average error of a set of data. It serves as a crucial indicator of how well the simulated data aligns with the regression line of the sample. In Eqn. 3.1, m_i denotes the measured value, s_i represents the simulated value, and n corresponds to the total number of measured data points. A positive MBE indicates that the model is under-predicting the measured data, while a negative MBE suggests over-prediction.

$$MBE = \frac{\sum_{i=1}^{n}(m_i - s_i)}{n} \qquad \text{Eqn. 3.1}$$

CV(RMSE) (*Coefficient of Variation of the Root Mean Square Error*) quantifies the extent of variability in the errors between the measured and simulated values. It is indicated as the model's capacity to calculate the overall load pattern shown in the data. The mean of measured values is indicated with the $\overline{m}$ in Eqn. 3.2. In this case, the value of p is suggested to be one (Reddy et al., 2006).

$$CV\ (RMSE) = \frac{1}{\overline{m}}\sqrt{\frac{\sum_{i=1}^{n}(m_i - s_i)^2}{n-p}} \times 100\ (\%) \qquad \text{Eqn. 3.2}$$

After generating the simulation model, initial simulation results are obtained, and the calibration procedure is conducted accordingly. The uncertainty of the data loggers is taken into consideration with ±1.0°C for temperature and ±3.5% for relative humidity. During the calibration, several modifications and improvements have been carried out including thermophysical and operational properties of the warehouse and they are listed below:

- Since the capacity of the warehouse is almost full every time, the schedule set is arranged accordingly. The lighting and electric equipment schedule is included along with the operational data collected from the interview with the staff.
- The volume of the warehouse has been divided into five zones vertically while analyzing the differences between different levels. Therefore, the identification of zone ventilation design flow rate has been modified for each zone so that air infiltration and ventilation conditions of the volume have been improved.

- Metal sandwich roof panels, concrete wall panels with insulation as well as detailed floor layers have been modified according to the information provided by the factory.

Hourly measurements and simulation results are used for the *MBE* and *CV(RMSE)* calculations. In Table 3.2, the MBE and *CV(RMSE)* are displayed for both temperature and relative humidity.

Table 3.2. Calibration results of the OpenStudio Simulations

		Temperature (°C)		Relative Humidity (%)	
	Height	MBE (%)	CV (RMSE) (%)	MBE (%)	CV (RMSE) (%)
July	2m	7.14	13.05	6.58	27.71
	4m	-7.08	15.67	21.04	35.10
	6m	-7.36	15.53	19.86	35.58
	8m	-5.94	15.11	18.87	33.72
	10m	7.93	11.01	3.92	36.19
August	2m	8.67	14.17	27.54	38.15
	4m	-6.34	15.76	7.31	26.52
	6m	-6.47	15.64	8.69	27.56
	8m	-5.42	15.28	6.09	24.98
	10m	8.94	12.13	23.15	43.44
September	2m	5.22	12.61	18.06	32.20
	4m	-9.88	17.71	7.53	28.45
	6m	-9.71	17.49	13.15	31.00
	8m	-9.64	17.62	7.80	27.71
	10m	8.94	10.34	19.14	44.37

According to ASHRAE Guideline 14 (ASHRAE, 2002b), obtained *MBE* value must be within ±10% and the *CV(RMSE)* value must be within ±30%. The temperature *MBE* and *CV(RMSE)* are within the ASHRAE Guideline 14 limits (ASHRAE, 2002b). However, the relative humidity error values are mostly out of scope for each indicator. The complex characteristics of the tobacco and thermal conditions of the tobacco warehouse prevent simulating the relative humidity fluctuations.

3.2.1.2.Building Performance Assessment

The relative importance of the design parameters for a tobacco warehouse building type was investigated through a case study model. For this case study, an existing tobacco warehouse as the preliminary building layout has been used. From this layout, an energy model of the building is constructed in OpenStudio because of the widespread usage of this software and support from experimental validation. Following the construction of the baseline model, the relevant input parameters for variation are selected and their probability distributions are defined.

The Monte Carlo Analysis (MCA) method was used to propagate the input uncertainties through EnergyPlus analyses and to produce an output distribution for the warehouse's annual energy consumption. To conduct the sensitivity analysis, both main effects and bilinear multivariate regressions were used to identify influential parameters and interactions. The building performance simulation and analysis processes contain different stages and are generalized into three main subjects, namely pre-processing, simulation, and post-processing (Figure 3.18).

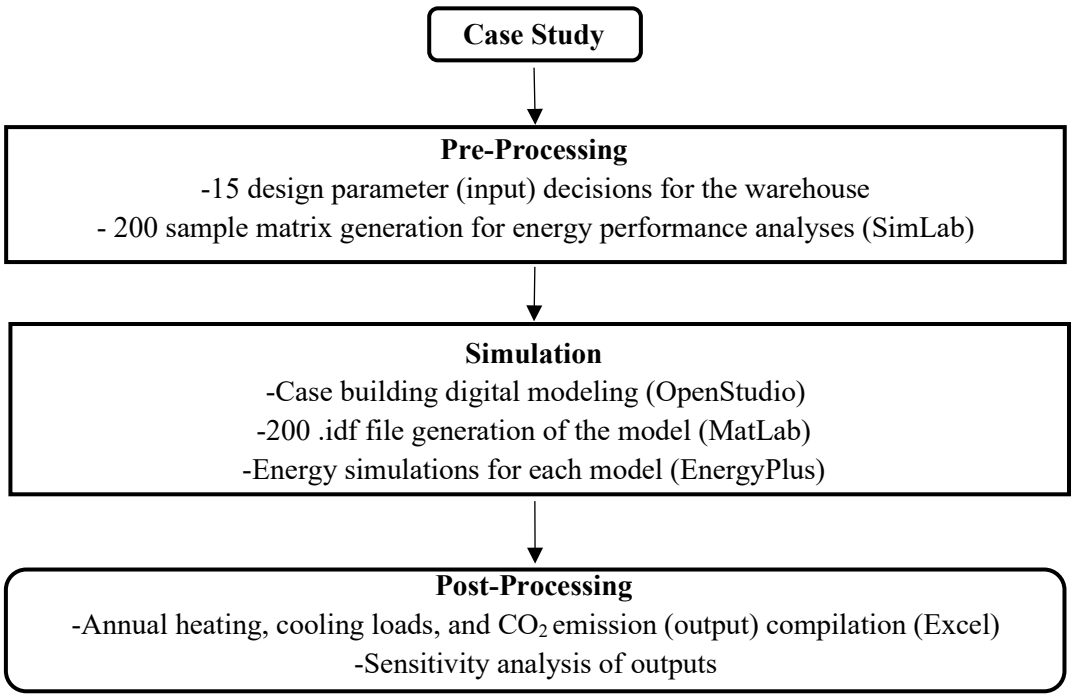

Figure 3.18. Visualization of the project simulation process

In general, pre-processing includes the selection of input parameters to be analyzed in terms of effects on the energy and environmental performance of the building and the preparation of sample files consisting of input parameter variations. Then, digitalization of the building, generation of energy simulation files, performing simulations, and compilation of the results are included in the simulation topic. Finally, post-processing is the part where the outcome collected from the process is analyzed by sensitivity analysis tools.

3.2.2. Pre-Processing

For the analyses, a total of 15 architectural design parameters are investigated. One of the four zones within the warehouse which is also selected for the field measurements is considered for initial analyses. Several parameters are not included such as variation of parameters related to the south and west facades since this zone has only two external facades.

Shading elements are applied by considering the orientations of the walls so that vertical application for the east facade and horizontal placement for the north wall is generated in the simulation model. Besides, the air infiltration range is assigned by considering the current situation inside the volume. Eqn. 3.3 is used for the calculation of the air change rate of the storage zone. Where 'n' indicates air changes per hour, 'q' is fresh air flow through the room (m^3/s) as well as 'V', for the volume of the room (m^3). The room has two fans with 34000 m^3/h air flow and the volume is 27250 m^3. The current air change rate in storage is calculated as 2.5 ACH.

$$n = 3600 \times q/V \qquad \text{Eqn. 3.3}$$

The architectural design parameters considered are all assumed to be continuous variables and indicated as opaque envelope thermal properties, shading and PV panel applications, and infiltration characteristics. Orientation was omitted as a variable due to the utilization of a predefined layout for the case study.

To account for the lack of prior knowledge about the probability distributions of architectural design parameters for tobacco storage warehouses, uniform distributions were assumed. This choice was made to minimize bias in the analysis results, as it does

not rely on any additional information beyond the maximum and minimum values of the parameters. Furthermore, the adoption of uniform distributions in uncertainty analysis of design parameters is recommended in building performance literature. In this approach, all values within the range of interest for design variables are considered equally probable (Tian, 2013).

The maximum and minimum values depending on the thermal and physical characteristics of input parameters are specified due to the common materials used for walls in the building sector in Turkey (Table 3.3). Table 3.3 presents the lower and upper boundaries of the uniform distributions explored for the architectural design parameters. These constraints were specifically chosen to encompass the acceptable design ranges currently available for each variable.

Table 3.3. Lower and upper boundaries for the architectural design parameters were investigated.

PARAMETERS		**UNITS**	**MIN VALUE**	**MAX VALUE**
Conductivity of Thermal Insulation Material	East facade	W/m.K	0.02	0.05
	North facade	W/m.K	0.02	0.05
	Roof	W/m.K	0.02	0.05
Thermal Insulation Material Thickness	East facade	m	0	0.2
	North facade	m	0	0.2
	Roof	m	0	0.4
Shading Projection Factor	East facade (vertical)	-	0.05	1
	North facade (horizontal)	-	0.05	1
Shading Angle	East facade (vertical)	°	0	90
	North facade (horizontal)	°	0	90
Solar Absorptivity	East facade	-	0.1	0.9
	North facade	-	0.1	0.9
	Roof	-	0.1	0.9
Air Infiltration Rate		ach	0	10
PV panels		-	Mounted (0)	Elevated (1)

After the applicable parameters and value ranges for variations are selected, a single MCA was used to examine the effect of input parameter uncertainty on the building energy consumption. MCA procedure is the analysis of building models by substituting a range of probability distributions for any factor that has uncertainty. By using probability distributions, variables can have different probabilities of different outcomes.

The annual heating and cooling consumptions of the building were selected as the output parameters of interest since the objective of the sensitivity analysis is to identify influential design parameters to help decrease the energy consumption of the building if possible. The annual consumptions are obtained through simulations of the building energy model over the course of an entire year with a Typical Meteorological Year (TMY) file used to define the weather conditions. Modifications are made within the weather file according to the meteorological values collected from the site.

A Latin Hypercube Sampling (LHS) method is implemented due to its efficient stratification properties, which allow for the use of more computationally demanding models such as EnergyPlus because a large amount of sensitivity and uncertainty information can be obtained with a relatively small sample size. A total of 200 simulations were created for the MCA using LHS to randomly sample from the distributions of all 15 parameters simultaneously. While it is stated that two-thirds of the input parameter number is adequate for these analyses, 200 different simulation scenarios are generated by MatLab, for improving the accuracy of a sensitivity analysis based on the MCA results.

3.2.3. Simulations

Digital modeling of the case building is provided by the simulation software, OpenStudio 2.3.0. Generally, there are two different approaches in digital modeling for thermal simulations. The first method includes simplifications through real projects by separating the whole project into zones so that the complexity of the model decreases as well as the time spent for simulations. The second approach is modeling the whole building according to the entire information in a detailed way. This method contains more complexity than the previous model and takes more time for simulations. However, the results present more accurate information. In this study, the digital model is simplified to accelerate the simulation process and decrease the model complexity by the zoning method.

Since the entire warehouse is separated by huge doors specialized for the efficient transportation of tobacco bales, four zones are created in the simulation model according to these separations of the actual warehouse. Then, only one of the four zones is selected for the simulations conducted for sensitivity analyses.

On the other hand, energy simulations are done by EnergyPlus 9.2.0 software. EnergyPlus data files (IDF) are created by using previously generated sample matrices by SimLab and the digital base model by OpenStudio. IDF files are obtained by assigning material properties indicated in sample matrices to the base model. Then 200 IDF files are created by MatLab and they include entire input parameter combinations assigned.

Annual energy consumption for heating and cooling of the building and annual operational CO_2 emissions are specified as output parameters for the sensitivity analysis. Therefore, EnergyPlus simulations are held for annual energy consumption for heating and cooling. The energy consumption results are collected for heating and cooling separately by EnergyPlus. Then, annual operational CO_2 emissions are calculated by acquired annual total energy consumption values. For this step, results are generated from 200 IDF files including combinations of different values of building input parameters.

In conclusion, input sample matrices and building performance simulation results are collected during the simulation stage. The following process requires the investigation of the relations between input parameters, and energy and environmental performance of the building.

3.3. CASES B&C: CFD Model

The increasing development of computers and the field of CFD have opened the possibilities of a low-cost yet effective method for modeling and simulation of airflow and heat transfer in warehouses with fewer experiments required. In this study, there are several main objectives of the CFD simulations and their connections to the field measurements. Initially, suitable methods to model the tobacco warehouse are identified. The following sections cover each of the topics focusing on detailed inputs and setups.

The dimensions of the modeled zone are 84x29 m. Since the building also has a hipped roof the height of the volume changes between 12.5 m and 14.5 m. Figure 3.19. demonstrates the three-dimensional CFD model.

The tobacco bales are not modeled entirely. Instead, each of the four stocking zones is modeled as one volume to simplify the geometry and decrease the density of the model. The load schedule of the warehouse is also observed during field measurements and since most of the time the warehouse works at full capacity, the bales are modeled in a dense placement. The general structure of the geometry and the calculation domain is shown in Figure 3.19.

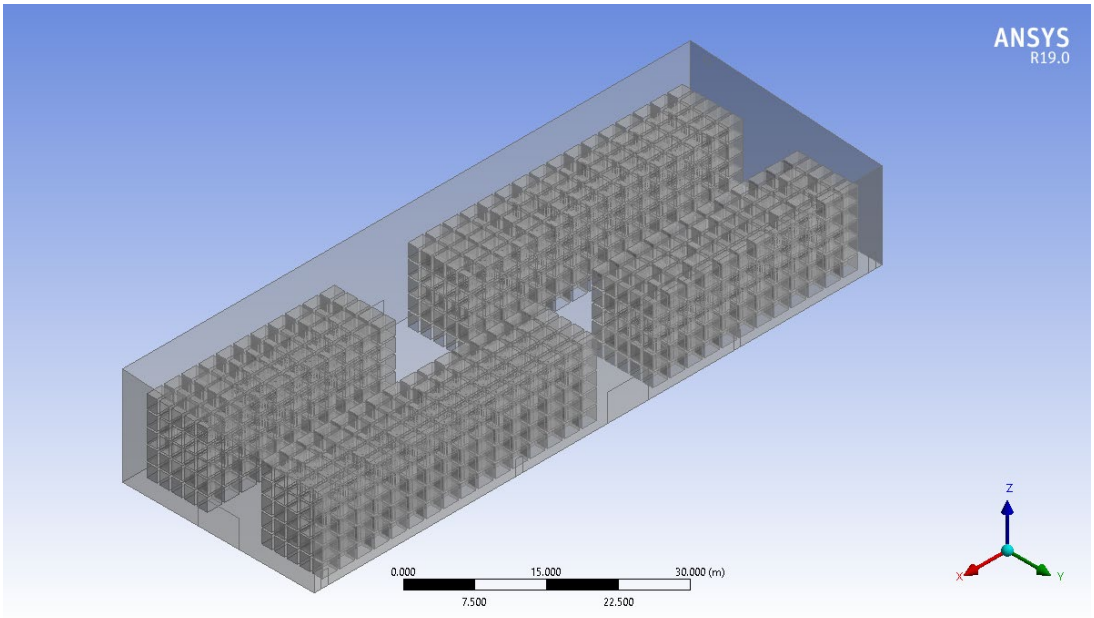

Figure 3.19. The calculation domain

Boundary conditions for the exterior walls, roof, and floor have been included in the simulations. The symmetry (zero heat flux specified) boundary condition is applied to the indoor walls. For the exterior walls and roof, mixed thermal conditions have been implemented. Accordingly, heat transfer coefficient values as shown in Table 3.4 are used for the simulations.

All the cases in this thesis are steady cases. The measurements were taken between 2020 June and 2021 October. The temperature conditions were changed for each month during this period. Furthermore, during the simulations, the temperature was monitored at certain points where the exact field measurements were recorded.

Table 3.4. Heat transfer coefficient calculations for roof, floor, and exterior walls

Construction unit	Building materials	Material thickness L (m)	Thermal conductivity k (W/mK)	Thermal resistance R (m^2K/W)	Overall heat transfer coefficient U (W/m^2K)
ROOF	Inner surface convective resistance			0.13	
	Roof panel	0.125	0.2	0.625	
	Rock wool	0.075	0.04	1.875	
	Brattice panels	neglected			
	Outer surface convective resistance			0.04	
Total				2.045	**0.49**
FLOOR	Inner surface convective resistance			0.17	
	Concrete slab	0.4	1.25	0.32	
	Vapor barrier	neglected			
	Gravel filling	0.25	0.9	0.278	
	Stabilized filling	0.5	2	0.25	
	Blockage	0.3	0.54	0.556	
	Outer surface convective resistance				
Total				1.573	**0.64**
EXTERIOR WALLS	Inner surface convective resistance			0.13	
	AAC	0.3	0.3	1.00	
	EPS insulation	0.04	0.04	1.000	
	AAC	0.3	0.3	1.00	
	Outer surface convective resistance			0.04	
Total				3.170	**0.32**

The values for outside temperature (Tout) and ground temperature were used as shown in Table 3.5. Outside monthly temperatures are the average temperature values for each month. In addition, the monthly ground temperatures are indicated to be close to the monthly outside air temperatures delayed by three months (EnergyPlus, 2022). Therefore, the ground temperature is calculated by averaging the air temperature of the previous three months.

Table 3.5. Outside and ground temperatures for selected periods

Month	Tout (°C)	Tground (°C)
January	9.4	12.8
February	10.4	10.9
March	13.3	10.3
July	29.1	25.2
August	29.2	27.4
September	25.6	28.0

3.3.1. Grid Generation

The variable y+, termed as the dimensionless wall distance, was used to find a suitable correct grid size near the walls and the standard wall functions require a range of $30 \leq y+ \leq 300$ for accurate prediction of the turbulent flow bounded by walls (Hussain et al., 2012). Therefore, an average y+: 75 was achieved in the model, which can guarantee an accurate prediction of airflow bounded by walls with the standard wall function (X. Liu et al., 2020).

The discrete equations were solved under the imposed boundary conditions with an iterative procedure using the Coupled pressure-velocity coupling algorithm. The surface-to-surface radiation model was adopted to solve the radiative transfer equation. A body force-weighted strategy for pressure was selected. Besides, the second order upwind spatial discretization method was chosen for density, momentum, turbulent kinetic energy, and turbulent dissipation rate.

The simulation was considered to have reached convergence when the monitored variables reached a stable state. To validate the models, the simulation outcomes were compared with measurement data. The steady-state situation was reached when errors of the mass and heat flow were less than 5%. A grid of 12.29 million hexahedral cells was used to obtain the simulation results. Meshing is not applied to the inside of the tobacco bales. Figure 3.20 shows the side section of the generated meshes from the three-dimensional model. Figure 3.21 is the partial and closer view of the meshing that is shown with red framing in Figure 3.20.

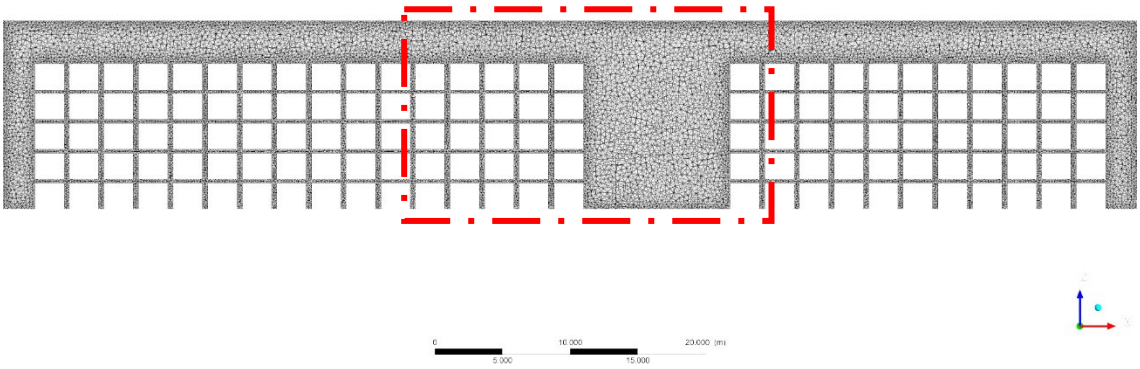

Figure 3.20. Side view of the meshing from the three-dimensional model

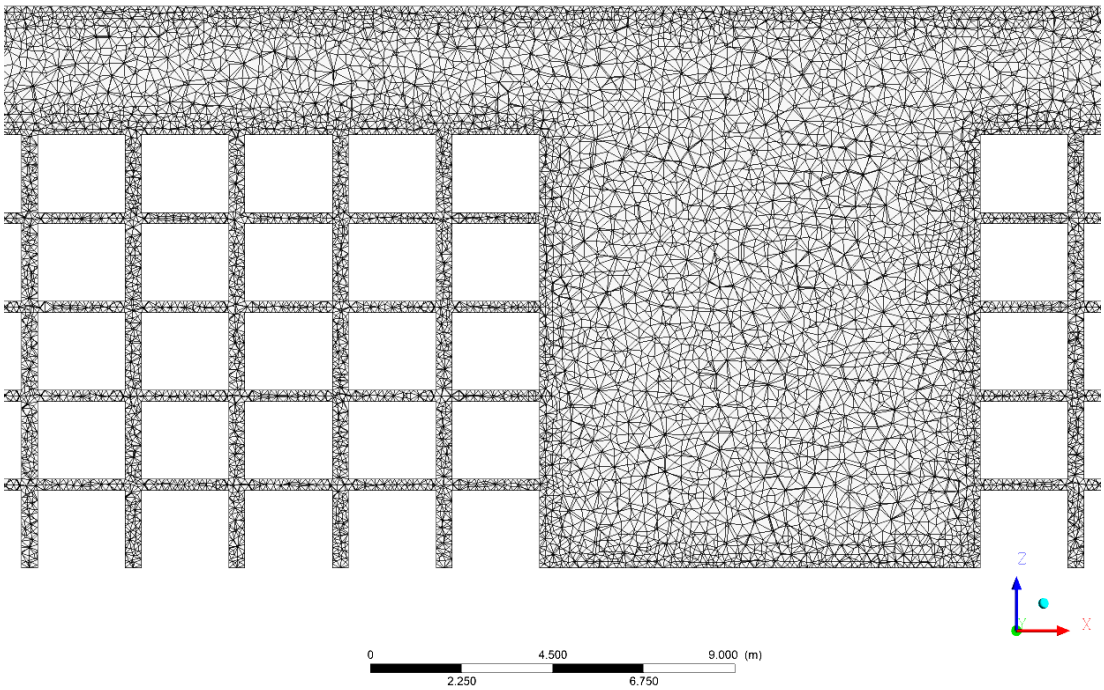

Figure 3.21. Partial view of the generated mesh from model

3.3.2. Governing Equations

To simulate the airflow within the CFD framework, the conservation equations are solved. These equations include the conservation of mass, momentum, and energy. The conservation of mass ensures that the net change in mass within a control volume is equal to the sum of the inflow and outflow of the fluid through its boundaries. The conservation of momentum states that the change in momentum of the fluid within the control volume is equivalent to the net momentum change across its boundaries, as well as the external forces acting on the control volume. The conservation of energy dictates that the total energy within a system remains constant, even as energy transforms between different forms.

In this study, the airflow is characterized by low speed and negligible density variations, allowing it to be treated as incompressible flow (ANSYS, 2018). The CFD model employs these conservation equations to govern the physical variables. Specifically, the equation of mass conservation can be written as:

$$\frac{\partial \rho}{\partial t} + \nabla \cdot (\rho \vec{v}) = 0 \qquad \text{Eqn. 3.4}$$

The general expressions for the conservation of momentum and energy of incompressible, Newtonian fluids are:

$$\frac{\partial \vec{v}}{\partial t} + (\vec{v} \,.\nabla)\, \vec{v} = -\frac{1}{\rho_0}\nabla p + \frac{\mu}{\rho_0}\nabla^2 \vec{v} + S \qquad \text{Eqn. 3.5}$$

$$\frac{\partial T}{\partial t} + \vec{v} \cdot \nabla T = \alpha \nabla^2 T \qquad \text{Eqn. 3.6}$$

In the given conservation equations, the variables *v, T, ρ* represent velocity, temperature, and density, respectively. The parameters *S, α, p*, and *t* correspond to the source term, thermal diffusion coefficient, pressure, and time, respectively. However, the change of the properties given in the equations from 3.4 to 3.6 according to time was not considered since the CFD problems were taken under steady-state conditions.

In this study, the CFD approach was studied separately for two different cases (B and C). In the first CFD case (CASE B), the above three conservation equations (Eqns. 3.4, 3.5, and 3.6) were used for thermal stratification in the tobacco warehouse, while the energy equation (Eqn. 3.6) was not used for CASE C. In this context, the following Boussinesq approach is used for CASE B.

The simulations conducted in this thesis employed the Boussinesq approximation to model buoyancy-driven force, which is a primary contributor to natural convection and thermal stratification. The Boussinesq approximation assumes that the density variation in a fluid is solely dependent on its temperature, resulting in a linear relationship between density and temperature. Compared to other density models, the Boussinesq approximation method is relatively straightforward to implement in simulations. The thermal expansion coefficient β (ANSYS, 2018) is defined as:

$$\beta = -\frac{1}{\rho}\left(\frac{\partial \rho}{\partial T}\right)_p \qquad \text{Eqn. 3.7}$$

Within the equation provided, ρ represents density, and T represents temperature. The thermal expansion coefficient is a necessary input for simulations employing the Boussinesq approximation. This approximation assumes a linear relationship between density and temperature. Therefore, the Boussinesq approximation is mathematically expressed as:

$$\rho_0 - \rho = -\rho_0 \beta (T - T_0) \qquad \text{Eqn. 3.8}$$

Within the provided equation, ρ_0 represents the reference value of density, and T_0 represents the reference value of temperature. The Boussinesq approximation states that the density variation is only important in the buoyancy term. By combining the force of gravity with the Boussinesq approximation as the source term, the momentum conservation equation can be formulated as follows:

$$(\vec{v} \,.\, \nabla)\, \vec{v} = -\frac{1}{\rho_0}\nabla p + \frac{\mu + \mu_t}{\rho_0}\nabla^2 \vec{v} + \vec{g} - \beta (T - T_0)\vec{g} \qquad \text{Eqn. 3.9}$$

Where μ is the dynamic viscosity, μ_t is the turbulent viscosity and $\vec{g}$ is the gravitational acceleration.

To solve the basic governing equations, it is necessary to use a turbulence model. The turbulent structure of the flow is considered by using the two-equation Re-Normalization group (RNG) *k-ε* model. This model had been applied to numerous indoor air flow problems with proper predictive accuracy. Besides the results specifically show that this model is suitable for simulating indoor airflow studies (Chen, 1995; Speziale et al., 1991; Zhiqiang et al., 2007).

Within this turbulence model, distinct transport equations were assigned to determine the values of turbulent kinetic energy, and turbulent dissipation rate. These quantities play a crucial role in calculating the turbulence viscosity, which is required for the momentum conservation equation.

Standard wall functions are applied for near-wall treatment. Moreover, the Second Order Upwind scheme and Coupled algorithm were used for space discretization and coupling between pressure and velocity in the numerical simulations. Besides, Body Force Weighted algorithm is used for spatial discretization of pressure.

3.3.3. CFD Modeling

The CFD analyses are studied under two cases. The first case (Case B) included the simulations conducted for decreasing thermal stratification, while the focus was given on improvements in indoor ventilation conditions in the second case (Case C).

3.3.3.1. Case B: Thermal Stratification

Case B is generated to observe the thermal stratification conditions inside the warehouse. On-site measurement data is used for stratification analyses. CFD model is generated according to these circumstances. Besides, the grid models pointed out in subsection 3.3.1 and the governing equations as well as the Boussinesq approximations mentioned in subsection 3.3.2 are used for CFD analyses.

The CFD model to study vertical temperature gradients inside the warehouse is modeled by assuming the volume is closed. Therefore, the fans and the openings are excluded from the model (Figure 3.22.). The grey walls indicate exterior walls exposed

to weather conditions and the transparent walls are adiabatic that are adjacent to the other volumes. As indicated in Chapter 3.1.4., six of the warmest and the coolest months are selected for analyzing vertical temperature gradients inside the volume.

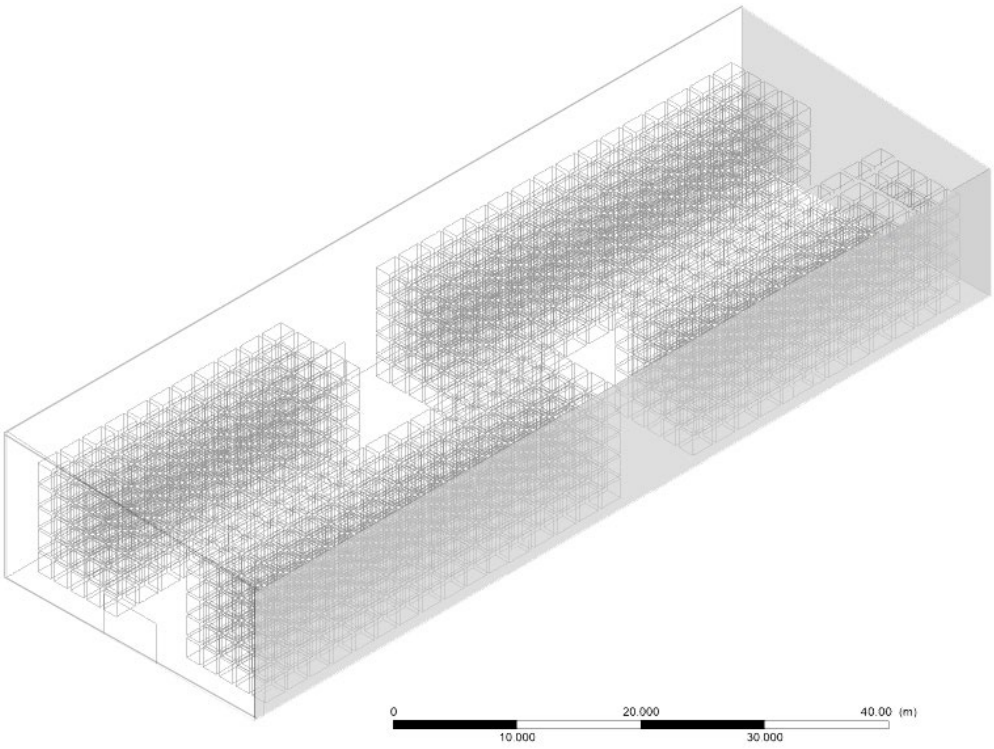

Figure 3.22. CFD model for thermal stratification studies

The generated model included energy equations and solar radiation information belonging to the studied location. Table 3.6 shows the monthly heat generation rates for each month and differences in solar radiation values according to different directions have also been taken into consideration. The values are calculated for roofs as well as north and east directions separately. Hourly solar radiation values, surface thicknesses, and absorptivity values of the surfaces are taken into account while calculating the heat generation rates. Besides, the inward transfer of the absorbed radiation is assumed to be two-thirds of the incoming radiation. Therefore, this assumption is included in the calculation of heat generation rate, as well. Accordingly, the values are calculated for July, August, September, January, February, and March. The surface-to-surface (S2S) radiation model is used for radiation heat transfer simulations.

Table 3.6. Monthly heat generation rates for the roof, north and east directions

Month	Direction	Hourly solar radiation (W/m^2)	Thickness (m)	Absorpt.	Heat generation rate (W/m^3)
	Roof	482.21	0.2	0.40	535.79
July	North	88.83	0.64	0.50	22.78
	East	246.12	0.64	0.50	63.11
	Roof	313.50	0.2	0.40	348.33
Aug	North	58.45	0.64	0.50	14.99
	East	229.07	0.64	0.50	58.74
	Roof	285.96	0.2	0.40	317.73
Sept	North	42.62	0.64	0.50	10.93
	East	188.15	0.64	0.50	48.24
	Roof	120.66	0.2	0.40	134.06
Jan	North	26.58	0.64	0.50	6.82
	East	111.97	0.64	0.50	28.71
	Roof	168.17	0.2	0.40	186.86
Feb	North	36.26	0.64	0.50	9.30
	East	146.36	0.64	0.50	37.53
	Roof	222.11	0.2	0.40	246.79
March	North	46.92	0.64	0.50	12.03
	East	167.54	0.64	0.50	42.96

The CFD simulations of the warehouse indoor temperature values are validated using the field measurement data of temperature distributions in the warehouse. The existing thermal stratification and the current indoor air conditions in the warehouse using the validated CFD models are simulated. With the validated CFD models of the

warehouse, different strategies of thermal destratification are simulated and compared to the existing situation to quantify the improvements.

3.3.3.2. Case C: Indoor Ventilation

Air conditioning in a large warehouse is particularly significant under very hot humid climatic conditions, as those occurring in many western parts of Turkey during the summer season. When comfort conditions required are not excessively demanding in large warehouses, efficient low-consumption ventilation systems are required. On the other hand, CFD techniques can be used in simulating the resulting temperature and velocity fields, allowing performance evaluation of different locations and spatial distributions of the diffusers. This can yield more efficient cooled air flows inside the warehouse, resulting in improved indoor conditions with equivalent energy consumption.

Under these circumstances, the indoor environment conditions of the storage zone are investigated by CFD analyses in terms of the ventilation conditions to analyze improvement possibilities. Grid models used for the analyses are explained under subsection 3.3.1. Besides, the governing equations used for CFD analyses are shown in subsection 3.3.2, whereas the energy equation is not used for indoor ventilation studies, unlike Case B analyses.

Figure 3.23 is the illustration of the CFD model used for the analyses in Case C. The grey-painted walls are the outer faces, and the other two are adiabatic walls neighboring other storage volumes. There are four transportation doors located on each wall and the width is 6 m and the height is 4 m. The wall facing to the outside has additional four doors with dimensions of 1x2.20 m and they are kept closed most of the time. Besides, there are two axial fans located on two walls facing outside. The features of the fans are 34000 m^3/h flow rate, 380 V, 1000 rpm speed, and 3 kW (4 HP) power with 0.95 m diameters.

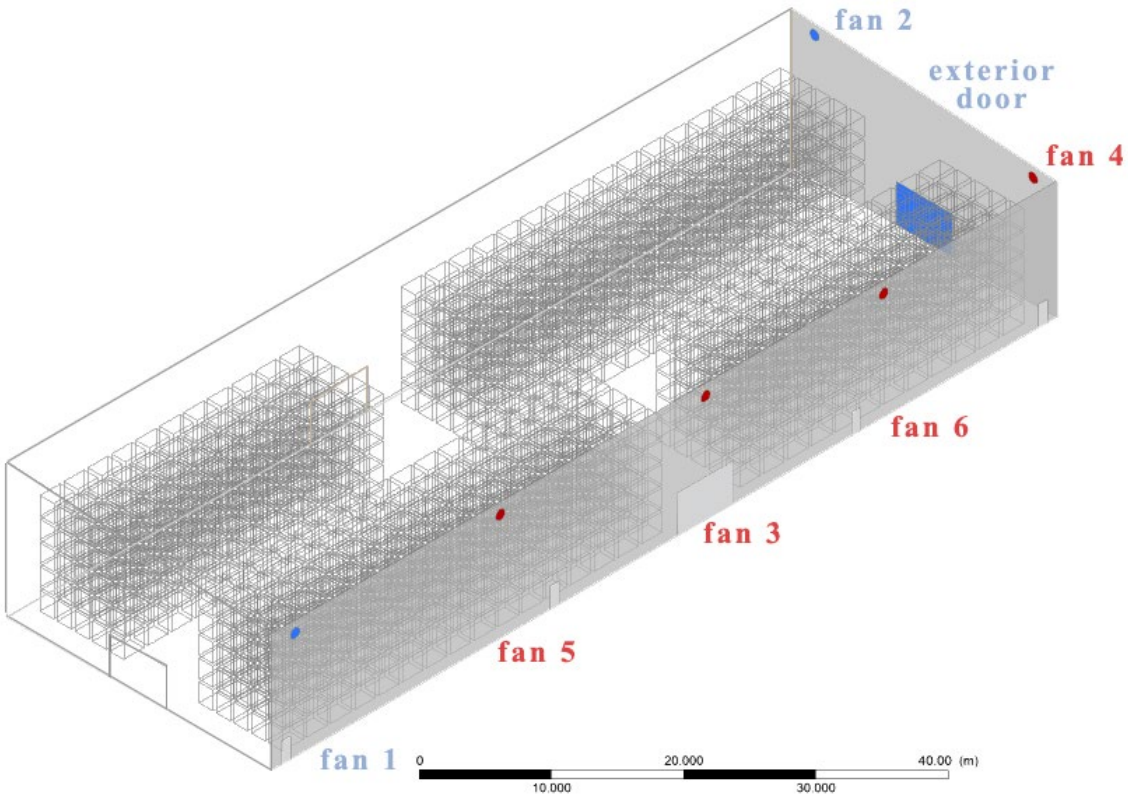

Figure 3.23. Existing and proposed fan locations

The blue-painted door is the exterior transportation door used for natural ventilation purposes and also assumed as opened for the studies in this thesis. The two blue-colored fans numbered 1 and 2 are existing fans. Besides, the possible additional fans (numbered 3-6) are included in the model and indicated in red color in the same figure.

CHAPTER 4

RESULTS

This chapter first shows the measured temperature from all five levels. What follows is the examination of input and output parameter correlations. Sensitivity analyses are conducted to observe the energy and environmental performance of the building, and the most important design parameters on building characteristics. Then, the CFD analysis results for the current case are presented for the warmest and the coldest months which is followed by the analyses for indoor thermal destratification. In the final part of the chapter, current hybrid ventilation conditions are examined and the scenarios for improving the indoor ventilation quality are simulated.

4.1. Experimental Measurement Results

Temperature-sensitive products such as tobacco require special indoor conditions for storage purposes. Therefore, one of the most significant criteria for product quality and preventing deterioration is to provide uniform temperature trends during the year. As indicated in Figure 4.1, for the studied building, July, August, and September are the warmest months while January, February, and March are the coldest and the most critical months for tobacco storage.

The data loggers located for measurements are numbered from 1 to 5 and indicated as H1, H2, H3, H4, and H5. The lowest number H1 indicates 2 m height from the ground level, H2 is for 4.5m, H3 is 7m, H4 is 9.5m while the fifth logger is indicating as H5 for the data logger located at 12 m. These vertical location assignments are used in all figures of this thesis unless otherwise specified.

The results shown in Figure 4.1 indicate that the storage space temperature deviates from the optimal range for storing baled tobacco, which is between 21-25°C. The green band in the figure shows the ideal temperature range, and it is apparent that the storage space's temperature exceeds this range in summer and winter.

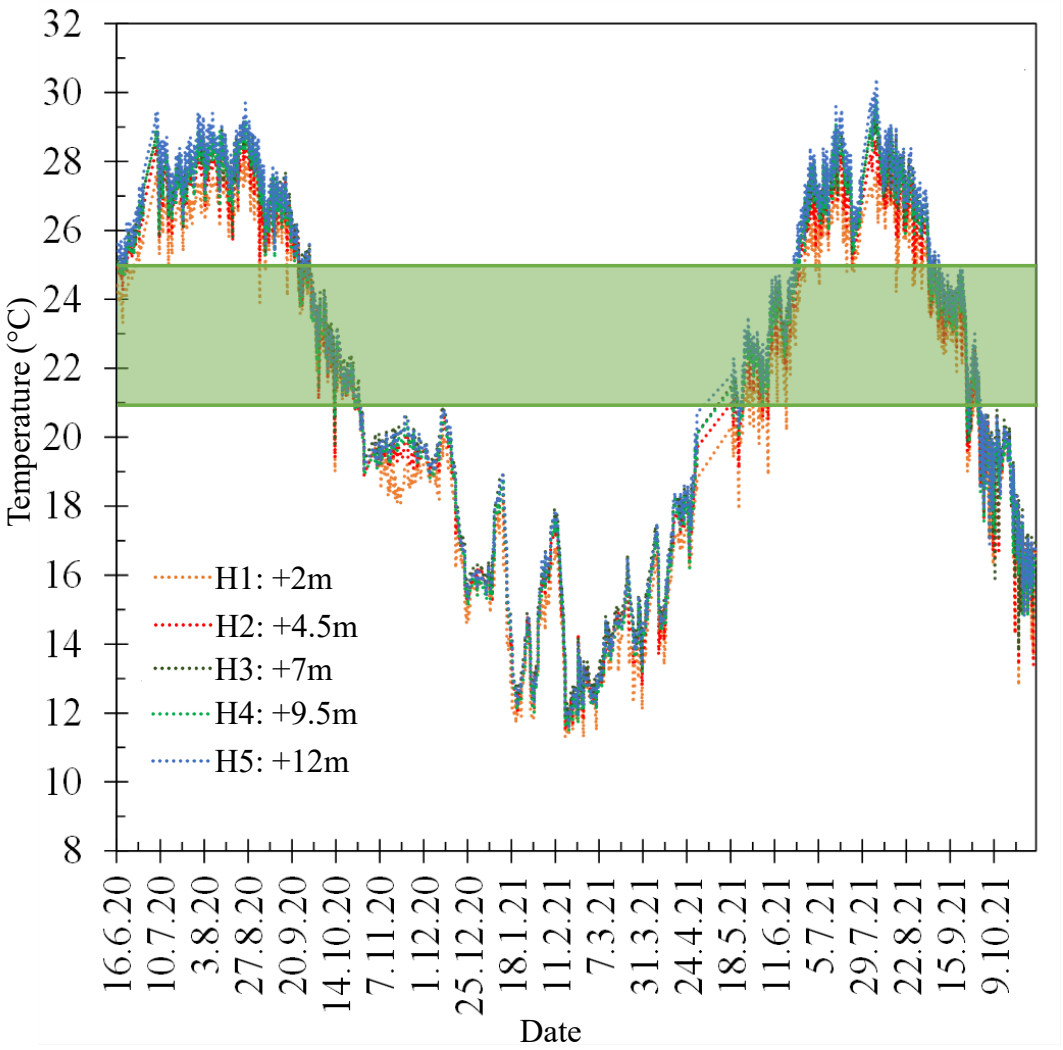

Figure 4.1. Yearly measured temperature data

In January, February, and March (the coldest months), the temperature inside the storage volume reaches around 11-12°C, which presents a problem as this temperature is more than 10°C below the optimal range. On the other hand, in July, August, and September (the warmest months), observing the temperature reaches up to 30°C, also gets problematic as the temperature goes beyond the optimal range. These temperature fluctuations can lead to deterioration in the stored tobacco, negatively impact its quality, and cause product losses. Therefore, it is crucial to regulate the storage temperature and maintain it within the optimal range to prevent the deterioration of the tobacco. The study's findings suggest that additional temperature regulation measures need to be implemented during the coldest and the warmest months to ensure that the temperature

remains within the optimal range. This could include using heating or cooling systems to adjust the temperature, as well as monitoring and adjusting the air flow.

Table 4.1 and Table 4.2 show the statistics about the measured vertical temperatures within the tobacco warehouse between 2020 June and 2021 October. Monthly maximum temperature differences between the highest and the lowest levels reach over 4°C while the fluctuations are between 1.8°C and 4.3°C. The vertical temperature gradient values change between 0.19 and 0.51.

Table 4.1. Measured temperature differences between 2020 June-December

	Monthly Max Temp. Differences (°C)	**Monthly Average Temp. Differences (°C)**	**Temperature Gradient (°C/m)**
2020 June	1.80	1.25	0.19
2020 July	2.70	1.52	0.28
2020 Aug	2.50	1.24	0.26
2020 Sept	3.70	0.74	0.39
2020 Oct	4.30	0.34	0.45
2020 Nov	2.40	0.96	0.25
2020 Dec	2.80	0.59	0.29

Table 4.2. Measured temperature differences between 2021 January-October

	Monthly Max Temp. Differences (°C)	**Monthly Average Temp. Differences (°C)**	**Temperature Gradient (°C/m)**
2021 Jan	3.20	0.60	0.34
2021 Feb	3.20	0.66	0.34
2021 March	2.90	0.49	0.31
2021 April	2.50	0.84	0.26
2021 May	2.80	1.44	0.29
2021 June	4.20	1.46	0.44
2021 July	3.80	1.48	0.40
2021 Aug	4.10	1.54	0.43
2021 Sept	4.80	0.93	0.51
2021 Oct	4.00	0.52	0.42

4.2. Numerical Analysis Results

4.2.1. CASE A: Energy Simulation Results

The post-processing section includes the examination of input and output parameter correlations. Sensitivity analyses are conducted to observe the energy and environmental performance of the building, and the most important design parameters on building characteristics. The impacts of input parameters are evaluated by using the sensitivity analysis method. Statistical analysis program, SimLab is used for sensitivity analysis. Initially, the sample files are exported, in terms of providing information about ranges of the input parameters. Then, generated Excel model output files created by using EnergyPlus simulation results of annual energy consumption for heating and cooling, and operational CO_2 emissions are assigned to the program.

After the specification of input and outputs, the regression-based sensitivity analysis method is selected. In this study, Standardized Rank Regression Coefficient (SRRC) is determined as an indicator to identify the sensitivity of each design parameter, which is based on a non-linear relation between the output and input parameters (Helton et al., 2006). Eventually, sensitivity analysis is conducted to clarify the most effective design parameters for the energy and environmental performance of the building.

Each parameter will have a value of significance between -1 and 1, where the negative sign points out that the output parameter value (annual energy, annual operational CO_2 emissions) will decrease when there is an increase in the input parameter value. On the contrary, the positive numbers point out the direct proportion of the input parameter value and the model output. Values higher than 0.9 are indicated as very effective, while a useless regression model implies values below 0.1 for the output variable (Saltelli et al., 1993). Therefore, input parameters having absolute values higher than 0.1 will be considered more influential design variables, as others, having values less than 0.1, will be classified as ineffective in increasing or decreasing annual energy consumption and environmental emissions.

Figure 4.2 indicates the most significant factors that have impacts on annual heating consumption characteristics for the selected zone of the warehouse. The lighter grey color is assigned for the values under the limit of 0.1, while darker implies the values above this limit.

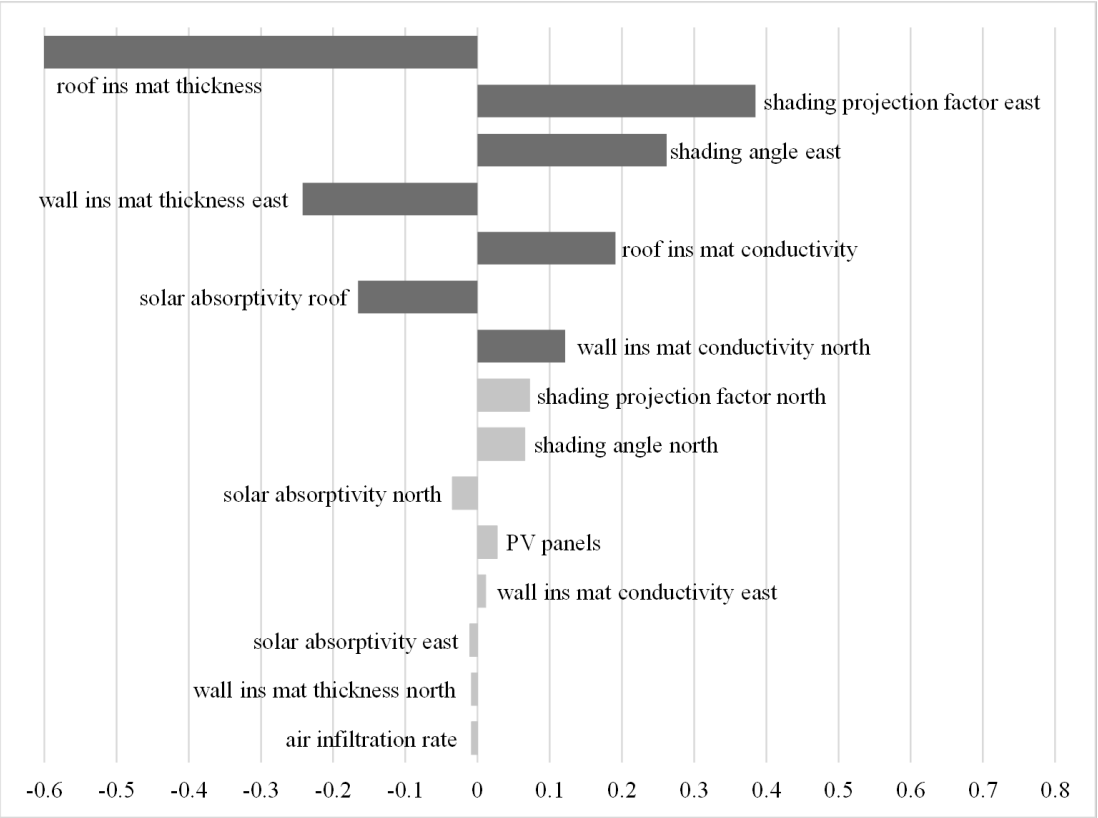

Figure 4.2. The most influential factors for annual heating consumption

The most important parameter affecting the annual heating consumption of the building is the roof insulation material thickness. The sensitivity value is 0.7 which means that the more insulation material thickness of the roof increases, the more annual heating consumption of the zone decreases. The second and third important parameters are the projection factor and the shading angle on the east facade with a value around 0.4 and 0.3.

The results mean that increases in the angle of the shading element and the projection length could cause increases in the heating requirements of the zone. It is caused by the cooling effects of shading elements within the zone. The following significant factor is related to increasing the insulation material thickness of the wall on the east facade, so that the annual heating consumption can decrease, as well. The variations in the roof insulation material conductivity and roof color are the following parameters that have an impact on the annual heating consumption. The last effective parameter is the conductivity of insulation material applied to the north facade.

Figure 4.3 shows the important relation between the design parameters and the annual cooling consumption of the selected zone. The most important parameter for the

annual cooling consumption is roof insulation material thickness with a value of 0.6. It means that the increases in the thickness can cause increases in the cooling requirements of the building as well. Secondly, the results show that the length and angle of the shading material applied to the east facade have a significant relation with cooling requirements.

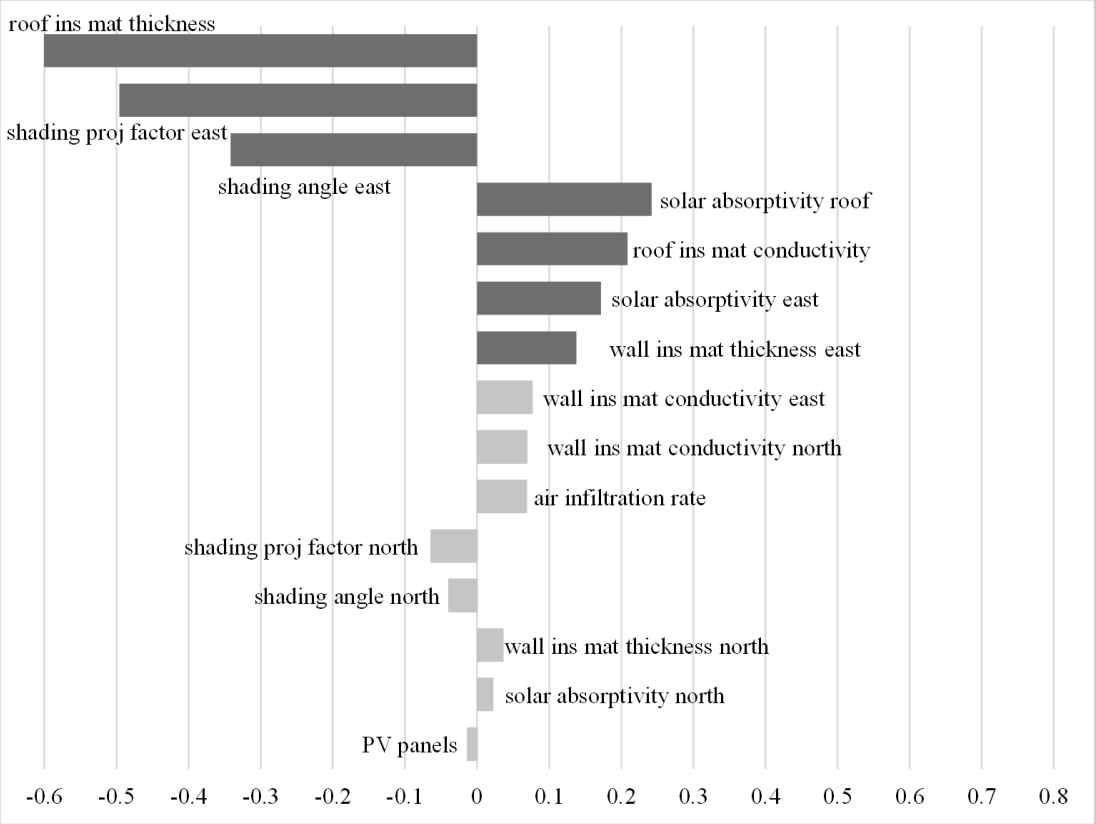

Figure 4.3. The most influential factors for annual cooling consumption

The following parameters, which are roof color, the conductivity of the roof insulation material and east facade color, and the insulation material thickness of this facade, have a direct relation with the cooling requirements as they increase, the cooling demand will diminish accordingly.

As a following step, operational CO_2 emissions are calculated manually to have more accurate results adapted to Turkey, by using the sum of annual heating and cooling consumption values. Total annual energy consumption values are multiplied by CO_2 emission factors specified in regulations on the energy performance of buildings; as 0.234 kg/kWh for natural gas and 0.819 kg/kWh for electricity. Then, these calculations are used

for the sensitivity analyses conducted. Figure 4.4 summarizes the sensitivity analysis results for operational CO_2 emissions.

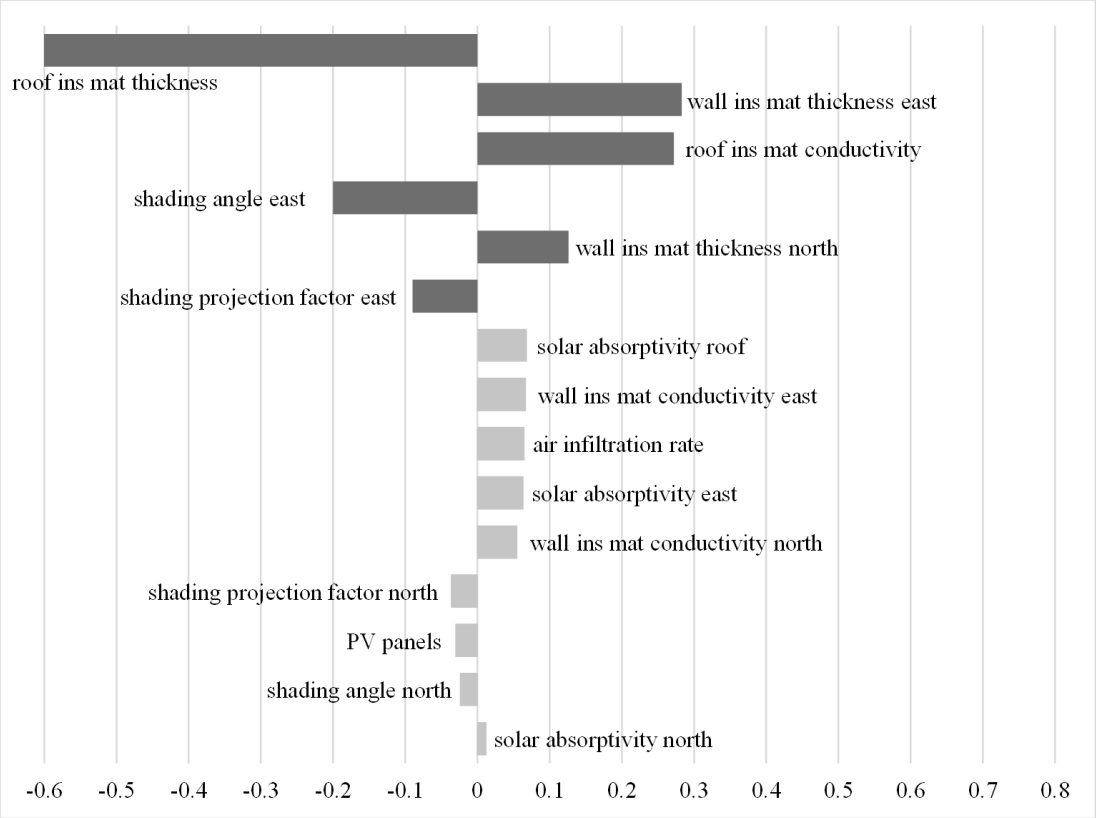

Figure 4.4. The most influential factors for operational CO_2 emissions

The most significant factor that has an impact on decreasing emissions is the thickness of the roof insulation material. Since the designated value is around 0.6, as the thickness increases it will cause an increase in CO_2 emissions.

The following parameters have much less impact on the output, for instance, east wall insulation material thickness and roof insulation material conductivity have effects with a value of nearly 0.3. The angle and projection factor of the shading material applied to the east facade have inverse impacts on the annual CO_2 emissions while increases in the insulation material thickness of the north facade cause increases in the emissions annually.

The results derived from the simulations and the analyses of the model are evaluated comprehensively. Accordingly, the relation between the input parameters and

the consumption and emission factors are analyzed simultaneously. It is observed that roof and wall insulation material thicknesses are two of the most influential factors for the energy and environmental performance of the building. Moreover, shading elements are another relatively significant parameter that needs attention. Besides, alterations in the thermophysical properties of the north facade and infiltration rates inside did not change the outcomes as much as previously stated parameters. The results also showed that the application of PV panels for increasing energy efficiency will not act as a shading element for the building.

Consequently, the overall evaluation of the analyses shows that it is important to focus on the thermophysical characteristics of roof materials and shading elements are essential for performance improvement strategies. In addition, various natural and mechanical ventilation approaches applied for warehouses need to be investigated, section of the most proper solutions and analyzing their effects on the same outcomes need to be studied as further study.

4.2.2. CASES B&C: CFD Analyses

The temperature results from the CFD simulations must be validated. In this section, the CFD results are compared with the measurement data. Then, the CFD analysis results for the current case are presented for the warmest and the coldest months which is followed by the analyses for indoor thermal destratification. Finally, current hybrid ventilation conditions are examined and the scenarios for improving the indoor ventilation quality are simulated. The exhaust air is mechanical, and the fresh air is natural (actually, with the negative pressure effect created by the fans) ventilation in these types of hybrid ventilation. A parametric numerical experiment is being carried out to effectively improve the indoor environment conditions (by sweeping more volume with less energy and reducing the amount of aged air) with the help of existing and additionally implemented wall-integrated fans through hybrid ventilation.

4.2.2.1. Model Validation

The warehouse building indoor thermal conditions are evaluated by using temperature measurements collected from the building. The months with the highest and

the lowest average temperature values inside the building are selected as the base cases. January, February, and March are the months with the lowest monthly average temperature values while July, August, and September are the months with the highest monthly average temperature values measured inside the building.

The simulations proceeded by comparing the temperature values taken from the measuring instruments placed at five vertical points in the warehouse with the temperature values at the points corresponding to the same locations in the CFD simulations. The simulations continued until the error percentages for each month are within the accepted ranges. Figure 4.5. shows the vertical temperature gradients inside the building according to the measurements and the computational model.

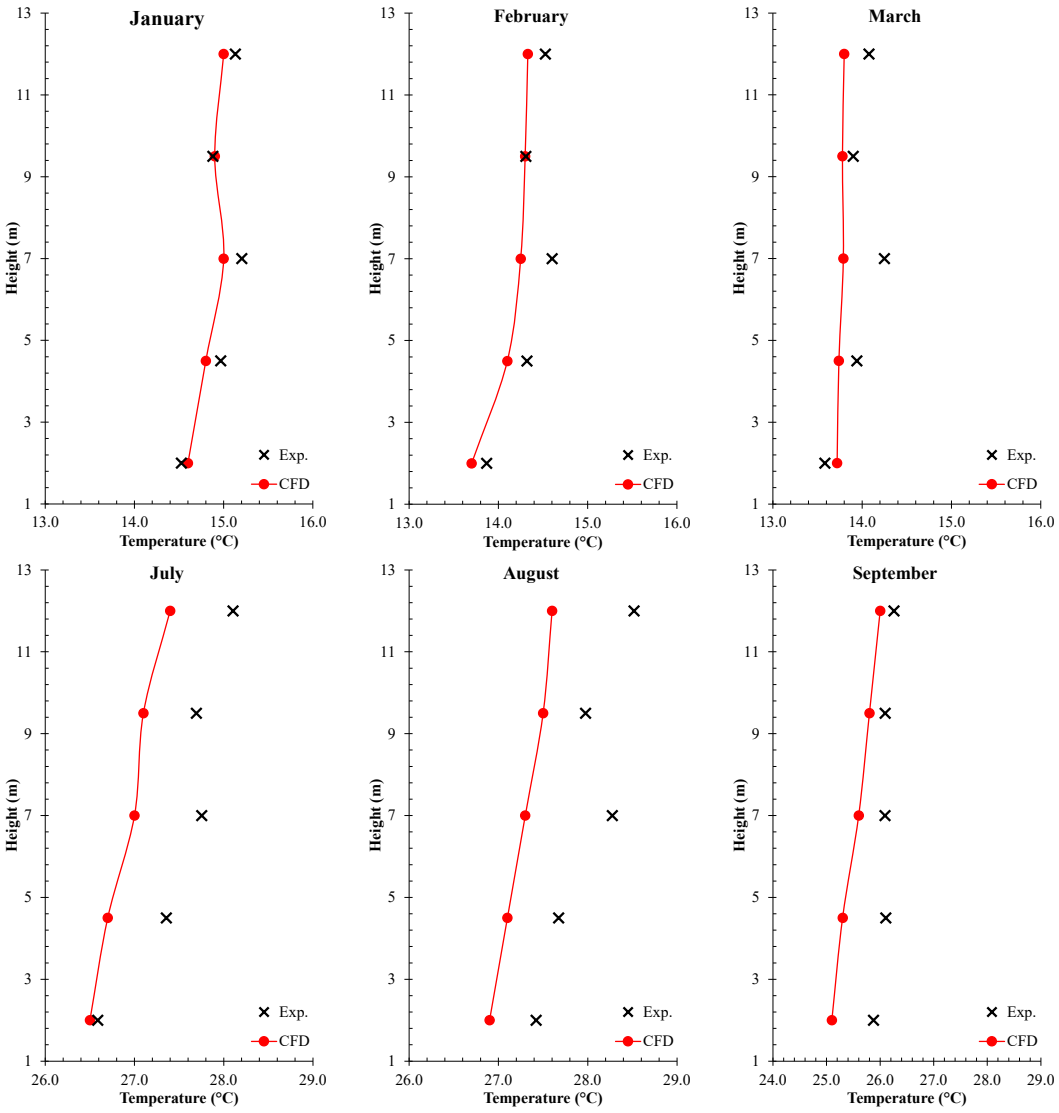

Figure 4.5. Comparison between experimental and CFD temperature results

As outlined in (Barbaresi et al., 2014), to determine the validity of a model and its results, it is necessary to compare the simulated temperatures with actual temperature data collected from the building. The assessment of the model's reliability involves examining the agreement between the simulated and measured temperatures, while the acceptability of the results is evaluated by analyzing the discrepancies between the simulated and recorded temperatures.

The monthly average of measurements taken at certain minute intervals and simulation results are used for the mean bias error (MBE) and coefficient of variation of the root mean square error [CV (RMSE)] calculations. Table 4.3 illustrates the vertical distributions of air temperature differences from the simulation and the on-site measurement. The MBE and CV(RMSE) values calculated according to the temperature (°C) measurements and simulation results, for summer and winter periods, are displayed in Table 4.3. The CV (RMSE)s of air temperature are 0.91%, 1.52%, and 1.92% for the coldest months of the year and 2.21%, 2.58%, and 2.19% for the summer months. The MBE of air temperature is 0.54%, 1.32%, and 1.31% for the coldest months and 2.03%, 2.47%, and 2.01% for the summer months. The CV (RMSE) and MBE% for the monthly temperature values are obtained within the acceptable tolerances (i.e., ±15% for CV(RMSE) and ±5% for MBE%), as defined in the ASHRAE Guideline 14 (ASHRAE, 2002b).

Table 4.3. Validation results of the CFD model

	January	**February**	**March**	**July**	**August**	**September**
CV (RMSE) (%)	0.91	1.52	1.92	2.21	2.58	2.19
MBE (%)	0.54	1.32	1.31	2.03	2.47	2.01

Figure 4.6 shows the planes used for the visualization of CFD analysis results. The location of the planes is selected specifically to cut out the doors and the tobacco bales so that the air movements through the doors and around the bales are shown in detail. There are three longitudinal and four transverse planes whose distances from the

walls are also indicated in the figure. Besides, the longitudinal planes are numbered (1), (2), and (3), and transverse planes are named (a), (b), (c), and (d). These signs are used to specify the planes in the following figures.

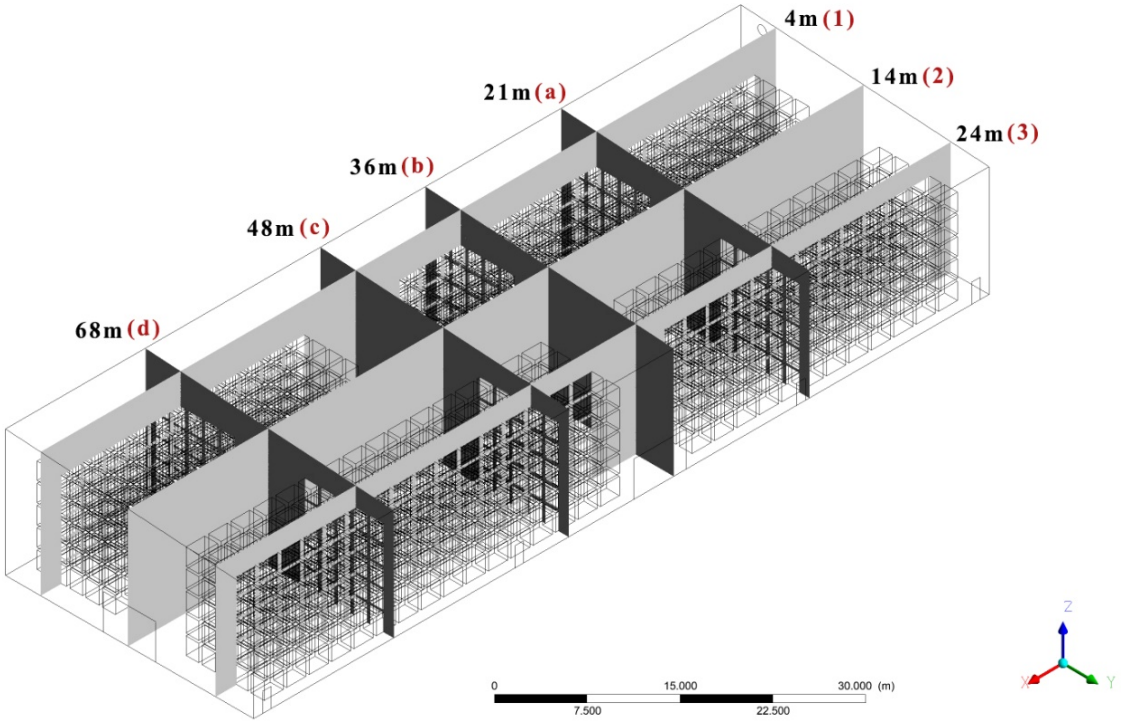

Figure 4.6. Location of the planes in the CFD model

4.2.2.2. CASE B: Thermal Stratification

The amount of vertical temperature stratifications varied depending on the height and time of year. Accordingly, a comprehensive study of the vertical temperature gradients between June 2020 and October 2021 was carried out. The methodology used was calculating the monthly average temperatures for five different levels monitored in the studied warehouse. The monthly average temperature values were used to represent the temperature profile for each month (Figure 4.7 and Figure 4.8).

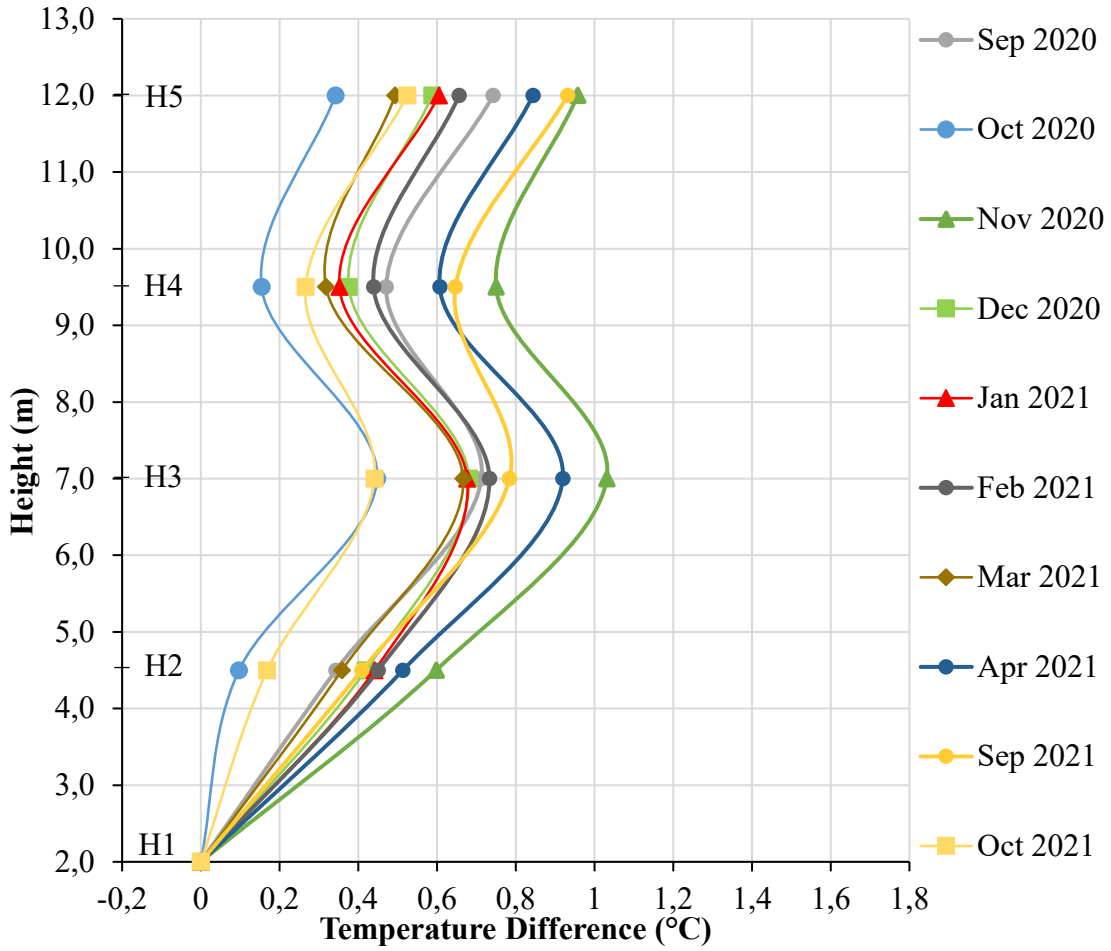

Figure 4.7. Curves of the vertical stratification of the monthly average temperatures from the fall to spring period

The vertical gradient of temperature inside the warehouse differed depending on the time of year and the impact of increasing outdoor temperature on increasing this gradient is also observed. During warmer months, the monthly average temperature differences between the upper and lower areas reach 1.5°C, while during cooler months, these variances decrease, averaging around 0.65°C with related values across all vertical profiles. This variation was attributed to temperature differences between the roof and the lower levels that were affected by the ground and outdoor air penetrations through the building's doorways.

During summer, the indoor air in the warehouse gets heated due to the maximum radiation absorbed by the roof. The lighter and less dense air remains in the upper part of the building, causing the temperature difference with the lower floors to increase. In addition, hot air infiltrations also stay in the higher zone. Nevertheless, the roof

temperature is lower than the ground and the lower levels of air in winter. This leads to the cooling of the top layer of air that has become heavier and sinks, resulting in air homogenization of the air and slighter variances. The colder outside air infiltrations additionally increase this trend.

Figure 4.8 shows that there is an increase of more than 1°C in temperature differences between the measured five meters during examining the monthly temperature curves during the warmer months. However, the increase in temperature differences is less distinct beyond that level, overlapping with the height of the transportation door openings, with some peaks in the area close to the roof. This observation shows that the air in the lower part of the building is more stable and layered, coupled with greater similarity of indoor and outdoor temperatures beyond five meters, air and outdoor infiltrations become homogeneous as altitude increases.

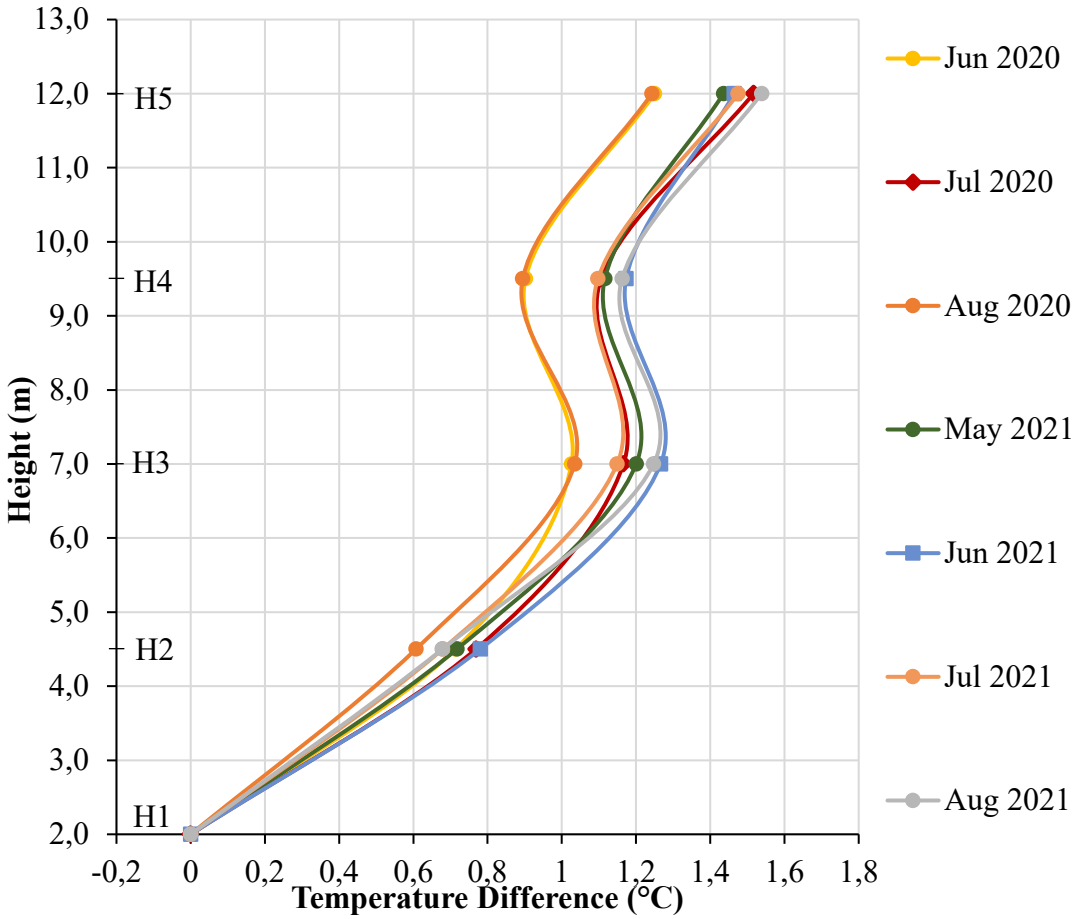

Figure 4.8. Curves of the vertical stratification of the monthly average temperatures for the summer period

Linear regression analysis was conducted for each monitored month in every warehouse to quantify temperature stratification. The model establishes a relationship between the temperature difference (ΔT) and the height above the ground, specifically comparing it to the temperature at the nearest lower point.

Table 4.4 presents the outcomes and coefficients obtained from the linear regression model executed in the warehouse. During months characterized by the highest levels of stratification (typically summer months), the model exhibited satisfactory adjustments, with average R^2 values ranging from 0.853 to 0.73.

Table 4.4. Results and coefficients of the linear regression model: R^2, standard error, and the temperature difference (ΔT)

Month	R^2	Error	(ΔT)
2020 June	0.73	0.14	1.25
2020 July	0.85	0.15	1.52
2020 August	0.73	0.17	1.24
2020 September	0.41	0.18	0.74
2020 October	0.12	0.19	0.34
2020 November	0.27	0.21	0.96
2020 December	0.03	0.17	0.59
2021 January	0.02	0.18	0.60
2021 February	0.08	0.17	0.66
2021 March	0.00	0.19	0.49
2021 April	0.21	0.21	0.84
2021 May	0.80	0.16	1.44
2021 June	0.77	0.17	1.46
2021 July	0.85	0.15	1.48
2021 August	0.81	0.19	1.54
2021 September	0.69	0.15	0.93
2021 October	0.51	0.14	0.52

The standard error of estimation was found to be close to the precision of the utilized sensors. As the temperature differences diminished, the R^2 values of the model also declined. However, this decline can be attributed to the fact that with reduced vertical temperature disparities, even slight errors or variations in sensor measurements gain

greater significance about the model's fit. Consequently, cases featuring lower R^2 values were linked to small temperature differences (ΔT), resulting in minor estimation errors. Thus, the chosen regression model provided valid outcomes for the study's objectives, enabling a comparison of average variation values across the observed months.

Indoor thermal stratification is one of the key aspects in the operation of the indoor environment of the warehouse, during summer especially since it allows one to understand the global thermal behavior of the construction. Although the stratification of the temperature decreases in the winter period, the distinct temperature drops are another critical factor for the hygrothermal behavior and ventilation of the building throughout the year. Therefore, in the following section, retrofit strategies that aim to decrease the vertical temperature gradients during summer as well as developing air conditioning proposals to increase the temperature during winter.

4.2.2.2.1. Improvements in Indoor Temperature Gradients

The on-site measurements and CFD simulations show that there is a vertical temperature gradient inside the warehouse, for six months examined. However, stored tobacco, like other hygroscopic products, requires certain temperature and humidity conditions to protect its quality. The constant conditions need to be provided in the studied warehouse as well, and the standards need to be maintained for all the stored tobacco bales. However, the vertical temperature gradients cause risky environments throughout the year. Therefore, two destratification methods are proposed for the months with higher temperatures as well as the coldest months.

Existing studies (X. Liu et al., 2020; Z. Wang et al., 2018) indicate that radiant floor realizes the most uniform vertical temperature distribution in the heating condition in large space buildings. Previous research (Rhee & Kim, 2015) recommends the floor surface temperature should be between 17°C and 29°C. Thus, the surface temperature of the radiant floor in this study is adjusted to 28°C in winter. The air temperature inside the volume increased to 21.0°C in the colder months, which decreases the sensible heating capacity handled by the ventilation system and magnifies the effect of the radiant floor. The radiant floor results in a more uniform vertical temperature distribution in winter.

The ceiling-type cooling components are commonly preferred in storage volumes, since they occupy no ground space, and are placed on upper levels off the floor

accordingly they are not exposed to damage caused by material handling equipment (Runsey, 2008). The ceiling-type cooling system temperature is assumed to be set to 22°C to provide the optimal indoor temperature for the tobacco bales.

Accordingly, radiant cooling from the upper level and radiant floor heating systems are applied to the warehouse. Then, the CFD simulations are conducted to observe their impact on the temperature gradient. During these simulations, parametric studies are conducted to find the optimal application for heating and cooling while considering the energy efficiency of the appliances.

Figure 4.9 and Figure 4.10 show velocity contours on planes (a), (b), (c), (d) and (1), (2), (3), indicating the floor heating and the ceiling-mounted cooling systems for six months. The velocity range changes between 0.0 and 0.8 m/s for the floor heating scenarios while the velocity is lower with values between 0.0 and 0.5 m/s for ceiling-mounted cooling operations. This difference is caused by the impact of buoyancy forces.

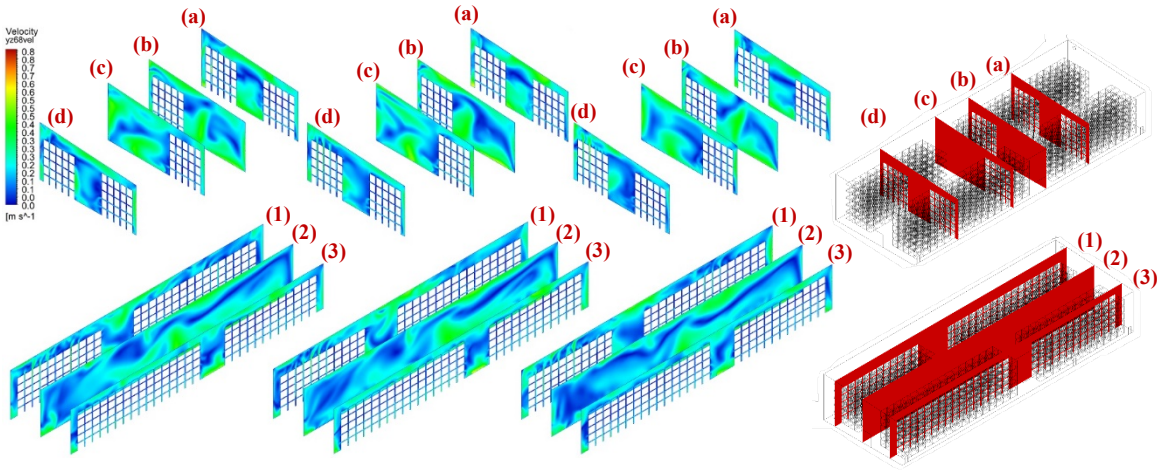

Figure 4.9. Velocity contours (0-0.8 m/s) of floor heating scenarios for (from left to right) January, February, and March

The velocity contours of the floor heating scenarios for three months are shown in Figure 4.9. The outcomes indicated that the effect of floor heating and additional buoyancy forces naturally dominates the air circulation in the space. It is shown that the movement of air decreases in March towards the end of the middle corridor.

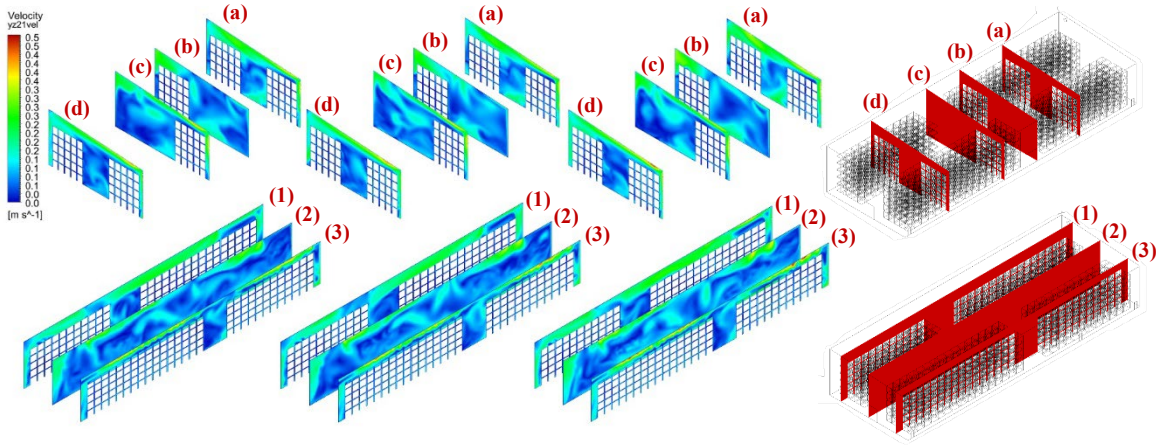

Figure 4.10. Velocity contours (0-0.5 m/s) of ceiling cooling scenarios for (from left to right) July, August, and September

The air gaps between the stacks of bales are also observed and the velocity is less than the other months in March as well. When the upper levels are also observed, the least movement in the air is observed in February. It is also correlated with the temperature gradient results which are shown in Figure 4.11. Despite the highest heating demands observed in February, the coolest month after floor heating simulations is also February. Therefore, the cooler air stays at the lower levels, while rises in heated air are observed in January and March.

Short planes cutting through the side corridors between bales also show different behaviors for three months. The more diffused air movement in these zones is also observed in January and March more than in February. Besides, the most diffused and the fastest air movement on the upper levels of the bales is also observed in January and March. This also shows the correlation between the similar heating demands of these two months, while the warehouse needs more heating energy than the other months.

The velocity contours collected from the CFD analyses for ceiling cooling scenarios are shown in Figure 4.10. The air velocity variations inside the volume are observed for three months. The results show that the highest velocities are observed in September. This result correlates with the vertical temperature gradient figure (Figure 4.11) as well. The air movements inside the volume are also the highest in September, concerning the highest temperature values. In July, air velocity has the lowest values which results in more stratified air activities. The corridor located in between the bales as well as the empty volumes in front of the side doors show that the air is not diffused to these areas as well.

The vertical temperature distributions for the cases of winter and summer periods are plotted in Figure 4.11 for comparison. An increasing temperature graph is expected to be observed within the months when the three-month periods are compared within the figure. This can be seen in Figure 4.11 (b), the differences are around 0.03°C/m. On the other side, when Figure 4.11 (a) is examined for winter months, it is observed that while the temperature values of January and March are close, February has lower temperature values.

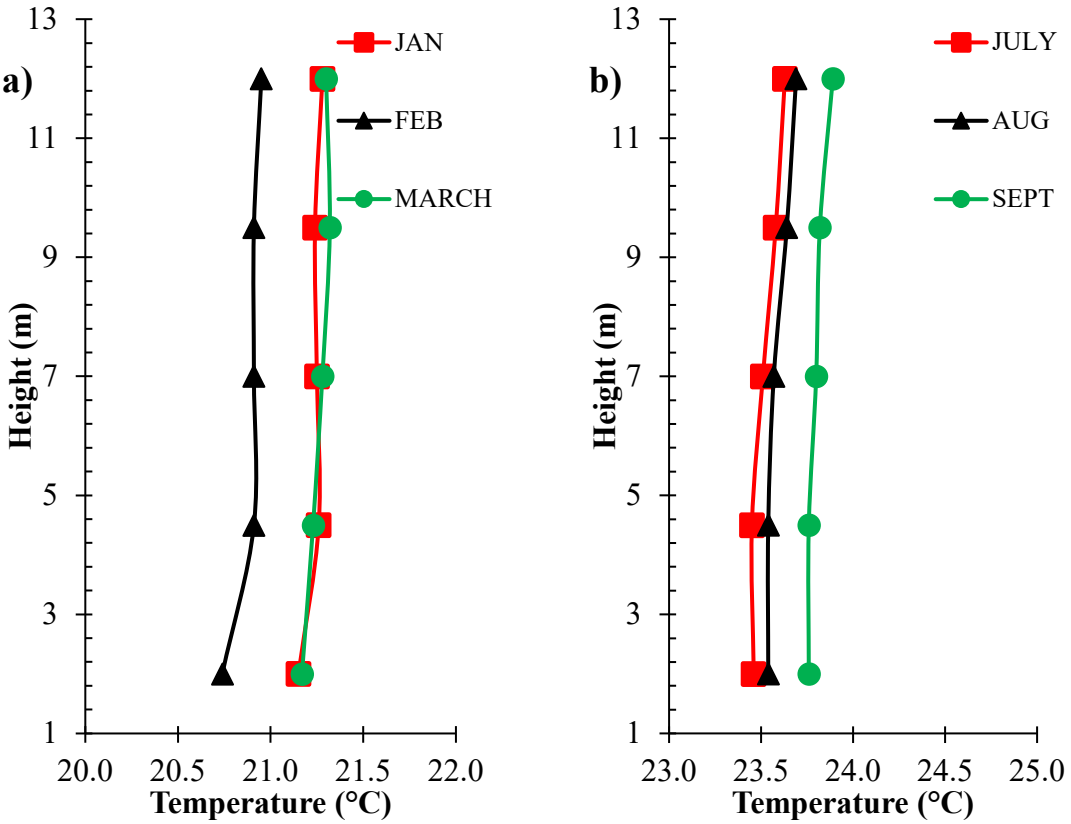

Figure 4.11. Vertical temperature gradient comparison among various months: (a) the coldest (floor heating) and (b) the warmest months (ceiling-mounted cooling)

As it is also previously shown in Figure 4.5, field measurements indicate that relatively lower indoor temperature values are observed in February and March within three months. This trend, which is observed in a different way than expected, is affected by the interventions during the material shipment. The reason for the observation of higher temperature values in January can also be seen in Table 3.1. The average

temperature in January is higher than in February and March. At the same time, solar radiation is higher in March. Since the heating radiant surface temperature is constant, the heat transfer values from the storage shell create differences on a monthly basis. At the same time, in addition to the effect of ventilation, it is seen that the thermal inertia of the building also affects the temperature graphs.

For the heating condition in the coldest months, the radiant heating condition has a diffused vertical temperature circulation as shown in Figure 4.11 (a). The average temperature rise in the volume is 6.9°C for three months when compared to the base case. Besides, the temperature gradient changes drop to 0.01°C/m and reach a maximum value of 0.02°C/m. Accordingly, it is shown in the figures that the vertical temperature gradient inside tends to be uniform in the heating situation. Therefore, the radiant floor heating reaches a uniform vertical temperature gradient in cooler months.

On the other hand, the ceiling-mounted cooling conditions have diffused vertical temperature circulations as shown in Figure 4.11 (b). The average temperature drop inside the volume is 3°C for three months when compared to the base case. In addition, the temperature gradient changes drop to 0.01°C/m and reaches a maximum value of 0.02°C/m. Therefore, it is shown in the figures that the vertical temperature gradient tends to be uniform in the cooling season as well. Consequently, ceiling-mounted cooling also provides a uniform vertical temperature gradient in warmer months.

After the CFD analyses have been conducted, the capacity of the heating and cooling units has also been calculated. According to the calculations, the monthly loads that would guide cooling and heating equipment capacity decisions are listed in Table 4.5 below.

Table 4.5. Monthly consumption values for thermal conditioning

Months		**Jan**	**Feb**	**March**	**July**	**Aug**	**Sept**
Required Capacities	**(kW)**	86.43	93.08	78.89	24.67	26.44	30.37
	(W/m^2)	36.78	39.61	33.57	10.5	11.25	12.92

Between the coldest months, the highest heating requirement is observed in February with 93.08 kW. In March the warehouse's heating demand is the least with 78.89 kW. The cooling consumption for the warmest months is between 25-30 kW. September is the most significant month to be considered for cooling demands since it has the highest value with 30.37 kW.

4.2.2.3. CASE C: Indoor Ventilation

The velocity outlet from each fan is 12 m/s. One of the fans is located on the north wall, while the other is installed on the east wall. The natural ventilation capacity of the zone is provided by the transportation door located on the north wall, as well. The door is 6 m wide with 4 m height.

CFD simulations are conducted to investigate the current situation of the natural and mechanical air conditioning environment of the warehouse. The base case scenario includes both fans running at full capacity and the transportation door being open to observe the maximum air movement inside.

It is shown in Figure 4.12 a) that the placement of the fans has an impact on the air movement inside the warehouse. The distance between the opened transportation door and fan 2 causes short-circuiting of the air so that the ventilation is not provided properly to the left side of the door. Since the air is sucked from fan 2 and goes through fan 1, the bales placed next to the exterior wall are the least ventilated zones. The air movement between the two fans is not evenly distributed, so there are unventilated zones even though the fans are assumed to perform at full capacity.

Two additional analyses are performed to observe the different fan operation scenarios. Figure 4.12 b) shows the velocity streamlines for fans working with 8 m/s capacity and c) shows the fans with different capacities as fan 1 working with 12 m/s and fan 2 with 6 m/s. It is seen that when fan 2 is working at half capacity, the air movement on the right-side increases while the bales located at the right side of the corridor are not exposed to air exchange.

On the other hand, air velocity around these bales and the corridor towards the door located in the exterior wall have higher values of air movement when both fans are working at 8 m/s capacity. The decrease in the fan 1 capacity increases the air movement

around the mid parts of the volume. However, when the capacity increases, since the suction of the air also increases, the air follows a more direct way to the outside.

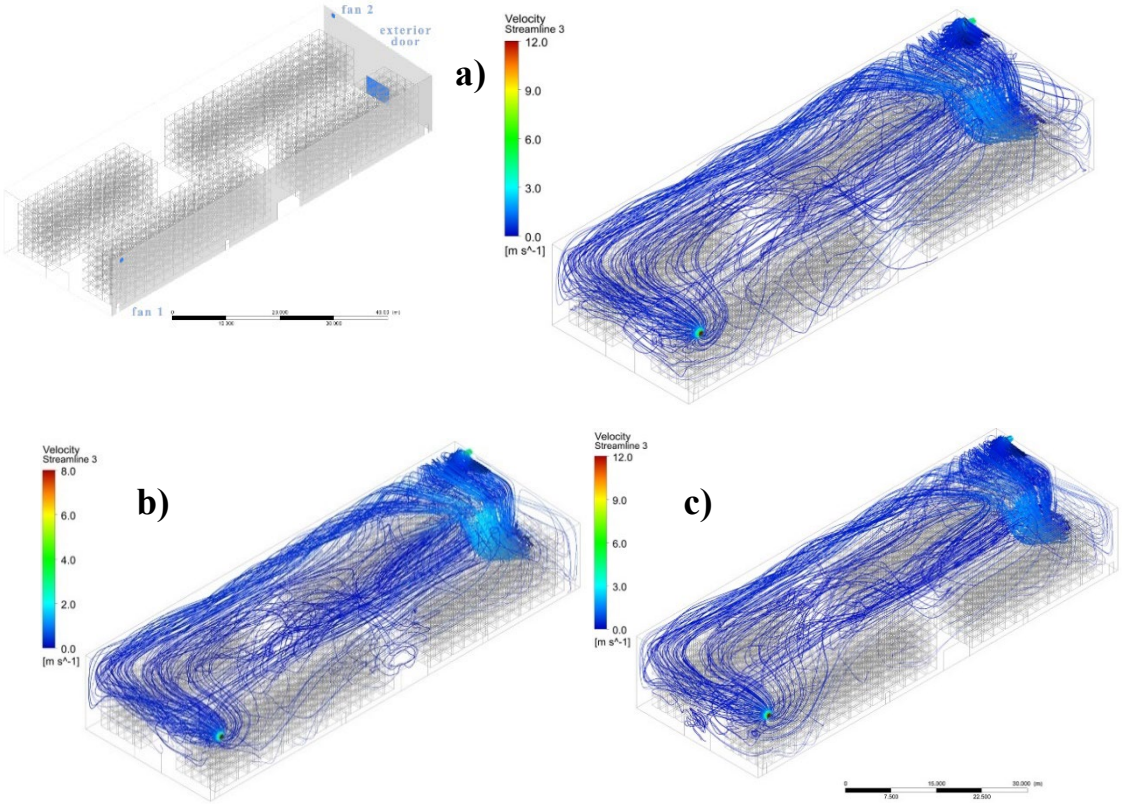

Figure 4.12. Current case fan scenarios; a) both at full capacity 12 m/s, b) both fans at 8 m/s, c) fan 1 at 12 m/s and fan 2 at 6 m/s

Figure 4.13 shows the velocity contours of the same scenarios. The locations of the planes are shown in Figure 4.6 with numbers (1), (2), and (3). The velocity contours of both stored bale sides, as well as the main corridor, are shown in these planes. The black arrows show the location and the direction of the incoming air. The changes in the air velocity are shown in more detailed sections. The more direct movement of the air in the first case is also seen in these contours. The passages of the air are more diffused in the last case. The simulations show that operating the fans at full capacity with higher amounts of energy does not guarantee increasing air movement around the bales. The location and the number of fans is also other indicators for improving the environmental conditions.

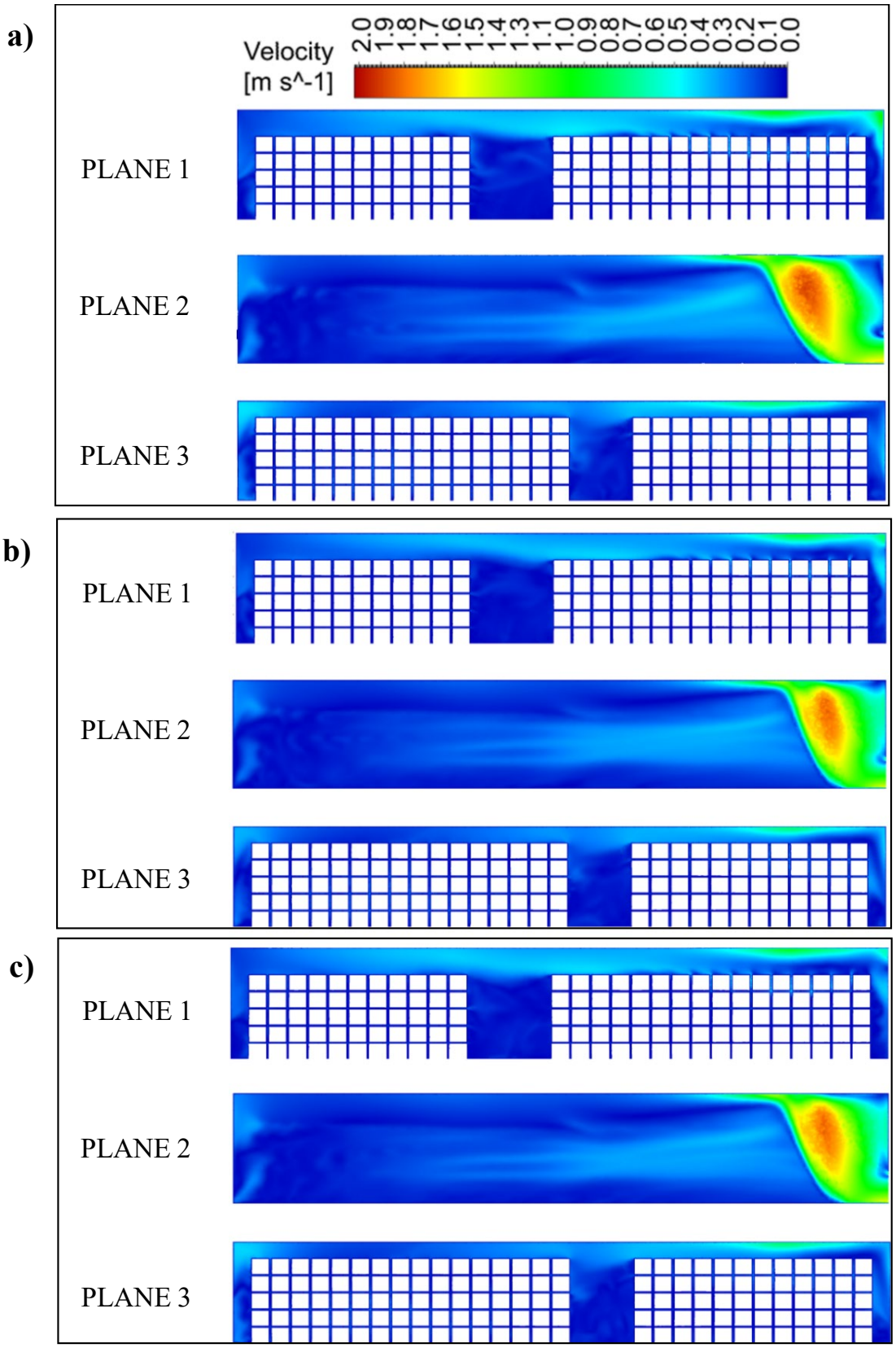

Figure 4.13. Velocity contours of the current case fan scenarios; a) both at full capacity 12 m/s, b) both fans at 8 m/s, c) fan 1 at 12 m/s and fan 2 at 6 m/s (Planes are 1,2 and 3; from top to bottom)

4.2.2.3.1. Scenarios for Indoor Ventilation Improvement

By observing the existing natural and mechanical ventilation conditions inside the warehouse, additional fan scenarios are taken into consideration. In the current situation, there are stagnant zones where air cannot exchange, and fresh air is not provided as well as a lack of diffused temperature gradients in various locations of the storage space. Accordingly, increasing the area that air is traveling as well as increasing the air exchange effectiveness is also one of the main aims of storage warehouses.

A properly working fan organization around the zone is supposed to improve execution on thermal comfort, required environment conditions for stored products, and energy efficiency. Firstly, the extreme case scenario is considered, and four different supplying fan additions (fans 3, 4, 5, and 6) are tested using the validated CFD model.

In this section, the CFD model has the same configuration as used in the validation work. Furthermore, additional fans are also assumed to have the same capacities as the existing ones. As indicated previously in Figure 3.23, fan 4 is included in the exterior wall with the operable transportation door, the location of the fan is symmetrical to the existing fan 2. Besides, three more fans are placed on the longer side of the room to work with the existing fan 1. Two of the fans are placed on the middle top of the two tobacco bale stacks and the third fan is located on top of the rarely used transportation door placed between those two stacks, at the same vertical level as the existing fan. With reference to the fans visualized in Figure 3.23, different cases for various fan arrangements are generated.

The current situation included three different cases of already mounted fans. Both fans are assumed to be working at full capacity in Case 1, both fans working at 2/3 capacity are indicated for Case 2, and Case 3 includes the first fan working at full capacity and the second fan working at half capacity.

When the additional four fans are included in the scenarios, two different cases are generated. Firstly, all the fans are assumed to be working at full capacity. While the second trial is focused on avoiding short-circuiting and stagnant zones of the air, at the same time refreshing the air inside at the optimal time. Accordingly, fan 1 which is located at the farthest location from the transportation door used for natural ventilation purposes, is assumed to be working at full capacity while the rates of the fans are reduced as getting closer to the outer door (fan 5: 9.6 m/s, fan 3: 7.2 m/s, fan 6: 4.8 m/s, fan 2 and 4: 2.4 m/s). These five cases are also shown in Table 4.6., comprehensively.

Table 4.6. Cases used for the simulations with various fan arrangements.

Cases		Door	Fan 1	Fan 2	Fan 3	Fan 4	Fan 5	Fan 6
Current Situation	**Case 1**	Open	12 m/s	12 m/s	--	--	--	--
	Case 2	Open	8 m/s	8 m/s	--	--	--	--
	Case 3	Open	12 m/s	6 m/s	--	--	--	--
Fan Additions	**Case 4**	Open	12 m/s	12 m/s	12 m/s	12 m/s	12 m/s	12 m/s
	Case 5	Open	12 m/s	2.4 m/s	7.2 m/s	2.4 m/s	9.6 m/s	4.8 m/s

The velocity streamlines of Case 4 and Case 5 are shown in Figure 4.14. It is shown in the figures that the air is more diffused inside of the volume at the full capacity scenario. However, the volume around fan 2 is not equally ventilated as the remaining zone. On the other hand, more diffused air ventilation around the opened transportation door is observed in Case 5. When the tobacco bales stacked around fan 1 are compared between the two cases, it is seen that the ventilation is more diffused with the full capacity in Case 4. When the fans work at full capacity, the velocity inside the volume reaches around 4 m/s values while working at various capacities the highest air velocity values increase to 3 m/s.

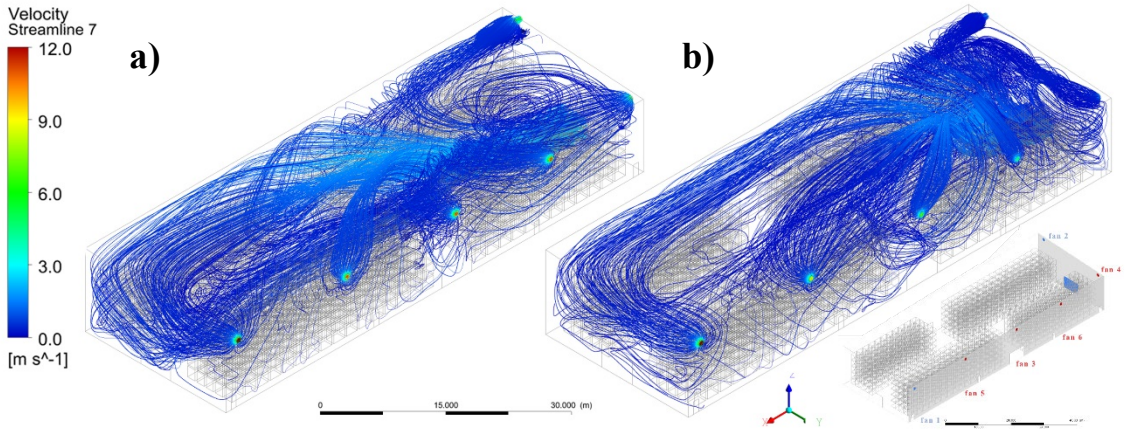

Figure 4.14. Velocity streamlines for the cases with additional four fans: a) Case 4, b) Case 5

4.2.2.3.2. Indoor Environment Conditions and Efficiency of Ventilation

The mean age of the air refers to a statistical measure indicating the time taken for all particles of fresh air to travel from the supply inlet to an arbitrary location. The air age, also known as AoA (Age of the Air), is a significant parameter in assessing environmental conditions as it reflects both air freshness and the distribution of fresh air. In numerical modeling, a transport model has been employed to analyze the air age. It is important to note that the local mean AoA is a passive quantity determined by the steady-state solution of air flow equations and does not impact the airflow patterns.

In ANSYS Fluent software, pre-existing models for calculating the mean AoA properties are not provided. A user-defined scalar (UDS) should be integrated into the CFD model in the pre-processing stage to find the mean AoA. As a result, the mean AoA equation needs to be incorporated into CFD simulation using user-defined functions (UDF). These UDFs are compiled into executable functions within the ANSYS Fluent solver (ANSYS FLUENT 15.0, 2013).

The UDF is used to calculate fluid residence time (Figure 4.15) and the UDS value is defined as zero at the inlet. UDS has units of time and represents the estimated residence time of fluid in the domain. A value of 0.7 is used for the turbulent Schmidt number. The UDFs are defined with five arguments: name, *c, t, dS*, and *eqn.* The "name" represents the UDF's name, while "*c*," "*t*," "*dS*," and "*eqn*" are variables passed by the ANSYS Fluent solver to the UDF. Similarly, for defining diffusivity, four arguments are used: *name*, *c*, *t*, and *i*. The UDF is responsible for calculating the diffusivity for a single cell and returning a real value to the solver.

```
#include "udf.h"
#include "prop.h"
#This defines the AoA diffusivity
DEFINE_DIFFUSIVITY (mean_age_diff, c, t, i)
{
return C_MU_EFF(c,t)/0.7;
}
#This defines the source
DEFINE_SOURCE (mean_age_source, c, t, dS, eqn)
{
real source;
source = C_R(c,t);
dS[eqn]=0;
return source;
}
```

Figure 4.15. UDF for calculating the mean AoA

Figure 4.16. shows the local mean AoA for the current case fan scenarios (Cases 1,2 and 3). The maximum AoA values reach up to 6500 seconds at the furthest side of the volume from the transportation door used for natural ventilation. This situation mainly occurs when both fans work at 8 m/s in Case 2. However, when both fans are working at full capacity in Case 1, the shortest time intervals are observed inside the volume. In this case, the fresh air movement reaches almost all the tobacco bales stored inside the zone.

When fan 1 works at full capacity and fan 2 decreases to half capacity in Case 3, it is observed that the mean AoA values are similar to the first case for the entire volume. It shows that reducing the fan 2 capacity can still provide fresh air inside the volume while the other works at full capacity. Therefore, more energy-efficient approaches can be followed for conditioning the storage without any compromise from the indoor environment conditions.

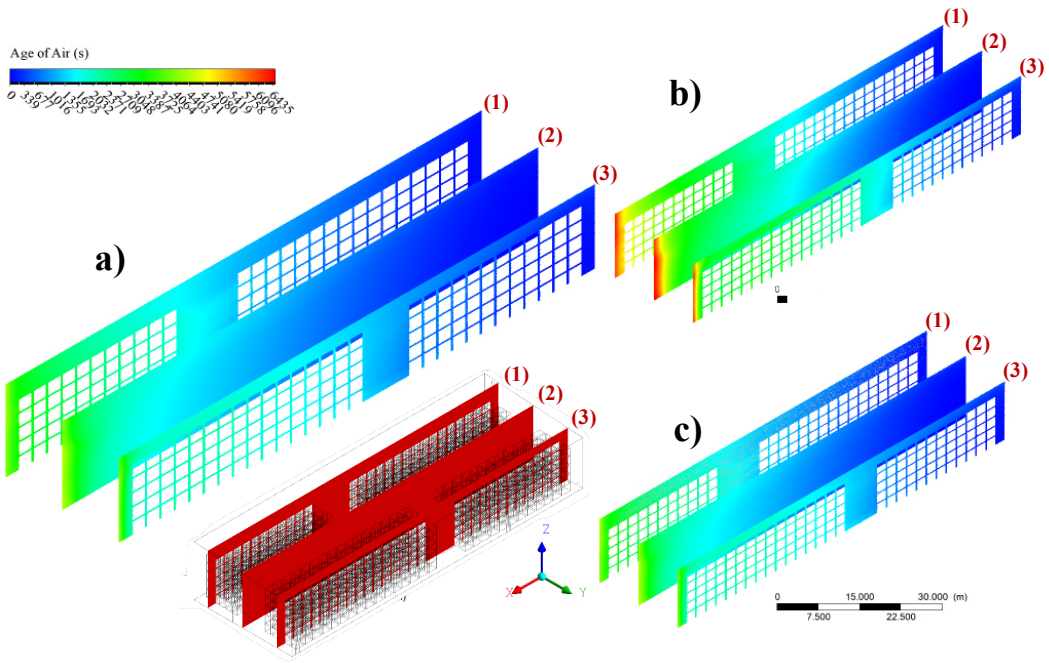

Figure 4.16. AoA at the current case fan scenarios; a) Case 1, b) Case 2, c) Case 3

The mean AoA along the x direction for six fans installed scenarios are visualized in Figure 4.17. The maximum aged air is around 3000 seconds, which is half of the time spent in previous cases. The most aged air is located at the farthest location from the supply air position. The location of the supply air shows a significant role in refreshing the air near and later at the end of the volume. However, due to the height of the supply air surface, the residence time of the air at upper levels is higher than in the lower zones.

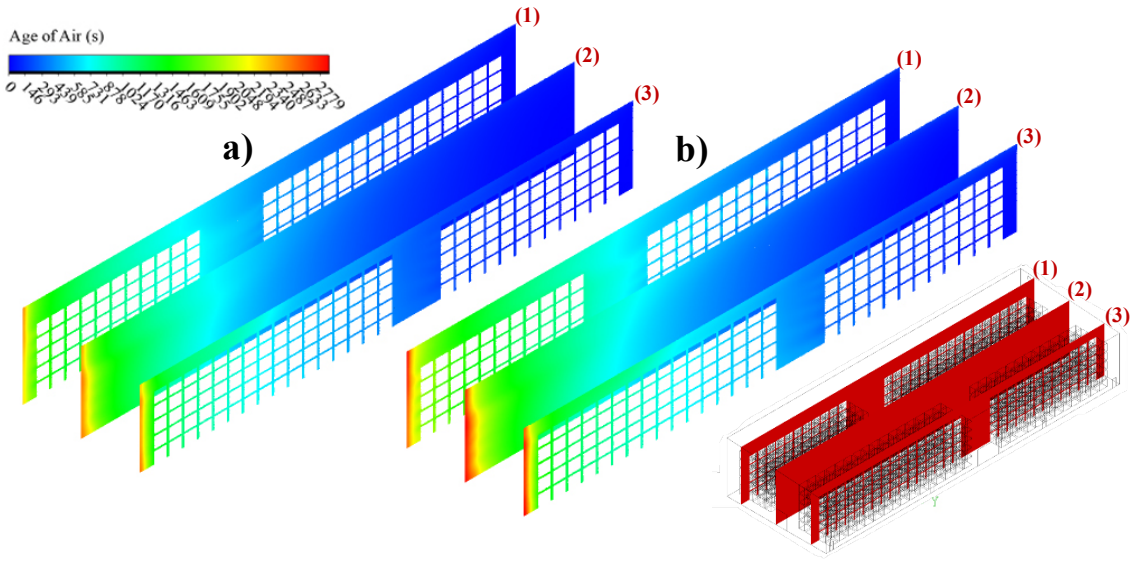

Figure 4.17. AoA at the cases with additional four fans; a) Case 4, b) Case 5

The spatially normalized mean AoA is averaged at the different vertical planes aligned to the floor and plotted along the z direction in Figure 4.18. Due to the horizontal convergence flow induced by the merging of thermal movements, the air near the supply air side of the room, where x is close to zero, is well refreshed. On the other hand, the aged air is transferred to the upper levels of the room.

The supply level shows a significant role in the location of refreshed air near the 4m level, while the air age at lower parts near zero has slightly higher residence times. However, as it gets closer to the roof level, the increase in the age of the air gradually slows down, and the difference in the age of air between different altitudes decreases.

The figure also shows that the close placement of a secondary fan to another fan or the fresh air source and keeping its capacity high as the other fans can cause higher values of the local mean AoA inside the warehouse (Figure 4.18). Short-circuiting between the openings occurs when they are located close to each other. This occurs when air enters through the supply openings and exits through the other without crossing the occupied zone.

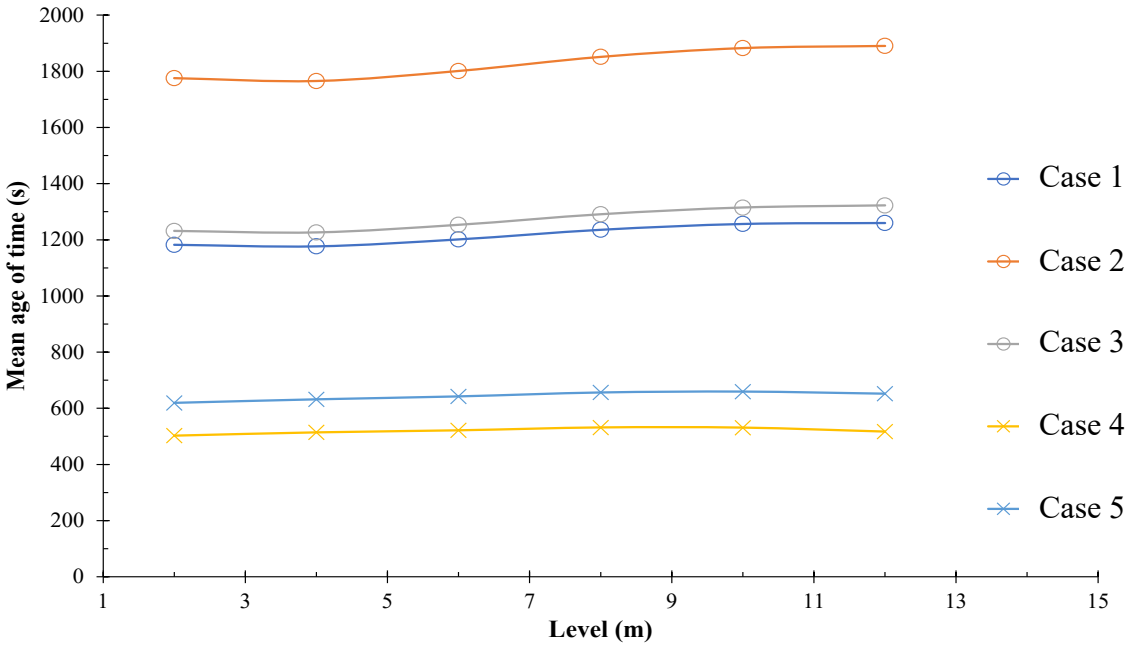

Figure 4.18. Spatial averaged mean AoA distribution within the planes along the z-direction

The description of air flow patterns, by air exchange efficiency (ε^a), involves assessing the local and average age of the air. This evaluation is achieved through calculations based on research of Davidson & Olsson, (1987) and the obtained 'ε^a' parameter (Mundt et al., 2004). To ensure the accurate design of subsequent numerical models, a comprehensive experimental and numerical study was conducted in multiple rooms within different buildings. The experimental results served as a reference point for validating the following numerical model.

The 'ε^a' parameter represents the correlation between the actual time required to completely replace the air in a given space, known as the return time (τ_t), and the average time it takes for air exchange to occur ($\bar{\tau}_{exc}$) (Sandberg, 1981). It is expressed as a percentage using the formula.

$$\varepsilon^a = \frac{\tau_t}{\bar{\tau}_{exc}} \times 100\ (\%) \qquad \text{Eqn. 4.3}$$

During experimental and numerical studies, the 'ε^a' parameter was determined by comparing the local mean age of the exhaust air (τ_e) to twice the average age of air within the room ($\bar{\tau}$), regarding an optimal theoretical model called the "piston model" (Sandberg, 1981).

$$\varepsilon^a = \frac{\tau_e}{2 \times (\bar{\tau})} \times 100\ (\%) \qquad \text{Eqn. 4.4}$$

The local mean age of the air (τ_e) is a statistical value representing the average time taken by fresh air particles to travel from the inlet to the specified point under investigation. By obtaining the average value of the local age of all the air in the room, the room's average age of the air ($\bar{\tau}$), was determined (Sandberg & Sjöberg, 1983).

The air change effectiveness function quantifies the contribution of an architectural design for air mixing within enclosed spaces. It represents the relationship between the time required for clean ambient air to replace the air within a space and the minimum flow rate necessary to achieve the same level of air quality. The air change efficiency function measures the air quality within enclosed spaces, while the age of the air assesses the quality of the flowing air. According to the minimum ACE 0.95 criteria for modern building regulations, for instance, the displacement air within the enclosed

volume must provide an air change effectiveness (ACE) higher than 0.95 for at least 95 % of the net lettable area (NLA) when measured by ASHRAE (2002a).

Table 4.7. shows the volumetric mean ages of air and air change effectiveness percentages collected from the results of the CFD simulations for each scenario. It indicates that the mean AoA declines depending on the air flow rate. Accordingly, as the air flow rate increases, less residence time of the air is observed. Although, the highest volumetric mean AoA yields up to 1843 s, operating fan 1 with full capacity and fan 2 with half capacity in Case 3 can decrease AoA down to 1285 s as well as increase the air change effectiveness. Furthermore, the installation of four additional fan scenarios can decrease mean AoA down to half with 651 s residency time for the air. It is also shown in the table that the highest air changes in an hour are provided by installing six fans and working them at full capacity in Case 4 with a value of 7.49 ACH. However, six fans at different capacities in Case 5 only provide only a 4 ACH air change rate.

Table 4.7. The mean AoA, air changes per hour, and air change effectiveness for all scenarios

Cases		Mean Age of Air (s)	Air Changes per Hour (ACH)	Air Change Effectiveness (%)
Current Situation	**Case 1**	1229.36	2.50	94.86
	Case 2	1842.93	1.66	94.62
	Case 3	1285.20	1.87	94.67
Fan Additions	**Case 4**	524.07	7.49	120.91
	Case 5	651.09	4.00	119.63

Between the current case situation cases, the shortest residency time for air is achieved when both fans are working at full capacity in Case 1. However, the close location of the secondary fan to the air intake changes the correlations between the AoA and the air change effectiveness. The comparison between base case scenarios also shows that increasing the capacity of the secondary fan near the fresh air income source (opened transportation door in this case) leads to higher values of mean AoA inside the warehouse, which also decreases air change effectiveness. Nevertheless, when the maximum number of operational fan scenarios are compared, the air residency inside is half of the current

situation scenarios. On the other hand, it is possible to see that the mean AoA inside the volume is similar between the two additional fan cases. Therefore, using different capacities of fans may provide the required air quality for the stored product inside. Besides, less energy would be used which can also support energy efficiency-oriented air conditioning approaches.

CHAPTER 5

DISCUSSIONS AND CONCLUSION

This thesis addressed the significant challenges faced by warehouses in terms of energy consumption and indoor environment conditions, highlighting the critical need for improving energy efficiency and promoting environmental sustainability. By investigating the influence of various architectural design strategies on thermal performance and emphasizing the importance of thermal destratification and air mixing strategies, valuable insights have been gained for industrial building designers and specialists.

5.1. Discussions

Warehouses are known for their substantial energy consumption and reliance on natural resources to maintain optimal indoor environment conditions. To address this challenge, there is a growing need for systematic approaches during the design stage to improve energy efficiency and environmental sustainability. This study presents a multi-faceted investigation focusing on two key aspects: (1) the impact of architectural design strategies on the thermal performance of naturally ventilated industrial buildings, and (2) the importance of thermal destratification and air mixing strategies for providing optimal indoor environment conditions for the stored products.

Using a sensitivity analysis approach, the study explores the influence of 15 architectural design strategies on the thermal performance of a tobacco warehouse located in İzmir, Turkey. Annual heating and cooling consumption, as well as operational CO_2 emissions, are evaluated across a range of thermal insulation and shading options, considering specific air infiltration and solar characteristics. The building is modeled using OpenStudio 2.3.0, with sensitivity analyses conducted using SimLab. The findings indicate that roof thermal insulation thickness, shading projection factor, and shading angle for the east facade are the most significant factors affecting the heating and cooling requirements of the warehouse. Furthermore, roof and east facade thermal insulation

thickness, along with the conductivity of the roof insulation material, significantly impact the operational CO_2 emissions.

Additionally, the study addresses the vertical and volumetric temperature gradients which are critical for the quality of the stored product and the necessity for thermal destratification as well as stabilizing the indoor air conditions. Field measurements and CFD simulations conducted in ANSYS FLUENT quantitatively assess these temperature gradients. The investigation also explores the effects of mechanical conditioning of indoor air with ceiling-mounted radiant cooling systems and floor-mounted heating systems through CFD-based numerical simulations. The results demonstrate the potential of the proposed cooling system to reduce indoor temperatures by 3°C and the heating system to increase indoor temperatures by 7°C. Moreover, the combined use of ceiling-mounted radiant cooling systems and floor heating systems helped to keep the indoor temperature between 21-25°C for the whole year. This enhances air conditioning effectiveness and temperature uniformity within the warehouse space.

Lastly, the air exchange impacts of various operational conditions for the existing two fans inside the warehouse are investigated through CFD simulations. To increase the air exchange quality an additional four fans are proposed. The comparison between the existing situation and the proposed scenarios are compared. The volumetric mean age of air is decreased to 1230 seconds in the current situation while additional fans can decrease the residence time of air to 525 seconds. The findings indicated that even though additional fans may decrease the mean age of air, maximizing the fan operation capacities is not obligatory to achieve increased air change effectiveness. It is seen that systematically analyzing various fan operations can increase environmental conditions as well as provide energy-efficient solutions.

The outcomes of this study offer valuable insights for industrial building designers and specialists. The identification of key design parameters, such as roof materials and shading elements, highlights their significant influence on the indoor environment and energy consumption. The integration of sensitivity analysis with building energy simulation tools provides a systematic approach to inform design decisions and improve performance. Moreover, the investigation of thermal air mixing and conditioning strategies in warehouses emphasizes the need for a combined experimental and numerical approach to optimize indoor environmental conditions. Ultimately, the study's findings and proposed retrofit assessment may contribute to the development of effective solutions

for warehouses storing temperature-sensitive products, ensuring optimal storage conditions, and mitigating the impact of temperature variations during logistic operations.

5.2. Conclusion

Warehouses are high-energy-consuming facilities that rely on natural resources to maintain indoor environment conditions. To enhance energy efficiency and environmental sustainability, systematic approaches are needed during the design stage. This study provides insights into the thermal performance and indoor environment conditions of warehouses, focusing on the impact of architectural design strategies and thermal conditioning techniques. Through a sensitivity analysis approach, the results revealed that roof thermal insulation thickness, shading projection factor, and shading angle for the east facade are key factors affecting the heating and cooling requirements of the warehouse. Additionally, roof and east facade thermal insulation thickness, along with the conductivity of the insulation material, significantly influenced the operational CO_2 emissions.

Furthermore, the study emphasized the importance of addressing vertical and volumetric temperature fluctuations within warehouses. Field measurements and CFD simulations demonstrated the effectiveness of mechanical conditioning strategies, such as ceiling-mounted radiant cooling systems and floor-mounted heating systems, in maintaining optimal indoor temperatures. The simulations revealed reductions in indoor temperatures during summer and increases in winter, resulting in a consistent temperature range of 21-25°C throughout the year. These findings highlight the enhanced air conditioning effectiveness and temperature uniformity achieved through these thermal destratification and air mixing techniques.

Additionally, the study explored the air exchange impacts of various operational conditions using CFD simulations. The proposed addition of four additional fans was found to improve environmental conditions as well as reduce the volumetric mean age of air. Importantly, the findings indicated that maximizing fan operation capacities is not necessary for increased air change effectiveness. Systematic analysis of different fan operations can achieve improved environmental conditions while ensuring energy efficiency.

Overall, this study offers insights for industrial building designers and specialists, highlighting the significant influence of design parameters, such as roof materials, shading elements, and insulation thickness, on the indoor environment and energy consumption. The integration of sensitivity analysis with building energy simulation tools provides retrofit possibilities for informed design decisions and performance improvement. Furthermore, this research emphasizes the necessity of employing a combined experimental and numerical approach to optimize indoor environmental conditions, particularly in warehouses that store temperature-sensitive products. The findings and proposed retrofit assessment may contribute to the development of effective solutions for warehouses storing temperature-sensitive products, ensuring optimal storage conditions, as well as addressing the challenges posed by temperature variations and minimizing the impact of these variations during logistic operations.

REFERENCES

Accorsi, R., Bortolini, M., Gamberi, M., Manzini, R., & Pilati, F. (2017). Multi-objective warehouse building design to optimize the cycle time, total cost, and carbon footprint. *The International Journal of Advanced Manufacturing Technology*, *92*(1–4), 839–854. https://doi.org/10.1007/s00170-017-0157-9

Andersen, K. T. (1998). Design of natural ventilation by thermal buoyancy with temperature stratification. *Proceedings of 6th International Conference on Air Distribution in Rooms*, 437–444.

Angel, B. W. F., Van Damme, D. A., Ivanovskaia, A., Lenders, R. J. M., & Veldhuijzen, R. S. (2006). *Warehousing Space in Europe: Meeting Tomorrow's Demand. A Pan-European Warehousing Trends Study by Capgemini and ProLogis*.

ANSYS. (2018). *Ansys Fluent User's Guide Release 19*.

ANSYS FLUENT 15.0. (2013). *UDF Manual, Release 15.0*. Chapter 2.

ASHRAE. (2002a). *ANSI/ASHRAE 129-1997 (RA 2002) Measuring Air-Change Effectiveness*.

ASHRAE. (2002b). *ASHRAE Guideline 14-2002: Measurement of Energy Demand and Savings. Atlanta: American Society of Heating, Refrigerating and Air-Conditioning Engineers*.

ASHRAE. (2017). *American Society of Heating, Refrigerating and Air-Conditioning Engineers (ASHRAE). 2017. ASHRAE Standards: standards for natural and mechanical ventilation. Atlanta, GA.*

Ataseven, Y. (2005). *Tobacco policies in the EU and Turkey - a comparative analysis*. Ankara University (in Turkish).

Ayata, T. (2009). Investigation of building height and roof effect on the air velocity and pressure distribution around the detached houses in Turkey. *Applied Thermal Engineering*, *29*(8–9), 1752–1758. https://doi.org/10.1016/j.applthermaleng.2008.08.018

Aynsley, R. (2005). Saving Energy with Indoor Air Movement. *International Journal of Ventilation*, *4*(2), 167–175.

B., L., J. D., S., & J. D., M. (1998). Air Velocity and High-Temperature Effects on Broiler Performance. *Poultry Science*, *77*, 391–393.

Barbaresi, A., De Maria, F., Torreggiani, D., Benni, S., & Tassinari, P. (2015). Performance assessment of thermal simulation approaches of wine storage buildings based on experimental calibration. *Energy and Buildings*, *103*, 307–316. https://doi.org/10.1016/j.enbuild.2015.06.029

Barbaresi, A., Torreggiani, D., Benni, S., & Tassinari, P. (2014). Underground cellar thermal simulation: Definition of a method for modeling performance assessment based on experimental calibration. *Energy and Buildings*, *76*, 363–372. https://doi.org/10.1016/j.enbuild.2014.03.008

Boon, C. R., & Battams, V. A. (1988). Air mixing fans in a broiler building —Their use and efficiency. *Journal of Agricultural Engineering Research*, *39*(2), 137–147. https://doi.org/10.1016/0021-8634(88)90136-9

Brandan, M., & Alejandra, M. (2012). *Study of airflow and thermal stratification in naturally ventilated rooms* [Massachusetts Institute of Technology]. http://hdl.handle.net/1721.1/74907

Calay, R. K., Borresen, B. A., & Holdø, A. E. (2000). Selective ventilation in large enclosures. *Energy and Buildings*, *32*(3), 281–289. https://doi.org/10.1016/S0378-7788(00)00054-2

Calegari, F., Calamari, L., & Frazzi, E. (2016). Cooling systems of the resting area in free stall dairy barn. *International Journal of Biometeorology*, *60*(4), 605–614. https://doi.org/10.1007/s00484-015-1056-0

Chen, Q. (1995). COMPARISON OF DIFFERENT k -ε MODELS FOR INDOOR AIR FLOW COMPUTATIONS. *Numerical Heat Transfer, Part B: Fundamentals*, *28*(3), 353–369. https://doi.org/10.1080/10407799508928838

Colicchia, C., Marchet, G., Melacini, M., & Perotti, S. (2013). Building environmental sustainability: empirical evidence from Logistics Service Providers. *Journal of Cleaner Production*, *59*, 197–209. https://doi.org/10.1016/j.jclepro.2013.06.057

Conti, J., & Holtberg, P. (2022). *International Energy Outlook 2022; Technical Report DOE/EIA-0484*.

Cook, P., & Sproul, A. (2011). Towards low-energy retail warehouse building. *Architectural Science Review*, *54*(3), 206–214. https://doi.org/10.1080/00038628.2011.590055

Daheng, Y. (2010a). Optimizing design scheme of energy saving in warehouse building based on grey relational analysis. *2010 International Conference on Logistics Systems and Intelligent Management (ICLSIM)*, *2*, 1090–1092. https://doi.org/10.1109/ICLSIM.2010.5461125

Daheng, Y. (2010b). Optimizing design scheme of energy saving in warehouse building based on grey relational analysis. *2010 International Conference on Logistics Systems and Intelligent Management (ICLSIM)*, 1090–1092. https://doi.org/10.1109/ICLSIM.2010.5461125

Davidson, L., & Olsson, E. (1987). Calculation of age and local purging flow rate in rooms. *Building and Environment*, *22*(2), 111–127. https://doi.org/10.1016/0360-1323(87)90031-X

Delsante, A. E., & Vik, T. A. (2000). *State-of-the-Art Report on Hybrid Ventilation*.

Dhooma, J., & Baker, P. (2012). An exploratory framework for energy conservation in existing warehouses. *International Journal of Logistics Research and Applications*, *15*(1), 37–51. https://doi.org/10.1080/13675567.2012.668877

Ding, T., Fang, L., Ni, J.-Q., Shi, Z., Sun, B., Wang, Z., & Yao, C. (2018). Optimization of Diffuser Parameters for Mixing Fans in Agricultural Buildings. *Applied Engineering in Agriculture*, *34*(2), 437–444. https://doi.org/10.13031/aea.12461

Doherty, S., & Hoyle, S. (2009). *Supply Chain Decarbonisation: The Role of Logistics and Transport in Reducing Supply Chain Carbon Emissions*.

Dominguez Espinosa, F. A., & Glicksman, L. R. (2017). Determining thermal stratification in rooms with high supply momentum. *Building and Environment*, *112*, 99–114. https://doi.org/10.1016/j.buildenv.2016.11.016

Elkington, J. (1998). Partnerships from cannibals with forks: The triple bottom line of 21st-century business. *Environmental Quality Management*, *8*(1), 37–51. https://doi.org/10.1002/tqem.3310080106

Estelles, J. I. (2018). Study of the ventilation system in a warehouse and a cooking school. In *Department of Building, Energy and Environmental Engineering: Vol. Masters De*.

Ezzeldin, S., & Rees, S. J. (2013). The potential for office buildings with mixed-mode ventilation and low-energy cooling systems in arid climates. *Energy and Buildings*, *65*, 368–381. https://doi.org/10.1016/j.enbuild.2013.06.004

FAOSTAT. (2022). *Food and Agriculture Organization of the United Nations [FAO]*. https://www.fao.org/faostat/en/#data/TCL

Federal Ministry for Economic Affairs and Energy. (2016). *Green Paper on Energy Efficiency*. https://www.bmwk.de/Redaktion/EN/Publikationen/green-paper-on-energy-efficiency.pdf?__blob=publicationFile&v=4

Fichtinger, J., Ries, J. M., Grosse, E. H., & Baker, P. (2015). Assessing the environmental impact of integrated inventory and warehouse management. *International Journal of Production Economics*, *170*, 717–729. https://doi.org/10.1016/j.ijpe.2015.06.025

Gilani, S., Montazeri, H., & Blocken, B. (2016). CFD simulation of the stratified indoor environment in displacement ventilation: Validation and sensitivity analysis. *Building and Environment*, *95*, 299–313. https://doi.org/10.1016/j.buildenv.2015.09.010

Gil-Lopez, T., Galvez-Huerta, M. A., O'Donohoe, P. G., Castejon-Navas, J., & Dieguez-Elizondo, P. M. (2017). Analysis of the influence of the return position in the vertical temperature gradient in displacement ventilation systems for large halls. *Energy and Buildings*, *140*, 371–379. https://doi.org/10.1016/j.enbuild.2017.02.017

Heiselberg, P. (2002). *Principles of hybrid ventilation*.

Helton, J. C., Johnson, J. D., Sallaberry, C. J., & Storlie, C. B. (2006). Survey of sampling-based methods for uncertainty and sensitivity analysis. *Reliability Engineering & System Safety*, *91*(10–11), 1175–1209. https://doi.org/10.1016/j.ress.2005.11.017

Ho, S. H., Rosario, L., & Rahman, M. M. (2010). Numerical simulation of temperature and velocity in a refrigerated warehouse. *International Journal of Refrigeration*, *33*(5), 1015–1025. https://doi.org/10.1016/j.ijrefrig.2010.02.010

Hongwei, X., Ivan L., B., G. Tom, T., & T. Lionel, B. (1994). Temperature and Humidity Profiles of Broiler Houses with Experimental Conventional and Tunnel Ventilation Systems. *Applied Engineering in Agriculture*, *10*(4), 535–542.

Huang, J., & Gurney, K. R. (2016). The variation of climate change impact on building energy consumption to building type and spatiotemporal scale. *Energy*, *111*, 137–153. https://doi.org/10.1016/j.energy.2016.05.118

Hussain, S., Oosthuizen, P. H., & Kalendar, A. (2012). Evaluation of various turbulence models for the prediction of the airflow and temperature distributions in atria. *Energy and Buildings*, *48*, 18–28. https://doi.org/10.1016/j.enbuild.2012.01.004

Jang, S., Cha, K., Yang, J., Lee, C., Shin, S., & Jo, C. (2007). Changes in water activity and physicochemical properties of burley tobacco as affected by storage and moisture contents. *J Korean Soc Tobacco Sci*, *29*, 59–65.

Karaman, S., Okuroğlu, M., Kızıloğlu, F. M., Memiş, S., & Cemek, B. (2009). Design of Proper Apple Storage Facilities for Karaman Province. *Tarım Bilimleri Araştırma Dergisi*, *2*(1), 145–154.

Karava, P., Athienitis, A. K., Stathopoulos, T., & Mouriki, E. (2012). Experimental study of the thermal performance of a large institutional building with mixed-mode cooling and hybrid ventilation. *Building and Environment*, *57*, 313–326. https://doi.org/10.1016/j.buildenv.2012.06.003

Kibar, H. (2012). DESIGN AND MANAGEMENT OF POSTHARVEST POTATO (Solanum tuberosum L.) STORAGE STRUCTURES. *Ordu Univ. J. Sci. Tech.*, *2*(1), 23–48.

Kibar, H., Maman, K., Gülbe, A., & Can, Ç. (2015). Design of Corn Storage Structure and Ventilation System for Igdır Province. *Journal of Agricultural Faculty of Gaziosmanpasa University*, *32*(1), 37–46.

Kitagawa, H. (2017). Environmental Policy Under President Xi Jinping Leadership: The Changing Environmental Norms. In *Environmental Policy and Governance in China* (pp. 1–15). Springer Japan. https://doi.org/10.1007/978-4-431-56490-4_1

Kobayashi, T., Sugita, K., Umemiya, N., Kishimoto, T., & Sandberg, M. (2017). Numerical investigation and accuracy verification of indoor environment for an impinging jet ventilated room using computational fluid dynamics. *Building and Environment*, *115*, 251–268. https://doi.org/10.1016/j.buildenv.2017.01.022

Kong, Q., & Yu, B. (2008). Numerical study on temperature stratification in a room with an underfloor air distribution system. *Energy and Buildings*, *40*(4), 495–502. https://doi.org/10.1016/j.enbuild.2007.04.008

Krautheim M., Pasel R, P. S. and G. JS. (2014). *City and Wind-Climate as an Architectural consultant*. Dom Publishers.

Lewczuk, K., Kłodawski, M., & Gepner, P. (2021). Energy consumption in a distributional warehouse: A practical case study for different warehouse technologies. *Energies*, *14*(9), 5–10. https://doi.org/10.3390/en14092709

Li, W. (2016). Numerical and Experimental Study of Thermal Stratification in Large Warehouses. Master Thesis. In *Ph.D.: Vol. Master of* (Issue April). https://spectrum.library.concordia.ca/981545/1/Weigang_MASc_F2016.pdf

Li, Y., & Heiselberg, P. (2003). Analysis Methods for Natural and Hybrid Ventilation - a Critical Literature Review and Recent Developments. *International Journal of Ventilation*, *1*(4), 3–20. https://doi.org/10.1080/14733315.2003.11683640

Liberati, P., & Zappavigna, P. (2010). A simulation model to predict the internal climatic conditions in livestock houses as a tool for improving building design and management. *Livestock Housing for the Future*, 117.

Liu, H., He, R., Tan, Q. Z., Huang, Z., Qi, Y. P., Ding, K. Z., & Zhou, M. M. (2011). Effects of Storage Conditions on Physical Properties of Cut Tobacco. *Advanced Materials Research*, *347–353*, 3041–3045. https://doi.org/10.4028/www.scientific.net/AMR.347-353.3041

Liu, X., Lin, L., Liu, X., Zhang, T., Rong, X., Yang, L., & Xiong, D. (2018). Evaluation of air infiltration in a hub airport terminal: On-site measurement and numerical simulation. *Building and Environment*, *143*, 163–177. https://doi.org/10.1016/j.buildenv.2018.07.006

Liu, X., Liu, X., & Zhang, T. (2020). Influence of air-conditioning systems on buoyancy-driven air infiltration in large space buildings: A case study of a railway station. *Energy and Buildings*, *210*, 109781. https://doi.org/10.1016/j.enbuild.2020.109781

Masanet, E. R. (2017). *Energy Technology Perspectives 2017: Catalysing Energy Technology Transformations*. OECD.

Mei, S.-J., Hu, J.-T., Liu, D., Zhao, F.-Y., & Wang, H.-Q. (2018a). Thermal buoyancy-driven flows inside the industrial buildings primarily ventilated by the mechanical fans: Local facilitation and infiltration. *Energy and Buildings*, *175*, 87–101. https://doi.org/10.1016/j.enbuild.2018.07.014

Mei, S.-J., Hu, J.-T., Liu, D., Zhao, F.-Y., & Wang, H.-Q. (2018b). Thermal buoyancy-driven flows inside the industrial buildings primarily ventilated by the mechanical fans: Local facilitation and infiltration. *Energy and Buildings*, *175*, 87–101. https://doi.org/10.1016/j.enbuild.2018.07.014

Mundt, E., Mathisen, H. M., Nielsen, P. V., & Moser, A. (2004). *Ventilation effectiveness. Guidebook n^{o}2* (E. Mundt, Ed.; First edit). Federation of European Heating and Ventilation Association REHVA.

Nunes, M. C. N., Emond, J. P., Rauth, M., Dea, S., & Chau, K. V. (2009). Environmental conditions encountered during typical consumer retail displays affect fruit and vegetable quality and waste. *Postharvest Biology and Technology*, *51*(2), 232–241. https://doi.org/10.1016/j.postharvbio.2008.07.016

Örüng, İ., Karaman, S., & Şirin, Ü. (2016). Nevşehir Yöresindeki Doğal Depoların Modern Depolarla Karşılaştırılması. *Nevşehir Bilim ve Teknoloji Dergisi*, *5*, 9–9. https://doi.org/10.17100/nevbiltek.210954

Owen, J. F. & I. (2010). *MegaFan Warehouse Case Study : Final Report*. *March*, 1–13.

Park, C.-E., Kim, Y.-S., Park, K.-J., & Kim, B.-K. (2012). Changes in physicochemical characteristics of rice during storage at different temperatures. *Journal of Stored Products Research*, *48*, 25–29. https://doi.org/10.1016/j.jspr.2011.08.005

Porras-Amores, C., Mazarrón, F., & Cañas, I. (2014). Study of the Vertical Distribution of Air Temperature in Warehouses. *Energies*, *7*(3), 1193–1206. https://doi.org/10.3390/en7031193

Pudleiner, D., & Colton, J. (2015). Using sensitivity analysis to improve the efficiency of a Net-Zero Energy vaccine warehouse design. *Building and Environment*, *87*, 302–314. https://doi.org/10.1016/j.buildenv.2014.12.026

R. W. Bottcher, G. R. Baughman, & L. B. Driggers. (1988). Temperature Stratification in Broiler Houses and the Effects of Ceiling Fans. *Applied Engineering in Agriculture*, *4*(1), 66–71. https://doi.org/10.13031/2013.26582

Rai, D., Sodagar, B., Fieldson, R., & Hu, X. (2011). Assessment of CO2 emissions reduction in a distribution warehouse. *Energy*, *36*(4), 2271–2277. https://doi.org/10.1016/j.energy.2010.05.006

Reddy, T. A., Maor, I., Jian, S., & Panjapornporn, C. (2006). *Procedures for Reconciling Computer-Calculated Results with Measured Energy Data*.

Rhee, K.-N., & Kim, K. W. (2015). A 50-year review of basic and applied research in radiant heating and cooling systems for the built environment. *Building and Environment*, *91*, 166–190. https://doi.org/10.1016/j.buildenv.2015.03.040

Rhee, K.-N., Shin, M.-S., & Choi, S.-H. (2015). Thermal uniformity in an open plan room with an active chilled beam system and conventional air distribution systems. *Energy and Buildings*, *93*, 236–248. https://doi.org/10.1016/j.enbuild.2015.01.068

Ries, J. M., Grosse, E. H., & Fichtinger, J. (2017). Environmental impact of warehousing: a scenario analysis for the United States. *International Journal of Production Research*, *55*(21), 6485–6499. https://doi.org/10.1080/00207543.2016.1211342

Rohdin, P., & Moshfegh, B. (2011). Numerical modeling of industrial indoor environments: A comparison between different turbulence models and supply systems supported by field measurements. *Building and Environment*, *46*(11), 2365–2374. https://doi.org/10.1016/j.buildenv.2011.05.019

Rojano, F., Bournet, P.-E., Hassouna, M., Robin, P., Kacira, M., & Choi, C. Y. (2018). Assessment using CFD of the wind direction on the air discharges caused by natural ventilation of a poultry house. *Environmental Monitoring and Assessment*, *190*(12), 724. https://doi.org/10.1007/s10661-018-7105-5

Rong, L., Nielsen, P. V., Bjerg, B., & Zhang, G. (2016). Summary of best guidelines and validation of CFD modeling in livestock buildings to ensure prediction quality. *Computers and Electronics in Agriculture*, *121*, 180–190. https://doi.org/10.1016/j.compag.2015.12.005

Runsey, I. (2008). Temperature and air distribution in refrigerated warehouses. A new dimension to energy savings. Food safety, Food supply. *Food Solutions. GDS Publishing Ltd.*

Rushton, A., Croucher, P., & Baker, P. (2017). *The Handbook of Logistics and distribution management* (6th ed.). Kogan Page.

Saïd, M. N. A., MacDonald, R. A., & Durrant, G. C. (1996). Measurement of thermal stratification in large single-cell buildings. *Energy and Buildings*, *24*(2), 105–115. https://doi.org/10.1016/0378-7788(95)00966-3

Saltelli, A., Andres, T. H., & Homma, T. (1993). Sensitivity analysis of model output. *Computational Statistics & Data Analysis*, *15*(2), 211–238. https://doi.org/10.1016/0167-9473(93)90193-W

Sandberg, M. (1981). What is ventilation efficiency? *Building and Environment*, *16*(2), 123–135. https://doi.org/10.1016/0360-1323(81)90028-7

Sandberg, M., & Sjöberg, M. (1983). The use of moments for assessing air quality in ventilated rooms. *Building and Environment*, *18*(4), 181–197. https://doi.org/10.1016/0360-1323(83)90026-4

Scharnow, R. (1986). *Codiertes Handbuch der Güter des Seetransports, VE Kombinat Seeverkehr und Hafenwirtschaft-Deutfracht/SeereedereiIngenieurhochschule für Seefahrt Warnemünde/Wustrow, Rostock Bd. 1: Stückgut A-K, Bd. 2: Stückgut L-Z, Bd. 3: Spezialgut*.

Schulze, T., & Eicker, U. (2013). Controlled natural ventilation for energy-efficient buildings. *Energy and Buildings*, *56*, 221–232. https://doi.org/10.1016/j.enbuild.2012.07.044

Seifhashemi, M., Capra, B. R., Milller, W., & Bell, J. (2018). The potential for cool roofs to improve the energy efficiency of single-story warehouse-type retail buildings in Australia: A simulation case study. *Energy and Buildings*, *158*, 1393–1403. https://doi.org/10.1016/j.enbuild.2017.11.034

Shi, H., Wang, R., Bush, L. P., Zhou, J., Yang, H., Fannin, N., & Bai, R. (2013). Changes in TSNA Contents during Tobacco Storage and the Effect of Temperature and Nitrate Level on TSNA Formation. *Journal of Agricultural and Food Chemistry*, *61*(47), 11588–11594. https://doi.org/10.1021/jf404813m

Shiao, T. F., Chen, J. C., Yang, D. W., Lee, S. N., Lee, C. F., & Cheng, W. T. K. (2011). Feasibility assessment of a tunnel-ventilated, water-padded barn on alleviation of heat stress for lactating Holstein cows in a humid area. *Journal of Dairy Science*, *94*(11), 5393–5404. https://doi.org/10.3168/jds.2010-3730

Speziale, C. G., Sarkar, S., & Gatski, T. B. (1991). Modeling the pressure–strain correlation of turbulence: an invariant dynamical systems approach. *Journal of Fluid Mechanics*, *227*, 245–272. https://doi.org/10.1017/S0022112091000101

Spindler, H. C., & Norford, L. K. (2009). Naturally ventilated and mixed-mode buildings—Part II: Optimal control. *Building and Environment*, *44*(4), 750–761. https://doi.org/10.1016/j.buildenv.2008.05.018

SPO. (2007). *9th Development Plan Alcohol, tobacco, and tobacco products industry SEC report (in Turkish)*.

Stoakes, P. J. (2009). *Numerical simulation of airflow and heat transfer in buildings* [Master of Science]. Virginia Polytechnic Institute and State University.

TEA. (2017). *Tobacco Experts Association [TEA]*. http://www.tutuneksper.org.tr/kaynaklar/fermantasyon/tabii-fermantasyon

Teitel, M., Levi, A., Zhao, Y., Barak, M., Bar-lev, E., & Shmuel, D. (2008). Energy saving in agricultural buildings through fan motor control by variable frequency drives. *Energy and Buildings*, *40*(6), 953–960. https://doi.org/10.1016/j.enbuild.2007.07.010

Tian, W. (2013). A review of sensitivity analysis methods in building energy analysis. *Renewable and Sustainable Energy Reviews*, *20*, 411–419. https://doi.org/10.1016/j.rser.2012.12.014

Tran, T. (2013). Optimization of Natural Ventilation Design in Hot and Humid Climates Using Building Energy Simulation. *Architecture*, *May*, 1–183.

Trust, C. (2007). *Carbon Footprint Measurement Methodology Version 1.3*. https://semspub.epa.gov/work/09/1142519.pdf

Tsai, T.-Y., Liou, R.-H., & Lin, Y.-J. P. (2014). An Experimental Study on the Indoor Environment Using Underfloor Air Distribution System. *Procedia Engineering*, *79*, 263–266. https://doi.org/10.1016/j.proeng.2014.06.341

TSMS. (2022). *Turkish State Meteorological Service*. İzmir İlinin İklim Durumu. https://izmir.mgm.gov.tr/files/iklim/izmir_iklim.pdf

Wang, B., Yu, J., Ye, H., Liu, Y., Guo, H., & Tian, L. (2017). Study on present situation and optimization strategy of infiltration air in a train station in winter. *Procedia Engineering*, *205*, 2517–2523. https://doi.org/10.1016/j.proeng.2017.09.984

Wang, J., Yang, H., Shi, H., Jin, T., Zhou, J., & Bai, R. (2017). Interacting effects of temperature, moisture content, and storage environment on tobacco-specific nitrosamines formation during burley tobacco storage. *Fresenius Environmental Bulletin*, *26*(3), 2114–2125.

Wang, L. L., & Li, W. (2017). A study of thermal destratification for large warehouse energy savings. *Energy and Buildings*, *153*, 126–135. https://doi.org/10.1016/j.enbuild.2017.07.070

Wang, X., Huang, C., Cao, W., Gao, X., & Liu, W. (2011). Experimental Study on Indoor Thermal Stratification in Large Space under Floor Air Distribution System (UFAD) in Summer. *Engineering*, *03*(04), 384–388. https://doi.org/10.4236/eng.2011.34044

Wang, Z., Luo, M., Geng, Y., Lin, B., & Zhu, Y. (2018). A model to compare convective and radiant heating systems for intermittent space heating. *Applied Energy*, *215*, 211–226. https://doi.org/10.1016/j.apenergy.2018.01.088

Wiedmann, T., & Minx, J. (2008). A definition of 'carbon footprint.' In H. Pertsova (Ed.), *A definition of 'carbon footprint'* (pp. 1–11). Nova Science Publishers.

Zhiqiang, J. Z., Zhao, Z., Wei, Z., & Qingyan Yan, C. (2007). Evaluation of Various Turbulence Models in Predicting Airflow and Turbulence Enclosed Environments by CFD: Part 1—Summary of Prevalent Turbulence Models. *HVAC&R Research*, *13*(6), 853–870.

APPENDIX A

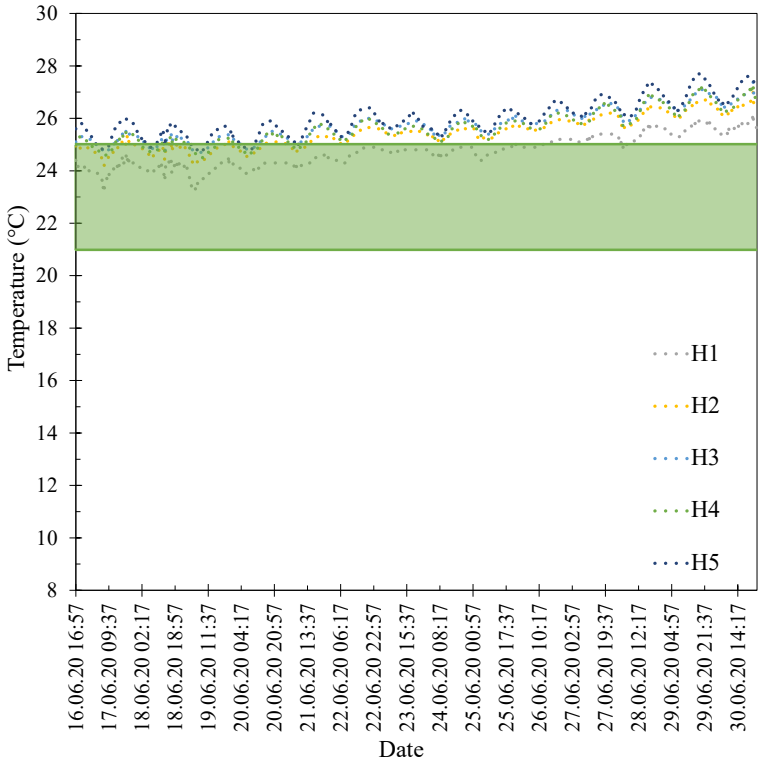

Figure A.1. Inside temperature measured in June 2020

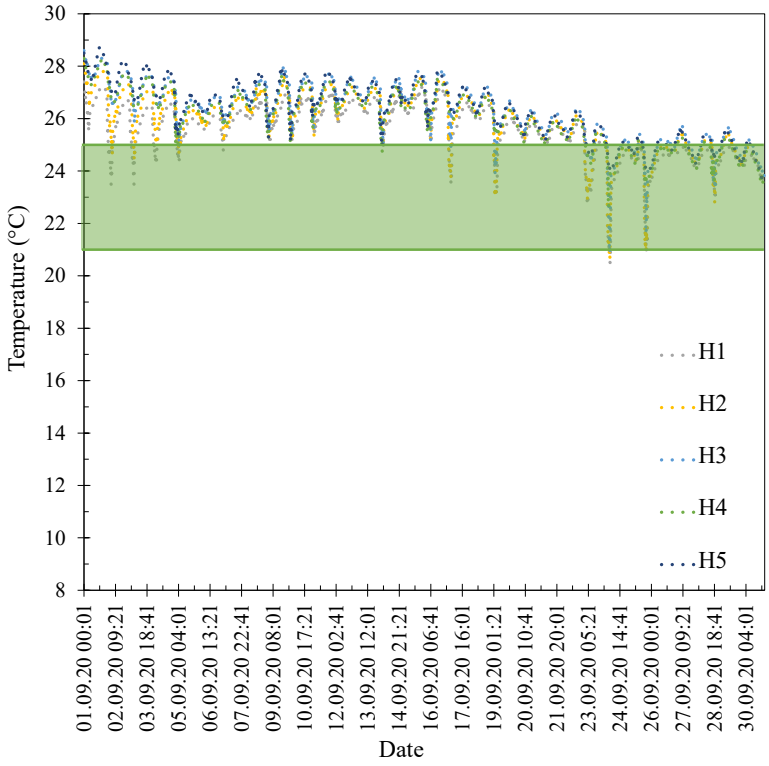

Figure A.2. Inside temperature measured in September 2020

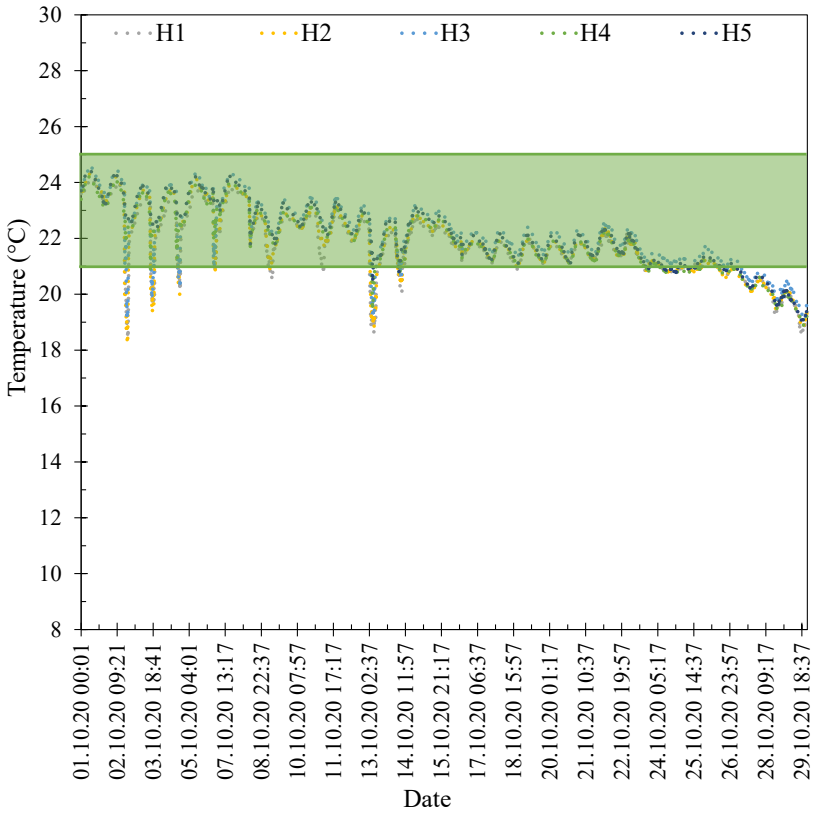

Figure A.3. Inside temperature measured in October 2020

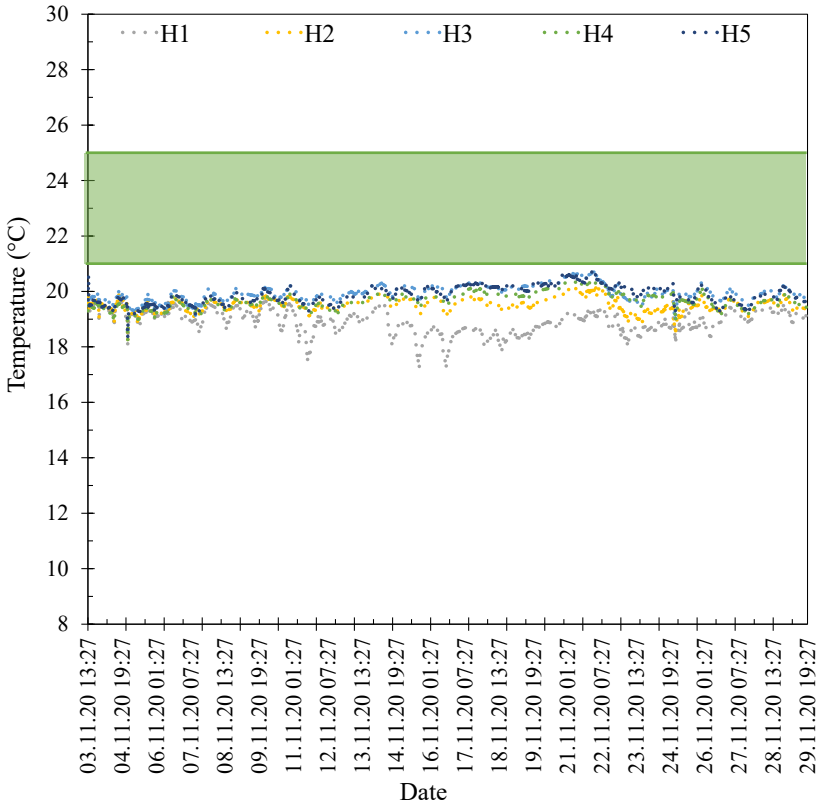

Figure A.4. Inside temperature measured in November 2020

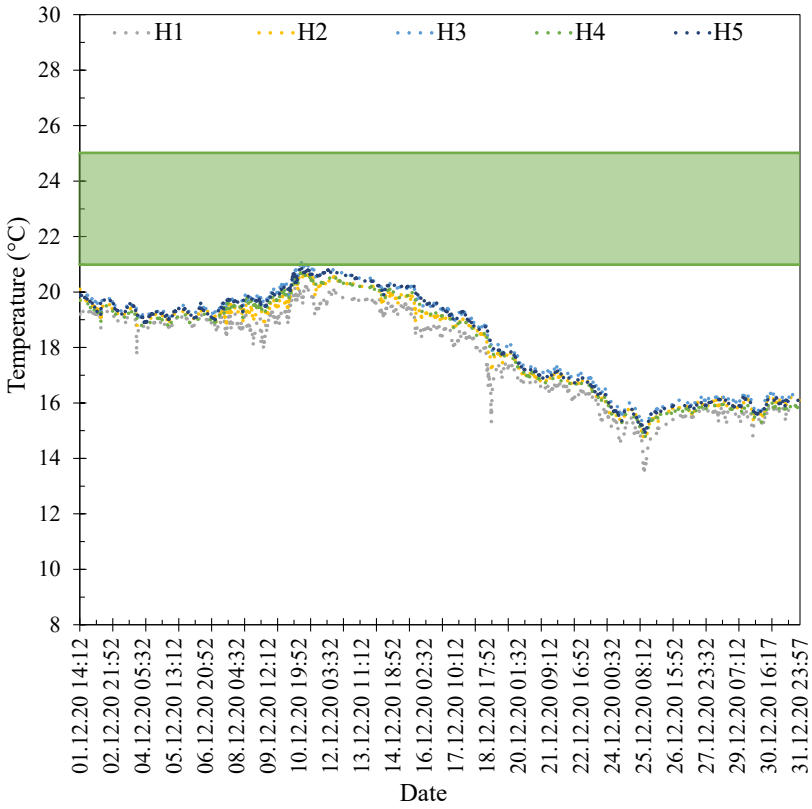

Figure A.5. Inside temperature measured in December 2020

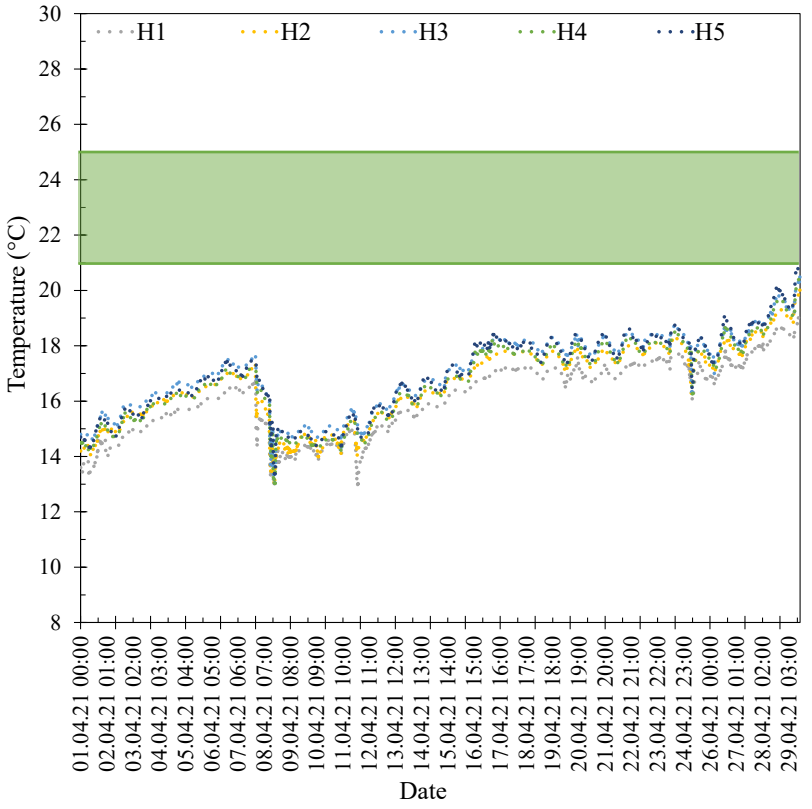

Figure A.6. Inside temperature measured in April 2021

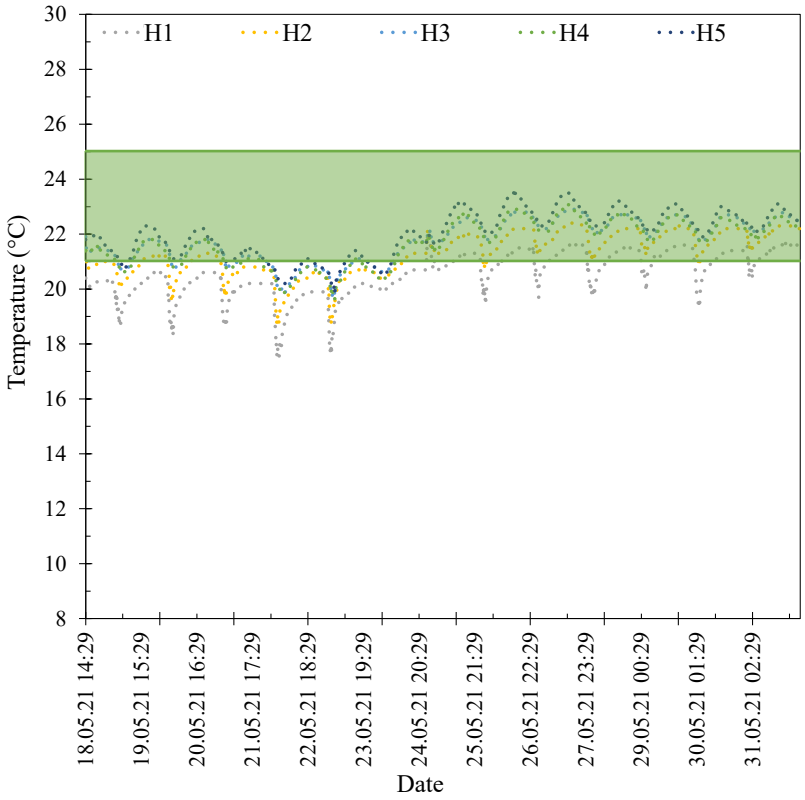

Figure A.7. Inside temperature measured in May 2021

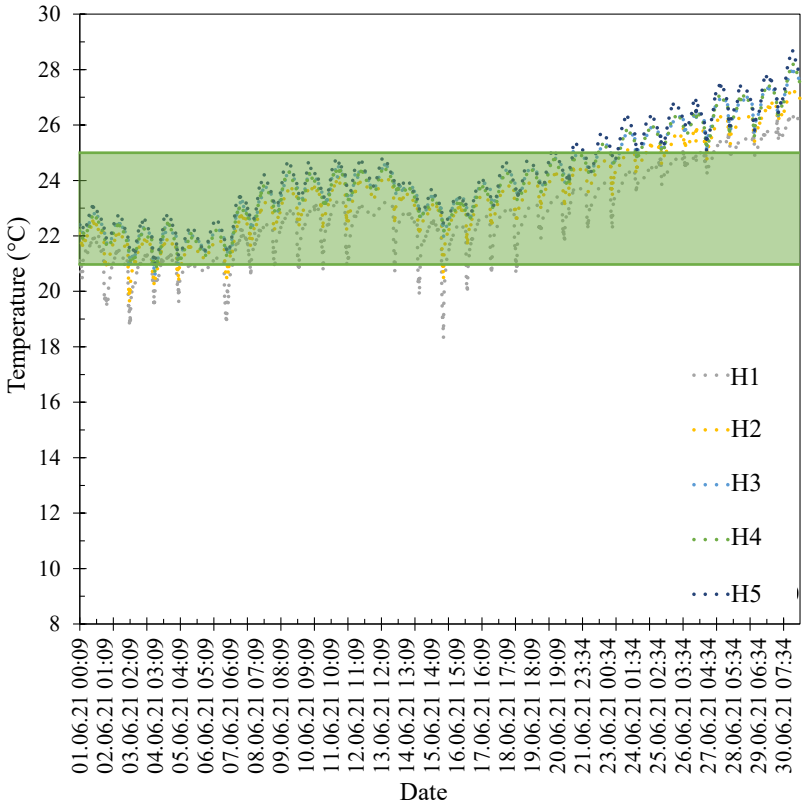

Figure A.8. Inside temperature measured in June 2021

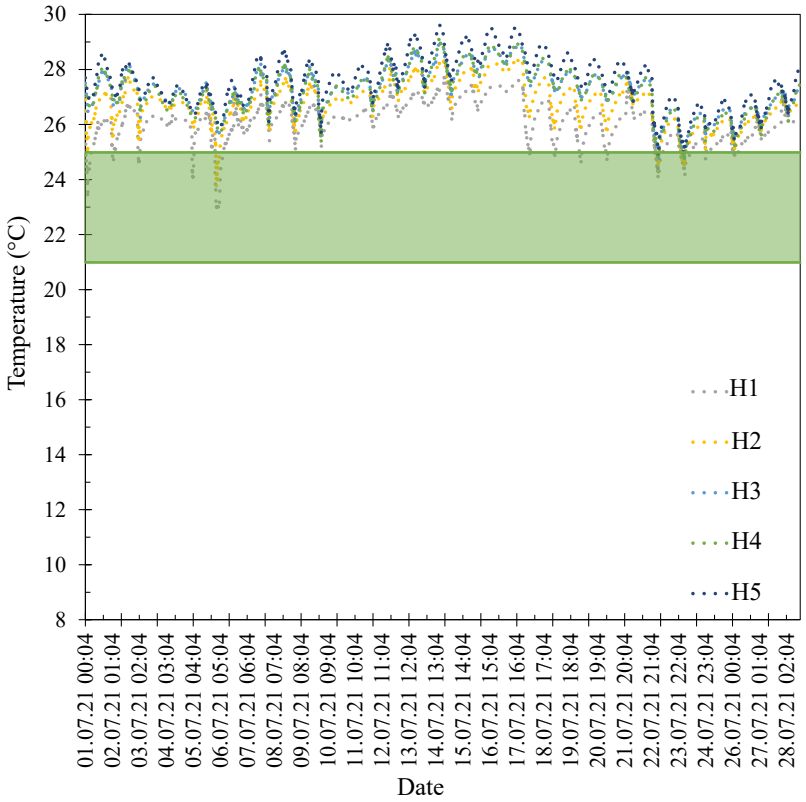

Figure A.9. Inside temperature measured in July 2021

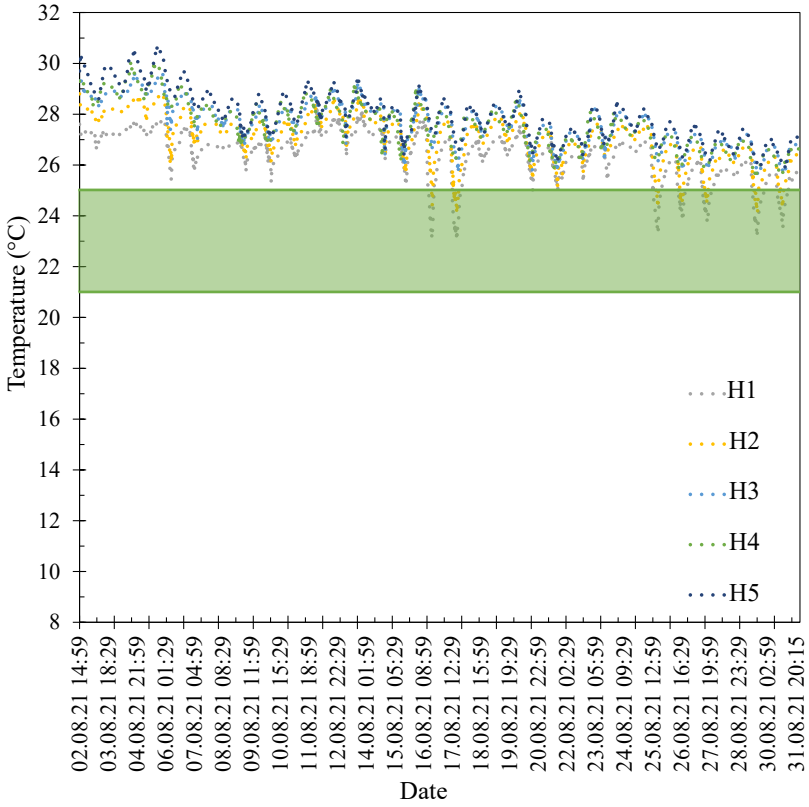

Figure A.10. Inside temperature measured in August 2021

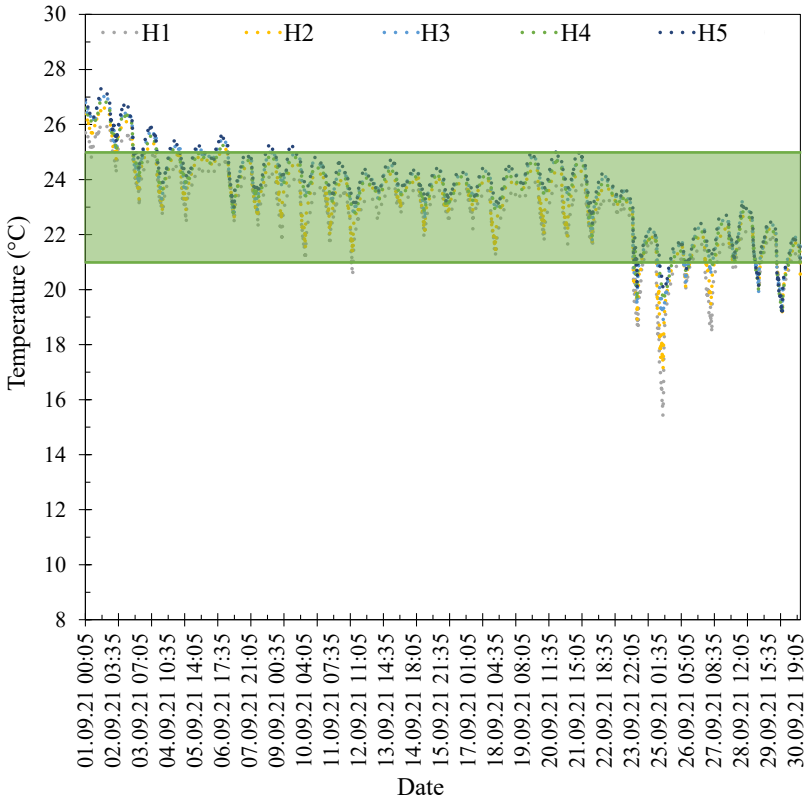

Figure A.11. Inside temperature measured in September 2021

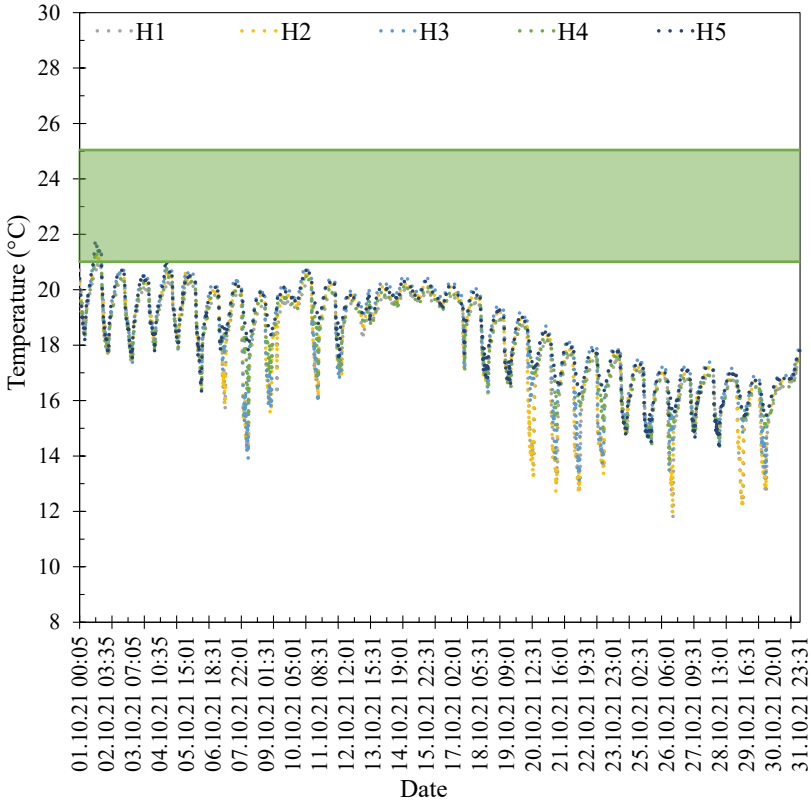

Figure A.12. Inside temperature measured in October 2021

APPENDIX B

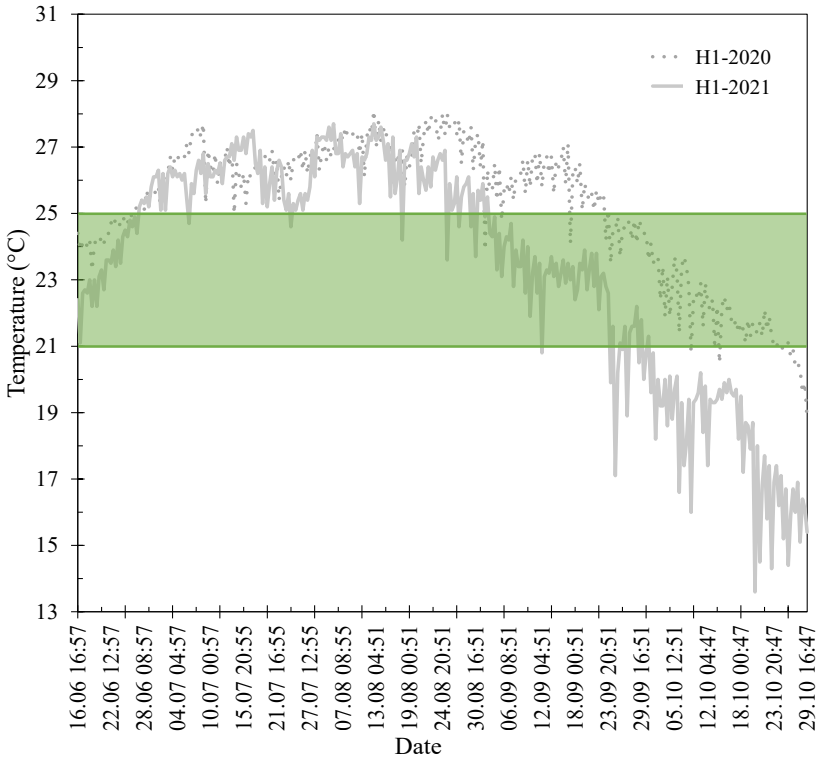

Figure B.1. Inside temperature values of 2020 and 2021 from the H1 level

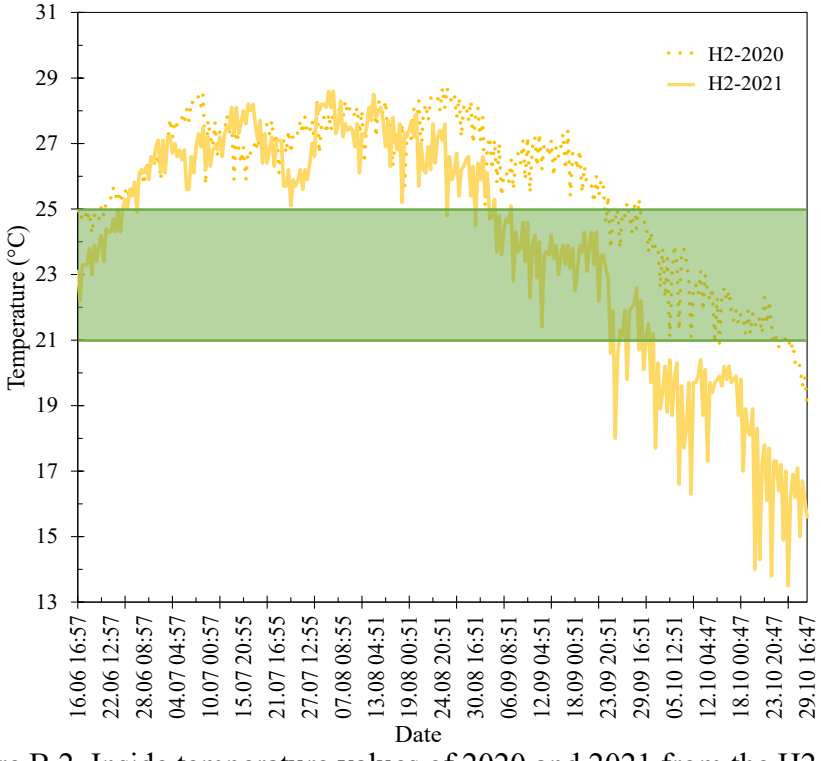

Figure B.2. Inside temperature values of 2020 and 2021 from the H2 level

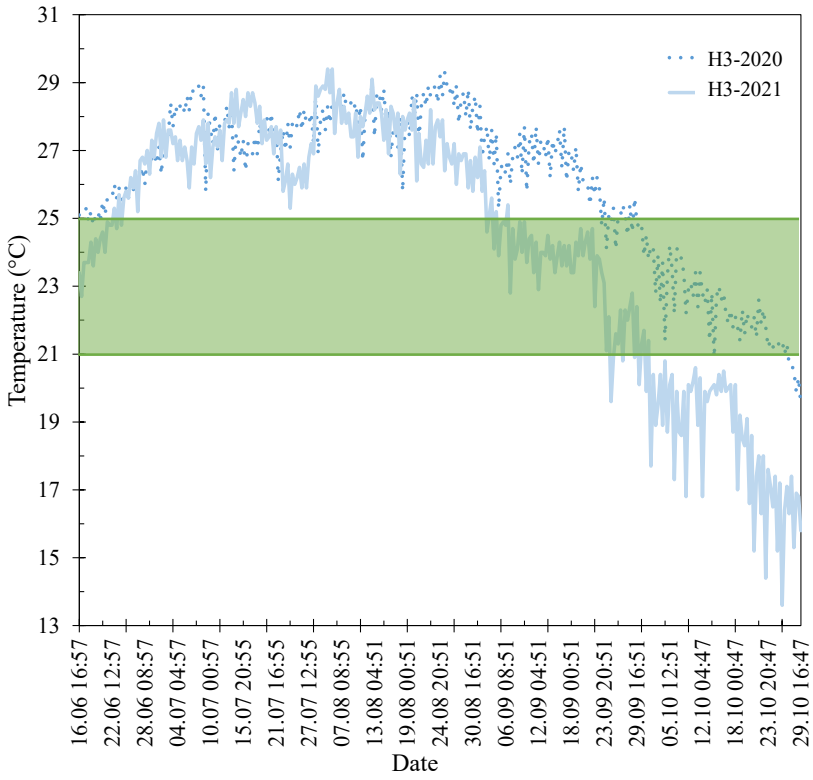

Figure B.3. Inside temperature values of 2020 and 2021 from the H3 level

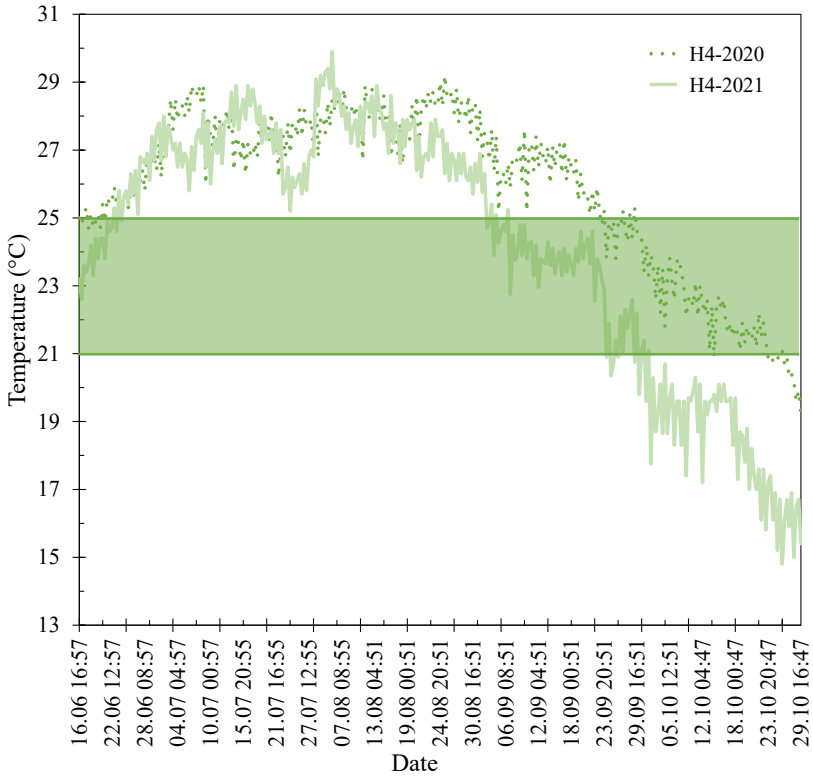

Figure B.4. Inside temperature values of 2020 and 2021 from the H4 level

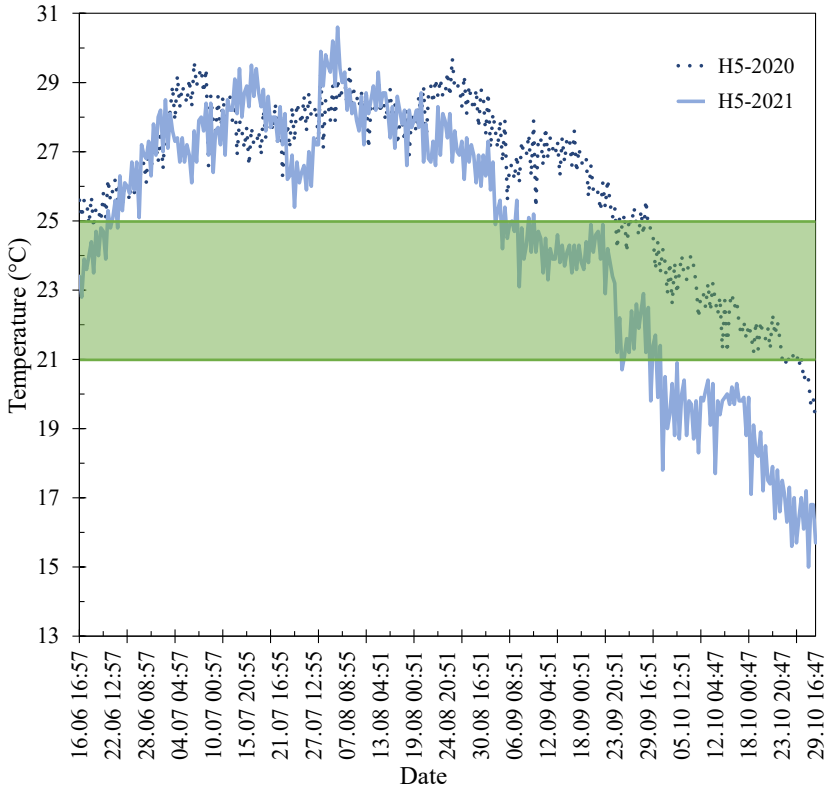

Figure B.5. Inside temperature values of 2020 and 2021 from the H5 level

APPENDIX C

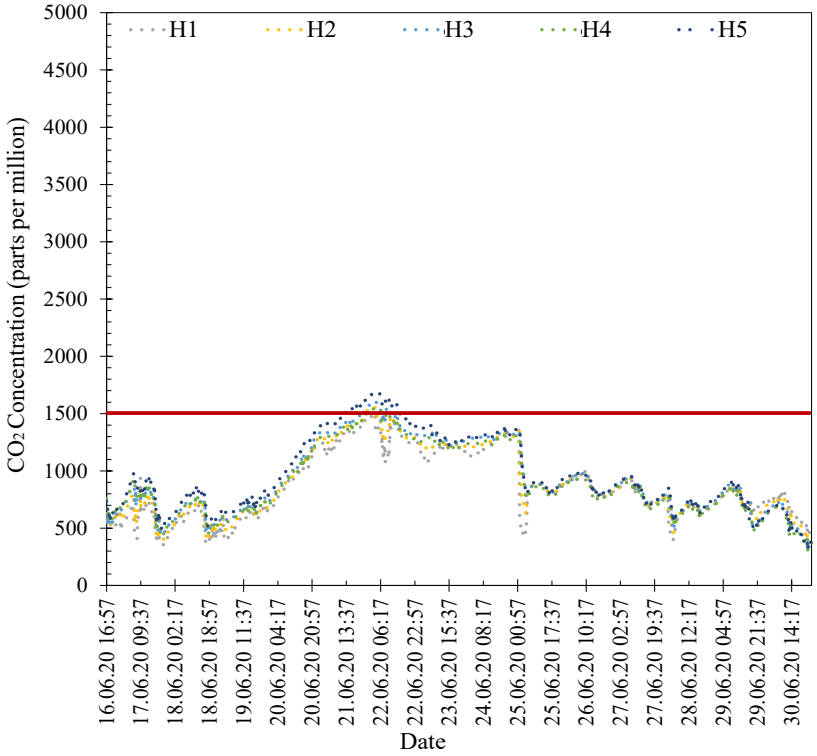

Figure C.1. CO_2 concentration values in June 2020

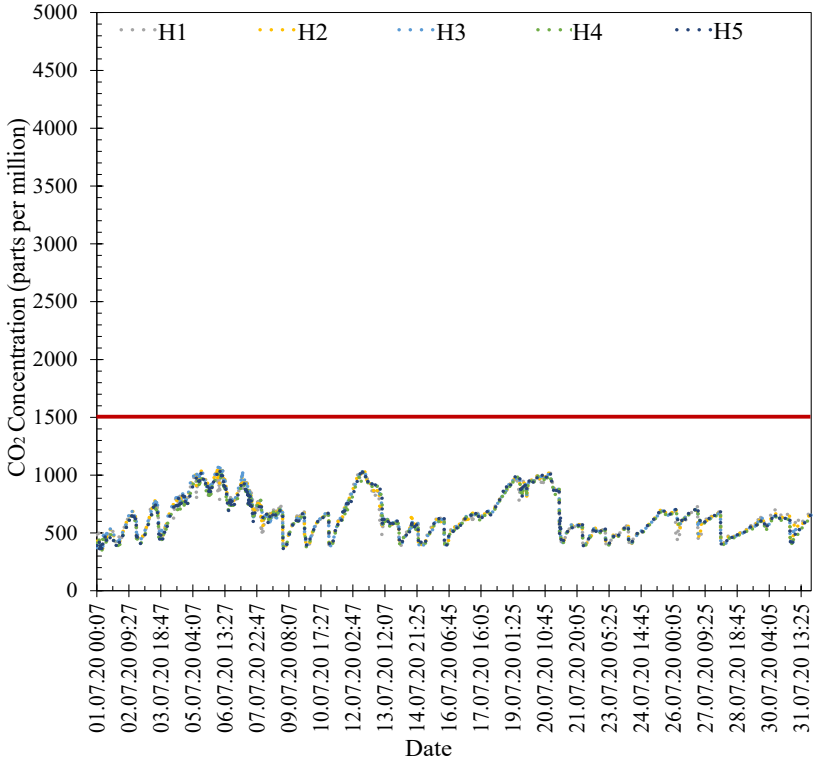

Figure C.2. CO_2 concentration values in July 2020

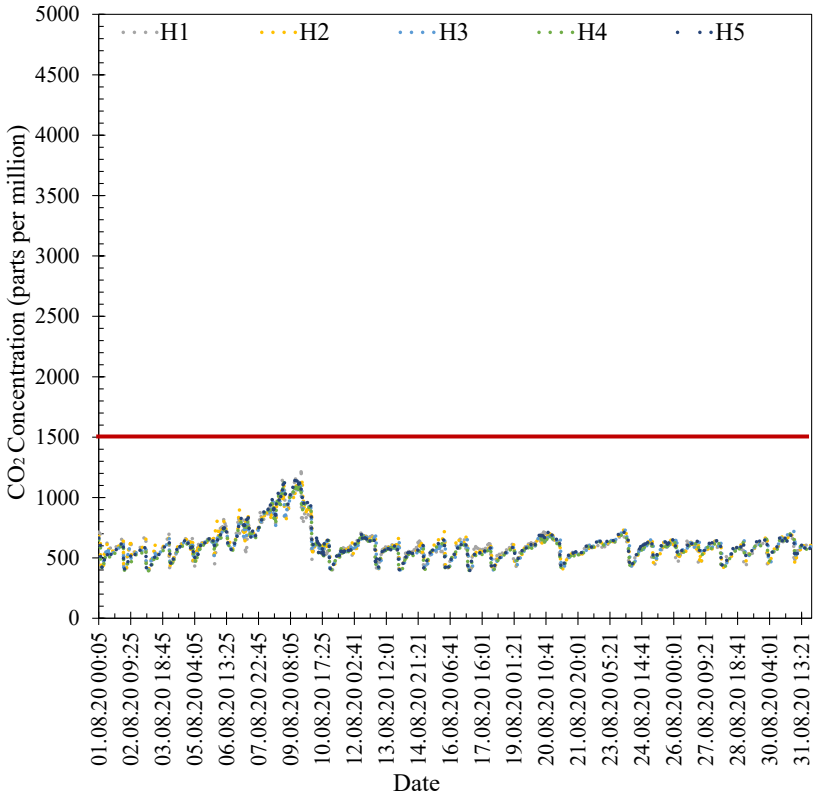

Figure C.3. CO_2 concentration values in August 2020

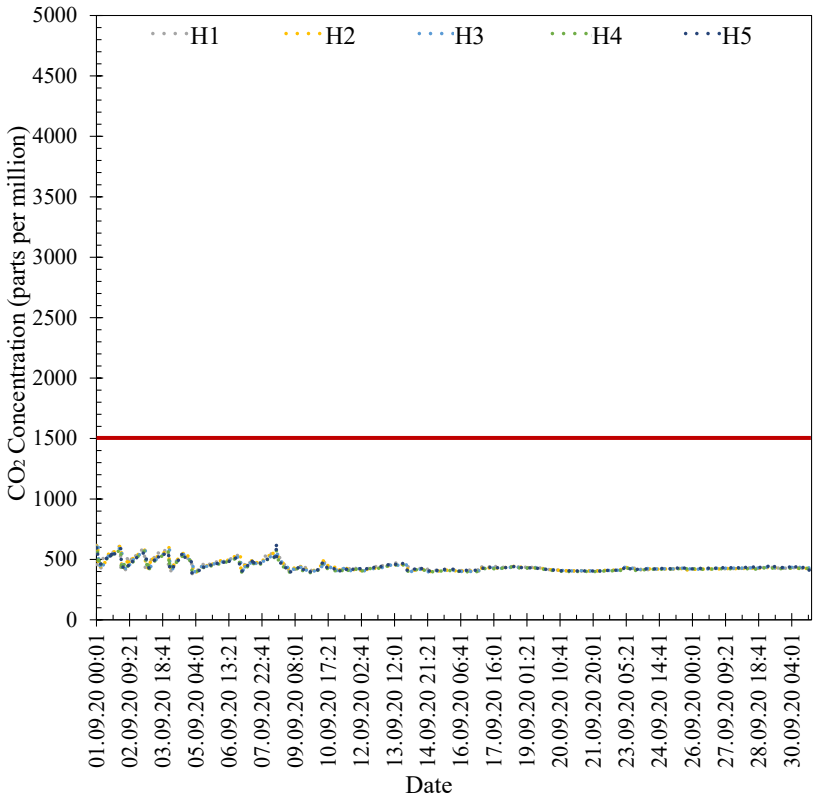

Figure C.4. CO_2 concentration values in September 2020

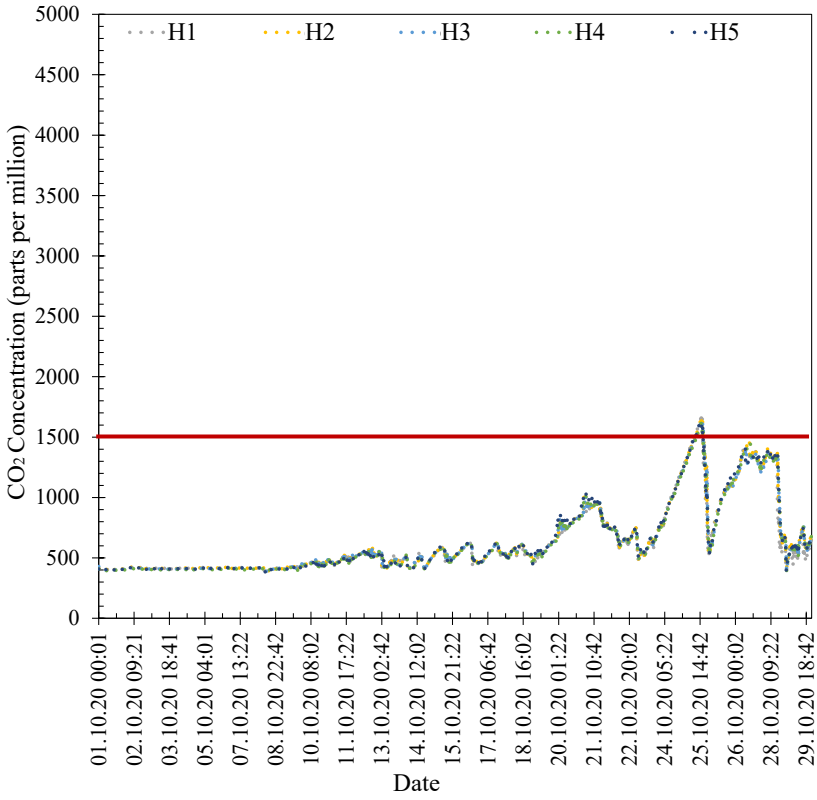

Figure C.5. CO_2 concentration values in October 2020

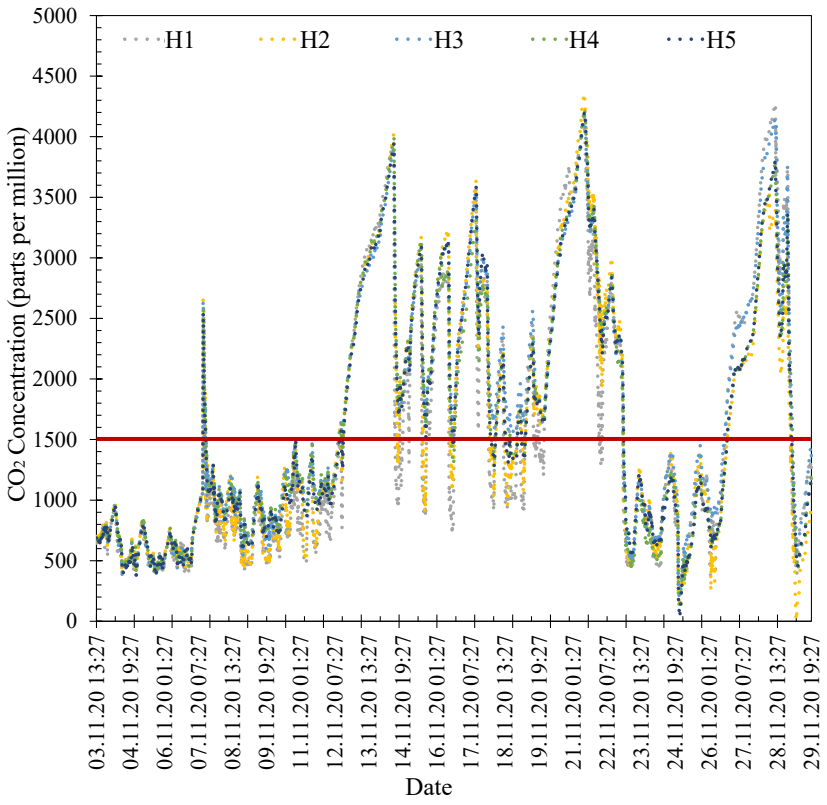

Figure C.6. CO_2 concentration values in November 2020

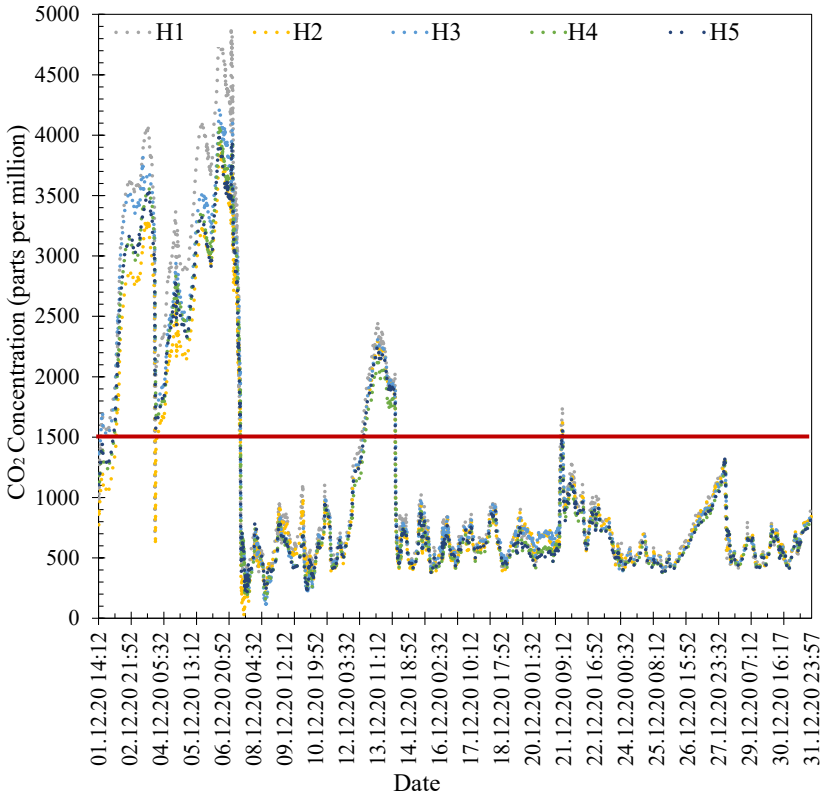

Figure C.7. CO_2 concentration values in December 2020

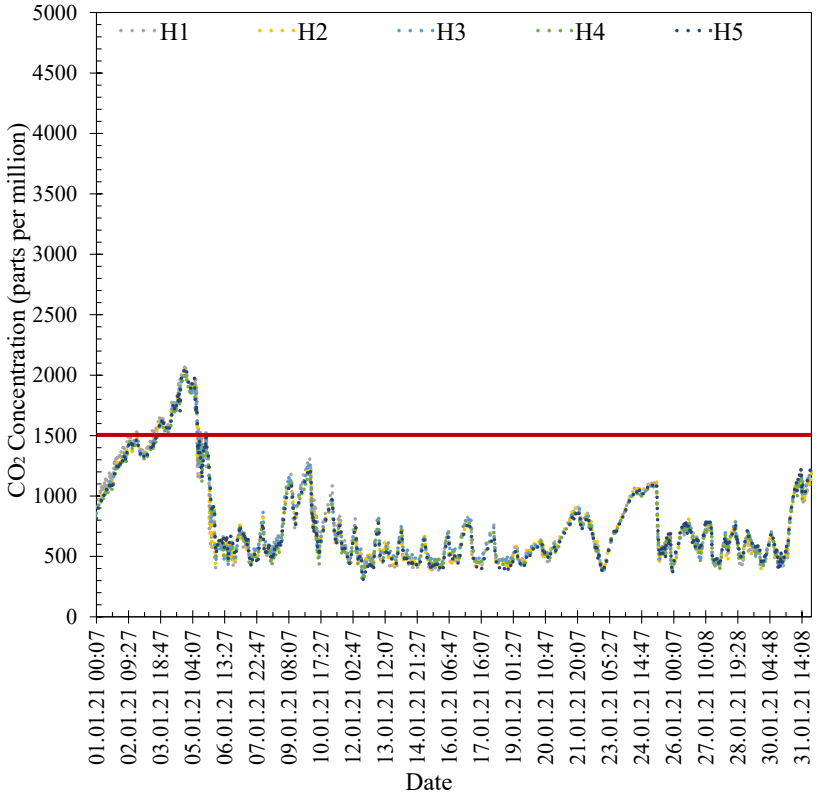

Figure C.8. CO_2 concentration values in January 2021

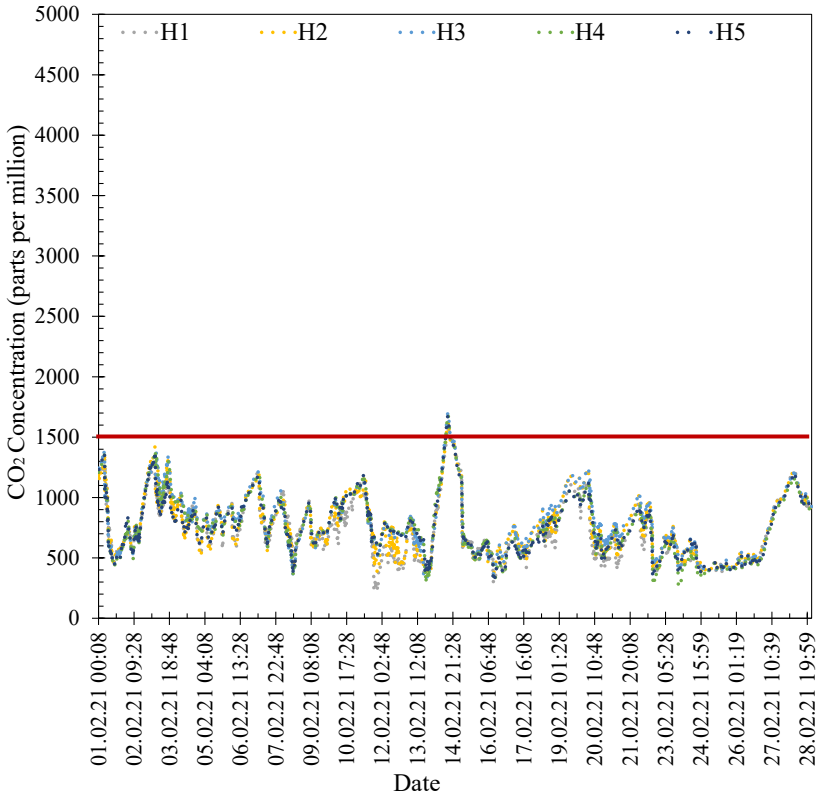

Figure C.9. CO_2 concentration values in February 2021

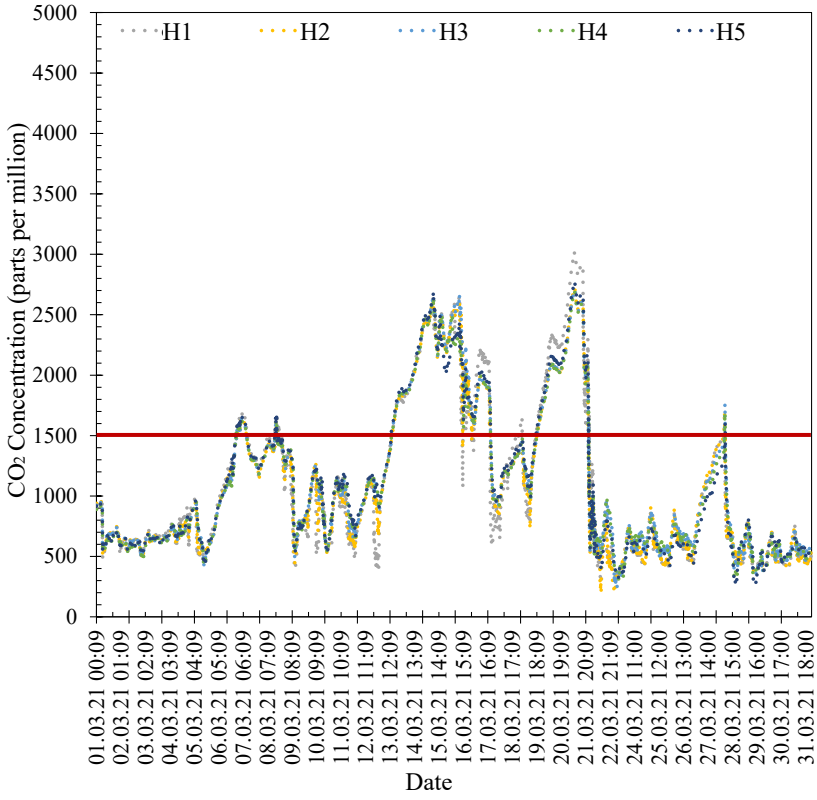

Figure C.10. CO_2 concentration values in March 2021

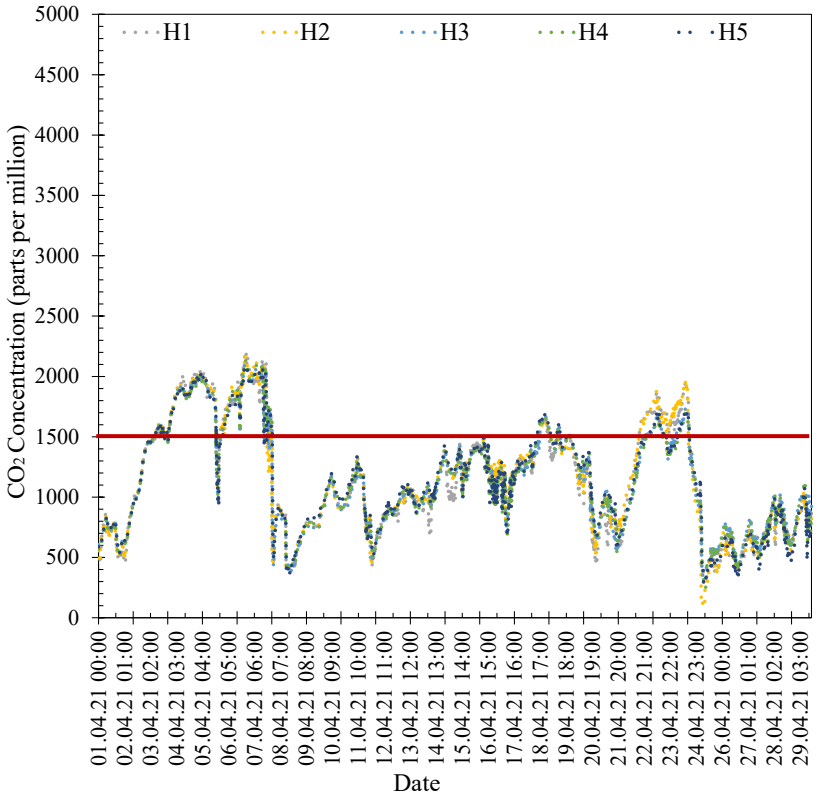

Figure C.11. CO_2 concentration values in April 2021

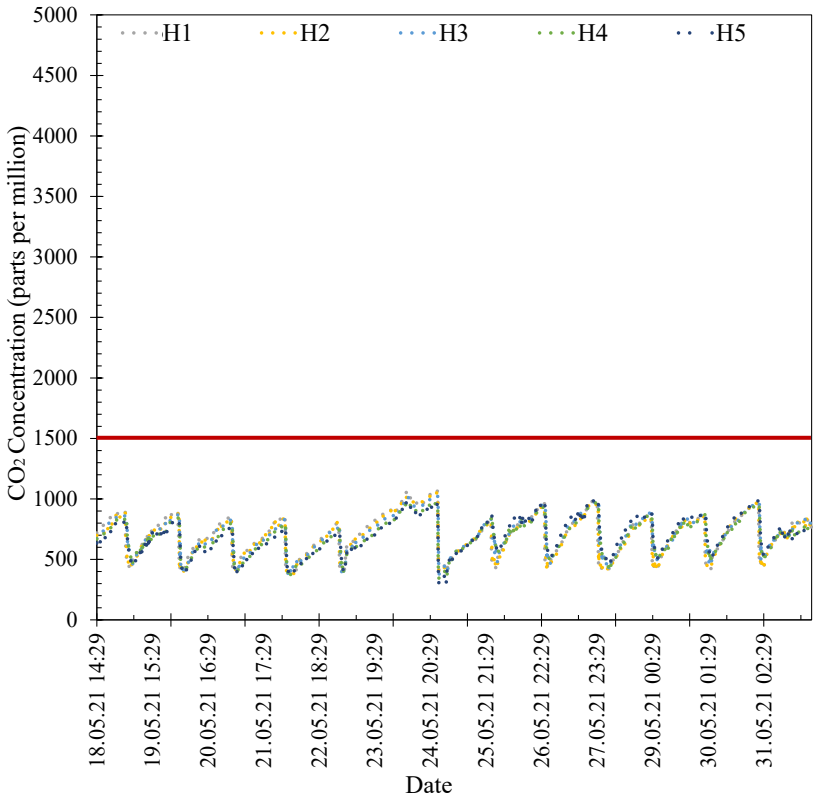

Figure C.12. CO_2 concentration values in May 2021

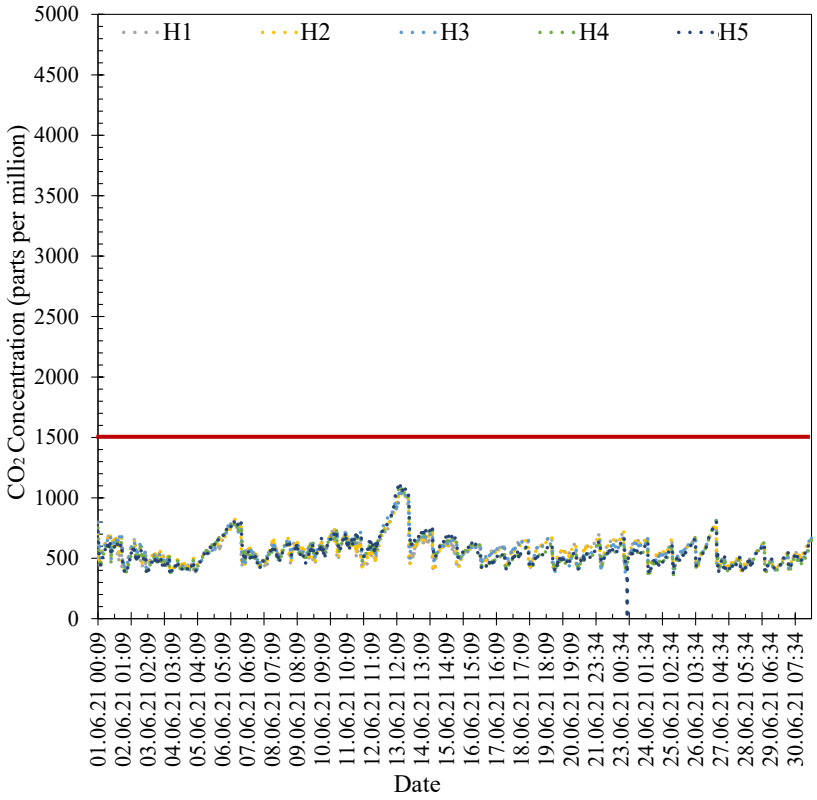

Figure C.13. CO_2 concentration values in June 2021

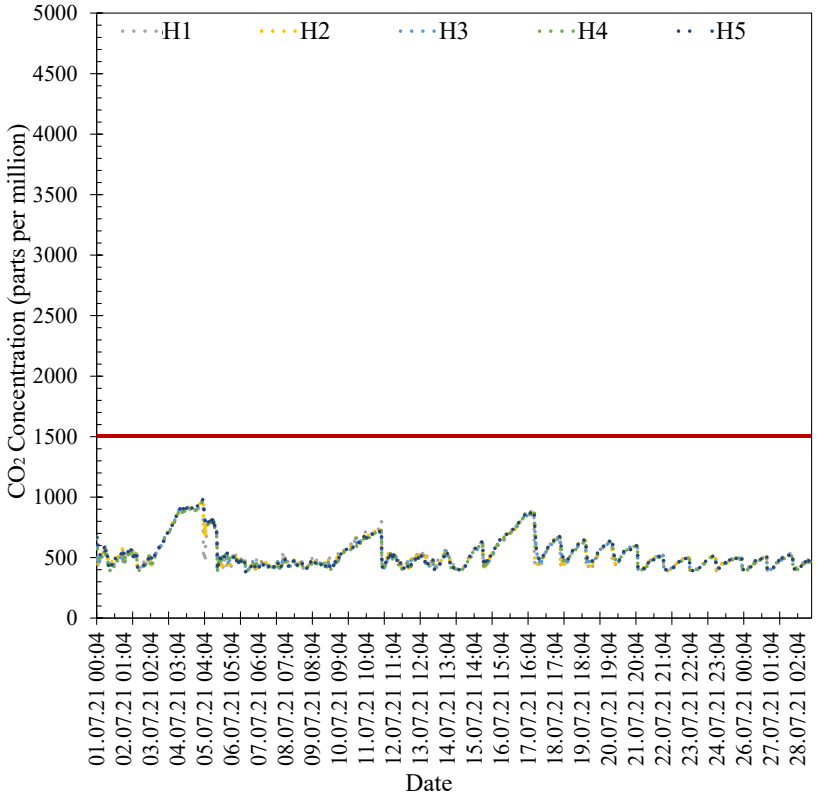

Figure C.14. CO_2 concentration values in July 2021

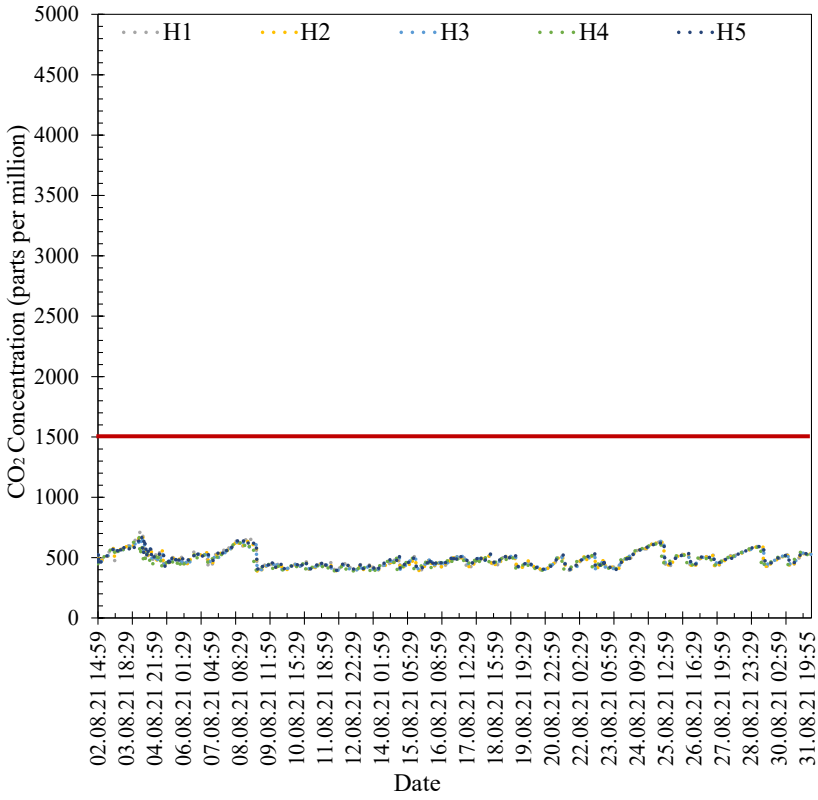

Figure C.15. CO_2 concentration values in August 2021

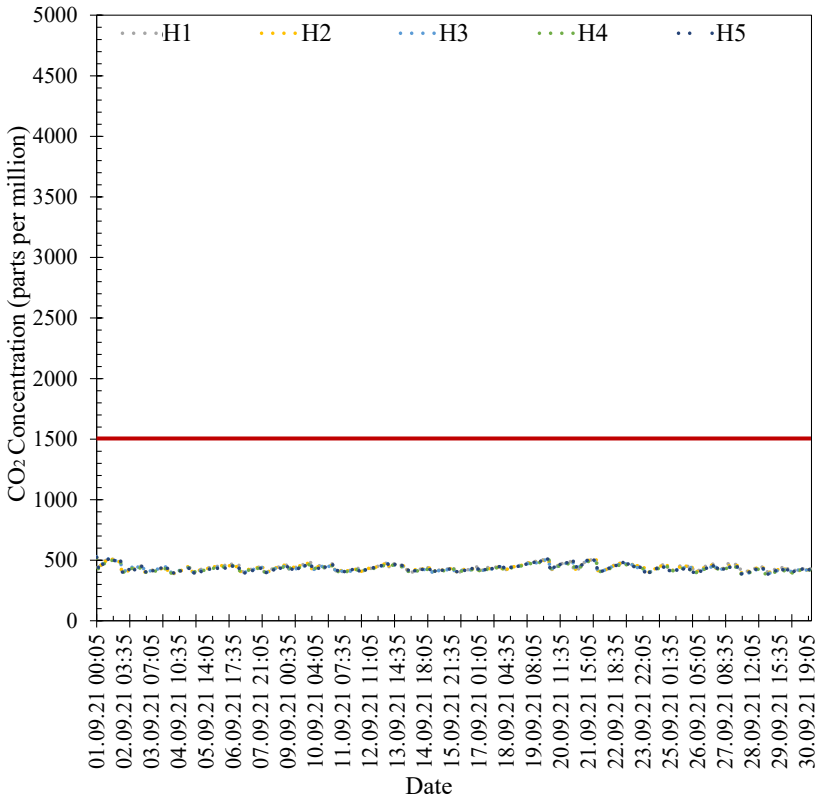

Figure C.16. CO_2 concentration values in September 2021

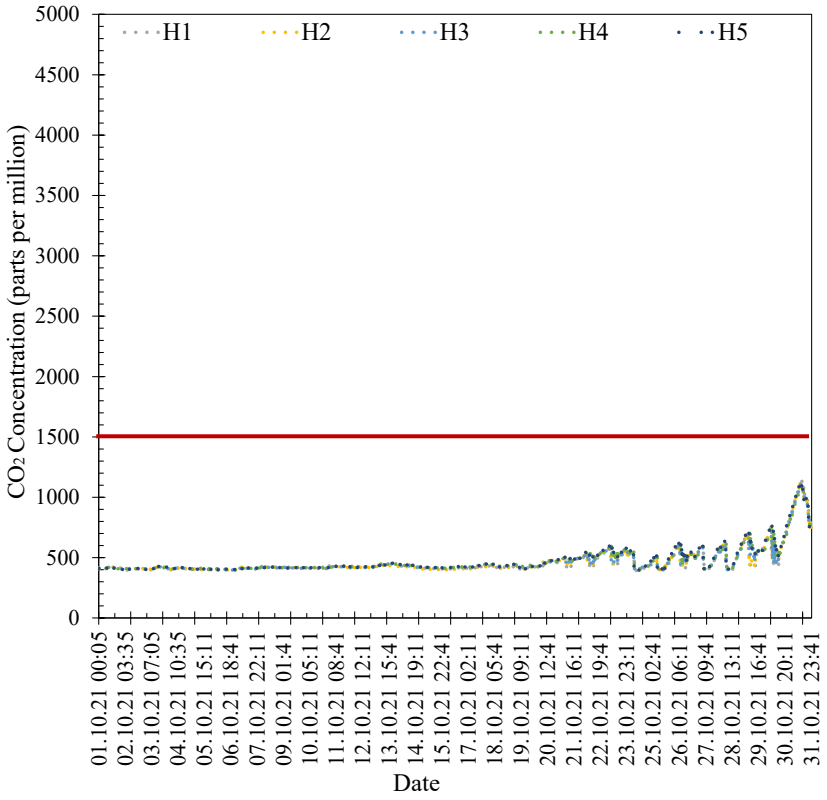

Figure C.17. CO_2 concentration values in October 2021

APPENDIX D

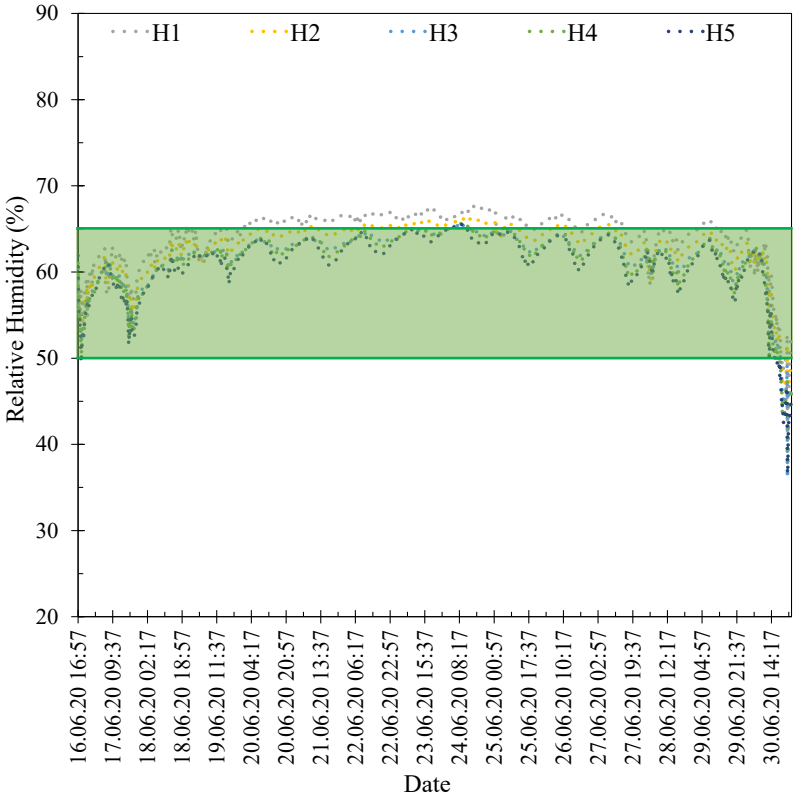

Figure D.1. Relative humidity values in June 2020

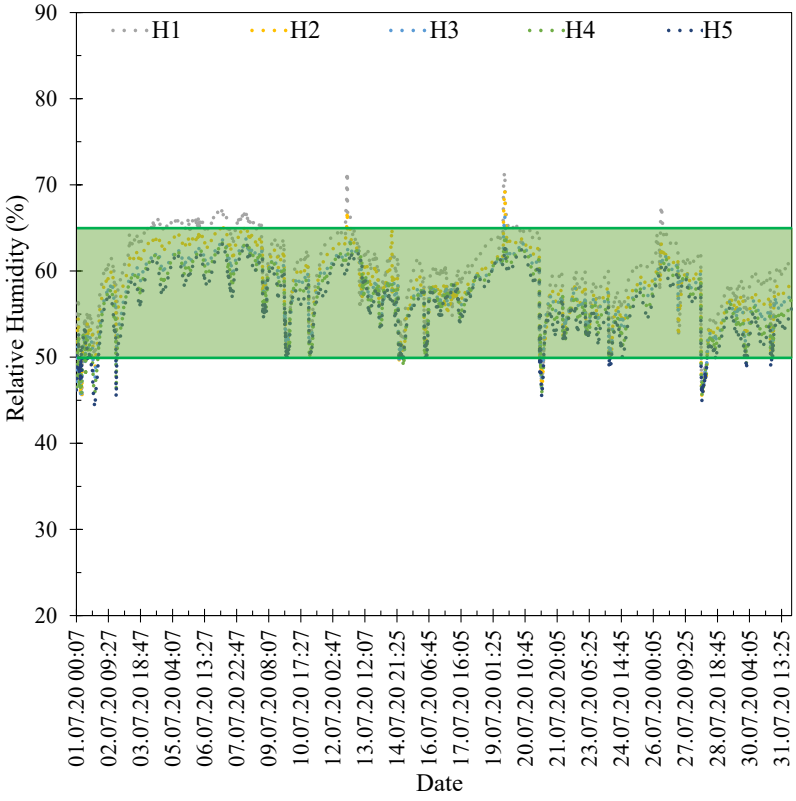

Figure D.2. Relative humidity values in July 2020

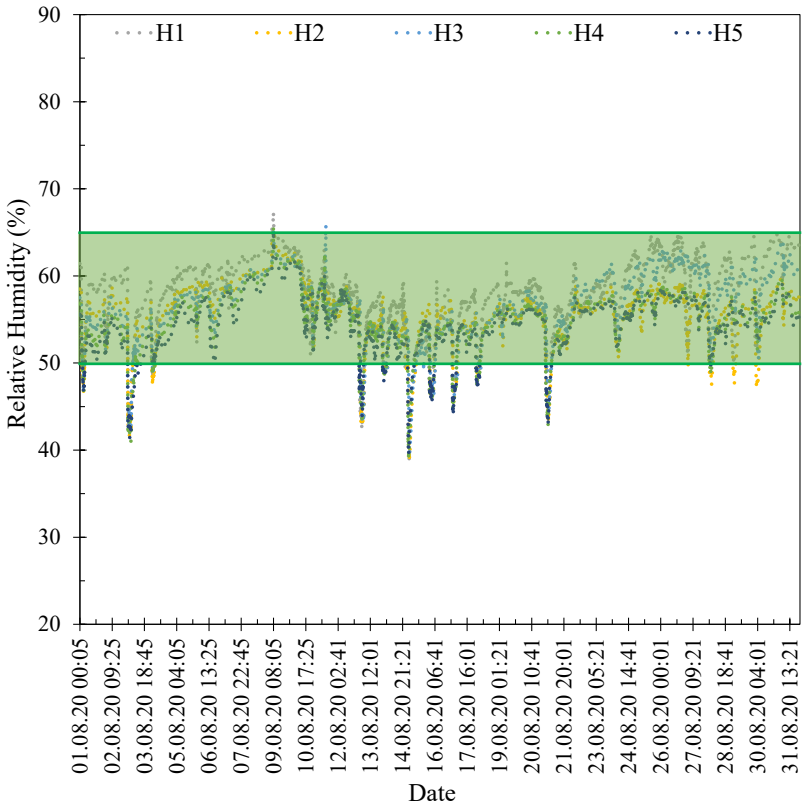

Figure D.3. Relative humidity values in August 2020

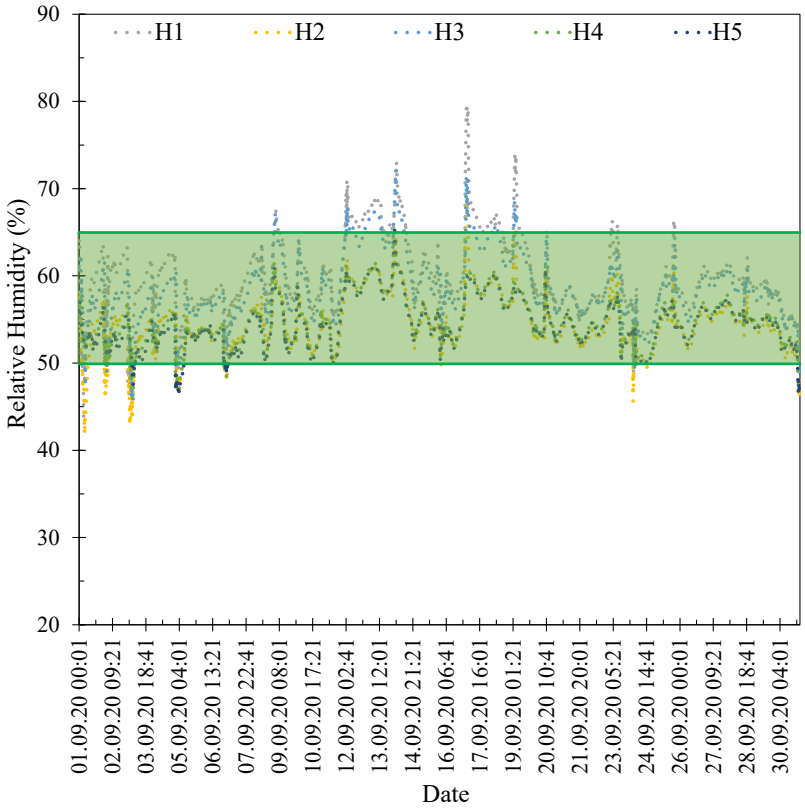

Figure D.4. Relative humidity values in September 2020

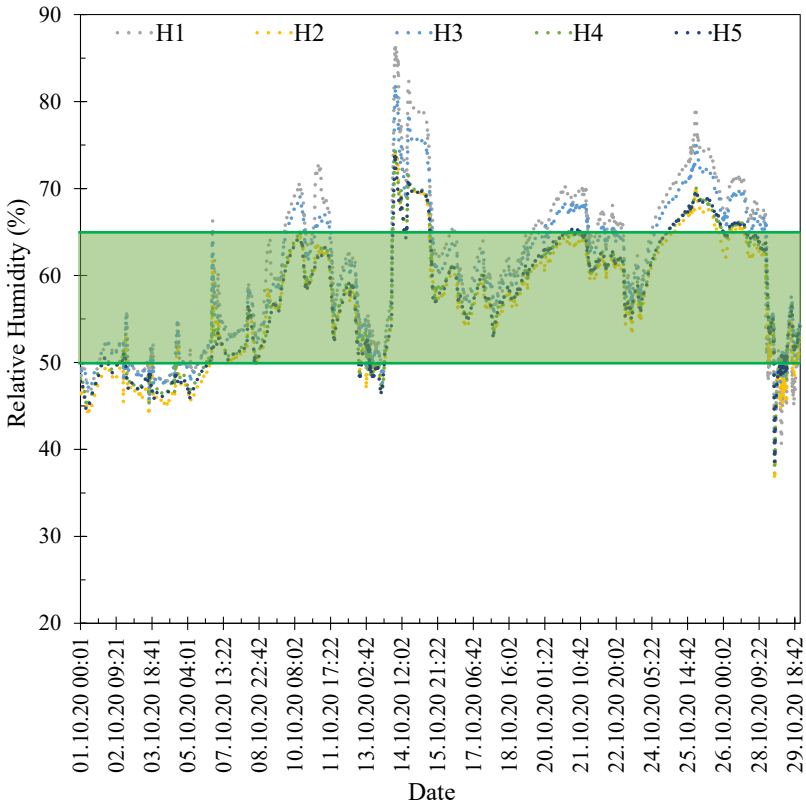

Figure D.5. Relative humidity values in October 2020

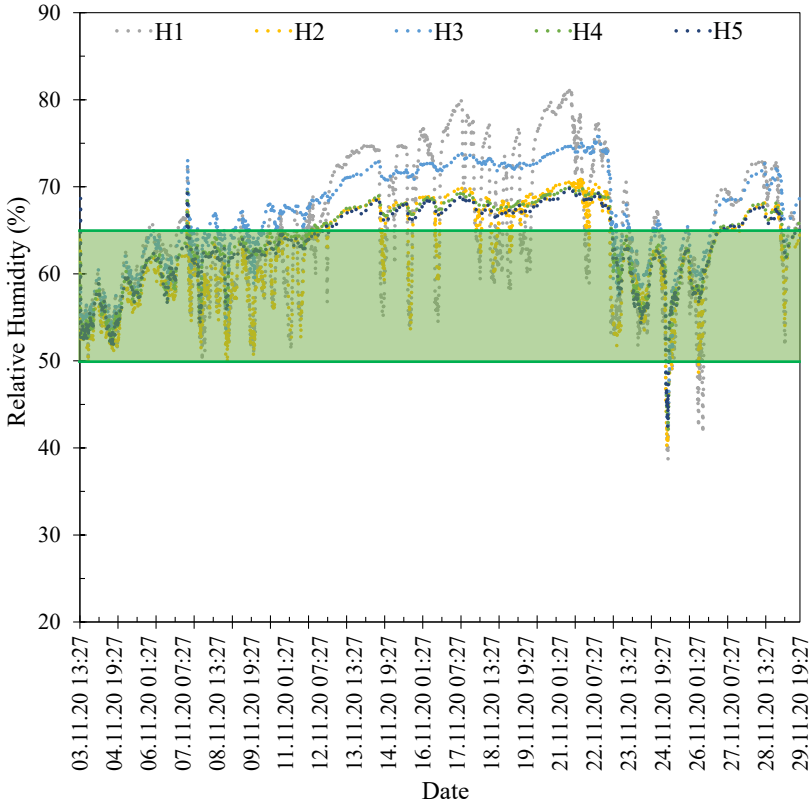

Figure D.6. Relative humidity values in November 2020

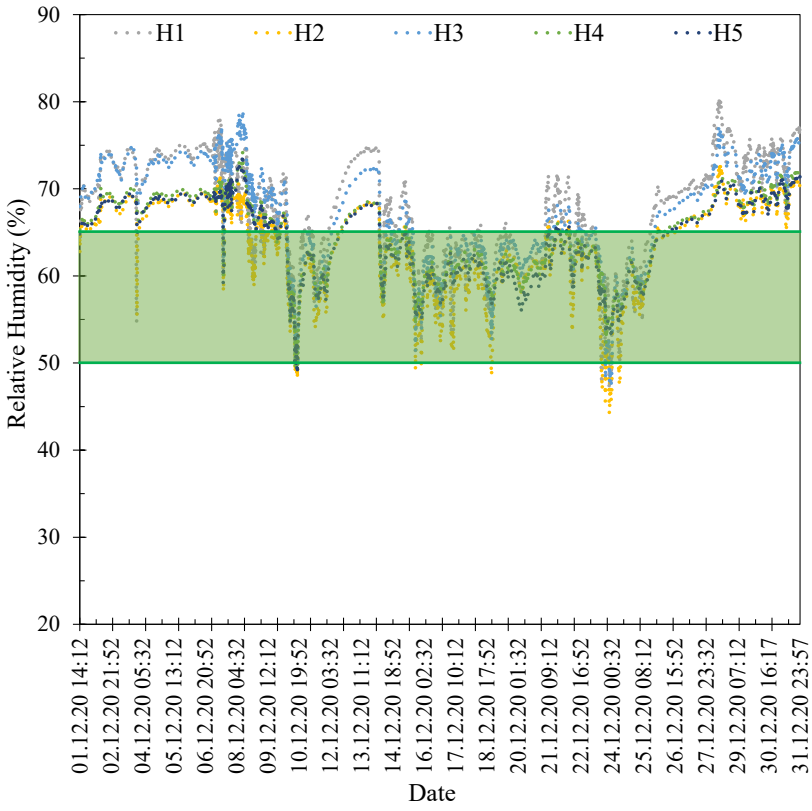

Figure D.7. Relative humidity values in December 2020

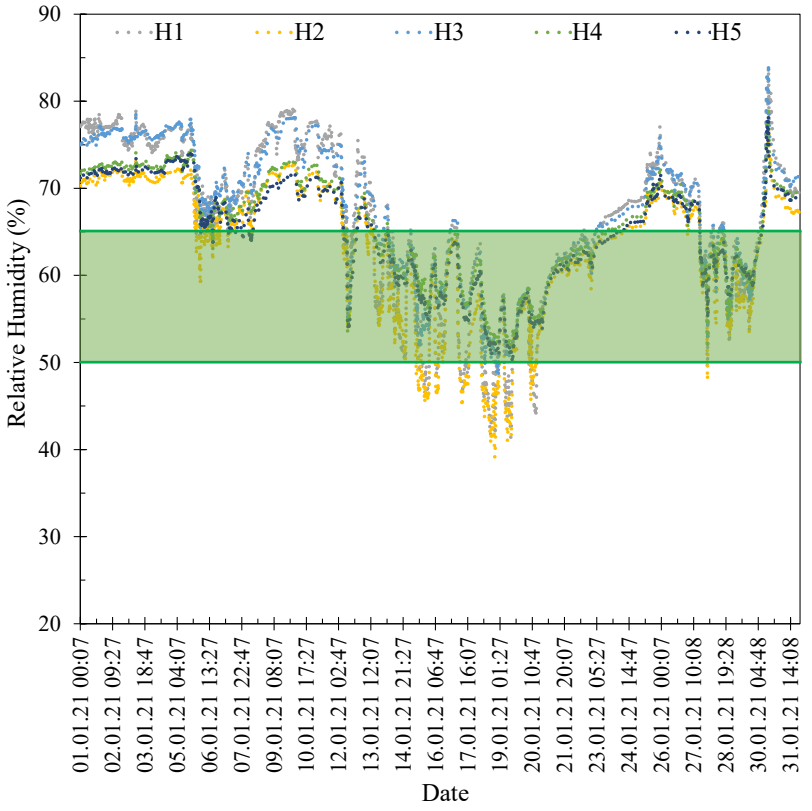

Figure D.8. Relative humidity values in January 2021

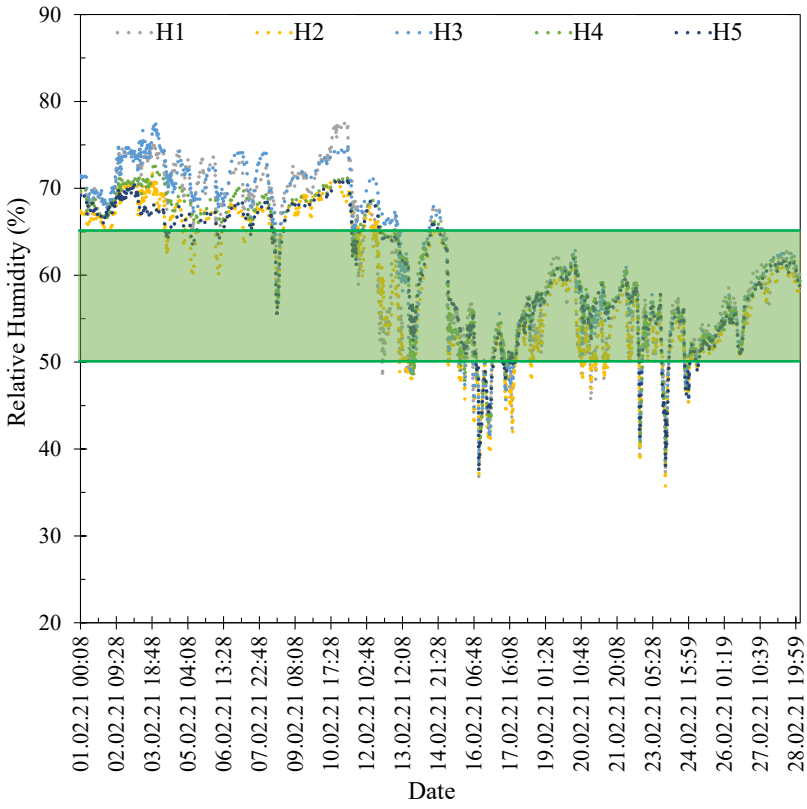

Figure D.9. Relative humidity values in February 2021

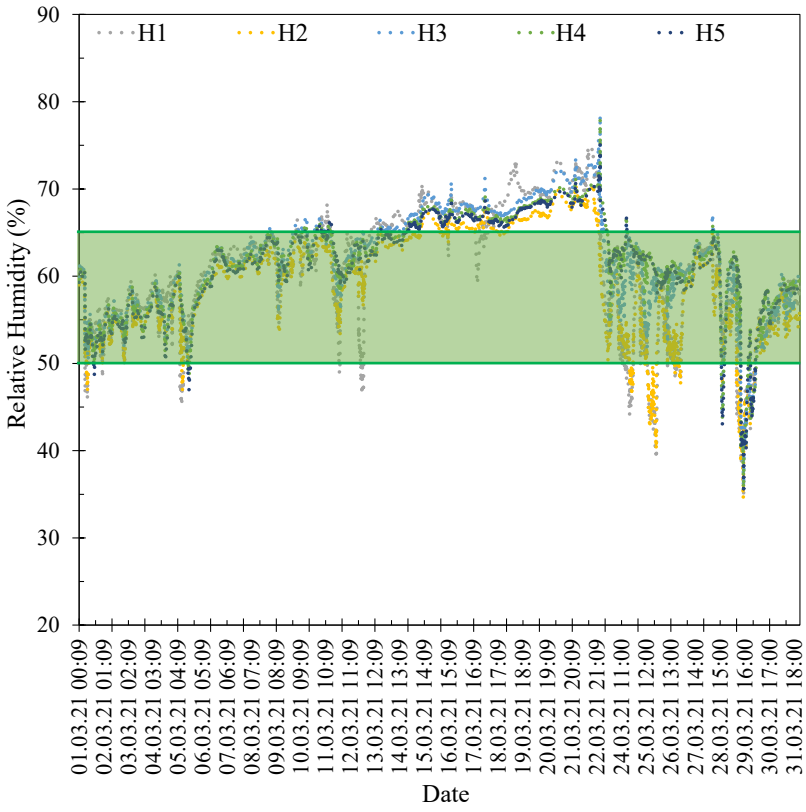

Figure D.10. Relative humidity values in March 2021

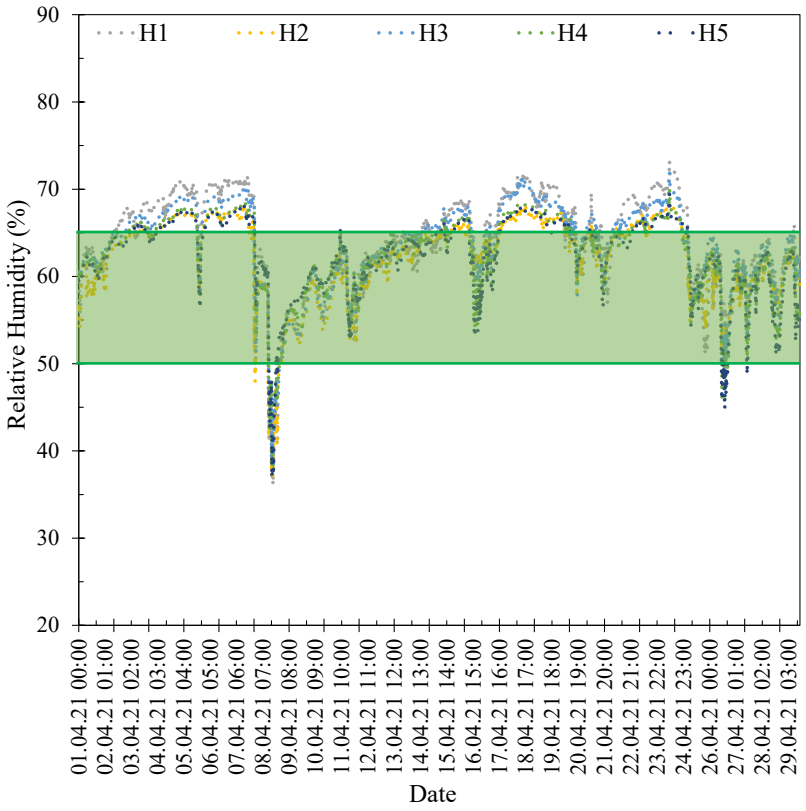

Figure D.11. Relative humidity values in April 2021

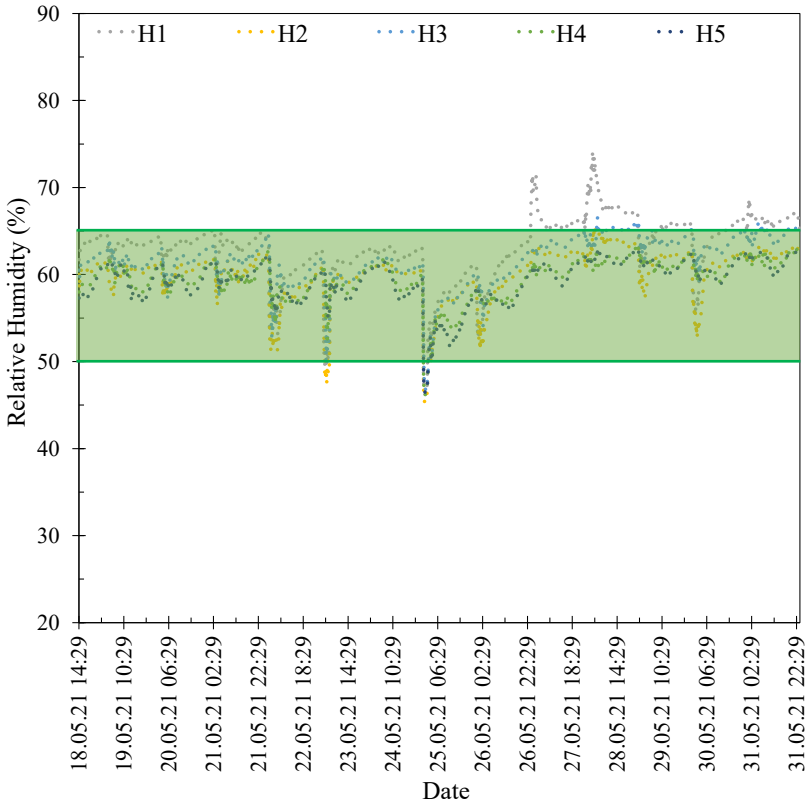

Figure D.12. Relative humidity values in May 2021

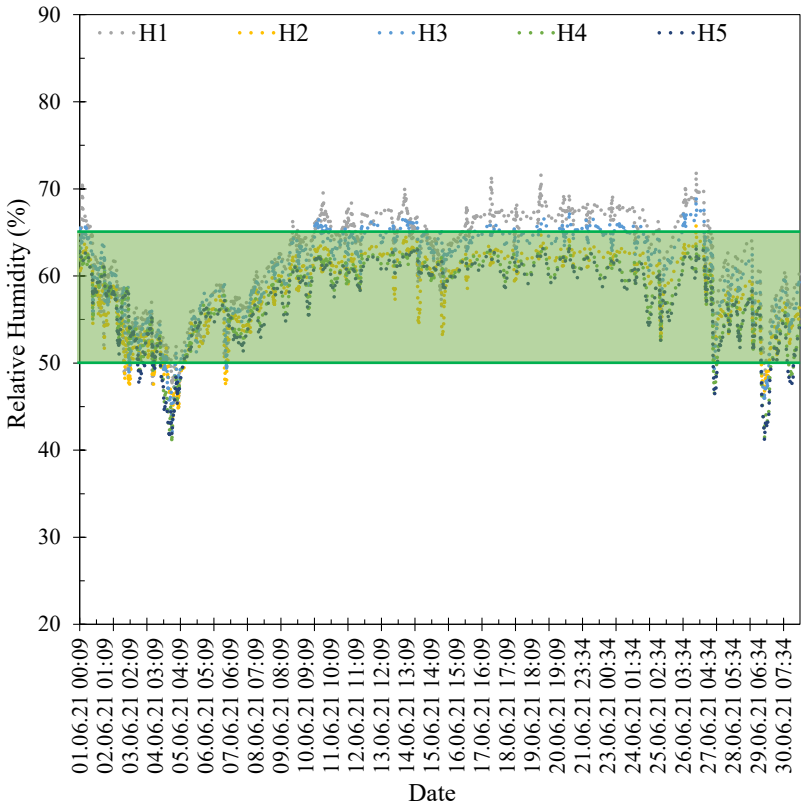

Figure D.13. Relative humidity values in June 2021

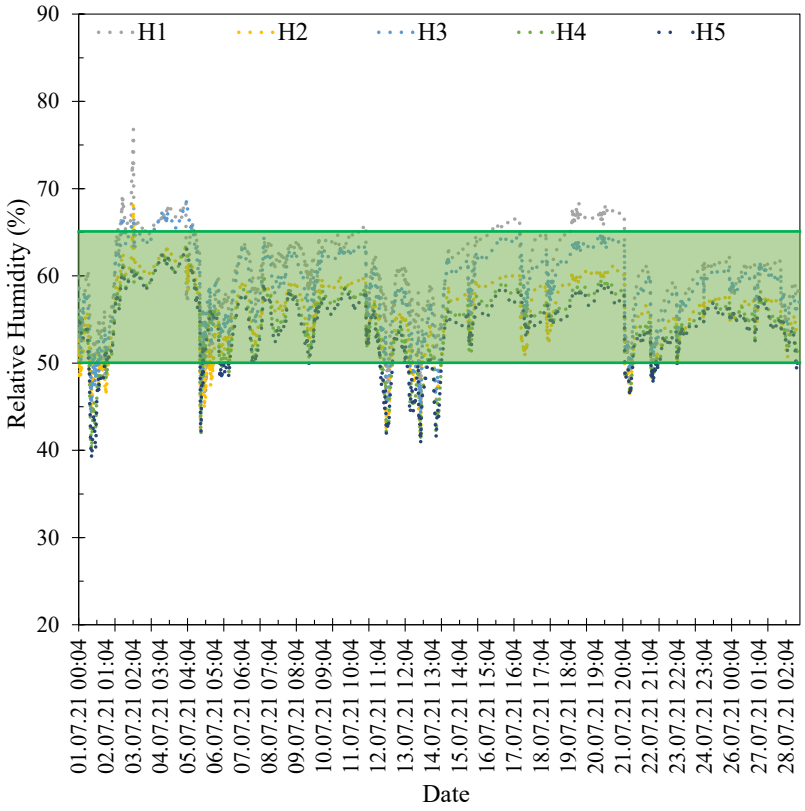

Figure D.14. Relative humidity values in July 2021

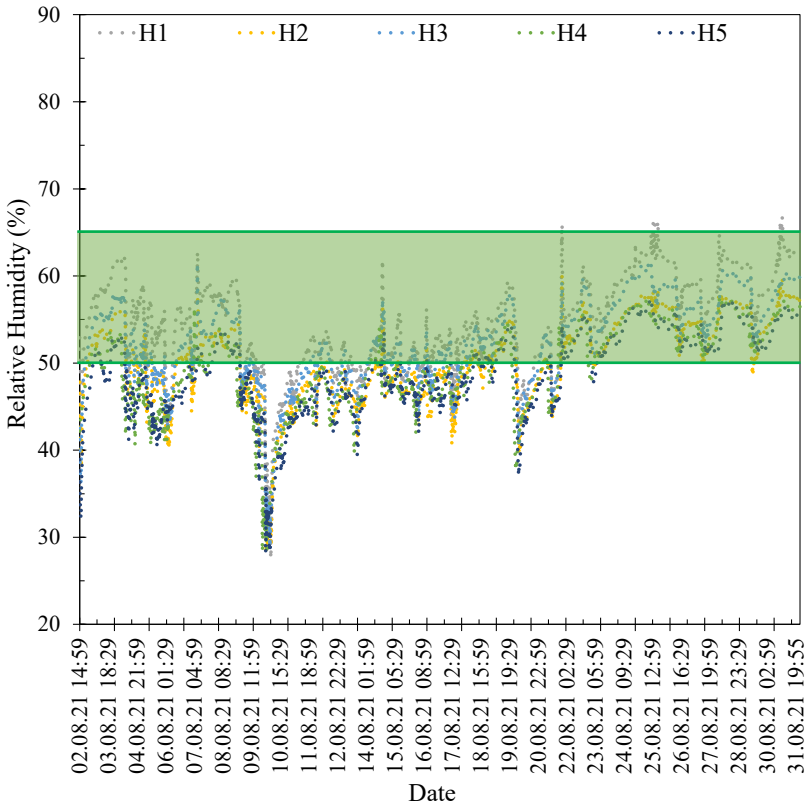

Figure D.15. Relative humidity values in August 2021

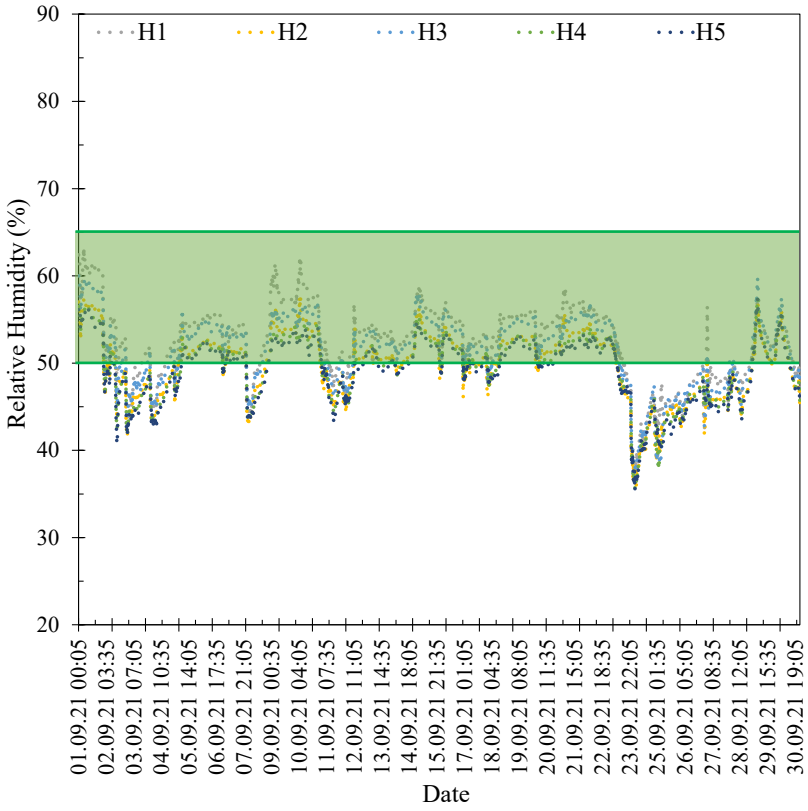

Figure D.16. Relative humidity values in September 2021

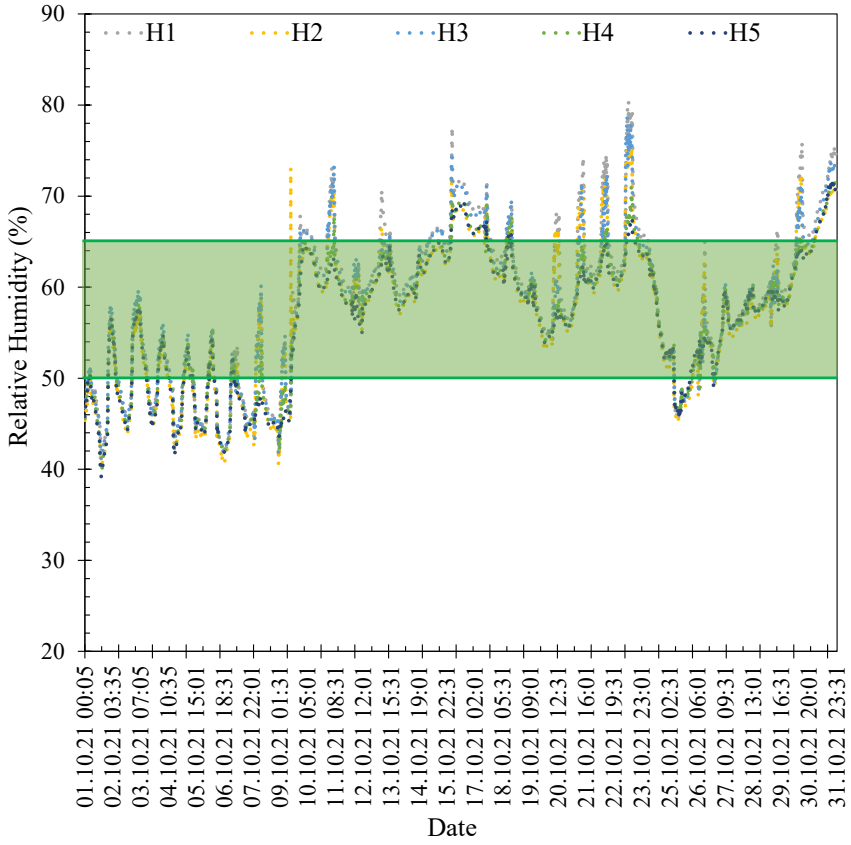

Figure D.17. Relative humidity values in October 2021

APPENDIX E

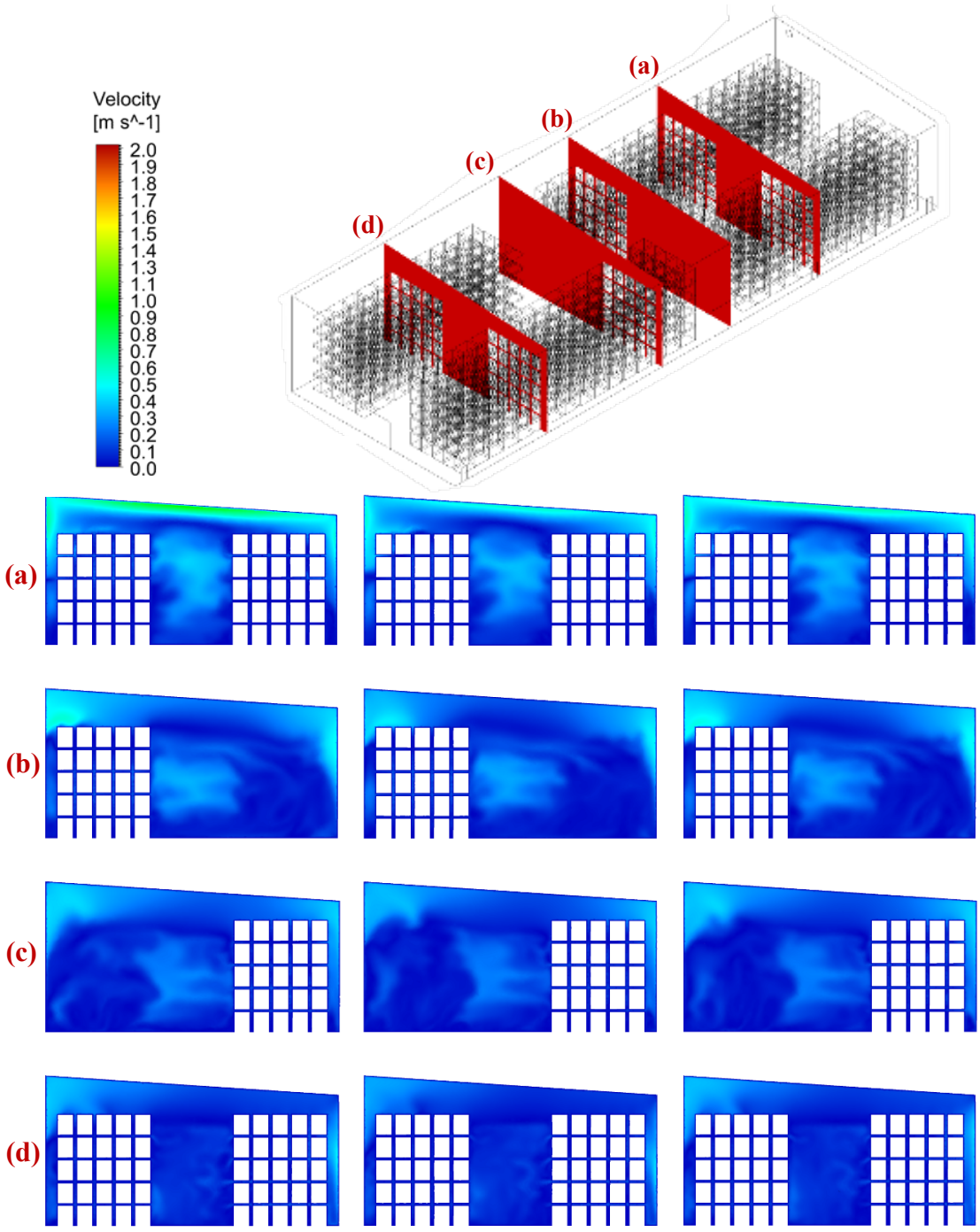

Figure E.1. Velocity contours on planes (a), (b), (c), and (d) for the current case fan scenarios; Case 1 (left), Case 2 (middle), Case 3 (right)

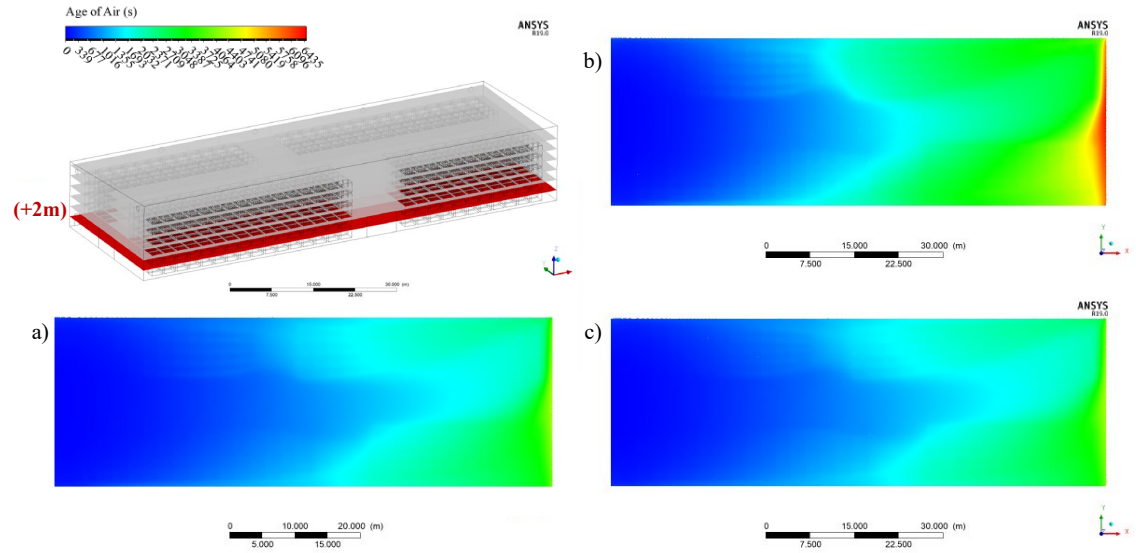

Figure E.2. AoA distribution within the 2 m plane along the z direction; a) Case 1, b) Case 2, c) Case 3

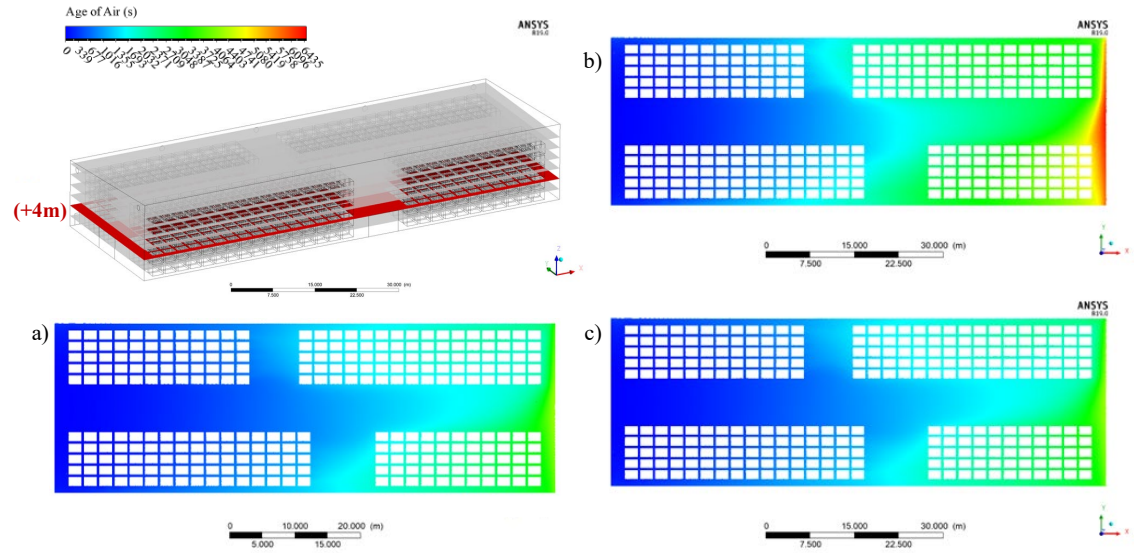

Figure E.3. AoA distribution within the 4 m plane along the z direction; a) Case 1, b) Case 2, c) Case 3

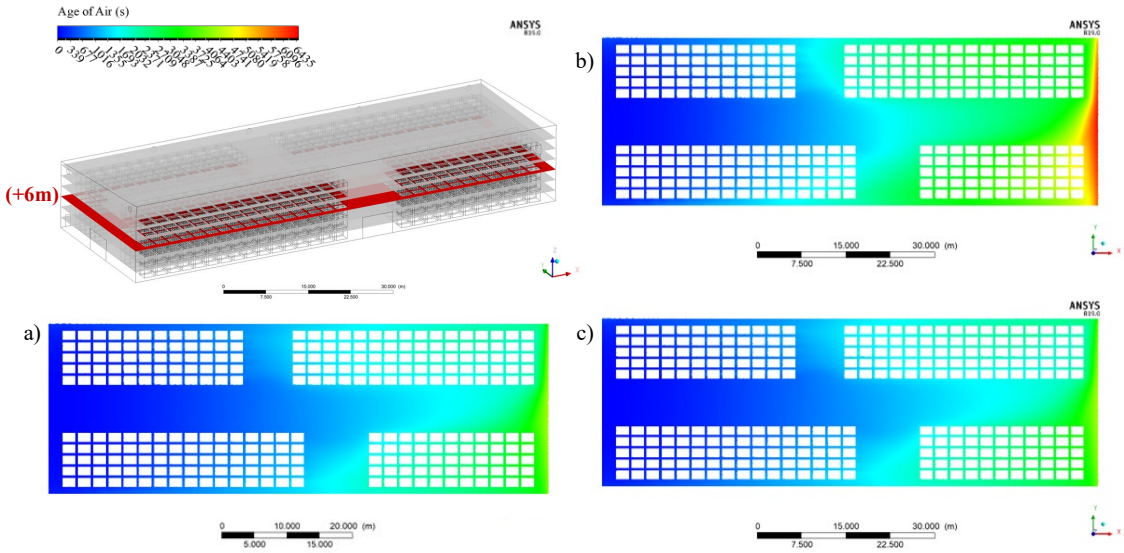

Figure E.4. AoA distribution within the 6 m plane along the z direction; a) Case 1, b) Case 2, c) Case 3

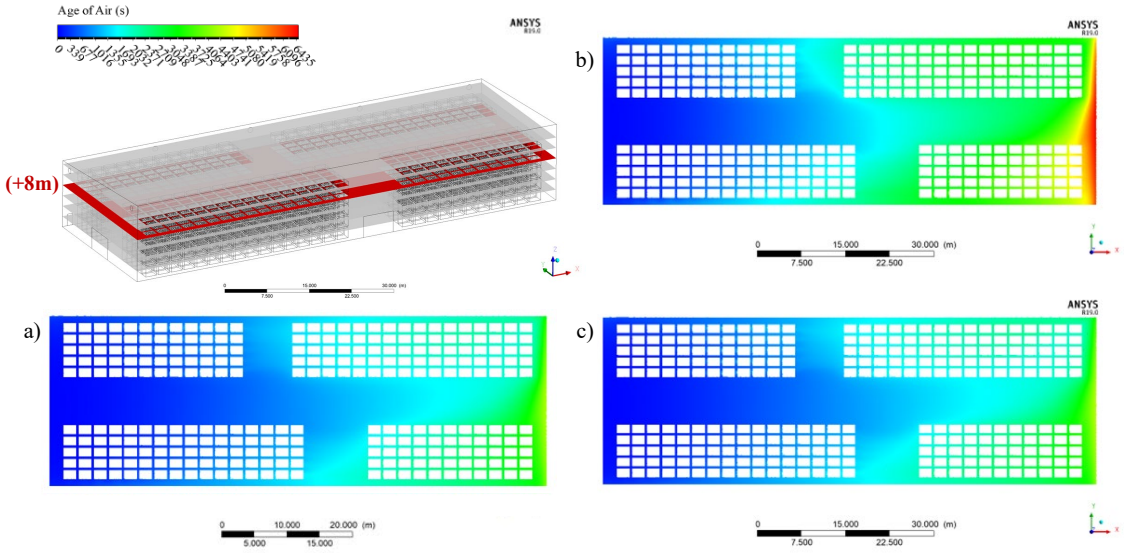

Figure E.5. AoA distribution within the 8 m plane along the z direction; a) Case 1, b) Case 2, c) Case 3

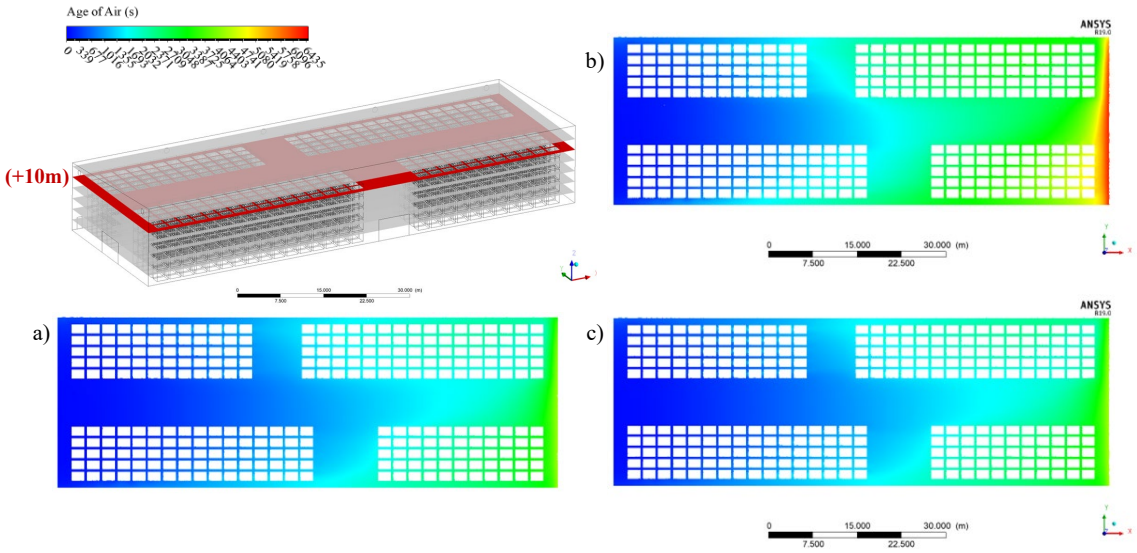

Figure E.6. AoA distribution within the 10 m plane along the z direction; a) Case 1, b) Case 2, c) Case 3

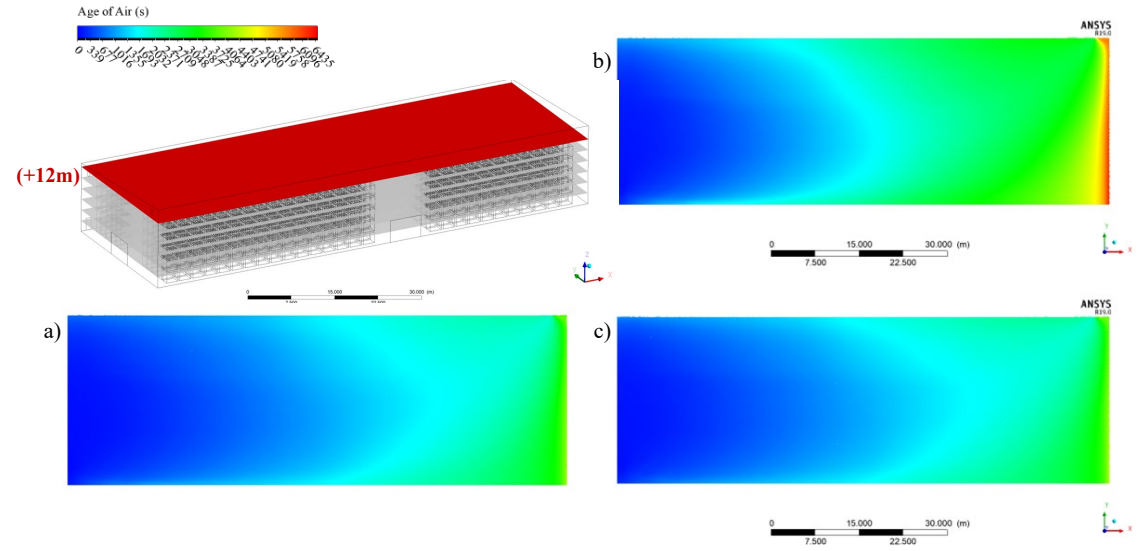

Figure E.7. AoA distribution within the 12 m plane along the z direction; a) Case 1, b) Case 2, c) Case 3

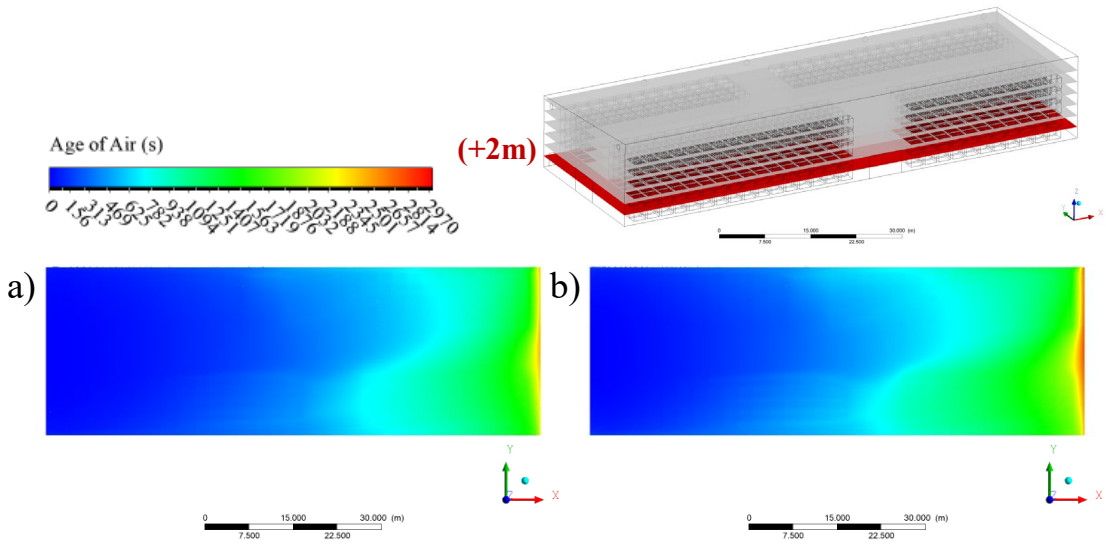

Figure E.8. AoA distribution within the 2 m plane along the z direction: a) Case 4, b) Case 5

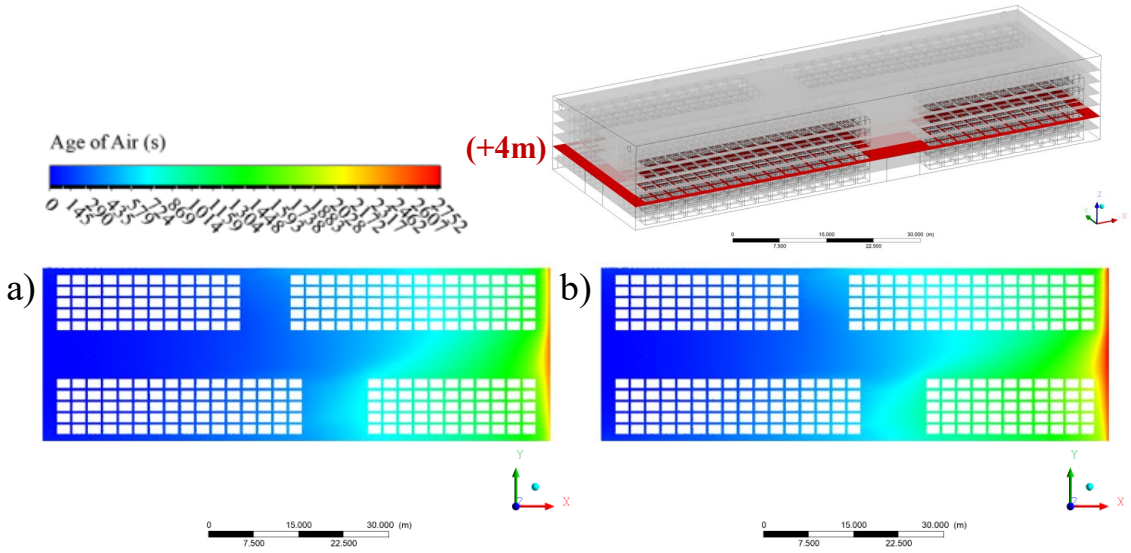

Figure E.9. AoA distribution within the 4 m plane along the z direction: a) Case 4, b) Case 5

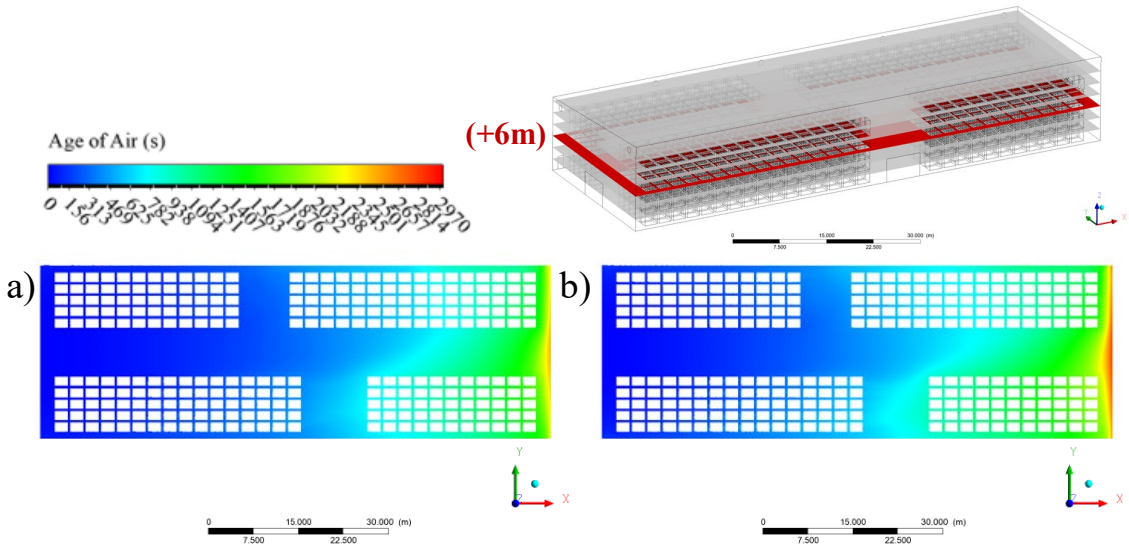

Figure E.10. AoA distribution within the 6 m plane along the z direction: a) Case 4, b) Case 5

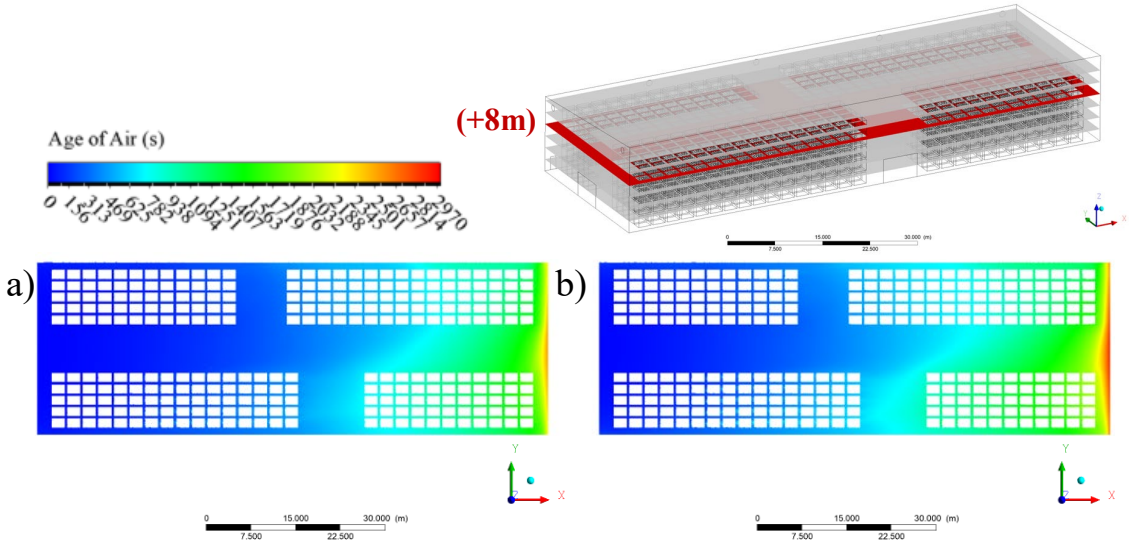

Figure E.11. AoA distribution within the 8 m plane along the z direction: a) Case 4, b) Case 5

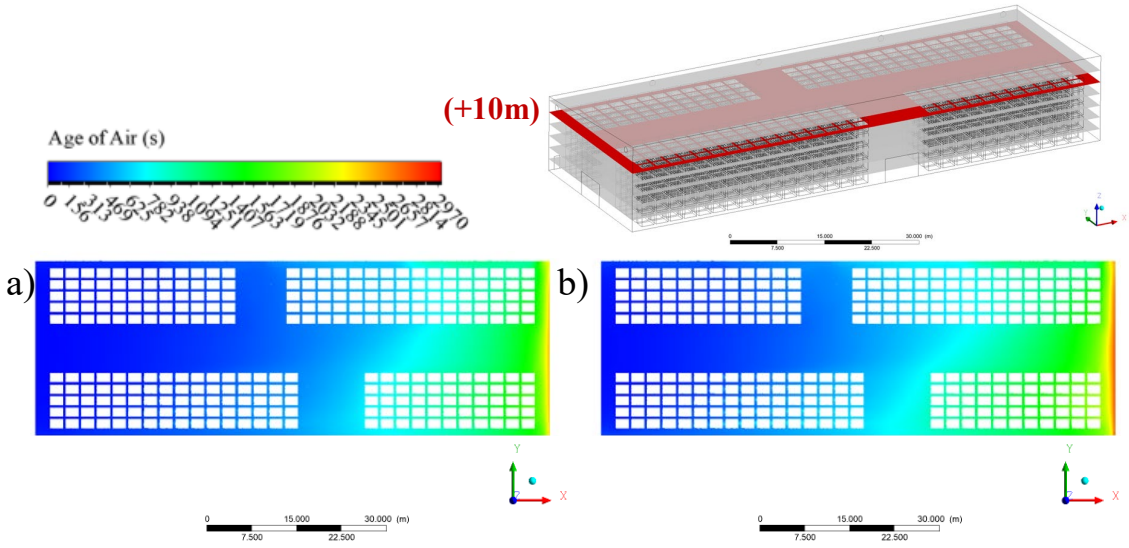

Figure E.12. AoA distribution within the 10 m plane along the z direction: a) Case 4, b) Case 5

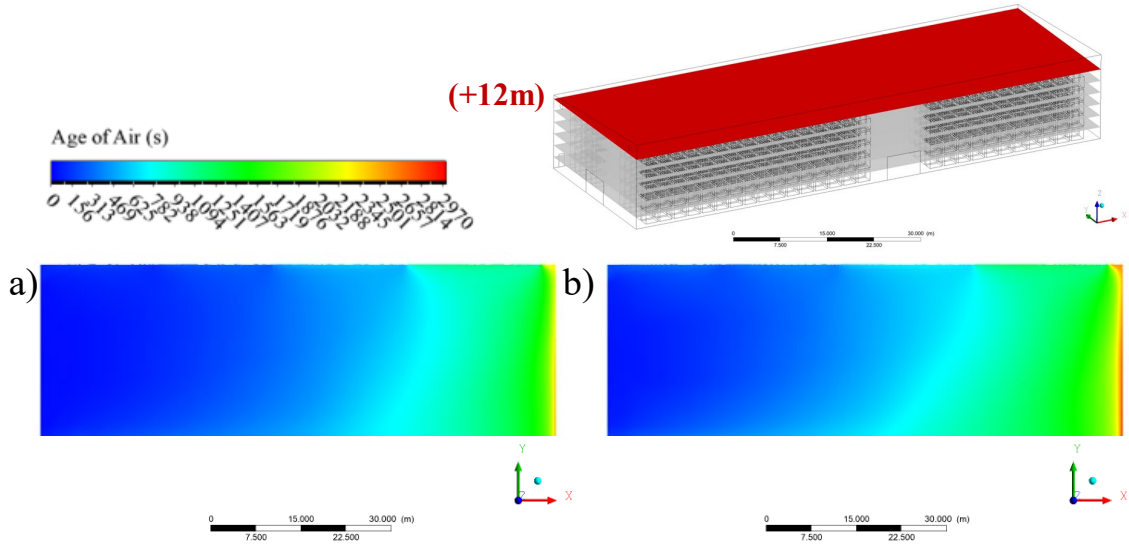

Figure E.13. AoA distribution within the 12 m plane along the z direction: a) Case 4, b) Case 5

VITA

PERSONAL

Surname Name: GERÇEK ŞEN Mümine

EDUCATION

Ph. D.	İzmir Institute of Technology. The Graduate School of Engineering and Science. Department of Architecture (2016-2023)
Thesis:	Investigations of Indoor Thermal and Air Flow Conditions in A Tobacco Warehouse
M. Sc.	İzmir Institute of Technology. Department of Architecture (2013-2016)
Thesis:	Energy and Environmental Performance-Based Decision Support Process for Early Design Stage of Residential Buildings
B. Arch.	Middle East Technical University. Department of Architecture (2007-2013)

WORK EXPERIENCES

İzmir Institute of Technology. Department of Architecture. Research Assistant (2014-…)

PUBLICATIONS

Gercek, M. and Arsan, Z. D. (2019). Energy and environmental performance-based decision support process for early design stages of residential buildings under climate change. *Sustainable Cities and Society*, 48, 101580.

Gercek, M. and Güçü, İ. (2019). The impacts of window-to-wall ratio and window orientation on building energy consumption and CO_2 emissions under climate change. *International Journal of Global Warming,* 18(3/4), 269-286.

Pekdoğan, T., Özen, G., Güçü, İ., and Gerçek, M., (2017). An Empirical Investigation of the Housing Price Dynamics across the Districts of İzmir. *Proceedings Books of International Congress on Politic, Economic and Social Studies 2017 (ICPESS) 3*(2), 200-211.

Gercek M. and Arsan Z.D., (2014). Impact of Energy Oriented Measures Over CO_2 Emissions of a Thermally Insulated Low-Rise Apartment Building in İzmir, Turkey. *ICONARP: International Journal of Architecture and Planning, 2*(2), 59-72.